United States
Environmental Protection
Agency

Environmental Research
Laboratory
Corvallis, OR 97333

EPA/600/3-90/078
September 1990

Research and Development

EPA

Biospheric Feedbacks to Climate Change: The Sensitivity of Regional Trace Gas Emissions, Evapotranspiration, and Energy Balance to Vegetation Redistribution

-- Status of Ongoing Research --

Edited By:
Hermann Gucinski, Danny Marks, and David P. Turner

Biospheric Feedbacks to Climate Change: The Sensitivity of Regional Trace Gas Emissions, Evapotranspiration, and Energy Balance to Vegetation Redistribution

-- Status of Ongoing Research --

Edited by:

Hermann Gucinski, Danny Marks, and David P. Turner

The information in this document has been funded by the U.S. Environmental Protection Agency as part of the Global Climate Research Program. The work presented here was conducted at the Corvallis Environmental Research Laboratory. This report has been subjected to the agency's peer and administrative review and it has been approved for publication as an EPA document.

Mention of trade names or commercial products does not constitute endorsement or recommendation for use.

Acknowledgements

The successful completion of this report would not have been possible without the support and assistance from a great number of individuals. We would like to acknowledge a few of those here. The editors would like to particularly recognize and thank Peter A. Beedlow, Technical Director, EPA Global Climate Research Program, Environmental Research Laboratory-Corvallis, for his support and assistance in the development of this report.

We also want to acknowledge the hard work and dedication of the Global Biogeochemistry Team and associated staff:

Joseph V. Baglio	George King	Donald L. Phillips
William G. Campbell	Greg Koerper	Derek Pross
Jayne Dolph	Bruce McVeety	Richard Vong
James Lenihan	Ronald P. Neilson	Andrew G. Wones
Kelly Longley		

We are grateful for the thoughtful criticism provided by the members of the public peer review panel for this report:

Frank Davis	University of California, Santa Barbara
Ralph Dubayah	University of Maryland
Upmanu Lall	Utah State University
Nikolas L. Nikolaidis	University of Connecticut
Phillip Sollins	Oregon State University
Nathan Stevenson	National Park Service
Denis White	NSI Technology Services, Inc.

We also want to thank several other scientists for their direct and indirect contributions to this effort:

Bert Drake	Smithsonian Environmental Research Center
Rik Leemans	National Institute of Public Health and Environmental Protection, Netherlands
Dennis Lettenmaier	University of Washington
Steve Running	University of Montana
Tom Smith	Oak Ridge National Laboratory
Starley Thompson	National Center for Atmospheric Research

BIOSPHERIC FEEDBACKS TO CLIMATE CHANGE: THE SENSITIVITY OF REGIONAL TRACE GASES EMISSIONS, EVAPOTRANSPIRATION, AND ENERGY BALANCE TO VEGETATION REDISTRIBUTION.
--STATUS OF ONGOING RESEARCH--

TABLE OF CONTENTS

EXECUTIVE SUMMARY

Implications of Global Climate Change

There is an emerging scientific consensus that global climate will change over the next several decades in response to increasing concentrations of greenhouse gases. However, there is less agreement on the magnitude and timing of that climate change. Among the major uncertainties are the role of atmospheric water vapor and clouds and the potential positive or negative feedbacks to climate change mediated by the biosphere. This document provides an analysis of the sensitivity of biospheric processes, including evapotranspiration, carbon storage in terrestrial ecosystems, and biogenic trace gas emissions that could affect the rate and extent of climate change through feedback processes.

Large Scale Data Requirements

Continental- and global-scale models require very large data bases to analyze patterns of precipitation, soil moisture, and other important processes which effect vegetation re-distribution. As a step towards development of spatially distributed models, data bases on terrain structure, soils, vegetation and land use, precipitation and runoff, air temperature, humidity, wind, solar radiation, and other parameters were assembled, evaluated for accuracy and reliability, and incorporated into suitable Geographic Information Systems (GIS).

Effects on Continental Scale Evapotranspiration

Simulation of potential evapotranspiration shows that climate change will alter evaporative stress across the U.S. Evapotranspiration affects the magnitude and spatial distribution of soil moisture and the regional water balance, which determines the condition and distribution of vegetation over the globe. Historical climate data were used to calculate potential evapotranspiration (PET) for the continental US by applying a turbulent transfer model to the hydrologic/climatologic data set. Results show that evaporative stresses are maximized in the southwestern US during summer. These findings differ from previous predictions based solely on air temperature. General circulation models (GCM) predict increases in wind, temperature and humidity for the continental U.S. Applying the GCM data to the evapotranspiration calculation illustrates how minor differences in predicted climate conditions can result in very different distributions of evaporative stress. Predictions of temperature, wind and humidity from the GFDL model lead to calculation of very high PET in the midwestern U.S., while the GISS model, leads to more modest increases in PET in the same region. These findings have important implications to the future of agriculture in this, the chief food-producing belt of the country.

Large-Scale Precipitation Analysis

An assessment of the utility of historical data for providing spatially distributed, large scale precipitation estimates indicates a low elevation bias in mountainous regions. Historical hydro-meteorological data were used to generate surfaces which characterize the spatial distribution of precipitation and runoff at regional- to continental-scales. A distributed water balance was used to assess the utility and limitations of historical data for providing estimates of precipitation across the continental U.S. The precipitation and runoff surfaces indicate a deficit in measured precipitation in comparison to measured runoff in mountainous regions of the western U.S. The incorporation of snow measurements into the precipitation record for these regions significantly improves the water balance calculations and enhances the utility of historical data for providing spatially distributed estimates of precipitation at scales compatible with GCM analysis.

Geostatistical Procedures for Spatially Distributing Climate Data

Simple interpolation techniques for distributing climatological data over the landscape fail to consider the effects of topography. For precipitation, this may result in considerable error in mountainous regions. Three geostatistical procedures, kriging, elevation detrended kriging, and co-kriging, applied to a small (300,000 km^2) northwest US river basin were evaluated for the precision and accuracy in the estimation of mean annual precipitation at a grid of points across the landscape. The latter two methods explicitly incorporate precipitation/elevation relationships, and yielded estimates with improved accuracy and precision. These methods appear promising for spatially distributing climate data consistent with topographic influences at this scale. The development of this approach to larger regions will require piece-wise estimation of sub-basins, or the development of an orographic precipitation model.

Re-distribution of Terrestrial Vegetation for a doubled CO_2 Climate

The potential redistribution of vegetation types in response to climate change has been estimated in several analyses using climate/vegetation correlation systems such as that of Holdridge combined with GCM climate scenarios. A review of results using five different GCMs revealed a general agreement in terms of the sign of the predicted change in the areal extent of specific vegetation types, i.e., deserts, boreal forest, and tundra biomes decrease, while grasslands and temperate and tropical forests generally increase in area. These changes reflect the increases in precipitation expected in temperate and tropical areas, and the effect of rising temperatures in high latitudes that displace or eliminate tundra and boreal biomes. The proportion of land surface

area changing from one vegetation type to another ranged from 16 to 56 % depending on the GCM used.

"Rule-based" Approaches to Vegetation Modeling

The present climate/vegetation models or correlations are based on relatively few climatic variables and in this study refinements are made by relating the seasonal timing and magnitude of temperature, precipitation and runoff patterns to the physiological requirements of specific vegetation types. For example, large winter precipitation allows a closed canopy forest to exist, while reduced winter precipitation produces a lower stature forest or savanna. Using seasonal precipitation and threshold values for different life-forms, the present model was calibrated and then tested for the biomes of the US. The overall success in predicting US biomes was 79%, with the best predictability at 94% for eastern forests, and the poorest success (0%) for a small grassland biome in northern California. Incorporation of potential evapotranspiration into the rule base is anticipated and this will allow application to future climates, e.g. doubled CO_2 climate scenarios, while "secondary" rules will improve model reliability by incorporating disturbance, such as fire, and biotic interactions, including the effect of CO_2 enrichment and changes of water use efficiency of plants.

Effect of Climate Change on Carbon Storage

An estimation of potential changes in storage of above- and below ground carbon in response to climate change was made based on the redistribution of vegetation types. Representative carbon pools were assigned to each vegetation type and the distribution of those vegetation types under the current climate and a double-CO_2 climate were used to predict changes in terrestrial carbon storage. Results from vegetation redistribution using four different GCMs and the Holdridge climate/vegetation correlation system were compared. All GCMs predicted a net flux of carbon from the atmosphere to the biosphere when considering just the aboveground biomass. This flux reflected increases in the areal extent of carbon rich vegetation types such as tropical humid forests. Two of the GCMs predicted a net loss of below ground carbon because of large decreases in the areal extent of tundra ecosystems with a high level of below ground storage. These analyses suggest the potential for a moderate negative feedback to global warming via accumulation of carbon in terrestrial ecosystems.

Climate Change and Isoprene Emissions

A global model was developed for estimating spatial and temporal patterns in the emission of isoprene from vegetation under the current climate and doubled-CO_2 climate scenarios. Current emissions were estimated on the basis of vegetation type, foliar biomass (derived from the satellite-generated Global Vegetation

Index), and global databases for air temperature and photoperiod. Doubled CO_2 climate emissions were estimated based on predicted changes in the areal extent of different vegetation types, each having a specific rate of annual isoprene emissions. The isoprene emissions under a doubled CO_2 climate were about 25 % higher than current emissions due mainly to the expansion of tropical humid forests which had the highest vegetation-specific emission rates. An increase in isoprene emissions could be expected to increase atmospheric concentrations of ozone and methane which are important greenhouse gases, however, detailed treatment of this question awaits incorporation of these emission surfaces into 3-D atmospheric chemistry models.

Research Directions

Fundamental questions remain about how ecological features can be characterized across different temporal and spatial scales and be integrated into predictive models of biosphere-climate interaction. Current GCMs do not include a realistic terrestrial biosphere, and operate at scales that are not ecologically meaningful. While these models are likely to improve over the next decade, it is important that we provide a link between terrestrial ecology and the atmospheric sciences in the context of climate change research. The work presented in this report is an important first step in this direction. Ecosystem models must be scaled up to regions comparable to GCM analysis, and equilibrium approaches to evaluating biospheric responses to climate change must give way to more dynamic or transient approaches.

Evaluation of ecosystem responses to climate change will require models which combine hydrology, nutrient cycling, and landscape ecology. Short- to mid-term research objectives require progress on three major fronts. The first is to improve the physical and mechanistic basis of models of the climate effects on biospheric processes so that they can be more effectively simulated for different climate conditions. This will require laboratory, growth chamber, and field experiments. A second is to develop simulation models of these processes which can be run at large regional- to global-scales. This will include an assessment of the effect of scaling on simulation of ecological processes, and development of "top down" models which treat features of the biosphere hierarchically. The third involves integrating these methodologies with efforts to improve both the spatial scale and characterization of the terrestrial biosphere in the next generation of GCMs.

BIOSPHERIC FEEDBACKS TO CLIMATE CHANGE: THE SENSITIVITY OF REGIONAL TRACE GASES EMISSIONS, EVAPOTRANSPIRATION, AND ENERGY BALANCE TO VEGETATION REDISTRIBUTION

– STATUS OF ONGOING RESEARCH –

INTRODUCTION

Hermann Gucinski and David P. Turner

NSI Technology Services, Inc.
U.S. Environmental Protection Agency
Environmental Research Laboratory
200 SW 35th Street
Corvallis, OR 97330
(503) 757-4600

There is an emerging scientific consensus that global climate will change over the next several decades in response to increasing concentrations of greenhouse gases (IPCC 1990). However, there is less agreement on the magnitude and timing of that climate change. Major uncertainties involve the role of atmospheric water vapor-cloud water balance, and the potential positive or negative feedbacks to climate change mediated by the biosphere.

The Global Change Research Program at the Corvallis Environmental Research Laboratory (ERL-C) was initiated in 1987 with the goal of examining potential effects of climate change on terrestrial ecosystems. The program has grown to focus in part on evaluation of biospheric feedbacks to climate change, especially as influenced by vegetation change. This area of research is of importance to EPA because of its influence on the rate and magnitude of climate change, and hence on the formulation of national policy regarding adaptation and mitigation. Early efforts at ERL-C have been on the development of climate/vegetation correlations that could be used to predict redistribution of vegetation types in response to climate change (Neilson et al. 1989). This work is in progress and more recent efforts have addressed the development of databases and distributed models for simulating atmosphere-biosphere interactions.

The work described in this document was performed during the 1990 Fiscal Year and represents the initial stages of a research effort that will extend into 1991 and beyond. The document is thus intended to report on work in progress in the areas of (1) examining spatial and temporal patterns in the current interaction between the biosphere and the atmosphere, (2) assembling and transforming the data bases required to understand vegetation dynamics and the biophysical constraints acting on the biosphere, and (3)

discussing approaches to quantifying biospheric feedbacks to climate change. The various chapters are a sampling of the range of research topics being addressed by the global change program at ERL-C.

Climate-vegetation interactions have been the object of study for some years. Research has aimed to clarify geographical patterns in vegetation distribution as they relate to climate, and to identify physiological mechanisms by which plant species are adapted to particular climate regimes. The reciprocal question, how plants or ecosystems influence the climate, has been addressed only recently. It is recognized that significant changes in global climate are likely to drive changes in the distribution of vegetation types. Major research questions must deal with how the flux in mass and energy from the biosphere influences climate under current conditions and how the flux will potentially influence climate as anthropogenically driven climate change begins to affect vegetation distribution.

The biosphere-atmosphere flux with which this document will be most concerned includes 1) water and water vapor, and 2) radiatively and photochemically important trace gases, particularly carbon dioxide (CO_2) and nonmethane hydrocarbons. A principal concern is how changes in vegetation in response to climate change will influence the flux.

The structure of the document is as follows: The introduction briefly reviews background material relating to several of the important feedback mechanisms and discusses research directions. We then begin with an examination of the necessary global data bases required for assessing factors which influence or produce biospheric feedbacks (II). There follows a series of chapters concerned with the hydrologic cycle. A spatially distributed turbulent transfer model is developed to evaluate the sensitivity of potential evapotranspiration to climate change (III). Continental-scale precipitation-runoff relationships for the U.S. are characterized to examine the utility of the historical precipitation record for providing spatially distributed

estimates of precipitation (IV). Thirdly, an evaluation of geostatistical procedures which could be used to estimate regional precipitation distribution and volume is presented (V). A "top down" approach for evaluating global vegetation redistribution in response to climate change is then presented (VI). The need to base this approach on mechanistic principles is examined in the chapter on a rule-based biome model (VII). The final chapters proceed from the estimates of current and future vegetation distributions to evaluate the effect of climate change on carbon storage and carbon releases (VIII), as well as on emissions of biogenic trace gases, which, by their importance in tropospheric chemistry, affect the concentration of greenhouse gases such as methane (IX).

Biospheric Feedbacks

The application of the concept of feedback to biological systems began with the development of cybernetics in the late 1940s (von Bertalanffy 1968). The concept arose in the field of engineering but it has been recognized that feedback is a basic mechanism of self regulation in organisms and at higher levels of organization. The basic idea is that a signal impinging on a component of a system initiates an output or change in output from that component which amplifies (positive feedback) or dampens (negative feedback) the magnitude of the original signal.

There are several applications for the feedback concept in the climate-biosphere system and it may be useful to make some distinctions based on spatial and temporal scales. In climate dynamics, the signal is a change in mean global temperature. In an equilibrium approach, one establishes what the climate would be, for example, under a doubled-CO_2 scenario with no change in the biosphere. General circulation models (GCMs), which account for the energy balance of the planet and atmosphere as well as the fluxes of water, permit such an evaluation. One then applies the climate scenario to models of the biosphere, determines how biospheric flux of mass and energy changes, and estimates how the new pattern of flux

would further influence the climate, again using a GCM. A specific example would be a potential increase in methane emissions driven by warming of high latitude wetlands. Since atmospheric methane would increase, and methane is a "greenhouse gas", the associated warming would be a positive feedback to the original doubled-CO_2 warming. Lashof (1989) has recently reviewed a variety of potential feedbacks to climate change using this approach and compared their relative magnitudes by reference to a gain factor.

The analysis of biospheric feedbacks using a dynamic or transient approach is considerably more complex. Here a GCM must be coupled to biospheric processes and run over time intervals from decades to centuries. At present, the biosphere is largely ignored in the GCMs. However, rapid strides are being made in this area of much needed research. Detailed process models for the hydrologic cycle, nutrient cycles and the exchange of trace gases and energy are being developed which will eventually be coupled to GCMs.

A brief review of some of the major feedback mechanisms is included here in order to put some of the material contained in this report in perspective.

Trace Gas Feedbacks

Water is the most important greenhouse gas, and is largely accounted for in terms of feedbacks in the global radiation budget of GCMs. There are several important greenhouse gases besides water vapor, including carbon dioxide (CO_2), methane (CH_4), nitrous oxide (N_2O), and ozone (O_3). Concentrations of these gases are not at chemical equilibrium in the atmosphere, an observation which has prompted the notion that the continuous processing of materials by the biosphere maintains their steady state (Lovelock 1989). Global budgets of these trace gases reveal that biological processes do indeed account for most

of the flux. Since the biosphere is expected to respond significantly to anthropogenically-induced climate change, the concentrations of the trace gases might also be influenced. This produces the potential for positive or negative feedbacks to climate change from the biosphere.

Carbon dioxide is the dominant trace gas among the non-water vapor greenhouse gases. Its concentration is determined by many factors collectively characterized as the global carbon cycle. That cycle includes large atmosphere-terrestrial biosphere and atmosphere-ocean flux. The flux is bi-directional, and the atmospheric and surface pool sizes remain relatively constant. There is a seasonal oscillation of approximately 10 ppm in the atmospheric CO_2 concentration in the northern hemisphere (Keeling et al. 1989) due to net photosynthesis in the summer and a release of CO_2 via respiration in the winter. A change in the flux rates to and from the atmosphere over longer time frames results in changes in atmospheric pool size.

The CO_2 concentration has varied widely over geological time, but has had a range between two and three hundred ppm over the last glacial-interglacial cycle, i.e., approximately 100,000 years (Barnola et al. 1987). Long term changes in CO_2 concentration appear to be responses rather than initiators of climate change and appear to be generally acting as positive feedbacks, i.e. changes in orbital forcings may initiate climate change but biospheric or other factors which change atmospheric CO_2 amplify the original change. The current global concentration is approximately 350 ppm, having risen from 280 ppm in the 1800's (Neftel et al. 1985) and about 200 ppm during the last glacial maximum (Barnola et al. 1987). Further increase in concentration over the next few decades is highly dependent on population growth and energy policy and is expected to be large enough to strongly impact the climate.

One of the mechanisms by which the atmospheric CO_2 concentration may change is via the storage of carbon in vegetation and soils. The warming since the last glacial maximum induced large changes in the distribution of vegetation types which may have influenced the rise from 200-280 ppm CO_2. Changes in above- and below-ground carbon pools may be a function of both changes in land surface area i.e. sea level changes, and changes in the areal extent of different biomes, each having biome-specific amounts of above- and below-ground carbon (Prentice and Fung in press). Evidence from the pollen record, for example, reveals the northward migration of boreal forest since the last glacial maximum (Davis 1981). The anticipated global warming of $3.5 \pm 1.5°C$ is likely to produce additional large changes in the areal extent of different vegetation types. We examine the associated changes in terrestrial carbon pools and related fluxes of CO_2 in chapter VIII of this document.

Methane and nitrous oxide have relatively long atmospheric lifetimes, 10 years and 120 years respectively. Atmospheric concentrations of both gases are also increasing currently, most likely due to anthropogenic factors, and they are predicted to account for approximately 25% of the increase in global temperature due to the "greenhouse effect" over the next several decades (Ramanathan et al. 1985). During previous periods of warming, atmospheric concentrations of these gases increased, suggesting they were part of a positive biospheric feedback to the warming (Khalil and Rasmussen 1989). However, there are large uncertainties about future feedbacks associated with methane and nitrous oxide (Lashof 1989). Biogenic sources may increase due to warming of high latitude biomes where there are large pools of potentially decomposable belowground organic matter. There may also be release of large amounts of pre-existing methane from marine sediments or from frozen high latitude soils.

Other biogenic trace gas emissions likely to increase with global warming include nonmethane hydrocarbons (NMHC). These compounds are emitted by most types of vegetation, but emissions vary

widely as a function of vegetation type and environmental variables such as temperature and light (Zimmerman et al. 1978). Oxidation of NMHCs reduces the concentration of the hydroxyl radical, thus serving to increase the atmospheric lifetime of methane and other important trace gases, and may result in production of tropospheric ozone, a significant greenhouse gas (Logan et al. 1981). The exponential rise of vegetative NMHC emissions with increasing temperature (Tingey et al. 1981) suggests that the warming associated with climate change is likely to increase the global emissions. There may also be increased emissions of NMHCs if the areal extent of forest ecosystems expands, as the modeling efforts in this document suggest will occur with a doubled-CO_2 climate. The corresponding increases in ozone and methane concentrations will be positive feedbacks to the climate warming.

Water Vapor Feedback

As noted, the dominant greenhouse gas in the Earth's atmosphere is water vapor; it provides a large potential feedback to climate change. About half the projected temperature increase in doubled CO_2 GCM runs is due to the positive feedback of increased atmospheric water vapor (Hansen et al. 1984). Much of the flux of water vapor from the land surface is from the vegetation, perturbations of which are likely to significantly alter the water vapor feedback (Shukla and Mintz 1982). Again, these biospheric processes are poorly modeled in current GCMs and are a current research objective in the modeling community.

Albedo Feedback

The Earth's albedo plays a significant role in its energy balance (Ramanathan et al. 1989) and hence its climate. As climate warms there is a simple positive feedback in that the area of highly reflective ice cap shrinks and more visible radiation is absorbed by the earth, a positive feedback. Much more complicated, and as yet not fully understood, is the relationship between the global balance of atmospheric water vapor and liquid water in the form of clouds, and the resulting balance in global albedo. Climate driven changes in vegetation cover and the distribution of vegetation types would also result in changes in the global albedo, although the magnitude of this effect may not be large (Dickinson and Hanson 1984). Future treatments of potential changes in global albedo due to vegetation change must include anthropogenic factors such as desertification (Sagan et al. 1979) and deforestation (Henderson-Sellers and Gornitz 1984).

Research Directions

Biospheric feedbacks to climate change operate across a wide range of spatial and temporal scales, and fundamental questions remain about how information at these scales can be integrated into predictive models, including present and future general circulation models. As a start, the current emphasis on equilibrium approaches to evaluating biospheric responses to climate change must give way to more dynamic or transient approaches. We have suggested, for example, that transitional releases of carbon during vegetation redistribution may produce sufficient feedbacks to alter equilibrium end points (King et al. 1990). Prediction of CO_2 fertilization effects on plants will likewise require an understanding of transition dynamics.

Integrating information at different spatial and temporal scales must remain a principal short- to mid-term research objective. This objective will require progress on three major fronts. The first would seek to describe biospheric and physical processes relevant to climate change at the plot or stand scale. A second would concern the ability to simulation these processes at broader spatial scales. The third would involve coupling of these simulations with GCMs such that there is two way interaction between the climate and the biosphere.

Evaluation of local or site-specific responses to climate change will require ecosystem models which combine hydrology, nutrient cycling and population biology. Driven by GCM climate scenarios, such models will become increasingly useful tools for evaluating the mechanisms which will dominate the response of particular sites to climate change.

The optimal approach to "scaling up" of responses from local sites to regional and global levels remains problematical. The varied spatial and temporal scales of relevant biospheric processes do not allow treatment of all processes simultaneously. Consequently, efforts will be required to develop models appropriate to each scale and one of the major research tasks of the next decade is to determine the optimum way of coupling such models.

These problems emphasize the need for concrete, short term research objectives, such as developing realistic capabilities for flux estimates at scales of hundreds of meters to kilometers. One approach used successfully in the past has been to bring a number of investigators to a common site. These scientists combine efforts to address questions such as the magnitude of biosphere/atmosphere fluxes of trace gases and energy. The First International Satellite Land Surface Climatology Program (ISLSCP) is the prototype for such efforts. In that case the surface/atmosphere flux of CO_2 was measured using both chamber and

eddy correlation techniques; open path FTIR or tunable dye laser now appear to be additional approaches for flux measurements which could be added to the suite of existing techniques. In combination with remote sensing of ecosystem processes, these measurement programs will contribute significantly to advances in our capacity to scale up from sites to regions.

Lastly is the problem of incorporating models of biospheric processes into GCMs. Current representations of the ground surface such as the Biosphere-Atmosphere Transfer Scheme (BATS) of Dickenson et al. (1986) have significant limitations. These models of biosphere/atmosphere interaction need improved treatment of physiological processes and will require high resolution global databases to be initialized and run. The increasingly sophisticated hardware and software associated with Geographic Information Systems will help in the development of appropriate databases for land surface features including topography, vegetation, soils, climate and land use. However, increased attention to spatial and temporal heterogeneity in relevant parameters is needed. In this regard, remote sensing offers considerable promise for initializing and eventually validating these models.

A Note on the Format of this Report

To reach the widest scientific audience, the report was assembled from chapters written as stand-alone manuscripts suitable for publication in the peer reviewed literature. While this introduces some unevenness in the document, we feel that the state of the science requires considerably more research before a comprehensive review of the role of biospheric feedbacks in climate change will be possible. This juxtaposition of research addressing a variety of issues and taking a range of approaches also highlights the need for increased inter-disciplinary collaboration and interaction to address the most critical, and in many ways most controversial, research issues. We see our efforts contributing in this arena, adding light

as well as heat to the debate. We well understand the incompleteness of the scientific record on the problem of forecasting the effects of global climate change, and well know the limitations of the contributions contained herein, but we see them as building blocks for improved future understanding.

Chapter VI, "Effects of global climate change on global vegetation," is included in this report as an integral part of the development of ideas for a rule-based approach to modeling vegetation change (Chapter VII), and as a basis upon which the assessment of the changes in terrestrial ecosystem carbon storage (Chapter VIII) and in plant emissions of trace gases (Chapter IX) is built. The chapter is also included in another report (King et al. 1990) because it fulfills a similar requirement there. We believe this duplication adds continuity and cohesiveness to both reports, and minimizes disruptive cross-references.

REFERENCES:

Barnola, J.M., D. Raynaud, Y.S. Korotkevich, and C. Lorius. 1987. Vostok ice core provides 160,000-year record of atmospheric CO_2. Nature 329:408-414.

Davis, M.B. 1981. Quaternary history and the stability of forest communities. In: D.C. West, H.H. Shugart & D.B. Botkin, eds., Forest Succession: Concepts and Application. Springer-Verlag, New York. 517 pp.

Dickinson, R., and B. Hanson. 1984. Vegetation-albedo feedbacks. In: J. Hansen and T. Takahasi, eds., Climate Processes and Climate Sensitivity. Geophys. Mono 29., Maurice Ewing, American Geophysical Union, Washington, DC. 5:180-186.

Dickinson, R.E., A. Henderson-Sellers, P.J. Kennedy and M.E. Wilson. 1986. Biosphere-Atmosphere Transfer Scheme (BATS) for the NCAR Community Climate Model. NCAR Technical Note, NCAR/TN-274+STR, National Center for Atmospheric Research, Boulder, Colorado, 69 p.

Hansen, J., A. Lacis, D. Rind, G. Russel, P. Stone, I. Fung, and J. Lerner. 1984. Climate sensitivity: Analysis of feedback mechanism. In: Climate Processes and Climate Sensitivity, Geophys. Monogr. Serv., AGU, Washington, DC 29:130-163.

Henderson-Sellers, A., and V. Gornitz. 1984. Possible climatic impacts of land cover transformations, with particular emphasis on tropical deforestation. Climatic Change 6:231-257.

Holdridge, L.R. 1947. Determination of world formulations from simple climatic data. Science 105:367-368.

Intergovernmental Panel on Climate Change. 1990. Scientific Assessment of Climate Change. Report for WGI Plenary Meeting.

Keeling, C.D., R.B. Bacastow, A.F. Carter, S.C. Piper, T.P. Whorf, M. Heimann, W.G. Mook, and H. Roeloffzen. 1989. A three-dimensional model of atmospheric CO_2 transport based on observed winds: Analysis of observational data. Geophys. Mono. 55:165-236.
pp 165-236. Geophysical Monograph 55. American Geophysical Union, Washington D.C.

King, G.A., J.K. Winjum, R.K. Dixon, L.Y. Arnaut (eds.). 1990. Responses and feedbacks of forest systems to global climate change. Report to the US EPA, Office of Research and Development. USEPA Environmental Research Laboratory, Corvallis, Oregon.

Khalil, M.A.K. and R.A. Rasmussen. 1989. Climate-induced feedbacks for the global cycles of methane and nitrous oxide. Tellus 41B:554-559.

Lashof, D.A. 1989. The dynamic greenhouse: Feedback processes that may influence future concentrations of atmospheric trace gases and climatic change. Climatic Change 14:213-242.

Logan, J.A., M.J. Prather, S.C. Wofsy, and M.B. McElroy. 1981. Tropospheric ozone: A global perspective. J. Geophys. Res. 96:7210-7254.

Lovelock, J.E. 1989. Geophysiology, the science of Gaia. Rev. Geophys. 27:215-222.

Neftel, A., E. Moor, H. Oeschger, and B. Stauffer. 1985. Evidence from polar ice cores for the increase in atmospheric CO_2 in the past two centuries. Nature 315:45-47.

Neilson, R.P., G.A. King, R.L. DeVelice, J. Lenihan, D. Marks, J. Dolph, W. Campbell, G. Glick. 1989. Sensitivity of ecological landscapes and regions to global climate change. Report to the US EPA, Office of Research and Development, USEPA Environmental Research Laboratory, Corvallis, Oregon.

Prentice, K.C., and I.Y. Fung. Bioclimatic simulations test the sensitivity of terrestrial carbon storage to perturbed climates. Nature. In press.

Ramanathan, V., R.J. Cicerone, H.B. Singh, and J.T. Kiehl. 1985. Trace gas trends and their potential role in climate change. J. Geophys. Res. 90:5547-5566.

Ramanathan, V., R.D. Cess, E.F. Harrison, P. Minnis, B.R. Barkstrom, E. Ahmad, and D. Hartmann. 1989. Cloud-radiative forcing and climate results from the earth radiation budget experiment. Science 243: 57-63.

Sagan, C., O.B. Toon, and J.B. Pollack. 1979. Anthropogenic albedo changes and the earth's climate. Science 206:1363-1368.

Shukla, J., and Y. Mintz. 1982. Influence of land-surface evapotranspiration on the earth's climate. Science 215:1498-1500.

Tingey, D.T., R. Evans, and M. Gumpertz. 1981. Effects of environmental conditions on isoprene emission from live oak. Planta 152:565-570.

von Bertalanffy, L. 1968. General Systems Theory. George Brazilla, Publ. New York. 295 pp.

Zimmerman, P.R., R.B. Chatfield, J. Fishman, P.J. Crutzen, and P.L. Hanst. 1978. Estimates on the production of CO and H_2 from the oxidation of hydrocarbon emissions from vegetation. Geophys. Res. Lett. 5:679-682.

A GEOGRAPHIC DATABASE FOR MODELLING THE ROLE OF THE BIOSPHERE IN CLIMATE CHANGE

WILLIAM G. CAMPBELL, DANNY MARKS,

NSI Technology Services Corp., Environmental Research Laboratory, US Environmental Protection Agency, Corvallis, Oregon

JOHN J. KINEMAN,

National Geophysical Data Center, National Oceanic and Atmospheric Administration, Boulder, Colorado

and

ROBERT T. LOZAR

Construction Engineering Research Laboratory, US Army Corps of Engineers, Champaign, Illinois

Abstract. Research into the effects of global climate change will require an integrated geographic database for landscape characterization, visualization, and modelling. An integrated, quality controlled, global environmental database. however, is not yet available. To answer this need, the US Environmental Protection Agency, in cooperation with National Oceanic and Atmospheric Administration's National Geophysical Data Center and the Army Corps of Engineers Construction Engineering Research Laboratory, is developing a global, quality controlled geographic database for use in regional, continental, and global modelling. This database will use an approach similar to that employed by the International Council of Scientific Union's Global Diskette Project for Africa. The database will use raster architecture for data storage and will rely on Geographic Information System technology for data access, retrieval, analysis, and output. Data access will not be tied, however, to any specific software package. Development of filters to reformat data will be actively encouraged. Although designed specifically for the EPA's Global Climate Research Program, the proposed database will, nevertheless, be available to the scientific community in general and should be particularly valuable for global and continental scale modelling.

1. Introduction

1.1. *Climate Change Research*

Increases in the atmospheric concentration of CO_2 and other greenhouse gases resulting from anthropogenic emissions are likely to alter forcing *functions that drive global climate, although uncertainties remain* regarding modelled distributions of temperature and precipitation (Dickinson, 1989; Schneider, 1989). Analyzing climate change effects will require a large scale interdisciplinary research effort and must include a coordinated research component for collecting and managing global data. To effectively analyze and model these large and complex datasets, flexible data management and analysis strategies need to be developed. This paper will present current efforts to develop global databases and tools for climate change research in association with the US Environmental Protection Agency's (EPA) Global Climate Research Program (GCRP). The GCRP is a large, interdisciplinary research effort designed to assess: 1) the role of the biosphere in climate, 2) the response of the biosphere to climate change, and 3) mitigative strategies related to management of the biosphere.

1.2. *Data Needs*

The research community has recognized the important role that geographic data play in assessing global change (ESRI, 1984; Rizzo, 1988; Tomlinson, 1988; Campbell *et al.*, 1989). To characterize the effects of climate change requires analysis of a wide variety of spatial data. This must include development of an integrated, quality controlled geographic database. The need for an integrated global database was addressed recently in the first meeting of the International Geographical Union's Global Database Planning Project (IGU, 1988). Tomlinson (1988), in his opening remarks at this meeting, stated "...there is a perceived need for geographical analysis and spatial data on a global scale". Similarly, the Committee on Earth Sciences (CES) has identified documentation of earth system change through observational programs and data management systems as the first integrating priority of the U.S. Global Change Research Program (CES, 1989).

Many different national and international organizations are currently involved in planning for or collecting data on a global scale, although these projects are in preliminary stages (e.g., International Geosphere-Biosphere Project, MINITOPO coordinated by the U.S. Defense Mapping Agency, etc.) and/or are designed to address specific needs such as the SOTAR (soils and terrain) working group (ISSS, 1986) and the World Digital Database for Environmental Sciences (Bickmore, 1988). Currently, a quality controlled, global geographic database for modelling does not yet exist, although some work has been done for individual continents (Kineman *et al.*, 1990) and ocean areas (Lozar, 1990).

A critical component of a global effects database must be Digital Elevation Models (DEMs). DEMs are a critical component because terrain structure largely controls energy balance and hydrologic response of the landscape as well as influencing the global distribution of vegetation. A geographic global effects database will play a key role in four general areas of research, including: 1) landscape characterization, 2) dynamic measurements, 3) surface generation, and 4) modelling.

1.2.1. *Landscape Characterization*

To properly characterize static components of the physical landscape, data on the distribution of soils, current vegetation/land cover, political/continental boundaries, terrain (elevation, slope, aspect), and geomorphic regions will be required. These data will be used to characterize the physical landscape, to determine the status and extent of resources, to provide information on the resources at risk, and to provide baseline information for models.

1.2.2. *Dynamic Measurements*

Information will be required on dynamic characteristics of the landscape, including temporal and spatial distributions of evapotranspiration, reflectance, albedo, soil moisture, and vegetative stress. Because of the need to characterize the temporal dynamics of large regions, remote sensing will be a critical element of the characterization efforts. These data will be used to assess the role of the biosphere in climate dynamics

as well as to assess potential effects of climate on the terrestrial components of the biosphere.

1.2.3. *Surface Generation*

New techniques will be developed to spatially distribute data from either point measurements or physically or empirically-based models. Information will be needed on the spatial and temporal patterns of precipitation, runoff, evapotranspiration, and temperature. These data will be used to: 1) estimate the spatial and temporal distributions of surface properties and their response to changing climate conditions, 2) measure the relative sensitivities of regions (biotic and/or physical) to changes in global climate, and 3) provide dynamic input to a variety of analytical procedures and predictive models.

1.2.4. *Modelling*

Much of the emphasis within climate effects research must be development and application of spatially distributed models, including models of regional energy balance, vegetation redistribution, and biogenic emissions. These models will require various types of data as inputs including measurements on static characteristics, dynamic surface properties, and generated surfaces. Future research efforts will require development and application of spatially distributed models at continental and global scales.

2. Data Requirements

2.1. *Spatial Data Handling Tools*

There are a variety of hardware and software options available for analyzing very large spatial datasets. We consider four primary options to be critical: 1) "open" or non-proprietary operating systems, 2) extensive use of "next generation" mass storage devices such as CD-ROMS and optical read/write disks, 3) ability to pre-process or filter data to conform to various format requirements, and 4) incorporation of Geographic Information System (GIS) technology for database access, retrieval, analysis, and output.

Reliance on non-proprietary operating systems (e.g., UNIX) dramatically increases flexibility of the proposed database by reducing the need to rely on a specific hardware vendor for accessing and analyzing the data. UNIX is also relatively hardware independent and is rapidly becoming the industry standard for workstations.

Next generation mass storage devices (e.g., CD-ROM) will be used as the primary distribution medium for the proposed database. Because of the cost efficiency of these devices, their use can significant increase the accessability and availability of large global databases to a wide variety of researchers. These devices are available for personal computers, workstations, as well as for mini-computer and mainframe environments. This technology has already been employed for geographic database management by the World Data Center-A in Boulder, CO under the auspices of the International Council of Scientific Unions (Allen, 1988; Clark and Kineman, 1988).

Development of filters to aid in the transference of data between various software packages will be critical. The emphasis on filters rather than "standard" software systems requires that "open" systems, particularly for input/output routines, must be actively encouraged. Systems with unknown or proprietary formats will be of limited use within this scheme. This "open" philosophy has several advantages over the use of a standard package including: 1) analyses can be application or need driven, 2) analyses can take advantage of the inherent strengths of particular software, and 3) the complexity of the chosen software can be varied depending on user expertise and complexity of application.

GIS will be required for database access, retrieval, analysis, and output. GIS have four essential components: 1) data input and verification, 2) data management, 3) data manipulation and analysis, and 4) data output (Aronoff, 1989). GIS are typically broken into two fundamental types depending on the method used to store spatial data. Raster systems (including hierarchical raster) store data as an array or hierarchical array of grid cells, while vector systems store data as a series of distinct spatial units called polygons (Burrough, 1986). Inherent strengths and limitations of these systems are listed in Table I. Because the basic

Table I Comparison of vector and raster systems

VECTOR

Advantages

- Good representation of phenomenological data structure
- Compact data structures
- Topology can be completely described with network linkages
- Accurate graphics
- Retrieval, updating and generalization of graphics and attributes are possible

Disadvantages

- Complex data structures
- Vertical aggregation of map layers creates difficulties
- Simulation is difficult because each unit has a different topological form
- Display and plotting can be expensive
- The technology is expensive
- Spatial analysis and filtering within polygons are impossible

RASTER

Advantages

- Simple data structures
- The combination of mapped data with remotely sensed data is easy
- Various kinds of spatial analysis are easy
- Simulation is easy because each spatial unit has the same size and shape
- The technology is cheap and is being energetically developed

Disadvantages

- Volumes of graphic data
- The use of large cells to reduce data volumes means that phenomenologically recognizable structures can be lost
- Crude raster maps are considerably less beautiful
- Network linkages are difficult to establish
- Projection transformation can be time consuming

(adapted from Burrough, 1986)

purpose of this proposed database is spatial modelling, raster will be the primary data type. Software that relies exclusively on the vector data structure will not be supported.

2.2. *Quality Assurance/Quality Control*

Quality assurance and quality control (QA/QC) for spatial data is in its infancy, particularly in GIS and spatial modelling environments (Chrisman, 1984; Burrough, 1986; Bailey, 1988; Goodchild, 1988; Campbell and Mortenson, 1989). Because analysis of spatial data and the application of spatial models do not lend themselves to classical QA/QC methodologies (e.g., replication), QA/QC must focus on identification and documentation of error associated with spatial data. At present, QA/QC of global and regional spatial data is very poor, with inadequate documentation and quality control, non-standard formats, and general inaccessibility.

In order to be a useful and viable component of global database efforts, QA/QC efforts must explicitly address defining, documenting, and tracking error and uncertainty of spatial data. The following elements must be addressed:

1) Research must be directed towards a basic understanding of errors associated with geographic analysis and spatial modelling. Although much work has been done with assessing and modelling errors associated with remotely sensed data, this effort must be expanded to spatial data in general.

2) Techniques must be developed that automate the tracking and/or documentation of spatial error through geographic processing and analysis. This must include consideration of the propagation of spatial error as it relates to overlay analysis and spatial modelling.

3) Procedures that will document and track error associated with entry of spatial data must be developed and/or refined. This is needed to better document or control errors resulting from digitization or scanning of base maps.

4) Documentation procedures for identifying error within spatial data, including tracking of map lineage, must be developed. This must include consideration of the spatial components of lineage, since global data will tend to be a horizontal integration of vastly different source materials.

5) Analogous methods to the scientific peer review process must be developed for review of spatial databases. This can include a network of research and test sites (including data centers, research institutions, U.S. and foreign agencies, universities, UN organizations, and others) to aid in evaluation and in developing data, systems, and methods.

Continuing research into the above-mentioned issues must be an integral research component within global database efforts, particularly because of the large reliance of the global change community on spatial data, geographic processing, and spatial modelling.

3. Database Development

3.1. *Approach*

The approach used in developing this database will consist of a series of steps, including:

1) Develop, in conjunction with other national and international data centers, a coherent, standardized, and quality controlled global environmental database of integrated regional and global data sets, including biotic, physiographic, hydrologic, edaphic, climatic, and other environmental factors derived from existing observations and remotely sensed data.

2) Develop, in conjunction with the database, appropriate analytical tools and methods for observational analysis and comparative studies of ecosystem and climate patterns.

3) Establish a peer review process and network for evaluation of the database and software development, and to ensure the scientific usefulness of these efforts in regard to the research needs of the global change science community.

4) Disseminate original datasets and various derivations as digital products for analysis, experimental design and modelling support.

5) Work closely with other groups to link the technology, data, and methods of spatial data analysis with research and applications, including theoretical/mathematical modelling.

6) Develop products for inclusion with the International Space Year and the International Geosphere-Biosphere Program.

3.2. *Cooperative Agencies/Roles*

Development of a geographic database will be a cooperative venture between three federal agencies: the U.S. Environmental Protection Agency's (EPA) Environmental Research Laboratory-Corvallis (ERL-C) in Corvallis, OR; the National Oceanic and Atmospheric Administration's (NOAA) National Geophysical Data Center (NGDC) in Boulder, CO; and the Army Corps of Engineers' (ACE) Construction Engineering Research Laboratory (CERL) in Champaign, IL. Data will be acquired, however, from a number of additional sources, including other federal agencies (particularly the US Geological Survey), cooperating universities, and national and international research centers.

Specific responsibilities of the three federal agencies (EPA, NOAA, and ACE) have been identified. The EPA, as the lead agency within the GCRP, will be responsible for program and project management and addressing the scientific questions regarding the role of the biosphere in climate change. Additionally, the EPA will provide direction on data requirements, geographic coverage priorities, and tool development. The NGDC will be responsible for global data management, analysis of status and trends of ecological resources, landscape characterization and visualization, and development of specialized data handling tools. Additionally, NGDC's

extensive contacts with other federal agencies and international research centers will form a bridge between the EPA and other organizations involved in global data collection. CERL is the developer of the GRASS Geographic Information System (ACE, 1988) and will be utilized for software development, including integration of spatially distributed models into the GIS environment, development of analytical tools within GRASS, and global data management activities. The three agencies will also perform cooperative research in a number of areas related to global data, including the development of quality assurance and quality control mechanisms, characterization and visualization techniques, spatial statistical techniques, and data management strategies related to spatial modelling.

3.3. *North American Prototype*

A North American prototype will be scheduled for immediate development, windowing existing databases from NGDC's existing global database and using a similar approach to that employed in the International Council of Scientific Union's Global Change Diskette Project for Africa (Kineman *et al.*, 1990). A detailed listing of the North American prototype database is presented in Table II.

4. Applications

The GCRP is using geographic data for a variety of analytical procedures and predictive models related to assessing the role of the biosphere in climate change. The following examples show the role geographic data play in analyzing and modelling these environmental data.

4.1. *Landscape Characterization*

Landscape characterization involves parameterizing static components of the landscape. To assess the role of terrain structure in controlling or influencing climate change, we have characterized the distributions of elevations across the continental U.S. using DEMs (Figure 1). The DEM data was overlaid with water resources regions obtained from the US Geological Survey (Figure 2 - USGS, 1978). Following overlay, hypsometric curves depicting the distributions of elevations were

Table II North American Prototype Database

Data	Resolution	Source
Monthly vegetation index for 1985 through 1988	10 minute	NOAA, 1990
Monthly temperature and precipitation anomalies	- - - -	UNEP, 1990
Average monthly temperature and precipitation	30 minute	Legates and Willmott, 1990
Monthly skin temperatures	10 minute	GSFC, 1979
Topography	10 minute	Kineman, 1989a
Percent water and urban cover	10 minute	Kineman, 1989b
Vegetation and reliability classes, soil classifications	1 degree	Wilson and Henderson-Sellers, 1985
Vegetation classes and albedo	1 degree	Matthews, 1983
Cultivation Intensity	1 degree	Matthews, 1983
Ecosystem classifications	30 minute	Olson *et al.*, 1983
Soil classifications	1 degree	Staub and Rosenzweig, 1987
Soil classifications	2 minute	UNESCO, 1973
Geographic and political boundaries	10 minute	CIA, 1990

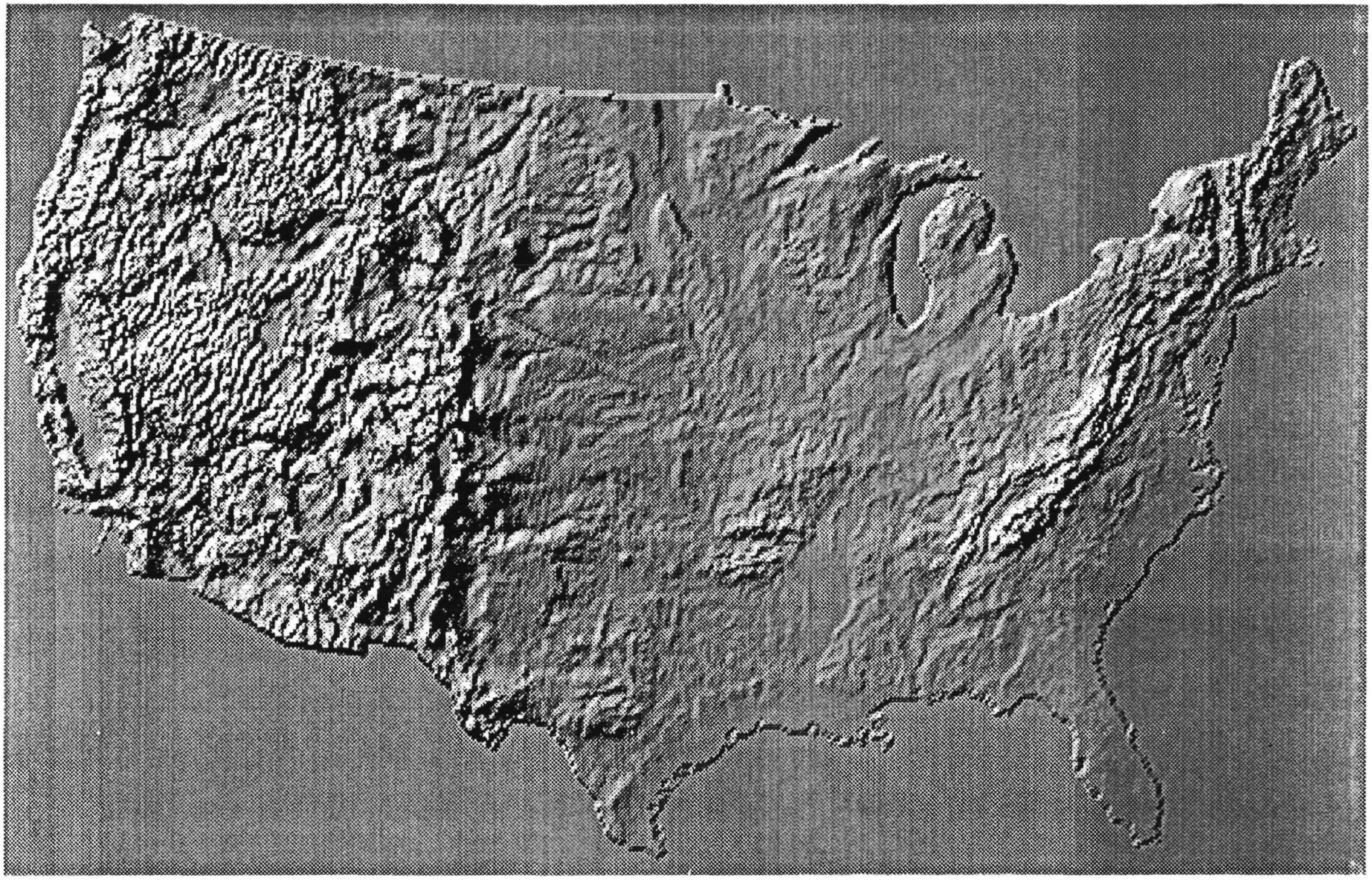

Fig. 1. Digital Elevation Model at 10 km resolution for the continental United States.

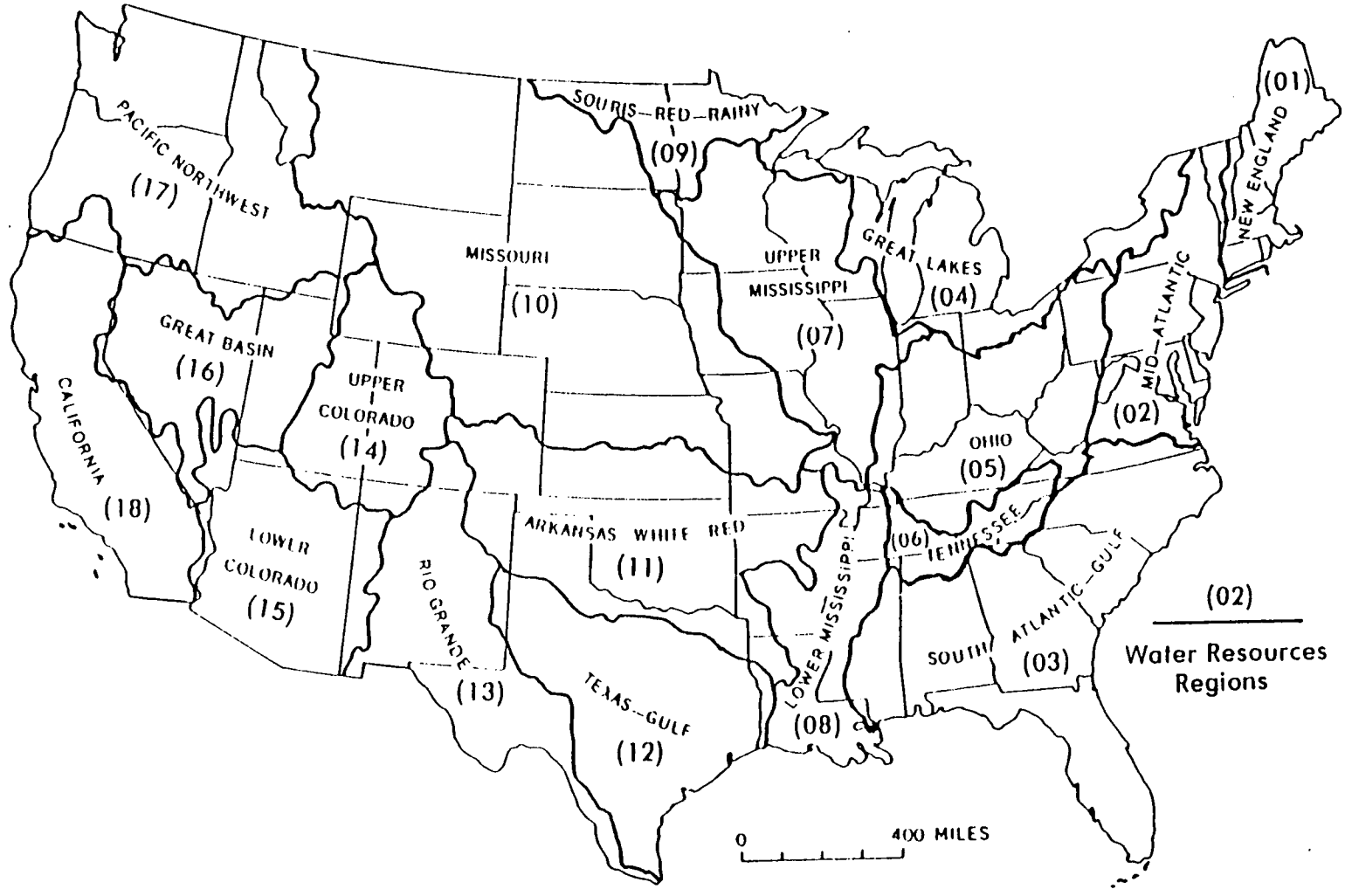

Fig. 2. Water resource regions for the continental United States.

generated for water resources regions and subregions (Figure 3). This data is being used in a quantitative analysis of the role of terrain structure on the surface energy balance and potential sensitivity of the landscape to climate change (see Chapter IX).

4.2. *Dynamic Measurements*

Measurements that characterize the dynamic properties of the landscape are required to assess the spatial and temporal changes in evapotranspiration, reflectance, albedo, soil moisture, and vegetative stress. To assess dynamic changes in vegetation over the globe, we have obtained information on the Global Vegetation Index (GVI - NOAA, 1990) formatted for use in the GRASS GIS (Figures 4 and 5). Empirical relationships between GVI and foliar biomass are being used to produce estimates of the temporal and spatial dynamics of estimated biomass for input to models predicting non-methane hydrocarbon emissions.

4.3. *Surface Generation*

Techniques to distribute measurements taken at a point in space (e.g., runoff, precipitation) over large geographic regions are being developed to analyze the spatial dynamics of selected variables and to provide input for spatially distributed models. In particular, distributed estimates of runoff and precipitation are required for areas ranging in size from large water resource regions (50,000 - 500,000 sq. km) to continental and global scales. This will include application of existing techniques (e.g., kriging) to larger areas to development and application of new techniques, such as spatially distributed modelling and artificial intelligence.

To assess the spatial and temporal dynamics of rainfall and runoff over large land areas, we have used historical data on precipitation (Quinlan *et al.*, 1987) and runoff (Wallace *et al.*, 1990) and distributed these measurements over the continental U.S. using an inverse distance algorithm. Figure 6 shows the long-term (1948-1988) average annual precipitation and runoff. The resulting data is being used in a preliminary analysis of the adequacy of the historical record for defining a distribution function of precipitation at the continental scale (Dolph, 1990; see also Chapter IV).

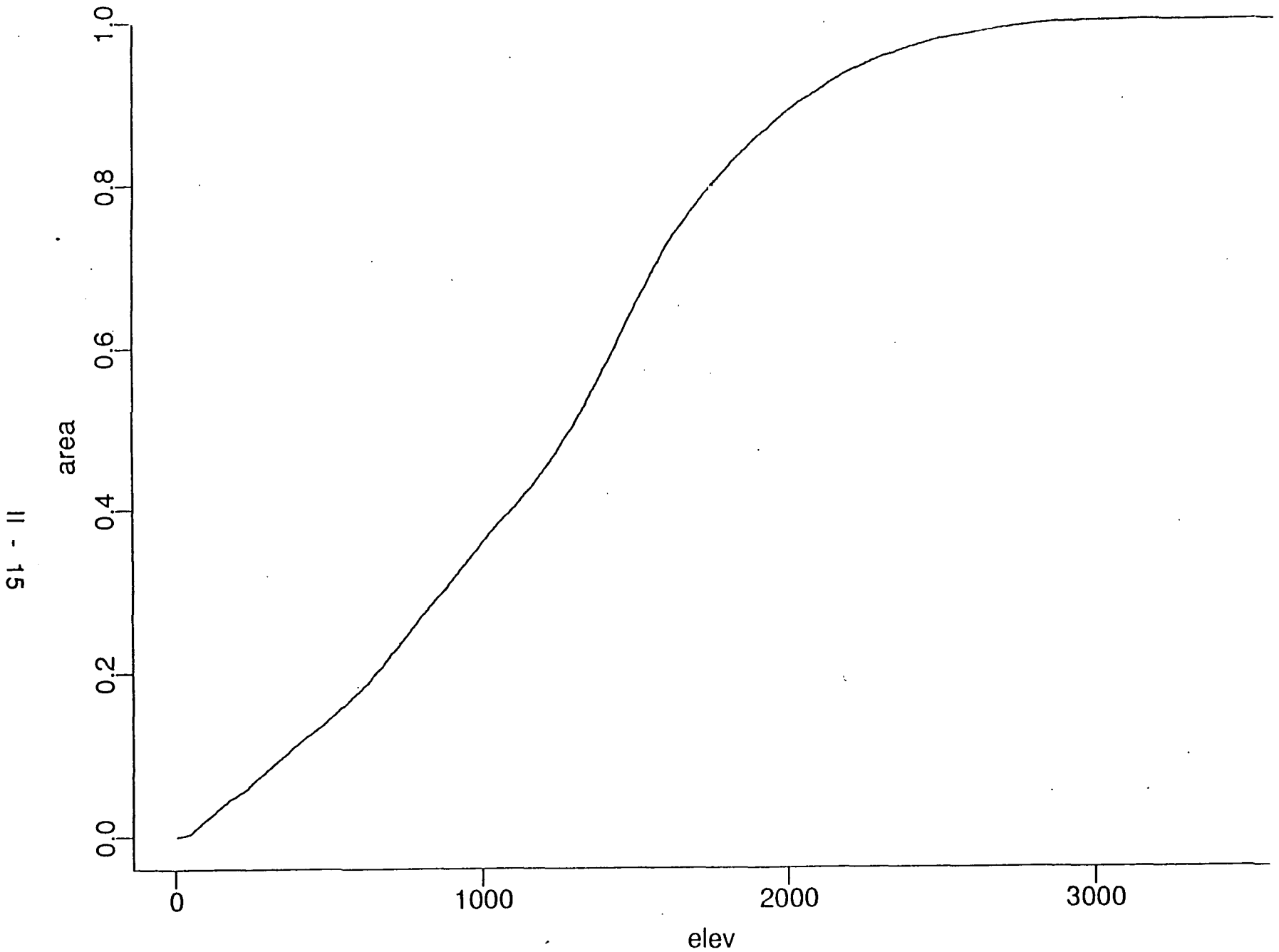

Fig. 3. Hypsometric integral for the Pacific Northwest water resource region.

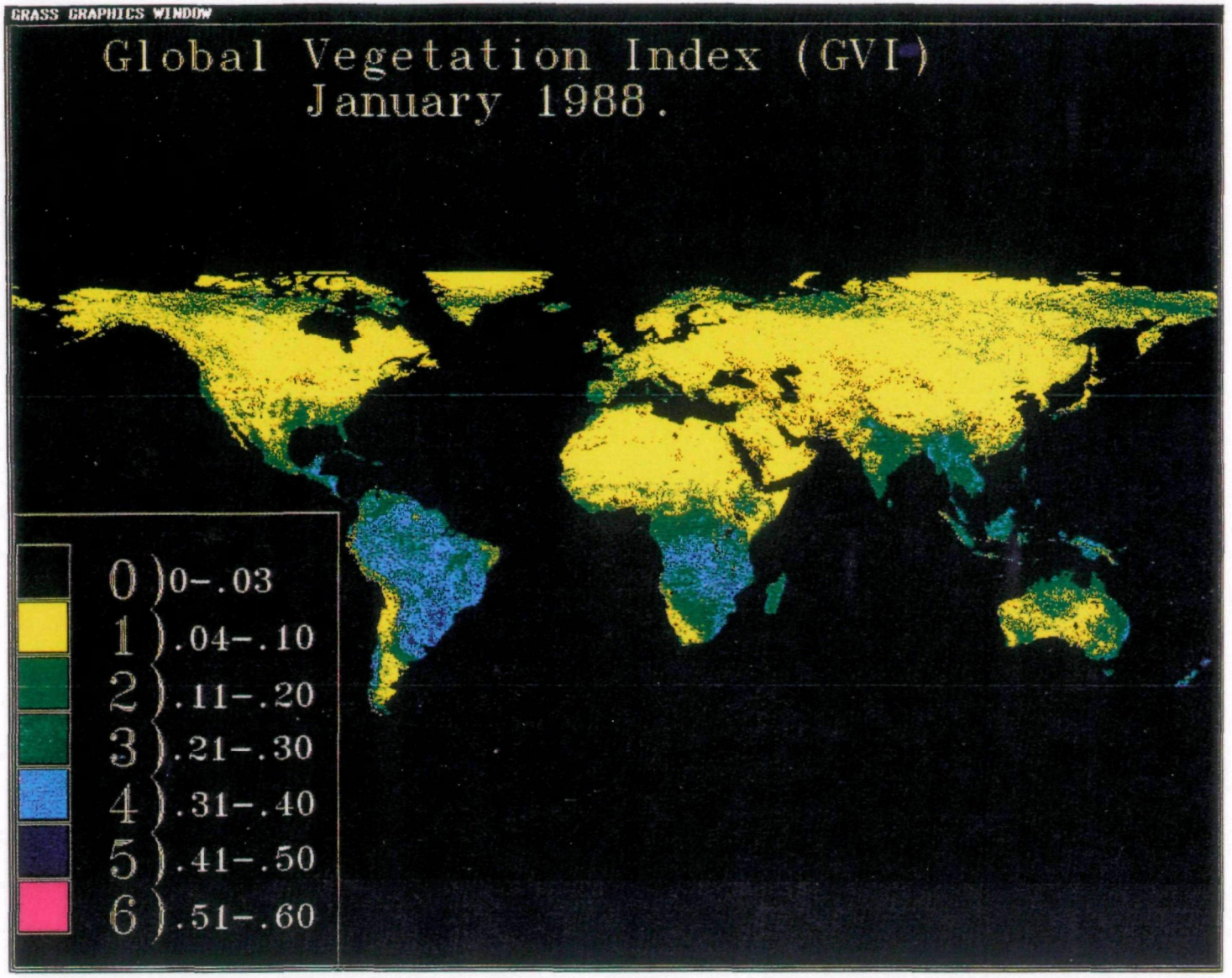

Fig. 4. Global Vegetation Index for January, 1988 (see also Chapter IX).

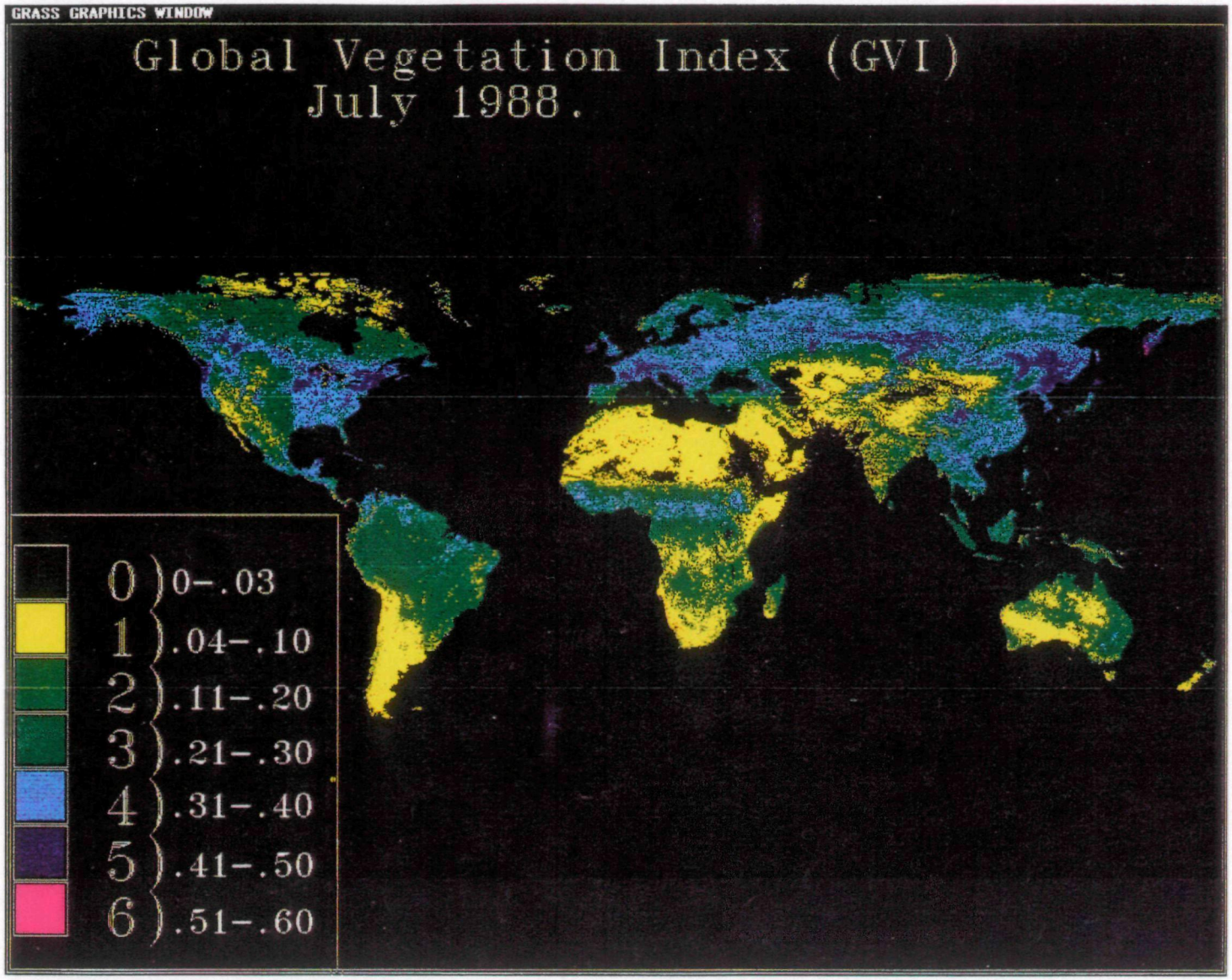

Fig. 5. Global Vegetation Index for July, 1988 (see also Chapter IX).

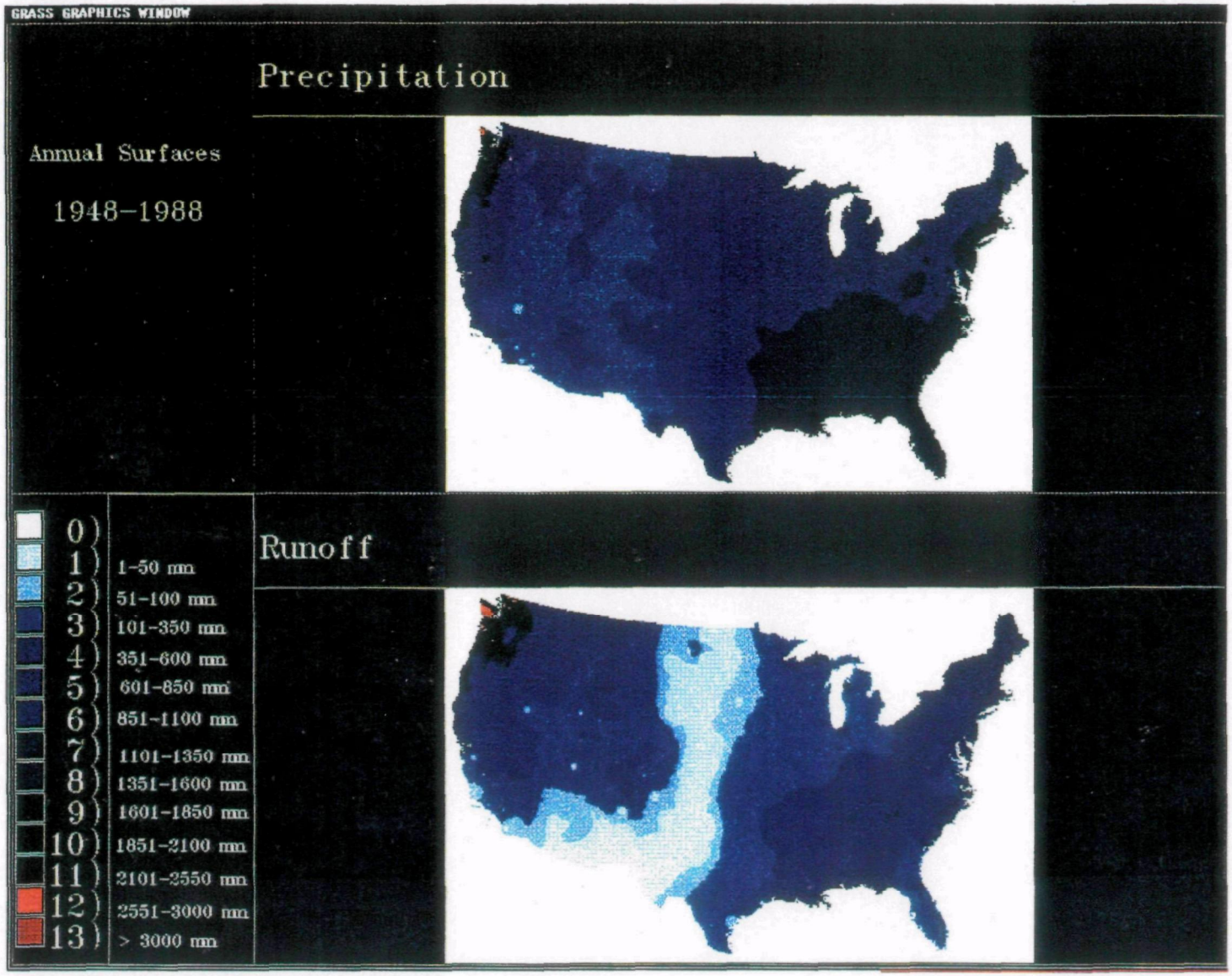

Fig. 6. Long-term (1948-1988) average annual precipitation and runoff surfaces for the continental United States (from Dolph, 1990; see also Chapter IV).

In addition to analyzing these data using simple interpolation techniques, we are also investigating the application of spatial statistical techniques to large areas. Phillips *et al.* (1990; see also Chapter V) investigated the application of three spatial statistical techniques for estimating the distribution of precipitation across the Willamette Valley in Western Oregon. The three techniques were (1) kriging, (2) kriging elevation-detrended data, and (3) cokriging with elevation as an auxiliary variable. Both detrended kriging and co-kriging showed improved estimates of precipitation when compared to simple kriging. The distribution of precipitation over the Willamette Valley using co-kriging is depicted in Figure 7.

4.4. *Modelling*

GIS provides a unique tool for modelling of spatial data, primarily through the development and application of spatially distributed modelling for energy and water balance, biogenic emissions, and vegetation redistribution. Marks (1990; see also Chapter III) has applied a spatially distributed turbulent transfer model to estimate the surface energy balance across the continental U.S. Critical inputs include Digital Elevation Models (e.g., see Figure 1), temperature, wind, and humidity. To create spatially distributed estimates of temperature, long-term monthly estimates were obtained from the Historical Climatological Network (Quinlan *et al.*, 1987). These data were then converted to potential temperatures (1000 mb surface), interpolated across the continental U.S. using an inverse-distance algorithm, and then re-mapped onto the DEM grid (Figure 8). The resulting temperature surface more accurately reflects the distribution of elevation across the U.S. than a simple interpolation scheme. This data can then be combined with distributed estimates of terrain structure, wind fields, and humidity, to provide model input for estimating Potential Evapotranspiration (Figure 9).

5. Discussion

An important consideration in designing a long-term plan for management and analysis of geographic data is the ability to adapt to new technology and adjust for future growth, in terms of data, hardware, and software.

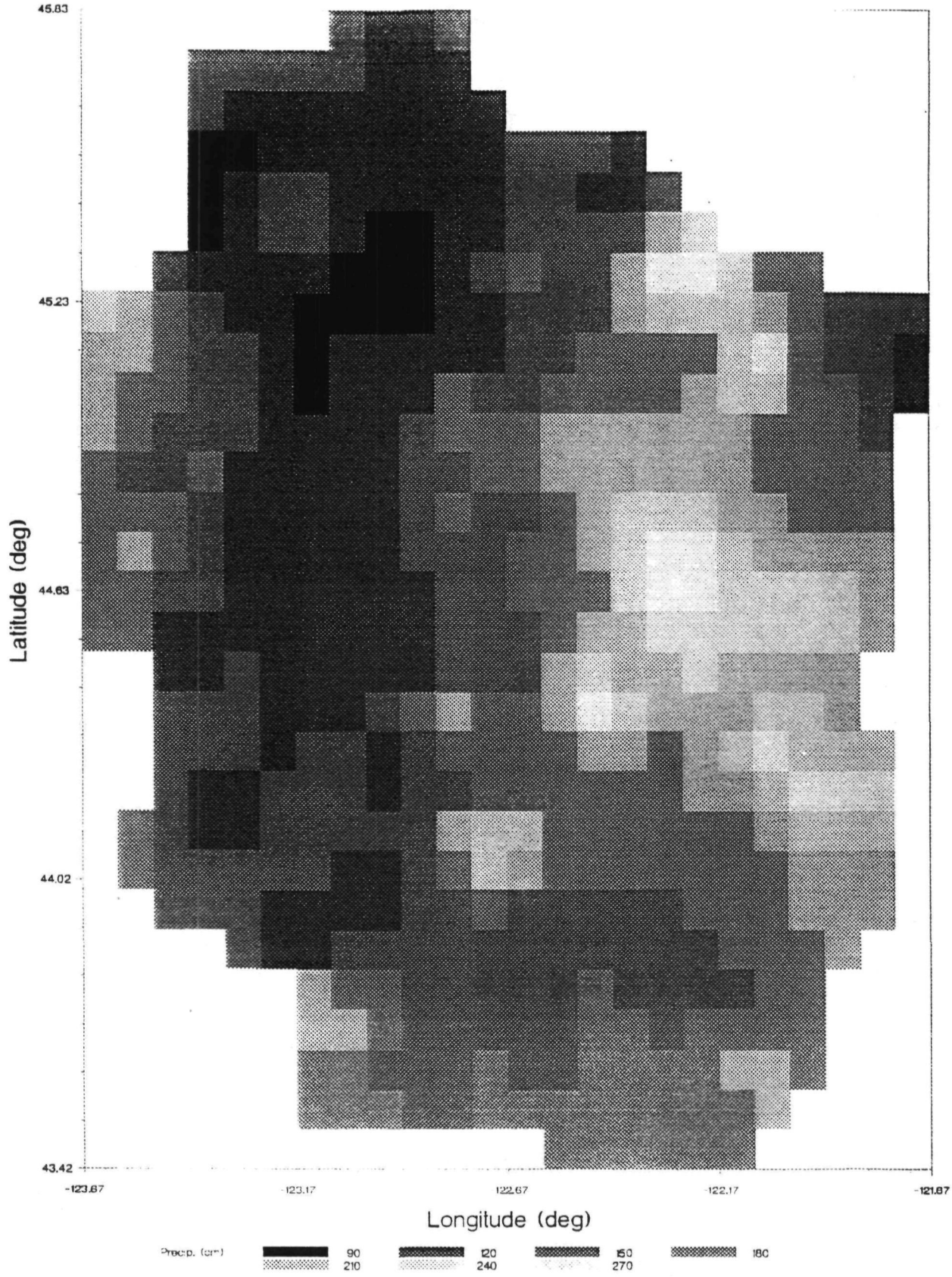

Fig. 7. Estimates of precipitation for the Willamette Valley, OR using cokriging (from Phillips *et al.*, 1990; see also Chapter V).

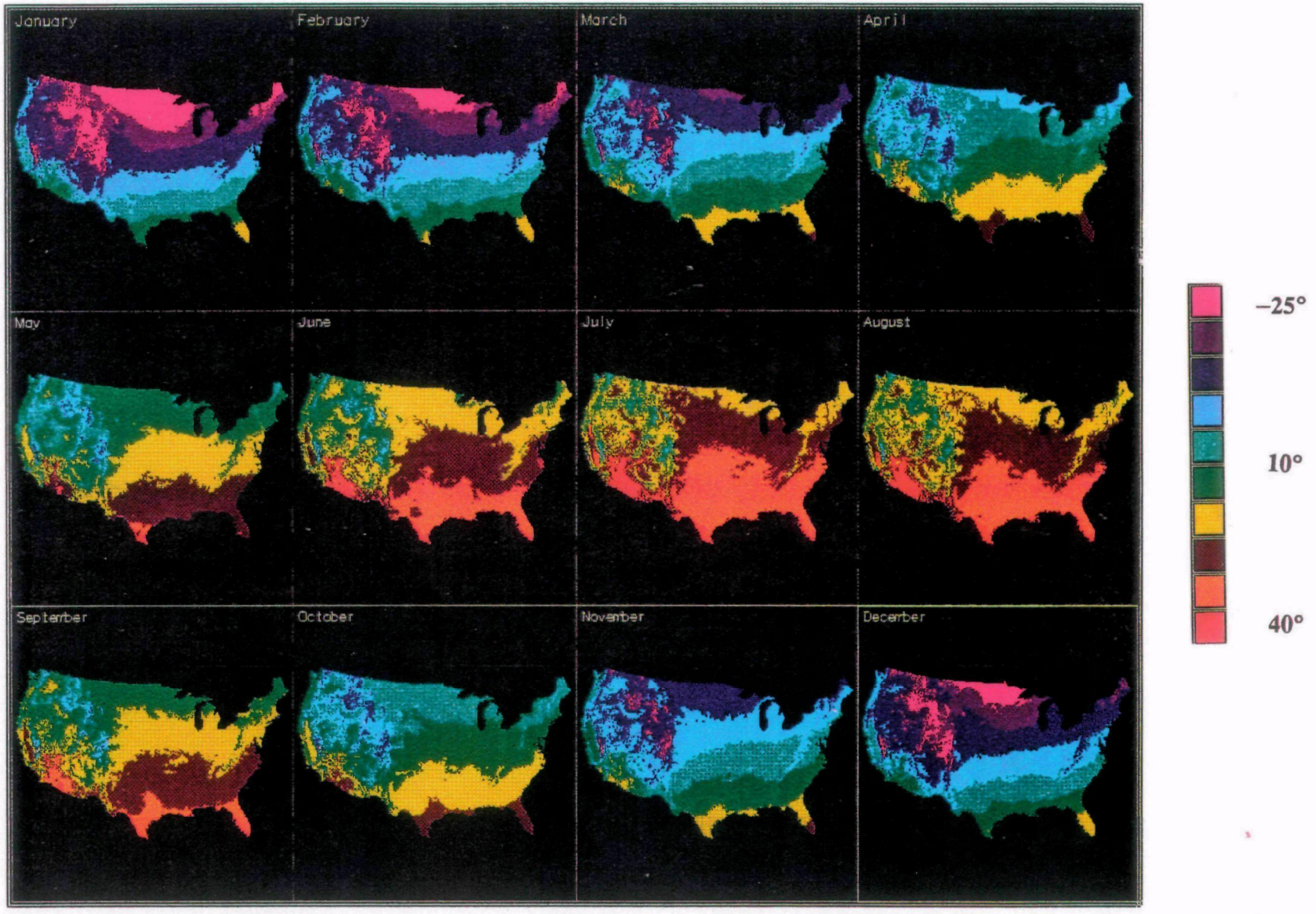

Fig. 8. Monthly air temperature for the continental United States (from Marks, 1990; see also Chapter III).

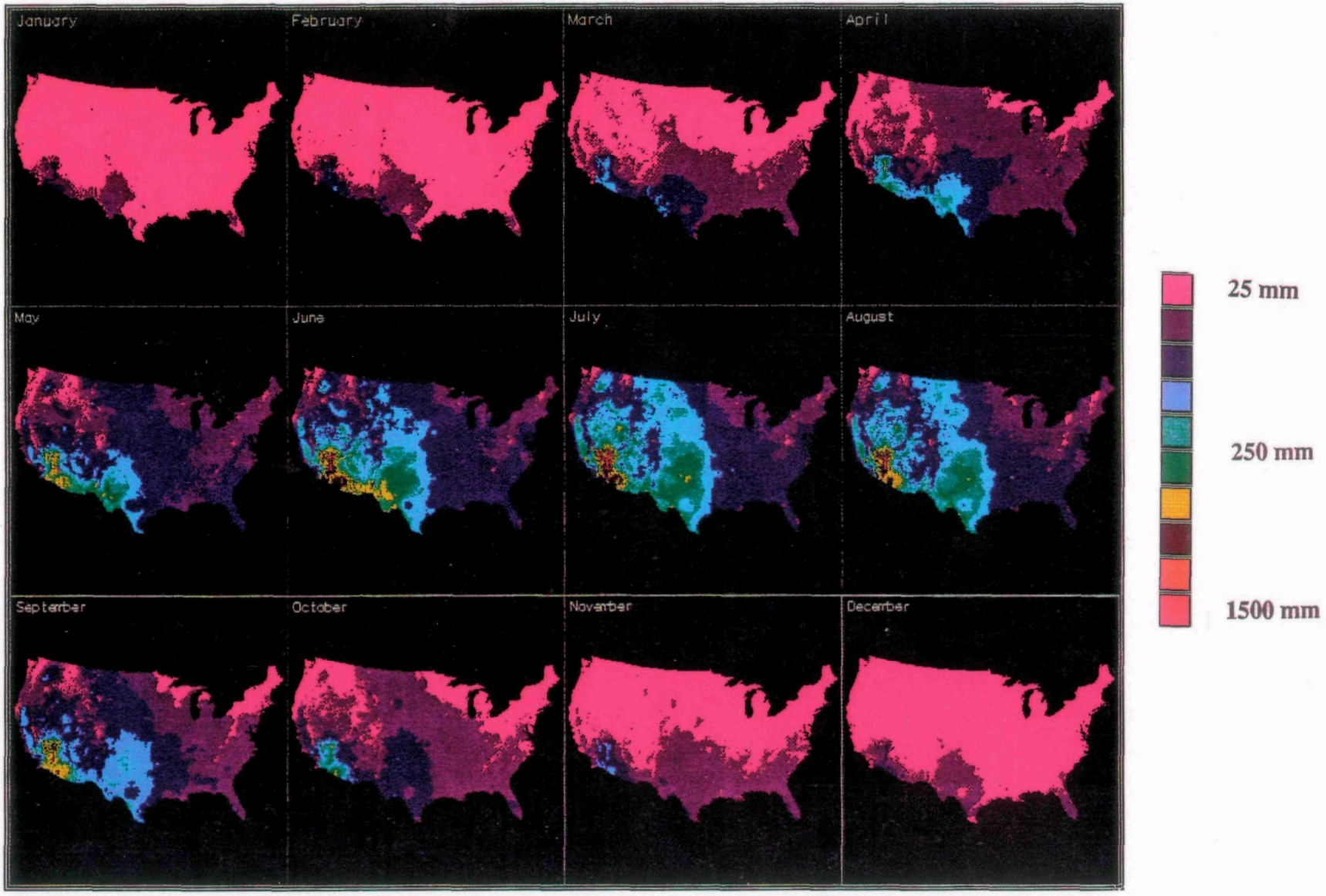

Fig. 9. Monthly Potential Evapotranspiration for the continental United States (from Marks, 1990; see also Chapter III).

Two general developments will guide the incorporation of new data. First, given the long timeframe of the global effects research, newer and better data will likely become available and can be added to the existing database. This will include data with better geographic coverage, and increasing spatial and temporal resolution. Secondly, given the large increases in the capabilities of workstations to effectively handle large, CPU-intensive applications, it is likely that future analyses and modelling will be able to more effectively handle applications such as fine resolution spatially distributed modelling and analysis of medium resolution remotely sensed imagery on a global scale. The reliance on open architecture should allow better adaptation to new technology.

Future software development efforts are likely to focus on two general areas. First, better analytical methods are needed for analyzing data in the spatial domain. Although GIS technology has increased the importance of spatial data in environmental analysis, much of the previous work has been in data management and cartographic applications, rather than spatial analysis and modelling. The specific needs of the GCRP require that better analytical tools be added to the list of current GIS capabilities, including but not limited to spatial statistical techniques, spatial and statistical queries, surface generation tools, and spatial modelling in the GIS domain. A second general area of development is system integration and/or filter development. Because of the complex problems facing researchers in the global arena, researchers must be able to draw on a variety of tools and software rather than be constrained by individual vendors and software packages. This emphasis on flexibility will aid in the analysis on climate change effects by focusing on the application while reducing software limitations.

References

ACE: 1988, *GRASS Users and Programmers Manual*, US Army Corps of Engineers Construction Engineering Research Laboratory, Champaign, IL.

Allen, J.H.: 1988, 'The World Data Center System, International Data Exchange and Global Change', in H. Mounsey and R. Tomlinson (eds.), *Building Databases for Global Science*, Taylor and Francis, Philadelphia, pp. 138-152.

Aronoff, S.: 1989, *Geographic Information Systems: A Management Perspective*, WDL Publications, Ottawa.

Bailey, R.G.: 1988, 'Problems with using Overlay Mapping for Planning and their Implications for Geographic Information Systems', *Environmental Management* **12**, 11-17.

Bickmore, D.P.: 1988, 'World Digital Database for Environmental Sciences (WDDES)', in H. Mounsey and R. Tomlinson (eds.), *Building Databases for Global Science*, Taylor and Francis, Philadelphia, pp. 181-191.

Burrough, P.A.: 1986, *Principals of Geographical Information Systems for Land Resources Assessment*, Clarendon Press, Oxford.

Campbell, W.G., Church, M.R., Bishop G.D., Mortenson, D.C., and Pierson, S.M.: 1989, 'The Role for a Geographical Information System in a Large Environmental Project', *International Journal of Geographical Information Systems* **3**, 349-362.

Campbell, W.G., and Mortenson, D.C.: 1989, 'Ensuring the Quality of Geographic Information System Data: A Practical Application of Quality Control', *Photogrammetric Engineering and Remote Sensing* **55**, 1613-1618.

CES: 1989, *Our Changing Planet: The FY 1990 Research Plan. The U.S. Global Change Research Program*, Committee on Earth Sciences, Executive Office of the President, Washington, DC.

CIA: 1990, *World Data Bank - II*, Central Intelligence Agency, National Technical Information Service, Washington, DC.

Chrisman, N.R.: 1984, 'The Role of Quality Information in the Long-term Functioning of a Geographic Information System', *Cartographica* **21**, 79-87.

Clark, D.M., and Kineman, J.J.: 1988, 'Global Databases: A NOAA Experience', in H. Mounsey and R. Tomlinson (eds.), *Building Databases for Global Science*, Taylor and Francis, Philadelphia, pp. 216-232.

Dickinson, R.E.: 1989, 'Uncertainties of Estimates of Climate Change', *Climatic Change* **15**, 5-13.

Dolph, J.E.: 1990, 'Characterizing the Distribution of Precipitation and Runoff over the Continental United States using Historical Data', *Journal of Geophysical Research* (submitted).

ESRI: 1984, 'Map of Desertification Hazards', in *Geographic Information Systems for Resource Management: A Compendium*, American Society for Photogrammetry and Remote Sensing, Falls Church, VA.

GSFC: 1979, *Skin Surface Temperature (SST) Data from HIRS2/MSU for 1979*, Goddard Space Flight Center, Greenbelt, MD.

Goodchild, M.F.: 1988, 'The Issue of Accuracy in Global Databases', in H. Mounsey and R. Tomlinson (eds.), *Building Databases for Global Science*, Taylor and Francis, Philadelphia, pp. 31-48.

IGU: 1988, *Building Databases for Global Science*, H. Mounsey and R. Tomlinson (eds.), Taylor and Francis, Philadelphia.

ISSS: 1986, *World Soils and Terrain Digital Database at a Scale 1:1M*, International Society of Soil Scientists, Wageningen, The Netherlands.

Kineman, J.J.: 1989a, *Improved USNAVY/NCAR Global 10 Minute Terrain Dataset in Image Format*, National Geophysical Data Center, Boulder, CO.

Kineman, J.J.: 1989b, *NOAA Monthly Vegetation Imagery on a 10 Minute Grid*, National Geophysical Data Center, Boulder, CO.

Kineman, J.J., Clark, D.M., and Croze, H.: 1990, 'Data Integration and Modelling for Global Change: An International Experiment', in *Proceedings of the International Conference and Workshop on Global Natural Resource Monitoring and Assessments: Preparing for the 21st Century*, Venice, Italy.

Legates, D.R., and Willmott, C.J.: 1989, *Global Surface Air Temperature and Precipitation, Long-period Grid Means*, National Center for Atmospheric Research, Boulder, CO.

Lozar, R.C.: 1990, 'CERL's Global Modelling Capability', presented at the North American NOAA Polar Orbiter User's Meeting, Washington, DC.

Marks, D.: 1990, 'The Sensitivity of Potential Evapotranspiration to Climate Change over the Continental United States', *Journal of Geophysical Research* (submitted).

Matthews, E.: 1983, 'Global Vegetation and Land Use: New High Resolution Data Bases for Climate Studies', *Journal of Climatology and Applied Meteorology* **22**, 474-487.

NOAA: 1990, *Global Vegetation Index User's Guide*, ed. K.B. Kidwell, National Oceanic and Atmospheric Administration, Washington, DC.

Olson, J.S., Watts, J.A., and Allison, L.J.: 1983, 'Carbon in Live Vegetation of Major World Ecosystems', *Environmental Sciences Division Publication No. 1997*, Oak Ridge National Laboratory, Oak Ridge, TN.

Phillips, D.L., Dolph, J.E., and Marks, D.: 1990, 'Evaluation of Geostatistical Procedures for Spatial Analysis of Precipitation', *Water Resources Research* (submitted).

Quinlan, F.T., Karl, T.R., and Williams, C.N.: 1987, *United States Historical Climatology Network Serial Temperature and Precipitation Data*, US

Department of Energy, Carbon Dioxide Information Analysis Center, Oak Ridge, TN.

Rizzo, B.: 1988, 'The Sensitivity of Canada's Ecosystems to Climatic Change', *Newsletter of the Canada Committee on Ecological Land Classification* **17**, 10-12.

Schneider, S.H.: 1989, 'The Greenhouse Effect: Science and Policy', *Science* **247**, 771-781.

Staub, B., and Rosenzweig, C.: 1987, *Global Digital Data Sets of Soil Type, Soil Texture, Surface Slope, and other Properties*, National Center for Atmospheric Research, Boulder, CO.

Tomlinson, R.: 1988, 'Opening Remarks', in H. Mounsey and R. Tomlinson (eds.), *Building Databases for Global Science*, Taylor and Francis, Philadelphia, pp. 1-9.

UNEP: 1990, *Monthly Temperature and Precipitation Anomalies for 1987 through 1988*, United Nations Environment Programme, Global Resource Information Database, Geneva, Switzerland.

UNESCO: 1973, *UNESCO/FAO Soil Map of the World.* United Nations Environment Programme, Global Resource Information Database, Geneva, Switzerland.

USGS: 1978, *The Nations Water Resources 1975-2000*, US Geological Survey, Washington, DC.

Wallace, J.R., Lettenmaier, D.P., and Wood, E.F.: 1990, 'A Daily Hydroclimatological Data Set for the Continental United States',*Water Resources Research* (submitted).

Wilson, M.F., and Henderson-Sellers, A.: 1985, 'A Global Archive of Land Cover and Soils Data for use in General Circulation Models', *Journal of Climatology* **5**, 119-143.

A Continental-Scale Simulation of Potential Evapotranspiration for Historical and Projected Doubled-CO_2 Climate Conditions

DANNY MARKS

NSI Technology Services, Inc.

U.S. Environmental Protection Agency,
Environmental Research Laboratory
200 S.W. 35th St.,
Corvallis, OR 97330,
(503) 757-4657;

TABLE OF CONTENTS

LIST OF FIGURES

A Continental-Scale Simulation of Potential Evapotranspiration for Historical and Projected Doubled CO_2 Climate Conditions

DANNY MARKS

NSI Technology Services, Inc.

U.S. Environmental Protection Agency,
Environmental Research Laboratory
200 S.W. 35th St.,
Corvallis, OR 97330,
(503) 757-4657;

ABSTRACT

Potential evapotranspiration $E_{T,P}$ was calculated over the continental U.S. for current climate conditions and for predicted conditions for a doubled CO_2 climate, using a turbulent transfer model presented by *Marks* [1988]. The simulation was done over a grid of 138,650 geographically referenced points representing a digital elevation model (DEM) of the U.S. at 10 km spacing. Data for air temperature T_a, vapor pressure e_a, and wind speed at 10 m above the surface u, were corrected for topographic effects, and used to generate surfaces at the same 10 km resolution. These surfaces represent a long-term average monthly time-series for the period between 1948-88. Relative changes in these parameters were estimated from $2\times CO_2$ scenarios from the GFDL and GISS GCMs. $E_{T,P}$ surfaces were calculated for both current and $2\times CO_2$ conditions.

The $E_{T,P}$ surface for current conditions shows evaporative stress maximized in the western U.S. in summer. This is significantly different from $E_{T,P}$ estimated from a *Thornthwaite* [1948] temperature-regression method which incorrectly shows evaporative stress maximized in the southeastern U.S. Both GCMs predict increases in wind, temperature, and humidity. The GFDL model predicts drier, windier conditions than the GISS model, and shows $E_{T,P}$ as very high in summer in the mid-western U.S. The GISS model predicts moister but less windy conditions, and also shows a modest increase in $E_{T,P}$ in the mid-western U.S. This analysis illustrates the importance of physically based estimates of evaporative stress for climate change analysis. It also shows that it is possible to evaluate the sensitivity of surface processes, such as $E_{T,P}$ at resolutions which are ecologically meaningful.

1. INTRODUCTION

Projected changes in the global climate driven by increases in atmospheric CO_2, indicate a significant change may occur in climatic conditions during the next 50 to 100 years [*Keeling*, 1973; *Manabe and Wetherald*, 1975, 1980; *Keeling and Bacastow*, 1977; *Thompson and Schneider*, 1982; *Ramanathan, et al.*, 1985; *Dickinson and Cicerone*, 1986; *Broecker*, 1987; *Hansen, et al.*, 1988]. This would affect the terrestrial biosphere through changes in the regional energy balance [*Dickinson*, 1983] which would alter the regional water cycle [*Strain*, 1985; *Eagleson*, 1978, 1982, 1986; *Lettenmaier and Burges*, 1978; *Lettenmaier and Gan*, 1990; *Lettenmaier and Sheer*, 1991; *Smith and Tirpak*, 1989], and have a profound effect on vegetation distribution [*Holdridge*, 1947; *Mather and Yoshioka*, 1968; *Botkin, et al.*, 1972; *Shugart and West*, 1977; *Solomon*, 1986] and condition [*Perrier*, 1982; *Gates*, 1983; *Eagleson and Segarra*, 1985]. Feedbacks between vegetation and climate, described in detail by *Hansen, et al.* [1984], *Dickinson and Hanson* [1984], and *Rind* [1984], would influence both the magnitude and timing of climate change by altering the surface albedo and radiation balance, soil moisture storage, evapotranspiration, and the water balance. Evapotranspiration, E_T, is the link between terrestrial hydrology, vegetation, and the climate system.

E_T is the combination of direct evaporation from the surface and transpiration from vegetation. They are combined because, for practical purposes, it is difficult to separate them in a natural environment. Direct evaporation from the soil is usually only a small percentage of total water loss [*Kramer*, 1983], while E_T has been estimated to be 50% or more of the annual precipitation at continental to global scales [*Budyko*, 1974; *Baumgartner and Reichel*, 1975; *Korzoun, et al.*, 1977; *Brutsaert*, 1986]. These studies of large-scale evapotranspiration have estimated E_T from regression relationships between air temperatures and measured evaporative loss [see, for example *Thornthwaite*, 1948; *Holdridge*, 1967; *Mather and Yoshioka*, 1968; *Budyko*, 1974; *Whittaker*, 1975; *Eagleman*, 1976; *Woodward*, 1987; *Stephenson*, 1989]. The limitations of this approach are pointed out by *Larcher* [1980], who notes that plants respond to solar radiation, humidity, temperature, wind, and soil moisture. Any of these can provide the stress to close the stomata and eliminate or reduce transpiration. An estimate of evaporative stress based solely on air temperature assumes that air temperature is functionally related to all of these other parameters, and is thus an effective surrogate for their interaction. Over a heterogeneous region, there are a multitude of combinations of humidity and wind which can occur at a given temperature. Under these conditions, evaporative stress is not adequately specified by air temperature.

This experiment is aimed at regional to continental scale analysis of evaporative stress. In this context, a region in the U.S. is on the order of one of the U.S.G.S. Hydrologic Regions, such as the Great Basin, the Upper Colorado, or the Missouri. This is an area the size of several states, or about a million km^2. At these regional scales, E_T has a strong influence on precipitation. *Shukla and Mintz* [1982] state that evaporation will influence local precipitation, but that this effect will vary regionally. Early estimates of the portion of regional precipitation derived directly from regional E_T were as little as 10-15% [e.g.: *Benton, et al.*, 1950; *Budyko and Drozdov*, 1953] but *Lettau, et al.*, [1979] reported as much as 71% of the precipitation in the Amazon basin is from local E_T, and *Salati and Vose*, [1984] estimated 48% of Amazon

basin E_T becomes local precipitation. An improved understanding of the current distribution and magnitude of E_T is needed to evaluate how its distribution and magnitude might be altered under projected $2\times CO_2$ climates.

Potential evapotranspiration $E_{T,P}$ is the atmospheric demand for water. $E_{T,P} = E_T$ over water, snow, or a moist vegetated surface; in most natural environments E_T is less than $E_{T,P}$. Thus $E_{T,P}$ can be used to estimate water stress or drought by determining the precipitation (P) excess or deficit, from the evaporative demand: $P - E_{T,P}$.

Rind, et al., [1990] used a variation of the Palmer drought severity index (*PDSI*) [*Palmer*, 1965], called the supply and demand drought index (*SDDI*), with climatic conditions from the GISS GCM to show how drought conditions are likely to increase during the next 50 years. Their analysis was carefully done, but at the very coarse resolution of the GISS GCM (7.83°×10°); it is very difficult to evaluate how increased $E_{T,P}$ will affect regional ecosystems, all of which occur at sub-grid resolution.

In this study, the distribution of $E_{T,P}$ is evaluated over the continental U.S. at a spatial resolution of 10 km, which accounts for the effects of topography at continental or regional scales, and for regions or ecosystems as small as 100 km^2. An aerodynamic turbulent transfer model, presented by *Marks* [1988] and *Marks and Dozier* [submitted] to calculate energy and mass flux from a snow cover was modified to accept geographically distributed input data to calculate $E_{T,P}$ over large regions. Historical data from a 30 to 40 year period between 1948 to 1988 for the U.S. were used for the analysis. Air temperature T_a, vapor pressure e_a, and wind speed u were aggregated into long-term monthly averages, corrected for elevation effects using methods detailed below, and interpolated to a 10 *km* grid over the continental U.S. These distribution surfaces are used as input to the turbulent transfer model to calculate a monthly time-series of $E_{T,P}$ for current, or $1\times CO_2$ conditions.

T_a, e_a, and u data from two GCMs (GISS and GFDL) † for both 1×- and $2\times CO_2$ runs of are converted to change ratios ΔR:

$$\Delta R = \frac{2\times CO_2}{1\times CO_2} \tag{1}$$

The ΔR values are interpolated, using an inverse distance squared method [*Isaaks and Srivastava*, 1989] to the same 10 *km* grid to form a change distribution surface. These are used to modify the T_a, e_a, and u distribution surfaces generated from the historical data to approximate the $2\times CO_2$ distribution surface, and to calculate a predicted $E_{T,P}$ distribution surface time-series for $2\times CO_2$ for both GCM predicted conditions. This experiment shows how GCM scenarios can be better integrated into known distributions of properties and processes at spatial resolutions which are fine enough to provide ecologically significant

†: Data from the GISS and GFDL GCMs were selected because they included air temperature, wind and humidity, and among the GCM scenarios from the group developed for the EPA report *The Potential Effects of Global Climate Change on the United States* [*Smith and Tirpak*, 1989] they generally represent the most extreme range of $2\times CO_2$ conditions predicted for these parameters over the U.S.

information. It also shows the importance of utilizing GCM predicted changes in humidity and wind, as well as air temperature, to evaluate the effects of climate change on biophysical processes such as $E_{T,P}$. The use of the physically-based turbulent transfer model to predict $E_{T,P}$ at this resolution, over the U.S., illustrates the importance of utilizing information about humidity gradients and wind to estimate evaporative sensitivity to changing climate forcings.

2. TURBULENT TRANSFER MODEL

The energy balance of the surface is expressed as

$$\Delta Q = R_n + H + L_vE + G + M \tag{2}$$

where ΔQ is change in surface energy, and R_n, H, L_vE, G, and M are net radiative, sensible, latent, conductive, and advective energy fluxes, respectively. In temperature equilibrium, $\Delta Q = 0$; a negative energy balance will cool the surface, decreasing it's temperature, while a positive energy balance will warm the surface. †

In most terrestrial environments, G and M are relatively small. Turbulent energy and mass flux at the Earth's surface is second only to radiation in importance for the energy balance of terrestrial ecosystems. Over land, net radiation R_n is of approximately equal magnitude to sensible H and latent heat exchange, L_vE [*Budyko*, 1974; *Baumgartner and Reichel*, 1975; *Korzun, et al.*, 1978]. However, because L_vE is usually negative (a heat loss), and H is usually positive (a heat gain), the sum of $H + L_vE$ is generally much smaller than R_n when integrated over a day or longer [*Marks and Dozier, submitted*].

The turbulent transfer of momentum, heat, and water vapor described by H and L_vE are the most complicated forms of energy exchange, and are not easily measured in a natural environment. The data required to calculate them are difficult to measure at a point, and they have a highly variable distribution over a topographic surface. Not only does significant energy transfer occur by turbulent exchange, but in most environments significant water loss can occur from sublimation, direct evaporation, or transpiration by vegetative cover [*Budyko*, 1974; *Baumgartner and Reichel*, 1975; *Korzun, et al.*, 1978; *Beaty*, 1975; *Stewart*, 1982; *Davis et al.*, 1984].

Tractable approaches to calculating sensible and latent fluxes have been summarized [*Fleagle and Businger*, 1980; *Brutsaert*, 1982]. The method used for this experiment was adapted from *Brutsaert* [1982] by *Marks* [1988] and *Marks and Dozier* [*submitted*]. A similar approach was used by *Martin, et al.* [1990] to estimate the sensitivity of E_T to climate change over several different types of vegetation in North America.

The data required for calculating turbulent transfer at each grid point are air density ρ, air and surface potential temperatures Θ_a, Θ_s, air and surface specific humidities q_a, q_s, wind speed u, and surface roughness z_0. The methodology for estimating these parameters over the U.S. will be discussed in a later

†: The sign convention used in this analysis is that a flux of energy or mass is negative if it is away from the surface, and positive if it is toward the surface.

section.

The equations to be solved at each grid point are:

Obukhov stability length:

$$L = \frac{u^{*3}\,\rho}{k\,g\left[\frac{H}{T_a\,C_p} + 0.61E\right]} \tag{3}$$

Friction velocity:

$$u^* = \frac{u\,k}{\ln\left[\frac{z_u - d_0}{z_0}\right] - \psi_{sm}\left[\frac{z_u}{L}\right]} \tag{4}$$

Sensible heat flux (positive toward the surface):

$$H = \frac{(\Theta_a - \Theta_s)\,a_H\,k\,u^*\,\rho\,C_p}{\ln\left[\frac{z_T - d_0}{z_0}\right] - \psi_{sh}\left[\frac{z_T}{L}\right]} \tag{5}$$

Mass flux (positive toward the surface):

$$E = \frac{(q - q_s)\,a_E\,k\,u^*\,\rho}{\ln\left[\frac{z_q - d_0}{z_0}\right] - \psi_{sv}\left[\frac{z_q}{L}\right]} \tag{6}$$

The latent heat flux is $L_v \times E$, or L_vE, where L_v is the latent head of vaporization ($\approx 2.5\times10^6\ \mathrm{J\,kg^{-1}}$), or sublimation ($\approx 2.8\times10^6\ \mathrm{J\,kg^{-1}}$). C_p is the specific heat of dry air ($1005\ \mathrm{J\,kg^{-1}\,K^{-1}}$). Measurement heights are z_u for wind, z_T for air temperature, and z_q for humidity. A measurement height of 10 m was used for all three in this experiment. a_H and a_E are the ratio of eddy diffusivity and viscosity for heat and water vapor, respectively; while there is some uncertainty associated with the value of these ratios, *Brutsaert* [1982] suggests that for most natural surfaces, $a_H = a_E = 1.0$. k is von Karman's constant (dimensionless), $k \approx 0.40$. g is the acceleration of gravity ($9.80616\ m\,s^{-2}$). d_0 is the zero-plane displacement height; *Brutsaert* [1982] also suggests $d_0 = (2/3)\,7.35\,z_0$. z_0 is the surface roughness length (m). For fairly smooth surfaces, z_0 ranges from 0.0001 to 0.005 m, though vegetation cover and terrain features can constrain the value to be much higher.

The ψ stability functions, ψ_{sm} for mass, ψ_{sh} for heat, and ψ_{sv} for water vapor, are:

Stable ($\zeta = \frac{z}{L} > 0$):

$$\psi_{sm}(\zeta) = \psi_{sv}(\zeta) = \psi_{sh}(\zeta) = \begin{cases} -\beta_s & 0<\zeta\le 1 \\ -\beta_s & \zeta>1 \end{cases}, \quad \beta_s = 5 \tag{7}$$

Unstable ($\zeta = \frac{z}{L} < 0$):

$$x = (1 - \beta_u \zeta)^{1/4}, \quad \beta_u = 16 \tag{8}$$

$$\psi_{sm} = 2 \ln\left[\frac{1+x}{2}\right] + \ln\left[\frac{1+x^2}{2}\right] - 2 \arctan x + \frac{\pi}{2} \tag{9}$$

$$\psi_{sh}(\zeta) = \psi_{sv}(\zeta) = 2 \ln\left[\frac{1+x^2}{2}\right] \tag{10}$$

Stewart [1982] in a sensitivity analysis of an early version of this model, showed that over snow, for all but the most extreme conditions, the three most critical terms in the above equations (3 thru 10) are the wind speed u, the temperature difference between the air and the surface $T_a - T_s$, and the humidity difference between the air and the surface $q - q_s$. Turbulent transfer of heat and mass is controlled first by the wind speed, and then by the temperature and humidity gradients between the surface and the air. Evaporation is controlled by wind speed and the humidity gradient as shown in the above equations. Air temperature T_a is only marginally involved through the calculation of the Obukhov stability length L (Eq. 3). The fact that evaporation is usually greater in summer, when air temperatures are warmer, is generally due to lower air humidities, and consequently higher humidity gradients between the surface and the atmosphere.

While the values for a_H, a_E, k, d_0, and z_0, cannot be precisely known, *Brutsaert* [1982] states that they can be estimated to within 10-20% of their true values from site considerations. Over an area the size of the U.S., this is a much more difficult problem. However, because these are basically scaling parameters, this uncertainty should affect the magnitude, but not the sign of the calculations, and, under most conditions, this effect should be relatively minor [*Stewart*, 1982].

This model was originally developed and tested as a point model over snow by *Marks* [1988] and used by *Marks and Dozier*, [submitted] as part of an energy balance study of an alpine snowcover. For this experiment it was incorporated into an image processing system, Image Processing Workbench (IPW), designed to provide tools for geographic data analysis, processing and display [*Frew*, 1990]. For this experiment, a_H, a_E, k, and d_0 are set to the constant values discussed above. Measurement heights, z_u, z_T, and z_q, are all set to a constant height above the surface. Data for air and surface temperature T_a, T_s, air and surface humidities q_a, q_s, wind speed u, elevation z, and roughness length z_0 are input as a multi-band image with the appropriate geographic coordinates.

3. GEOGRAPHIC DATA SURFACES FOR CURRENT CLIMATE CONDITIONS

The data used for this analysis were organized into a geographic information system (GIS) described by *Campbell et al.* [submitted]. This system is compatible with a variety of both raster and vector GIS software formats, but this analysis was done using only raster data and processing tools. Most of the processing was done using Image Processing Workbench (IPW) [*Frew*, 1990]. Data projection, management, and display was done using the GRASS GIS software system, Version 3.2, which was acquired from the

U.S. Army Corps of Engineers as a Beta release [*USACE*, 1988].

Digital Elevation Grid

The base-layer of the GIS system used in this analysis is a digital elevation model (DEM) of the continental U.S. sampled at a 5′ latitude and longitude spacing. It was acquired from the NOAA National Geophysical Data Center in Boulder Colorado on CD-ROM as part of the data distribution *Geopyhysics of North America* [*NOAA*, 1989]. This database was re-projected into an Albers Equal-Area Conic projection [*Snyder and Voxland*, 1989] at a uniform 10 km grid spacing. This is a grid of 295 rows by 470 columns, with 138,650 grid points. When the boundary of the U.S. is used to mask the file, 77,857 grid points are within the area used for analysis. The minimum elevation is $-121\,m$ located in Death Valley, California, and the maximum elevation is $3790\,m$, located in the Sierra Nevada, California. **Figure 1** is a shaded relief map of this data layer, showing the distribution of relief and topography across the U.S.

Elevation-Corrected Air Temperature Surfaces

Monthly average air temperatures were extracted from the Historical Climatology Network (HCN) database for the years 1948-87 [*Quinlan, et al.*, 1987; *Karl, et al.*, 1990]. Data from 1211 stations within the continental U.S. were used to construct long-term monthly averages for this 40 year period. **Figure 2.a** shows the distribution of measurement sites across the U.S. The spatial distribution is adequate across much of the U.S., except for Nevada, the southwest deserts, Texas, and the Dakotas. In general, however, high elevation areas particularly in the western U.S., are not well represented by these data. Regional variation in air temperature is largely controlled by variations in air pressure caused by topographic structure. From the equation of state for an ideal gas and the hydrostatic equation [*Byers*, 1974], we can show how air temperature changes with elevation and pressure:

$$C_p\,dT_a = -\left[\frac{R\,T_a}{m\,P}\right] g\rho\,dz$$

This reduces to:

$$dT_a = -\left[\frac{g}{C_p}\right] dz$$

where T_a is the air temperature (K), P is the air pressure in Pascals (Pa), ρ is the air density ($kg\,m^{-1}$), z is the elevation (m), R is the gas constant ($8.3143\,J\,mol^{-1}\,K^{-1}$), m is the molecular weight of dry air ($28.9644\,kg\,m^{-3}$), g is the acceleration due to gravity ($9.80616\,m\,s^{-2}$) and C_p is the specific heat of dry air at constant pressure ($1005\,J\,kg^{-1}\,K^{-1}$).

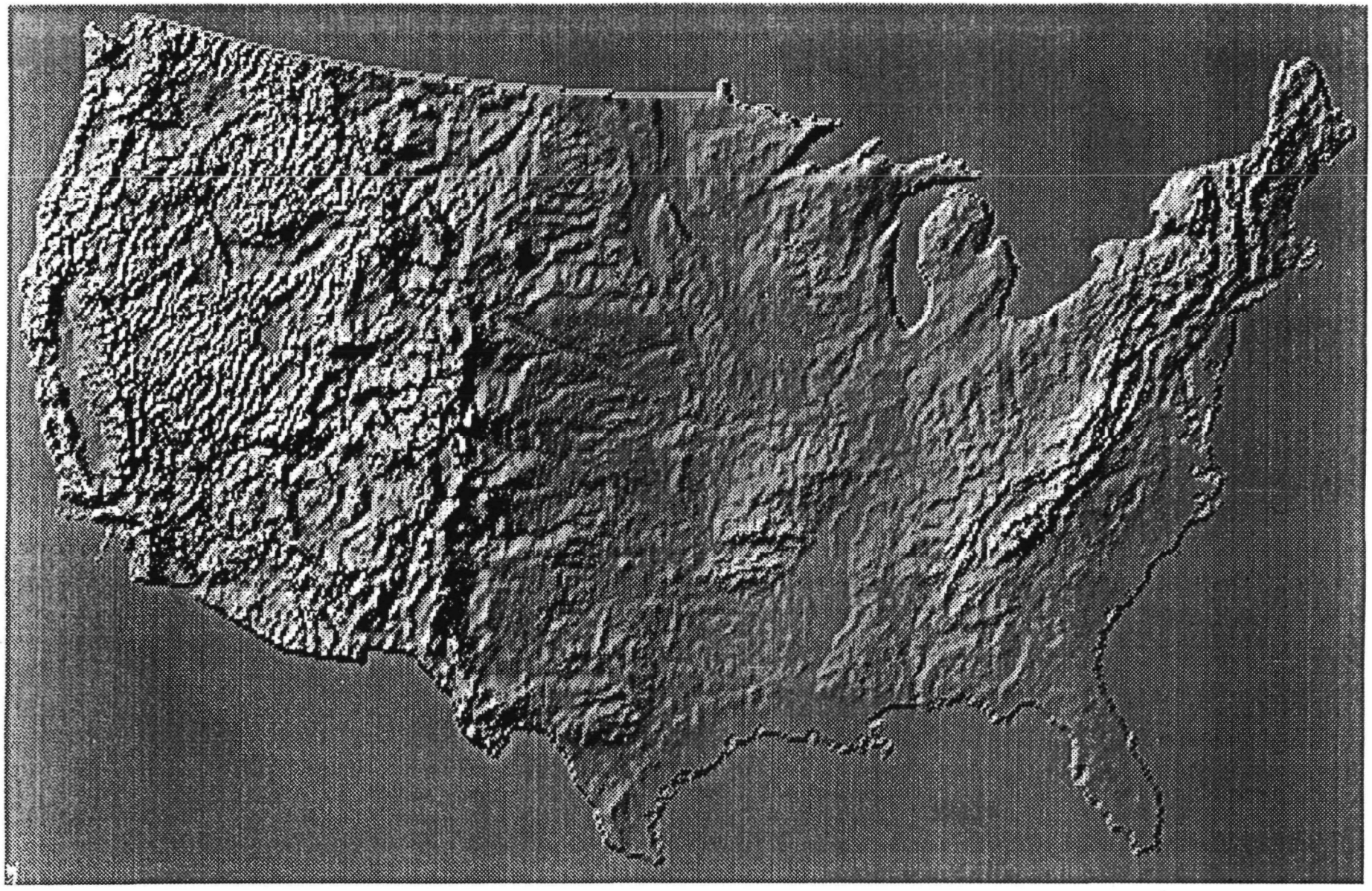

FIGURE 1: Shaded relief map of the U.S. computed from 10 km grid DEM (77,857 points).

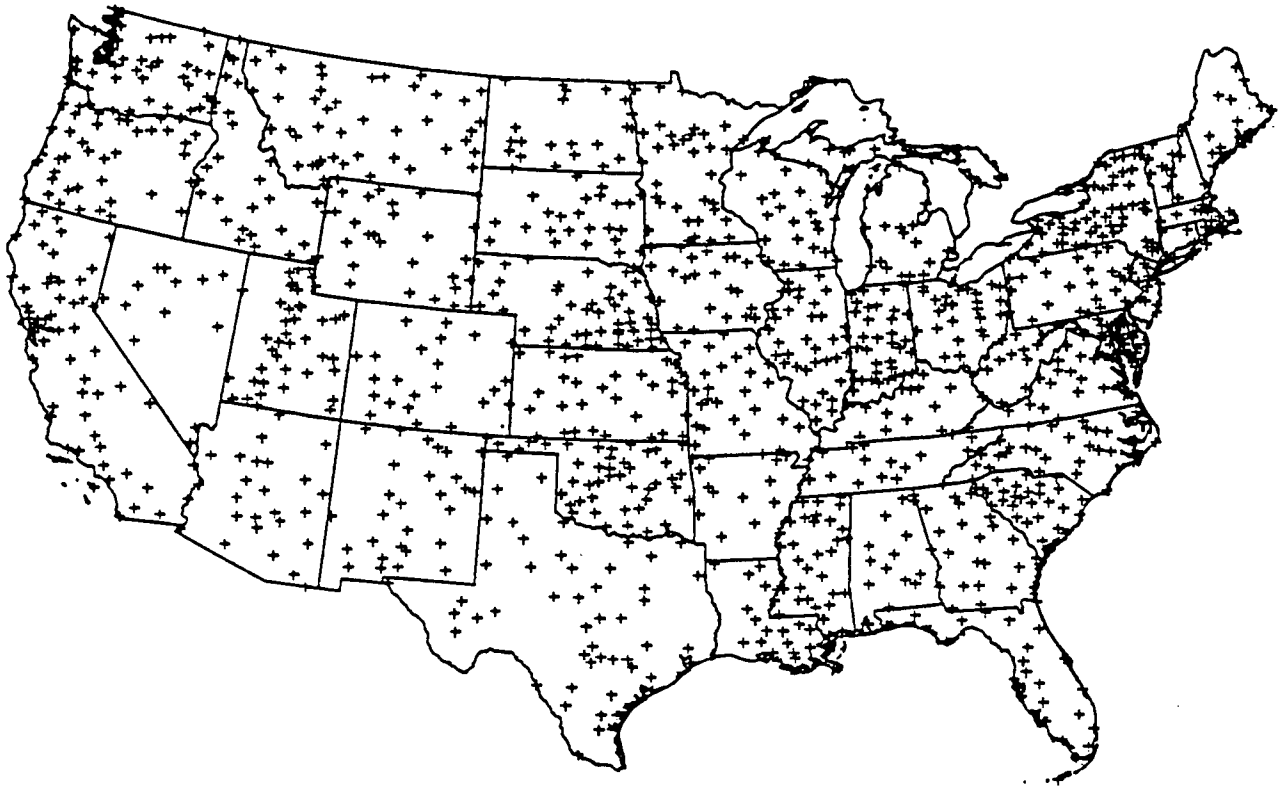

FIGURE 2.a: Location of Historical Climatology Network (HCN) data measurement sites.

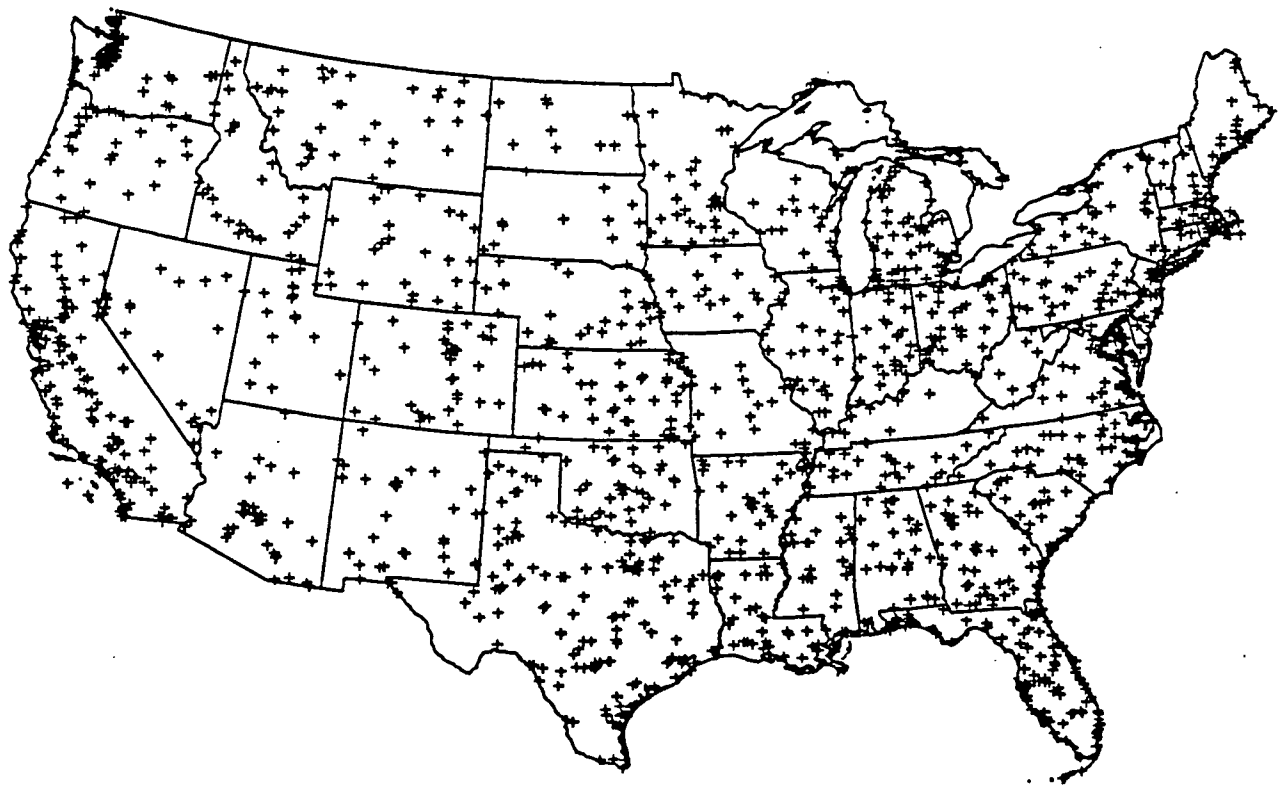

FIGURE 2.b: Locations of U.S. airport measurement sites, Climate Data for Planet Earth database.

Equation 12 defines the adiabatic temperature change with height in the atmosphere. The decrease in temperature at higher elevations is caused by a combination of adiabatic cooling, and local or regional surface interaction with the atmosphere. To extend air temperature data from the irregular measurement network to a uniform grid across the U.S. we must systematically account for topographic effects in the interpolation procedure.

To achieve this, topographic effects were removed from the measured air temperatures by converting them to their sea-level equivalent prior to interpolation, and then the sea-level air temperatures interpolated to the 10 km grid were re-converted to the appropriate air temperature for the elevation from the DEM. Air Temperatures T_a were converted to their sea-level equivalent, or potential temperatures Θ_a:

$$\Theta_a = T_a[\frac{P_0}{P_z}]^{R/mC_p} \qquad 13$$

where P_0 and P_z are air pressures in Pa at sea level, and elevation z, respectively. The HCN measurement site elevations were used to derive the air pressures using the hydrostatic equation (equation 11, above). This procedure effectively eliminates the elevation effects on the measured temperatures, but retains latitude/longitude effects by scaling air temperatures to their equivalent at the $100\,kPa$ level (approximately sea level), making them directly comparable. They were then interpolated to the geographic grid spacing of the DEM data using a simple linear inverse distance squared algorithm [*Isaaks and Srivastava*, 1989] †

resulting in a geographic surface of Θ_a for the U.S. Eq. 13 was then inverted using the Θ_a surface and the DEM elevation surface to map T_a back onto the elevations of the DEM grid.

Figure 3 shows the long-term average monthly time series of elevation corrected T_a for the U.S. Though the elevation correction was fairly simple, it gives a result which is quite different from other attempts to distribute air temperature over large regions [e.g.: *Legates and Willmott* 1990]. These efforts have been able to show the general spatial variation of air temperature, and some latitudinal trends, but have made no attempt to correct for topographic effects. The temperature surfaces used in this analysis represent the first large regional-scale temperature database which is elevation-corrected.

---

†: The inverse distance squared interpolation is:

$$V_{GP} = \frac{\sum_{i=1}^{n} v_i/d_i^2}{\sum_{i=1}^{n} 1.0/d_i^2}$$

where V_{GP} is the interpolated value at a grid point, v_i is the measured value of the i^{th} nearest neighbor, d_i is the distance to the i^{th} nearest neighbor, and n is the number of nearest neighbors considered. While the interpolation is setup to search up to 12 nearest neighbors, there is little impact on the result beyond 4 to 6, unless they are tightly spaced so that the distances are all similar. This algorithm was selected over other more complex methods such as spline interpolation [*Eubank*, 1989] because it is numerically simple, computationally relatively fast, and is an exact interpolation method (the interpolated surfaces are constrained to go through the input data points). Other methods will be investigated in future experiments

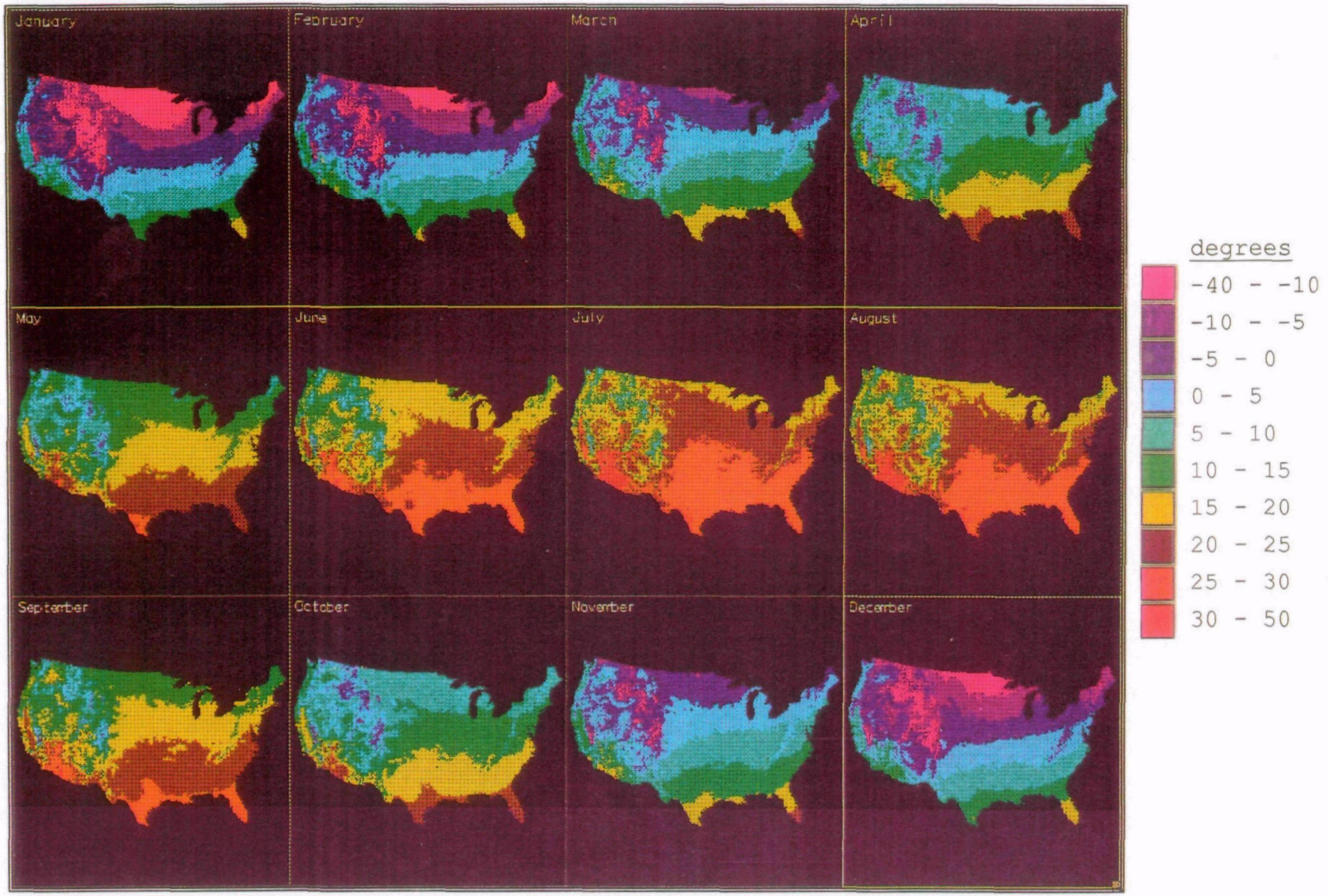

FIGURE 3: Monthly air temperature T_a surface under historical climate conditions.

Persistent local features such as valley inversions, are not accounted for, but the temperature surfaces show significant detail in the monthly average temperatures. Both topographic and latitudinal temperature features are illustrated. A surprising number of relatively small regional features such as the Columbia Gorge in the Pacific Northwest, the Sierra Nevada, White Mountains, and the Owens Valley in eastern California, the Grand Canyon, and the southern Appalachians show clear differences in temperature at various times of year.

Elevation Corrected Humidity Surfaces

Daily dew point temperatures were extracted from National Climatological Data Center Archive (NCDC) data supplied on CD-ROM by *WeatherDisc Associates, Inc.* [*WeatherDisc Assoc., Inc*, 1990]. These data are described in detail by *Spangler and Jenne* [1988]. Dew point temperatures from the Worldwide Airfield Summaries database for 1565 airport measurement sites in the continental U.S. were aggregated into a long-term average monthly time series for 1960-87. **Figure 2.b** shows the distribution of airport measurement sites across the U.S. As with air temperature, in most regions the distribution is adequate, except for Nevada, the southwestern deserts, Texas, and the Dakotas, and high elevation sites are severely under represented. Topographic correction for dew point temperature is more uncertain than for air temperature. Dew point temperature not only diminishes with elevation, but it is constrained to be equal to or less than the local air temperature. Dew point temperatures were converted to vapor pressures e_a (Pa), and then combined with the appropriate T_a from the temperature surfaces to calculate temperature-corrected relative humidity RH:

$$RH = \frac{e_a}{e_{a,sat}} \qquad 14$$

where $e_{a,sat}$ is the saturation vapor pressure at T_a. T_a from the temperature surfaces was used in this calculation because T_a derived from the airport database was frequently inconsistent with the HCN derived temperature surfaces. This was due to differences in observation time and the relatively coarse resolution of the 10 km grid when locating measurement stations. Air temperatures measured at airports also tend to be biased because they are usually measured over tarmac.

Temperature-corrected RH's were then interpolated to the geographic grid spacing of the DEM data and the T_a surfaces, using the same inverse distance squared method [*Isaaks and Srivastava*, 1989], used for air temperatures, resulting in a geographic surface of RH for the U.S. RH was used for the interpolation, rather than vapor pressure e_a because RH tends to be more stable over mountainous regions than e_a [*Marks and Dozier*, 1979]. Eq. 14 was then inverted, using the T_a and RH surfaces to map e_a onto the DEM grid.

Figure 4 shows the long-term average monthly time series of elevation corrected e_a for the U.S. While this correction is not as physically-based as the T_a correction, the spatial distribution of humidity is much smoother than that of temperature, and the elevation-corrected e_a surfaces represent the only humidity database of this type. The values e_a are generally low during winter across the U.S., with higher humidities during the summer.

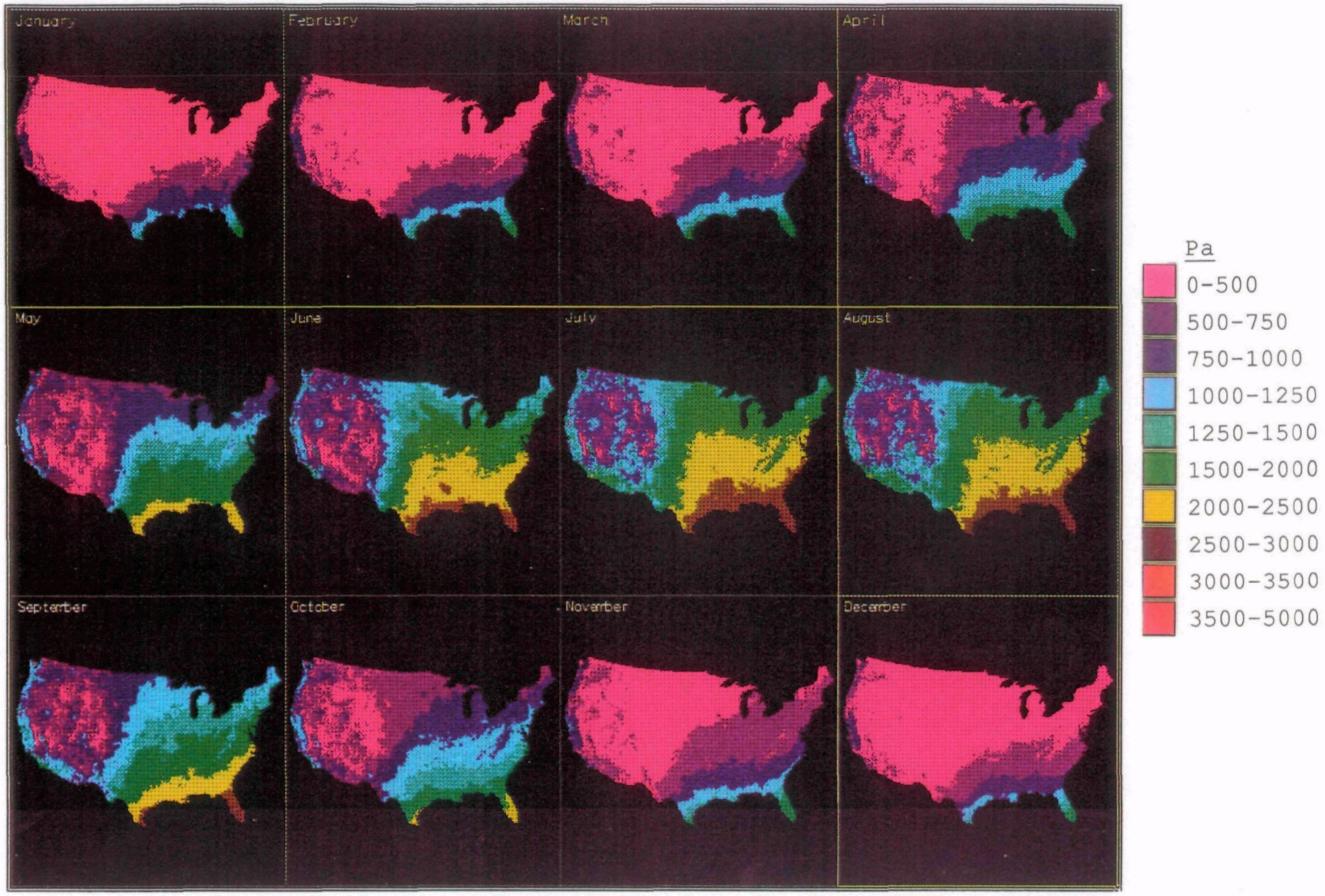

FIGURE 4: Monthly vapor pressure e_a surfaces under historical climate conditions.

The Southeast is consistently humid, with very high humidities during the summer. High humidities occur along the eastern seaboard during summer, but are absent during colder months. Many of the same regional features that were evident on the T_a surfaces are also evident on the e_a surfaces. High elevations are consistently drier, throughout the year. The "summer monsoon" in the Southwest is also evident from the incursion of higher humidities during July and August.

Wind Surfaces for the Continental U.S.

Synoptic wind data for the continental U.S. are nearly non-existent at space and time scales required for this analysis. National Meteorological Center (NMC) Grid Point Data are available that provide twice daily estimates of wind speed at two or three pressure heights (850, 500, and 250 mb) over a 10 minute (≈ 20 km) grid which covers the U.S. [e.g.: *Jenne*, 1970 *Jenne*, 1990]. While it may be possible to derive wind surfaces from these data, the data were not available in a usable format for testing at the time of this experiment.

The Department of Energy had developed a wind database described in *Wind Energy Resource Atlas* [*Elliott, et al.*, 1986]. These data are available in digital form for seasonal averages for the continental U.S. The averaging periods of the data are variable, and unspecified, as the database was designed for locating wind energy systems, not hydro-meteorological analysis. As *Elliott, et al.* [1986] explains, they are based on a combination of surface measurements, and upper air data such as radiosonde and the NMC data described above. They have been topographically corrected to account for higher wind speeds over ridges and mountains. The data were resampled from a 1/3×1/4 ° latitude-longitude grid to the same 10 km DEM grid as the T_a and e_a surfaces, using the same inverse distance square method. No attempt was made to account for the greater topographic detail in the DEM grid.

Figure 5 shows the long-term seasonal time series of wind speed at $10\,m$ (u_{10m}) for the U.S. The data surfaces show the expected increases in wind speed in areas of high topographic relief. Higher wind speeds occur in winter, and lower during summer. The data used to develop the wind surfaces were compiled to estimate wind power potential over the U.S. and are based on conservative estimates of wind speed [*Elliott, et al.*, 1986]. In many areas, actual monthly wind speeds are probably higher. While these wind surfaces are imperfect, they are the best synoptic wind data available at this time, and are adequate for this analysis.

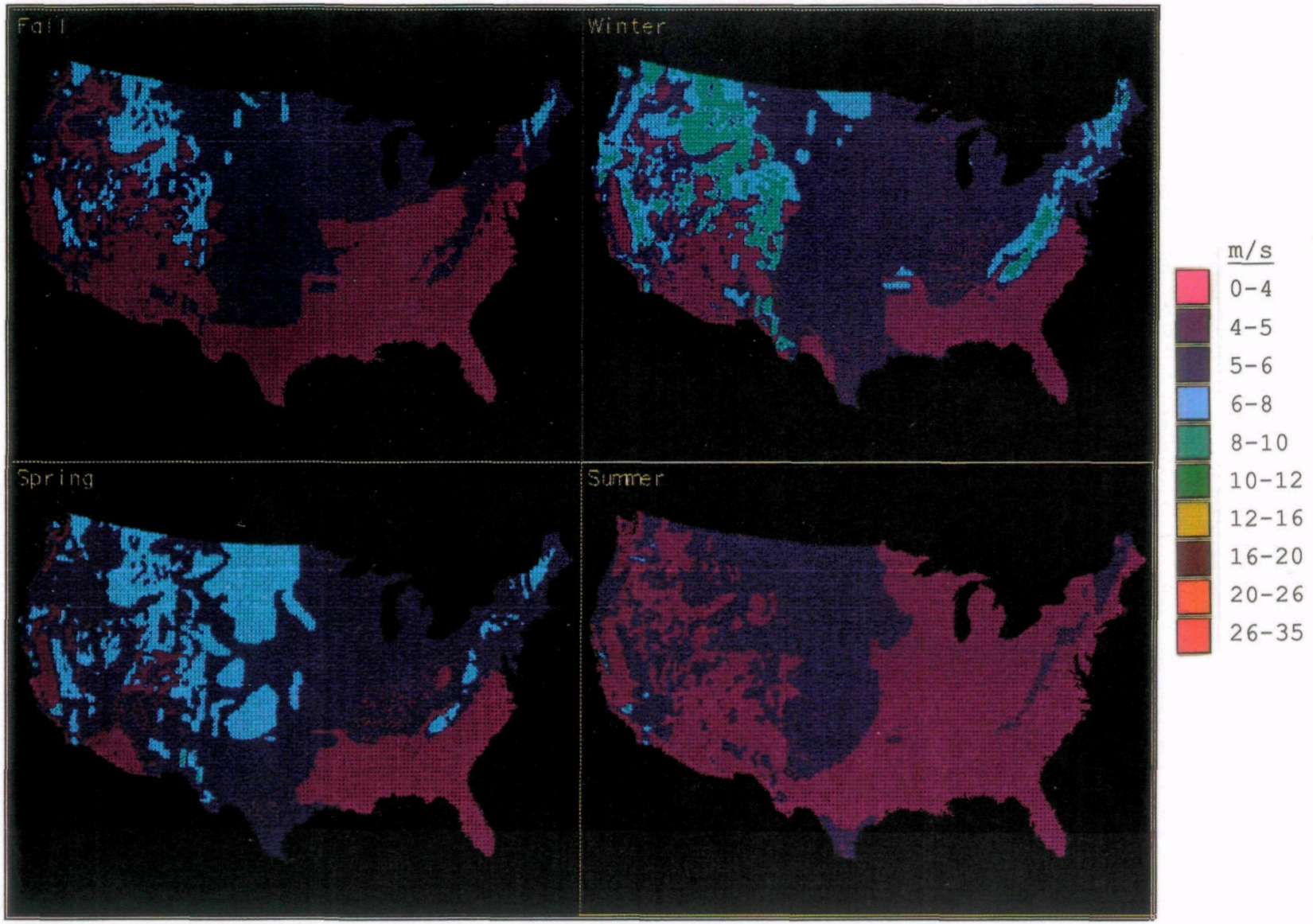

FIGURE 5: Seasonal wind speed u_{10m} surfaces, under historical climate conditions (DOE wind database).

4. GEOGRAPHIC DATA SURFACES FOR PREDICTED 2×CO_2 CONDITIONS

Data from the NASA Goddard Institute of Space Studies (GISS) and the NOAA Geophysical Fluid Dynamics Laboratory (GFDL) GCMs were extracted from the doubled CO_2 climate scenario data assembled for the EPA assessment of potential climate change effects [*Smith and Tirpak*, 1989]. These were selected because they included wind and humidity, as well as temperature and because they represent the most extreme range of $2time CO_2$ conditions predicted for these parameters over the U.S. A detailed description of the GCM data is given by *Jenne* [1990]. The GFDL resolution is $4.5 \times 7.5°$, and the GISS resolution is $8 \times 10°$ latitude-longitude. Values for air temperature, humidity, and wind for present conditions (1×CO_2), and for 2×CO_2 were used to generate ratios of the relative change in these parameters ΔR, as shown in Eq. 1. This approach to using GCM scenario data was presented by *Parry, et al.* [1987] and *Parry and Carter* [1989], and was used for precipitation analysis in the EPA report to congress [*Smith and Tirpak*, 1989]. The ratio approach is used because the actual values predicted by the 1×CO_2 GCM runs are inconsistent with historical data distributions in both time and space. This is caused by the coarse resolution of the GCMs, the lack of a realistic topography which influences parameters such as temperature, wind, humidity, and precipitation, and the relatively crude parameterization of surface properties within GCMs [*Rosenzweig and Dickinson*, 1986; *Schlesinger*, 1988].

Developing ratios for wind and humidity, which are based on absolute scales, is straightforward. Air temperature in °C must be first transformed to K. When temperature is transformed to K, the change ratios ΔR are generally between 1.01 and 1.02, and are not very different from predicted absolute temperature changes. Because of this, the absolute temperature change ΔT_a (K) is used in place of ΔR for the estimating GCM-predicted T_a, to avoid rounding errors.

Values of ΔR for humidity and wind, and ΔT_a for air temperature, were interpolated from the GCM grids to the $10\,km$ DEM grid using the inverse distance squared algorithm discussed above [*Isaaks and Srivastava*, 1989]. ΔR surfaces for humidity and wind are multiplied by the e_a and u_{10m} surfaces described in the previous section. The ΔT_a surfaces are added to the T_a surfaces, to generate T_a, e_a, and u_{10m} surfaces for the predicted $2\times CO_2$ conditions for the GFDL and GISS GCMs.

Figure 6 summarizes the temperature, humidity, and wind data surfaces for current conditions as predicted by historical data, and for 2×CO_2 conditions, as predicted by the GISS and GFDL GCMs. In general, both GCMs predict increases in all three meteorologic parameters. There is little difference between GFDL and GISS predicted T_a and e_a except during June, July, August, and September. Over this interval, the GFDL model predicts higher temperatures, and lower humidities than the GISS model. Compared to the GFDL model, wind speeds u_{10m}, are higher for the GISS model in winter and fall, about the same in the spring, and then substantially lower in summer. Though this temporal trend is not as great in the base-case historical data, it is generally similar.

FIGURE 6: Synopsis of historical climate data and GCM-predicted 2×CO_2 T_a, e_a, and u_{10m}. Comparison based on mean values for each parameter, over U.S. DEM grid.

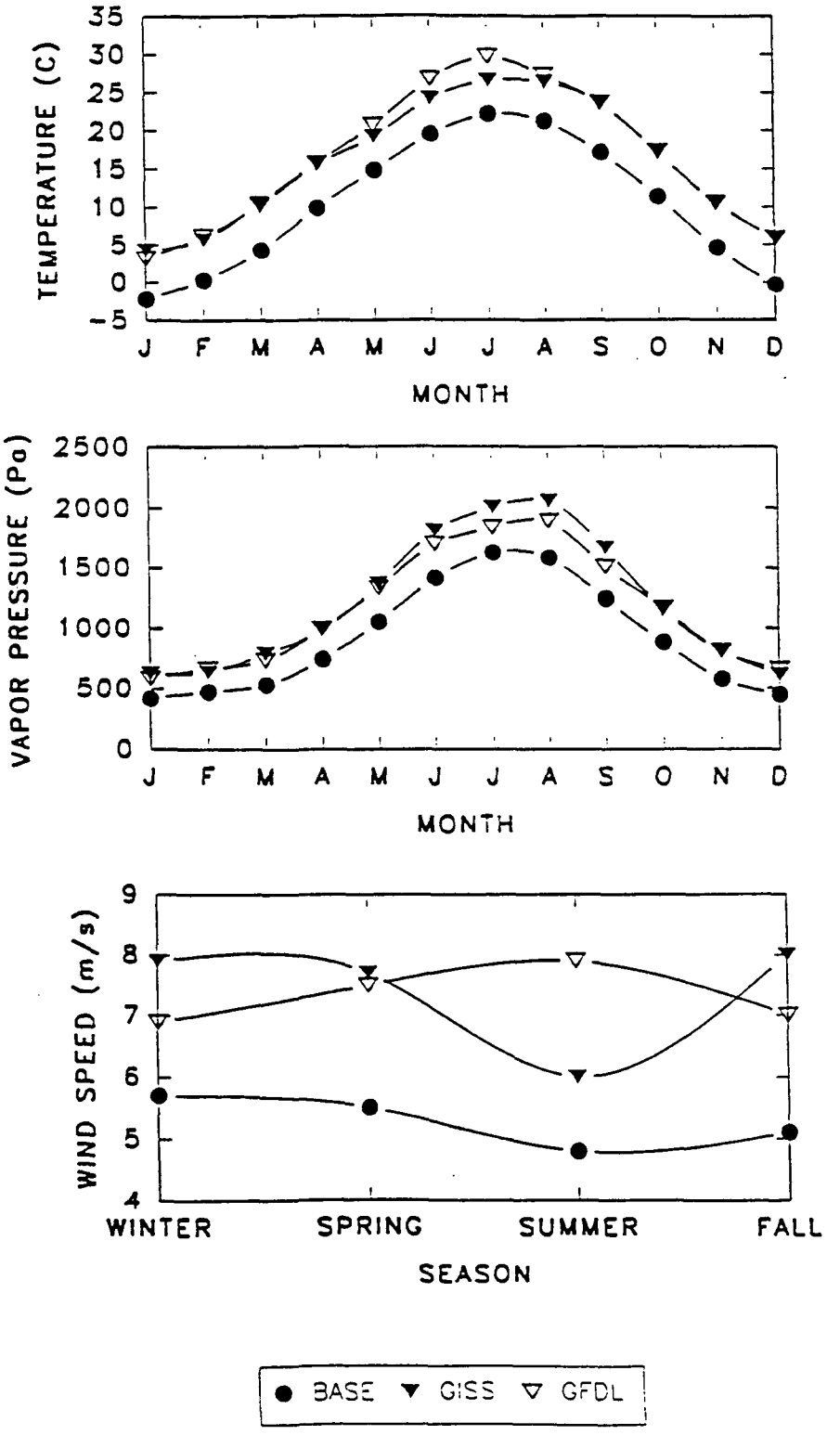

The GFDL model predicted substantially higher winds in summer. The GFDL surfaces are drier, warmer, and windier than the GISS surfaces in summer, when the maximum $E_{T,P}$ occurs. As shown in Eq. 6, the combination of higher humidities, and lower wind speeds during summer will lead to lower $E_{T,P}$ for the GISS-predicted conditions, while the lower humidities and higher wind speeds during summer will lead to much higher predictions of $E_{T,P}$ for the GFDL-predicted conditions.

Figures 7 and **8** show the distribution of T_a for the GFDL and GISS 2×CO_2 conditions. These show that warmer conditions prevail throughout every month of the year in comparison to the historical climate conditions shown in **Figure 3**. During the winter months there is little difference between the GISS and GFDL temperature predictions, but during summer the GFDL predictions are substantially warmer. For the base-case (**Figure 3**), air temperatures gradually increase from winter through spring to summer, and then decrease in the fall. In the GISS prediction (**Figure 8**), the temperatures are higher, but this same progression occurs. For the GFDL prediction (**Figure 7**), winter and fall temperatures basically agree with the GISS temperatures. However, during the months of June, July and August, the GFDL model predicts substantially higher temperatures for the entire country.

Figures 9 and **10** show the distribution of e_a for the GFDL and GISS 2×CO_2 conditions. More humid conditions prevail throughout most months of the year in comparison to the historical climate conditions shown in **Figure 5**. During the winter months there is little difference between the GCM predictions and the historical data predicted base-case. During summer the GFDL model predictions are only slightly more humid, while the GISS model predicts higher humidities throughout most of the country, especially the Southeast. This condition persists into the fall.

Predicted wind surfaces are shown in **Figures 11** and **12**, for the GFDL and GISS 2×CO_2 conditions. These surfaces show increased wind across the U.S. during all seasons of the year in comparison to the historical climate conditions shown in **Figure 6**. They also display interesting artifacts caused by the coarse resolution of the GCM computational grids. Wind appears to be somewhat less stable in the GCMs than are air temperature or humidity, showing a much more erratic progression from one season to the next as shown in **Figure 6**. In particular, the GFDL wind surfaces (**Figure 11**) show relatively low wind speeds just west of the Great Lakes region during spring, but extremely high wind speeds in the same region during summer. The GISS wind surfaces (**Figure 12**) show a similar transition in wind speeds in around the Great Lakes region from summer to fall.

doesn't really
argue strongly 1vs 2×CO2

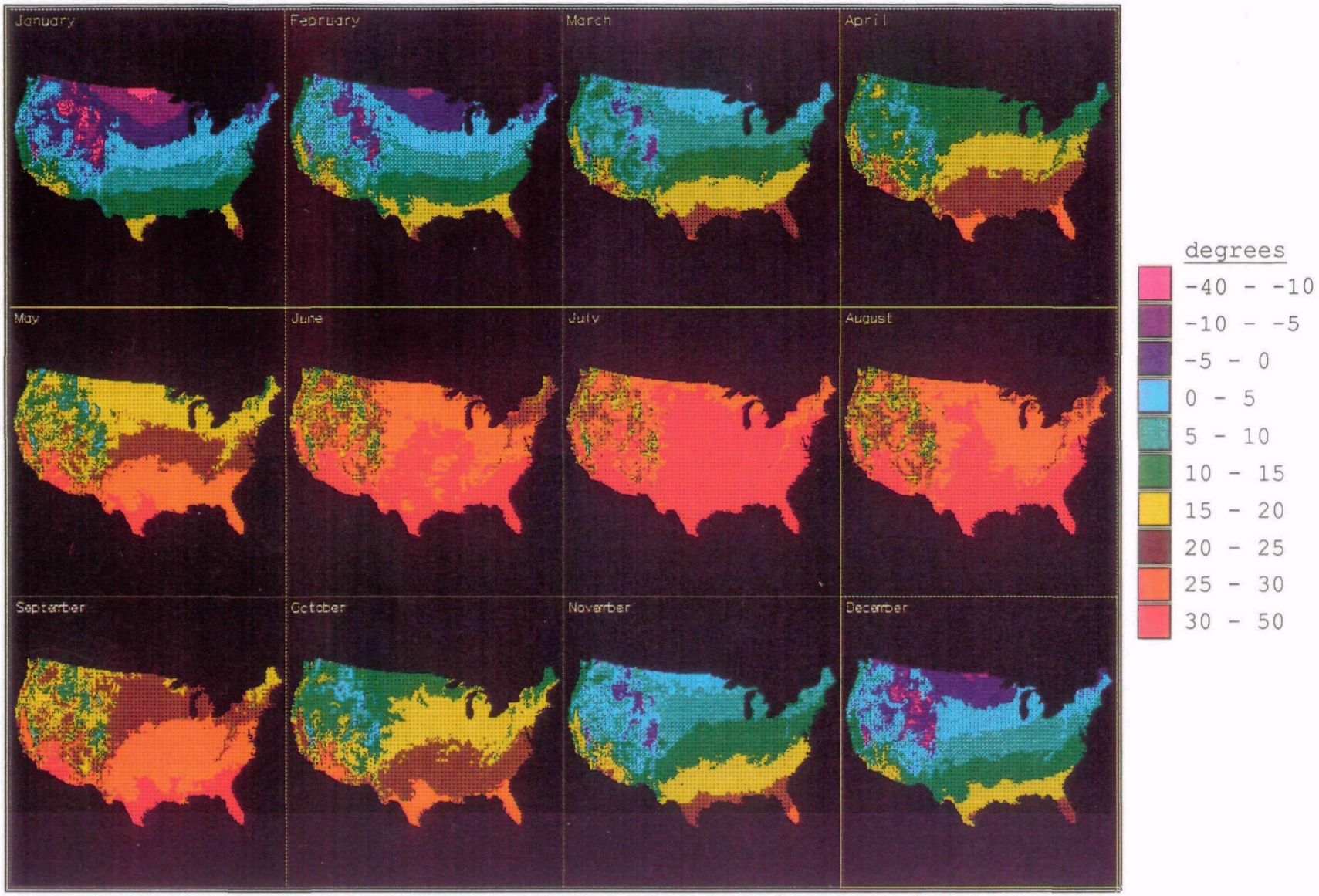

FIGURE 7: Monthly air temperature T_a surfaces for conditions predicted by the GFDL model for $2\times CO_2$.

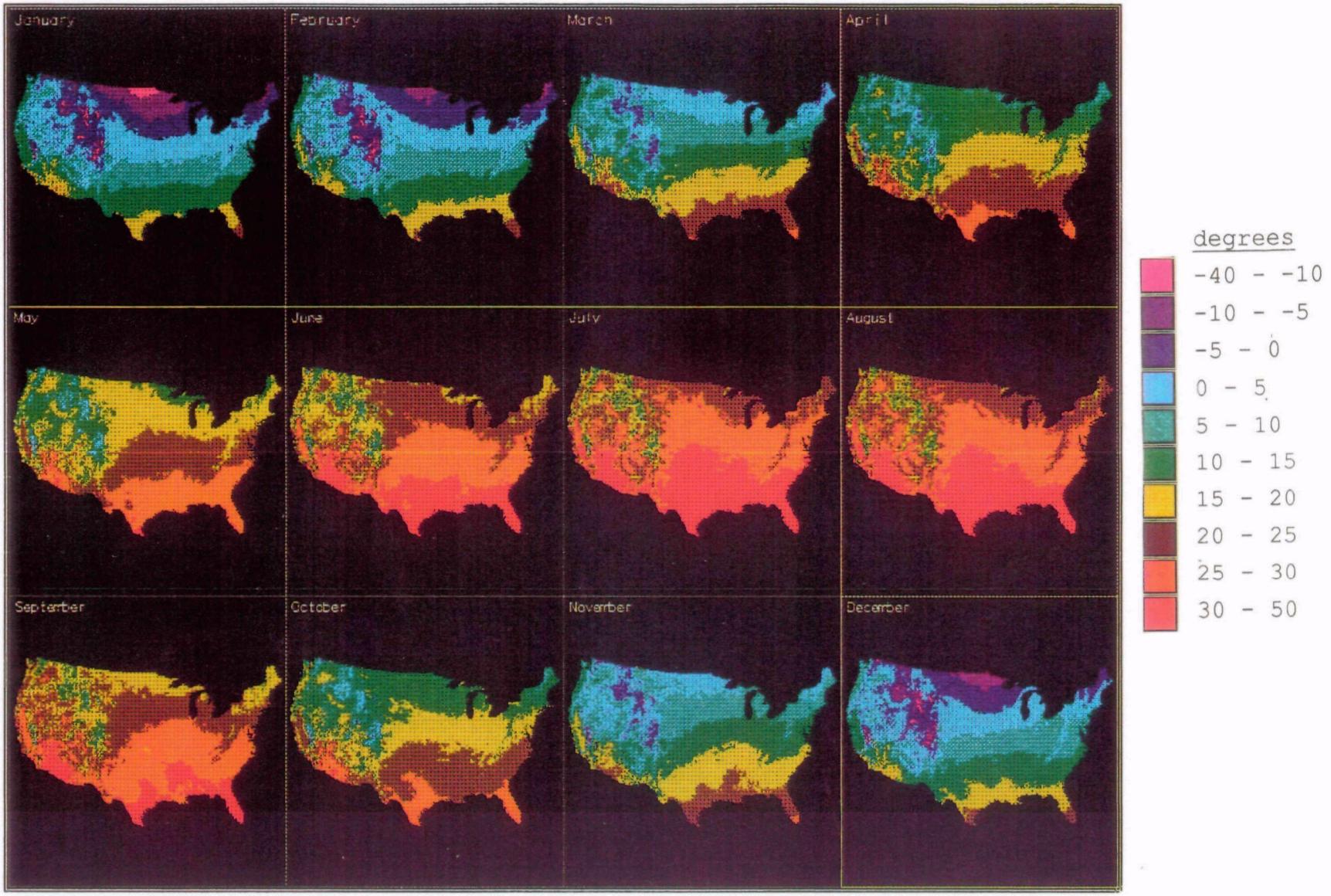

FIGURE 8: Monthly air temperature T_a surfaces for condidtions predicted by the GISS model for $2\times CO_2$.

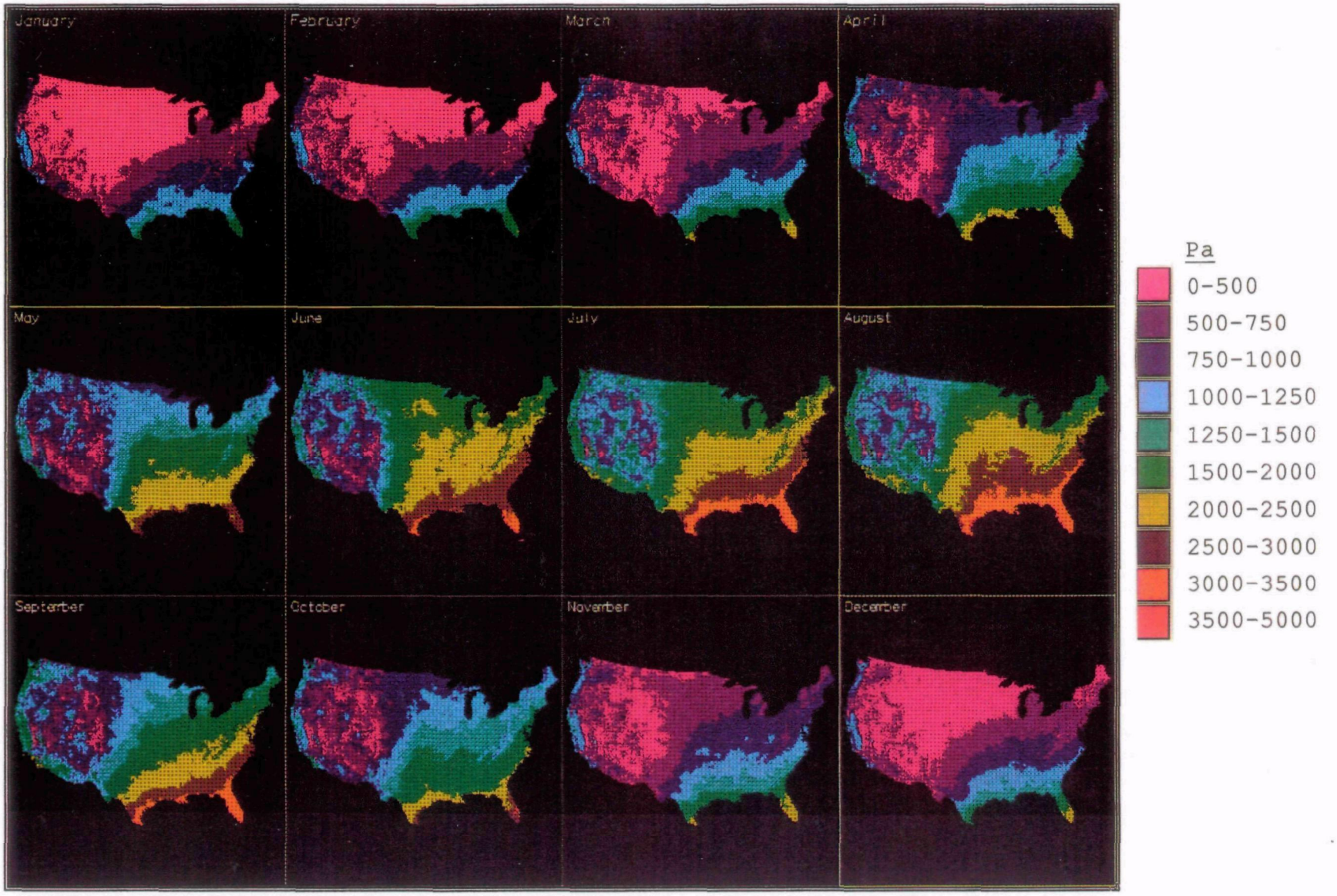

FIGURE 9: Monthly vapor pressure e_a surfaces for conditions predicted by the GFDL model for $2\times CO_2$.

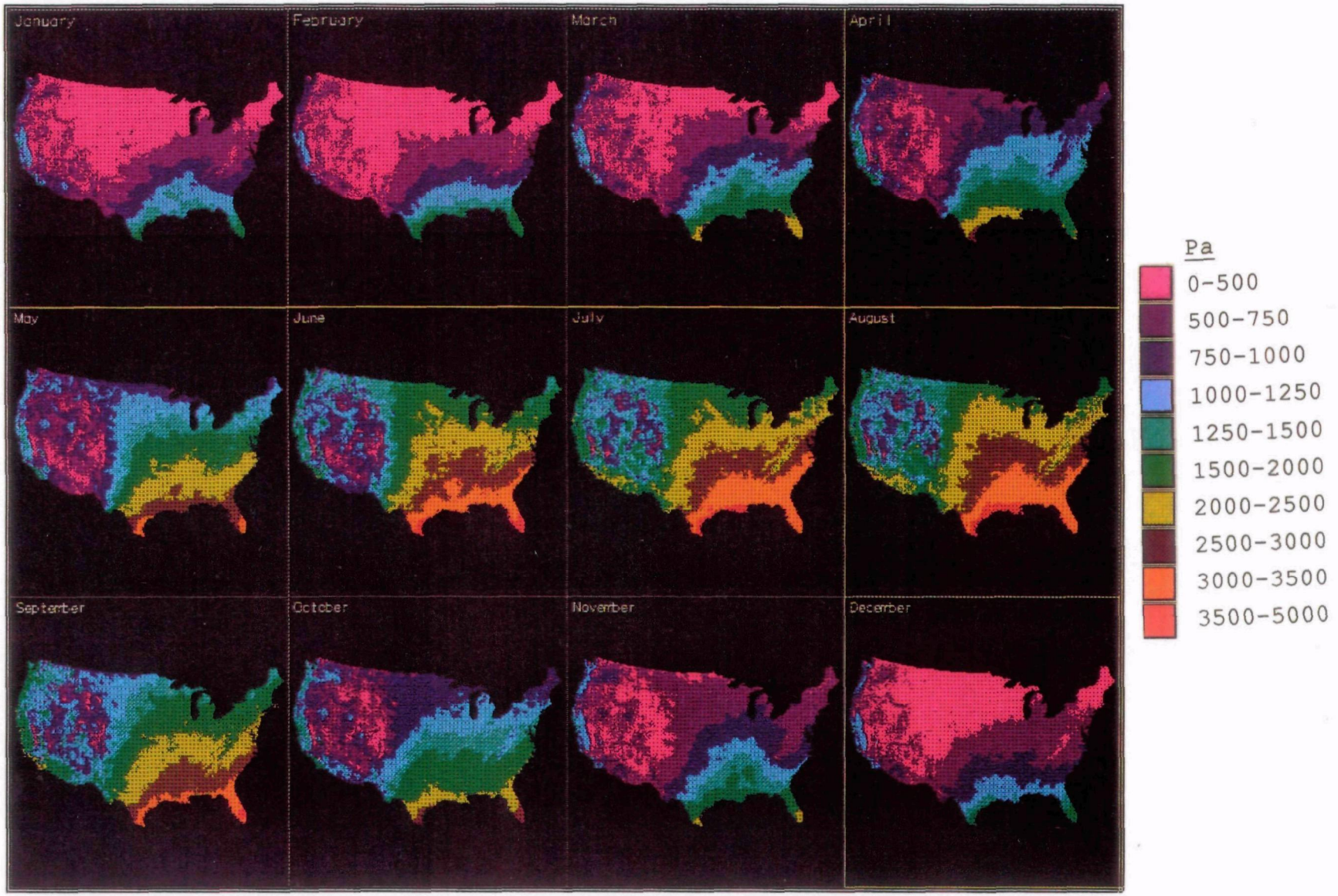

FIGURE 10: Monthly vapor pressure e_a surfaces for conditions predicted by the GISS model for $2\times CO_2$.

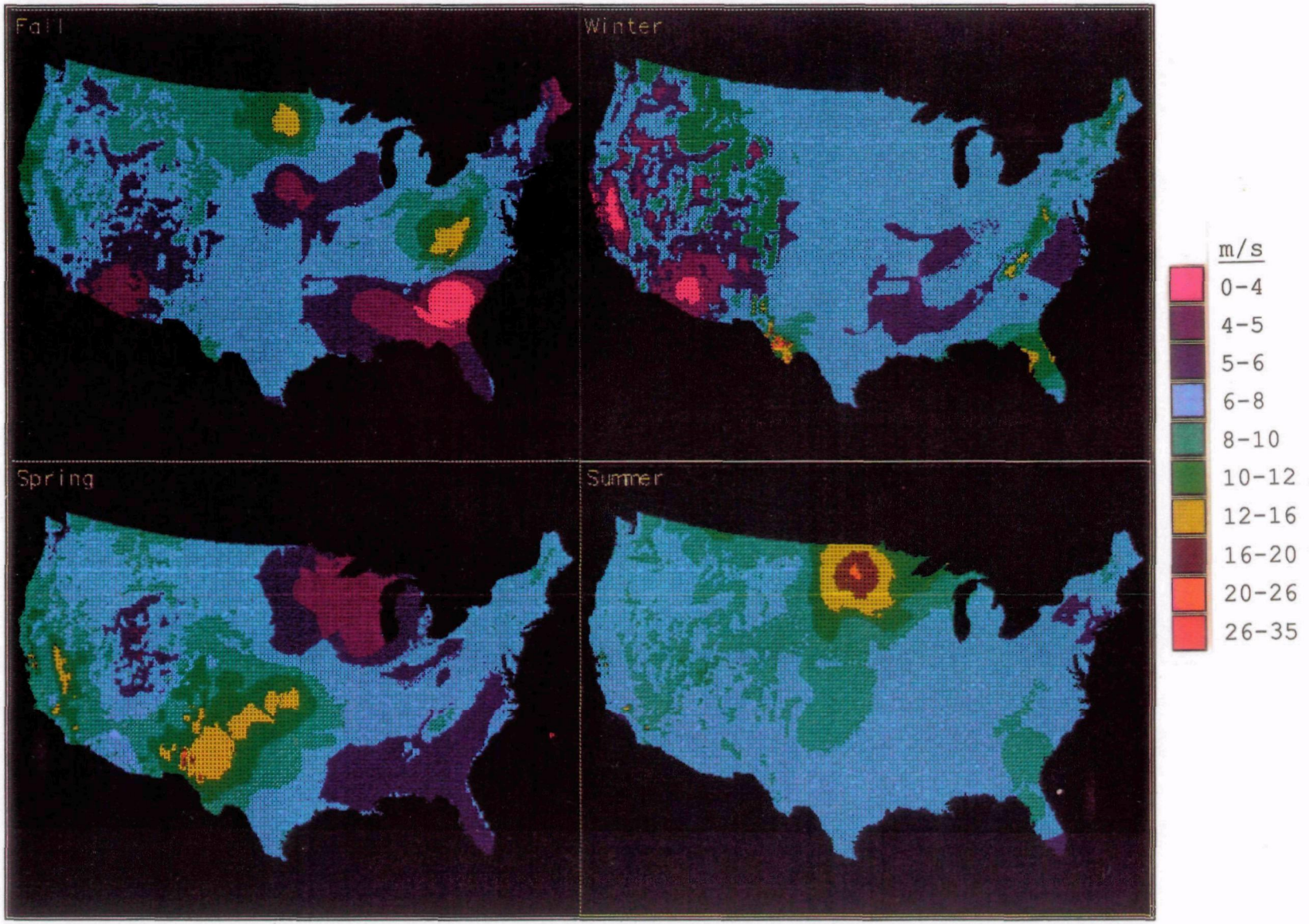

FIGURE 11: Seasonal wind speed u_{10m} surfaces for conditions predicted by the GFDL model for $2\times CO_2$.

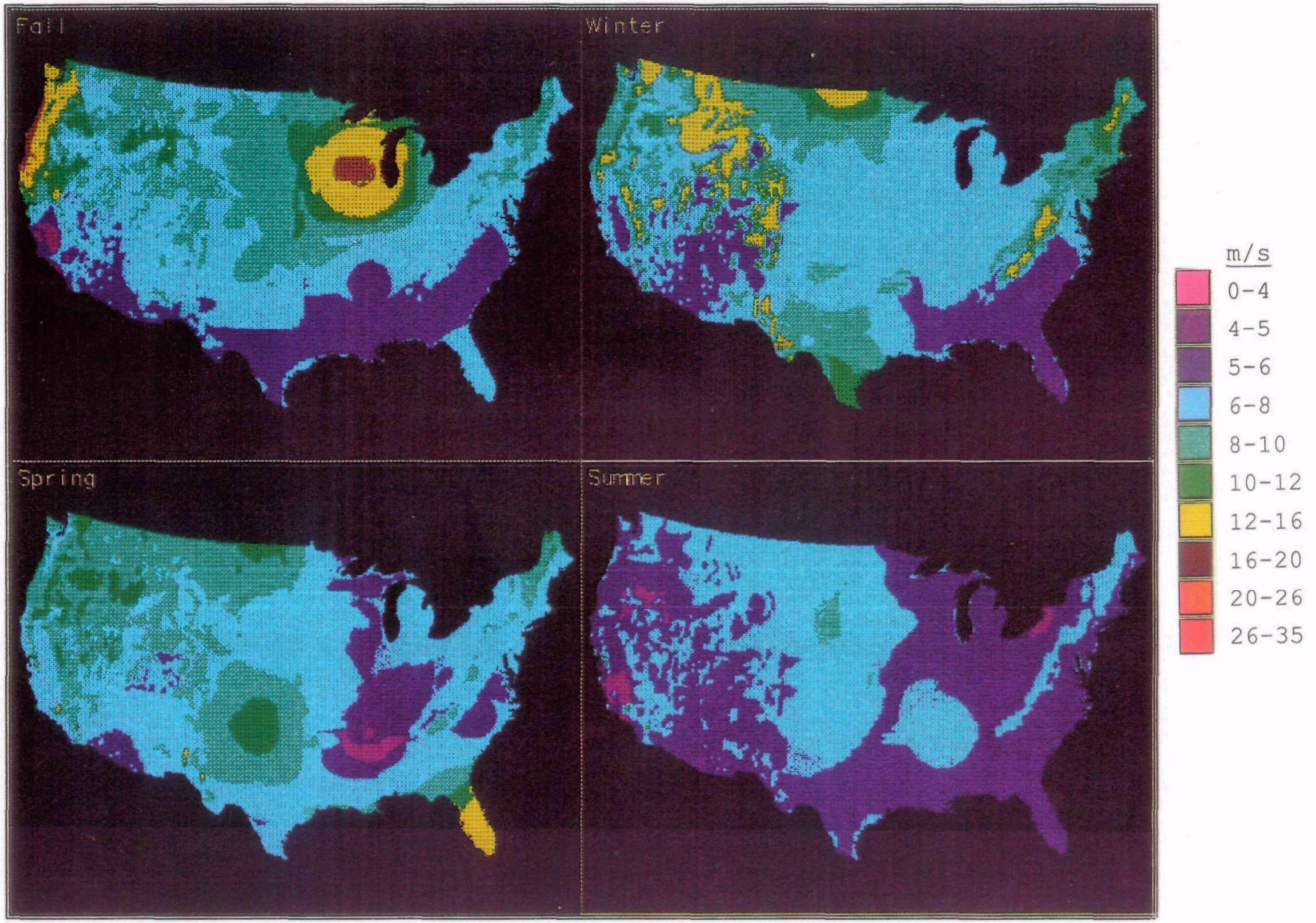

FIGURE 12: Seasonal wind speed u_{10m} surfaces for conditions predicted by the GISS model for $2\times CO_2$.

5. POTENTIAL EVAPOTRANSPIRATION ($E_{T,P}$) OVER THE U.S.

The turbulent transfer model presented above was used to calculate evaporation E surfaces for the historical data predicted base-case and the GCM predicted $2\times CO_2$ conditions. For this experiment, evapotranspiration E_T was considered equivalent to E. Because potential evapotranspiration $E_{T,P}$ is being modeled, the surface is assumed to be saturated, so the surface vapor pressure $e_s = e_{s,sat}$, the saturation vapor pressure at the surface temperature T_s; therefore E_T as calculated by the model is actually $E_{T,P}$.

A surface temperature T_s database from which long-term monthly average T_s could be derived was not available for this analysis. The monthly average surface temperature can be approximated from monthly average air temperature over most surfaces. A notable exception is over snow or ice, which cannot exceed 0°C. For this experiment, the average air temperature T_a, adjusted for topographic effects as discussed in the previous section, was assumed to be equal to the average monthly surface temperature T_s. If actual surface temperature data were available, it is unlikely that the average monthly T_s would differ significantly from average monthly T_a, except under the circumstances listed above. Measured, or satellite derived surface temperature would allow us to test the model at a time-step of days to weeks, rather than for average monthly conditions.

Vapor pressure at the surface e_s was derived from the saturation vapor pressure at T_s. The roughness length z_0 scales the turbulent interaction between the atmosphere and the surface.

For a given set of climatic conditions, a smooth surface such as bare soil or grassland, will have a small z_0, which will reduce turbulent interaction and reduce evaporation; a rough surface such as a forest canopy, will have a larger z_0, which will increase turbulent interaction and increase evaporation [*Brutsaert*, 1982]. Numerous estimates of z_0 over smooth surfaces such as grass, soil, snow, etc., have been made, [e.g.: *Sutton*, 1953; *Kondo*, 1962; *Chamberlain*, 1966 and *Businger et al.*, 1971] *Deacon* [1973] estimated z_0 over mixed vegetation in England, and *Fichtl and McVehil* [1970] estimated z_0 over tropical vegetation and forests in Florida. Few measurements of z_0 exist, however, over mid-latitude forests. *Brutsaert* [1982] shows that z_0 can be derived for different vegetation and other porous surfaces from canopy height, density, and leaf-area-index (LAI). These data, however, were also not available for this experiment.

In the absence of detailed monthly foliar biomass, leaf-area-index (LAI) data, or vegetation height and density, the surface roughness length z_0 was assigned a constant value related to a grassland or prairie over the grid. This was selected because it was a conservative value, that should under-estimate $E_{T,P}$ in most instances. $E_{T,P}$ should be overestimated over snow, water, and some desert regions, but it will underestimated over forested regions, particularly mountainous regions where winds speeds may be high. Because the purpose of this experiment is to estimate the distribution of $E_{T,P}$ over the U.S. within a reasonable range, the uncertainty in the estimate of z_0 should not detract from the results.

T_a, T_s, e_a, e_s, u_{10m}, and z_0 data surfaces were assembled into a six-band data image. The model was run at each DEM grid point within the continental U.S., to derive the average monthly $E_{T,P}$ surfaces from historical average monthly climate conditions as shown in **Figure 13.**

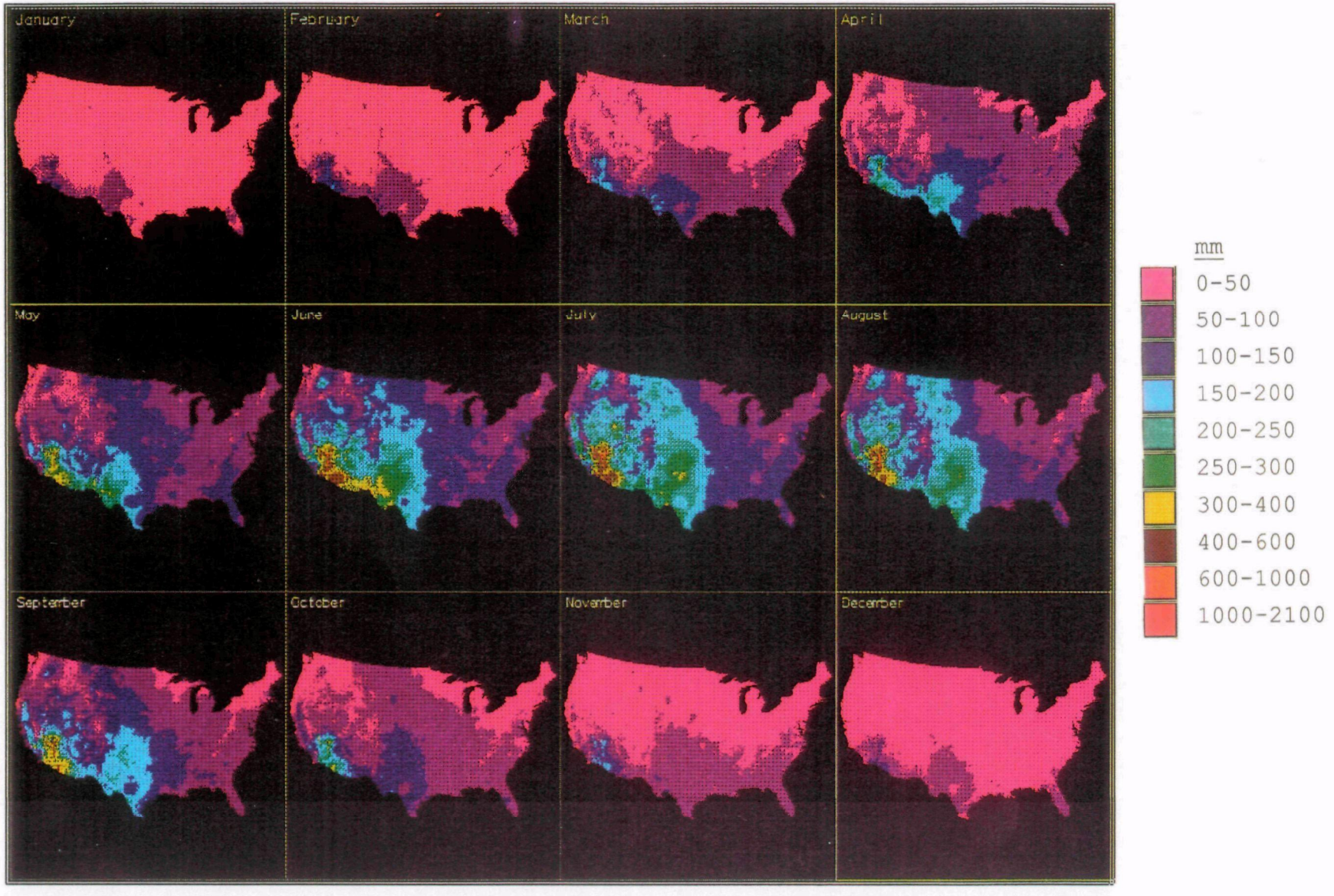

FIGURE 13: Calculated potential evapotranspiration $E_{T,P}$, for historical climate data.

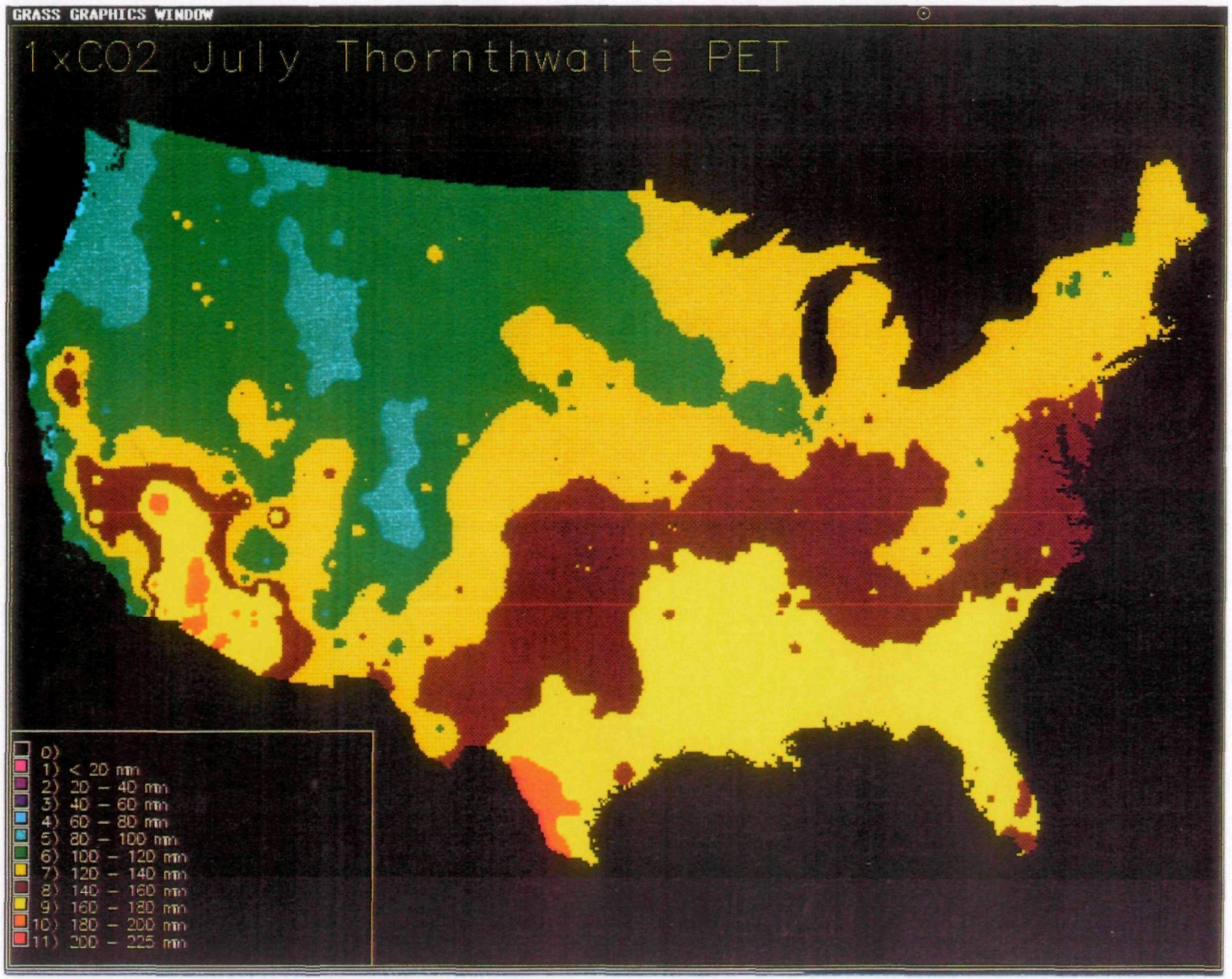

FIGURE 14: Thornthwaite estimate of $E_{T,P}$, using the temperature-regression method for average July conditions, historical climate data.

Winter $E_{T,P}$ is relatively low throughout the U.S. By March it begins to increase in the southwest and by late spring, has increased in the southwest, and the inter-mountain west. In summer it is highest in the southwest, but substantially higher throughout the west and the grain-belt in comparison to the east and the southeast.

This is significantly different from the result obtained when $E_{T,P}$ is estimated by regressing air temperature against measured evaporation [e.g.: *Thornthwaite*, 1948]. **Figure 14** is a July $E_{T,P}$ surface derived using the *Thornthwaite* [1948] temperature-regression method which has been commonly used to estimate potential evapotranspiration over large areas [e.g.: *Thornthwaite and Mather*, 1955; *Holdridge*, 1967; *Mather and Yoshioka*, 1968; *Budyko*, 1974; *Whittaker*, 1975; *Eagleman*, 1976; *Woodward*, 1987; *Stephenson*, 1989]. It predicts the high values in the southwest deserts and also in the southeast, and the along the eastern seaboard. The inconsistencies inherent in predictions of $E_{T,P}$ based solely on air temperature, without consideration of wind and humidity, are clearly apparent. As the data presented in the previous section show (and as anyone who has ever been to those regions in July will attest) high humidities and low wind speed dominate the southeastern U.S. in summer, which reduces the humidity gradient $q - q_s$, and the friction velocity u^*, as shown in Eq. 5.

Figures 15 and **16** show $E_{T,P}$ for conditions predicted by the GFDL and GISS $2\times CO_2$ GCM runs. While change in $E_{T,P}$ is minimal during winter, both GCMs show increases in $E_{T,P}$ during spring and summer. The GFDL $E_{T,P}$ surfaces show substantial increases, especially in the southwest and midwest, but the GISS surfaces show more moderate increases. This is primarily because the GFDL model predicts a warmer, windier, and drier environment, with large increases in temperature and wind, but only moderate increases in humidity, as shown in **Figure 6**. The GISS model predicts a warmer, more humid environment, with relatively uniform increases in temperature, wind, and humidity.

Figures 17 and **18** show difference surfaces ($2\times CO_2$ – HistoricalClimate) for $E_{T,P}$ calculated from conditions predicted by the GFDL and GISS $2\times CO_2$ GCM runs and $E_{T,P}$ calculated for historical climate conditions. Both models predict increases in spring and summer $E_{T,P}$ for the $2\times CO_2$ conditions. The GFDL model shows increased $E_{T,P}$ in California's Central Valley, while the GISS model shows increased $E_{T,P}$ in southern Florida. Though the GFDL model shows large increases in $E_{T,P}$ during summer, while the GISS model show only modest increases, both models show increase in $E_{T,P}$ in the midwestern grain-belt during spring and summer growing seasons.

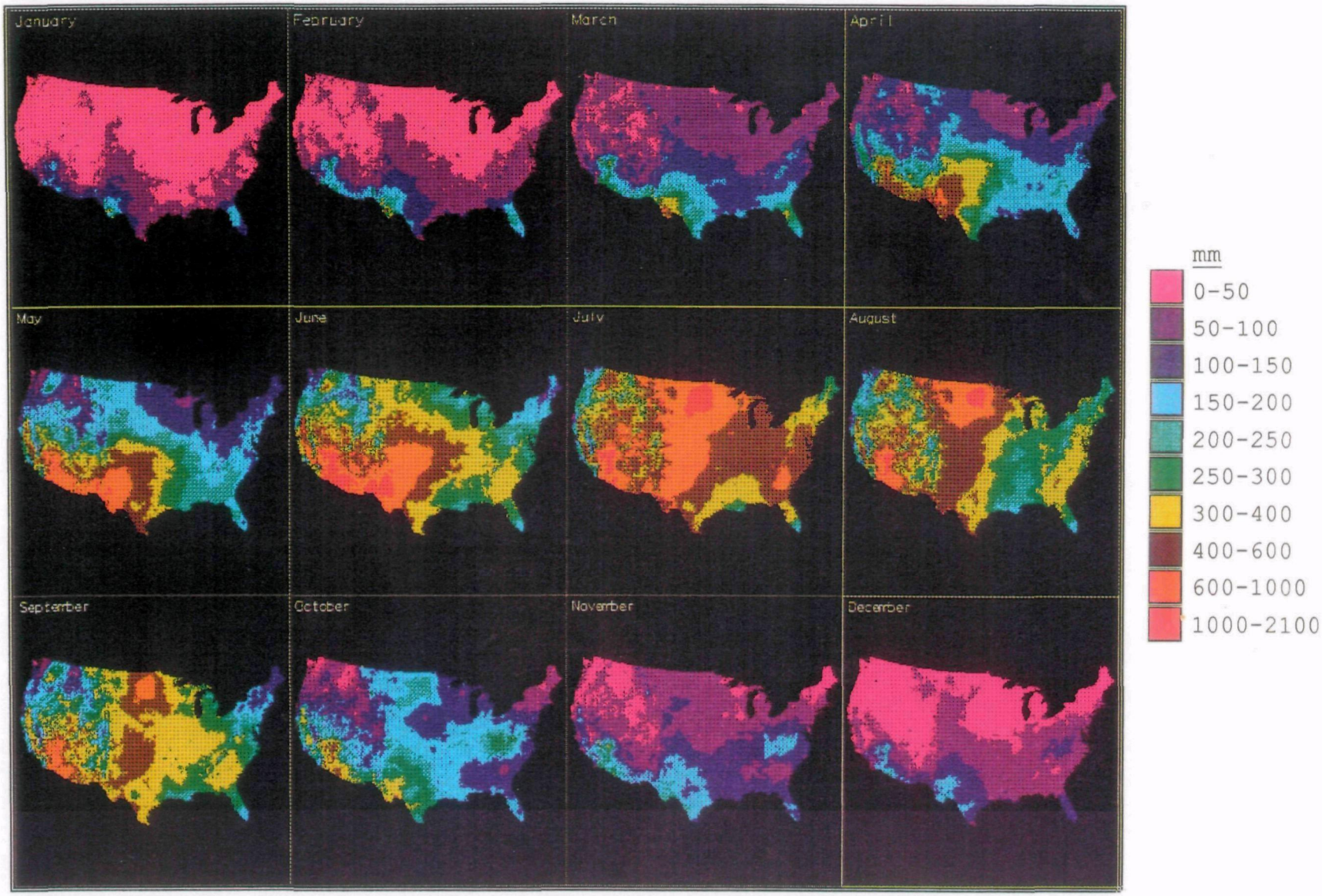

FIGURE 15: Calculated potential evapotranspiration $E_{T,P}$ for conditions predicted by the GFDL model for $2\times CO_2$.

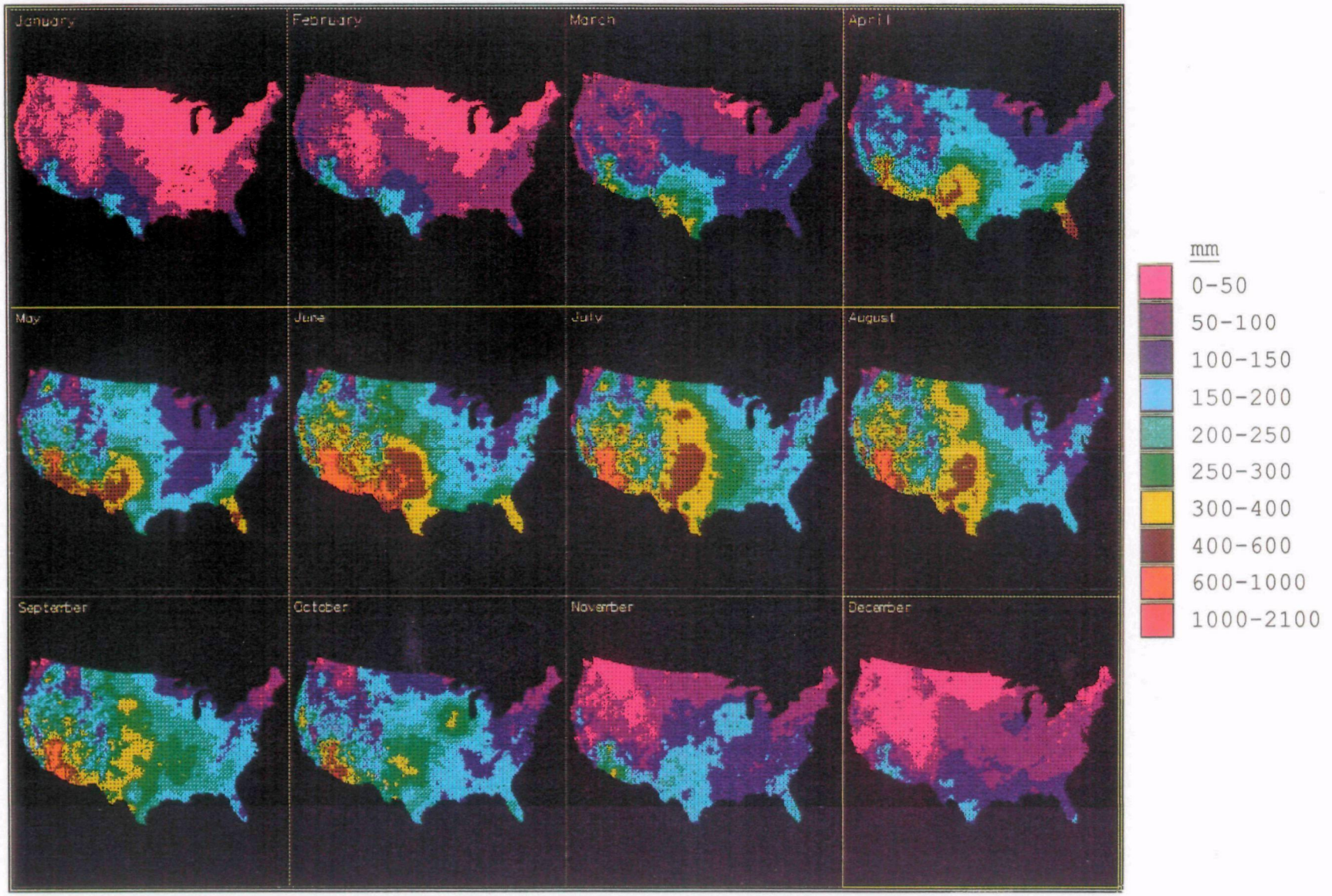

FIGURE 16: Calculated potential evapotranspiration $E_{T,P}$ for conditions predicted by the GISS model for $2\times CO_2$.

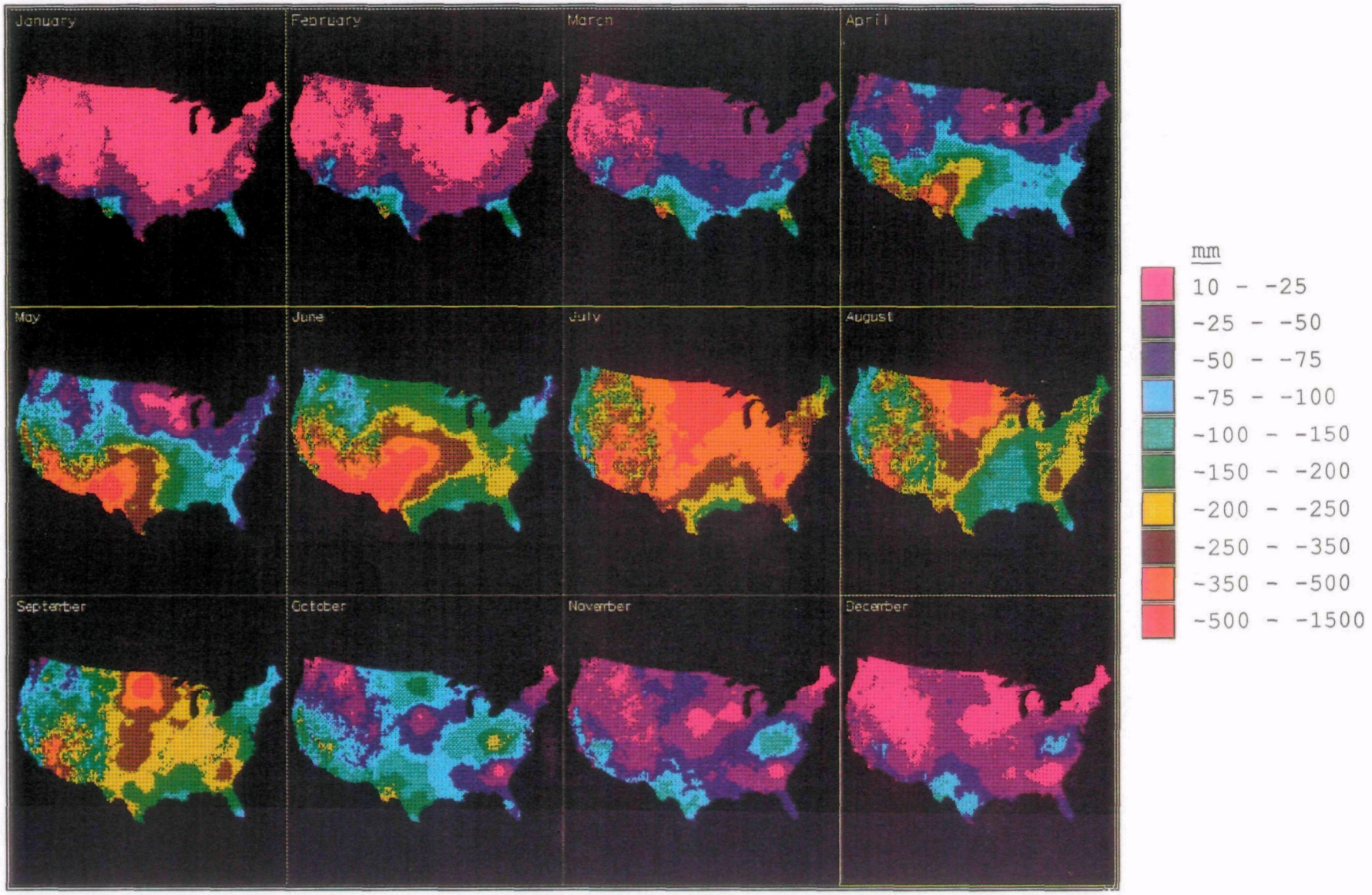

FIGURE 17: Difference Between 2×CO_2 and historical climate preditions of $E_{T,P}$ for the GFDL model..

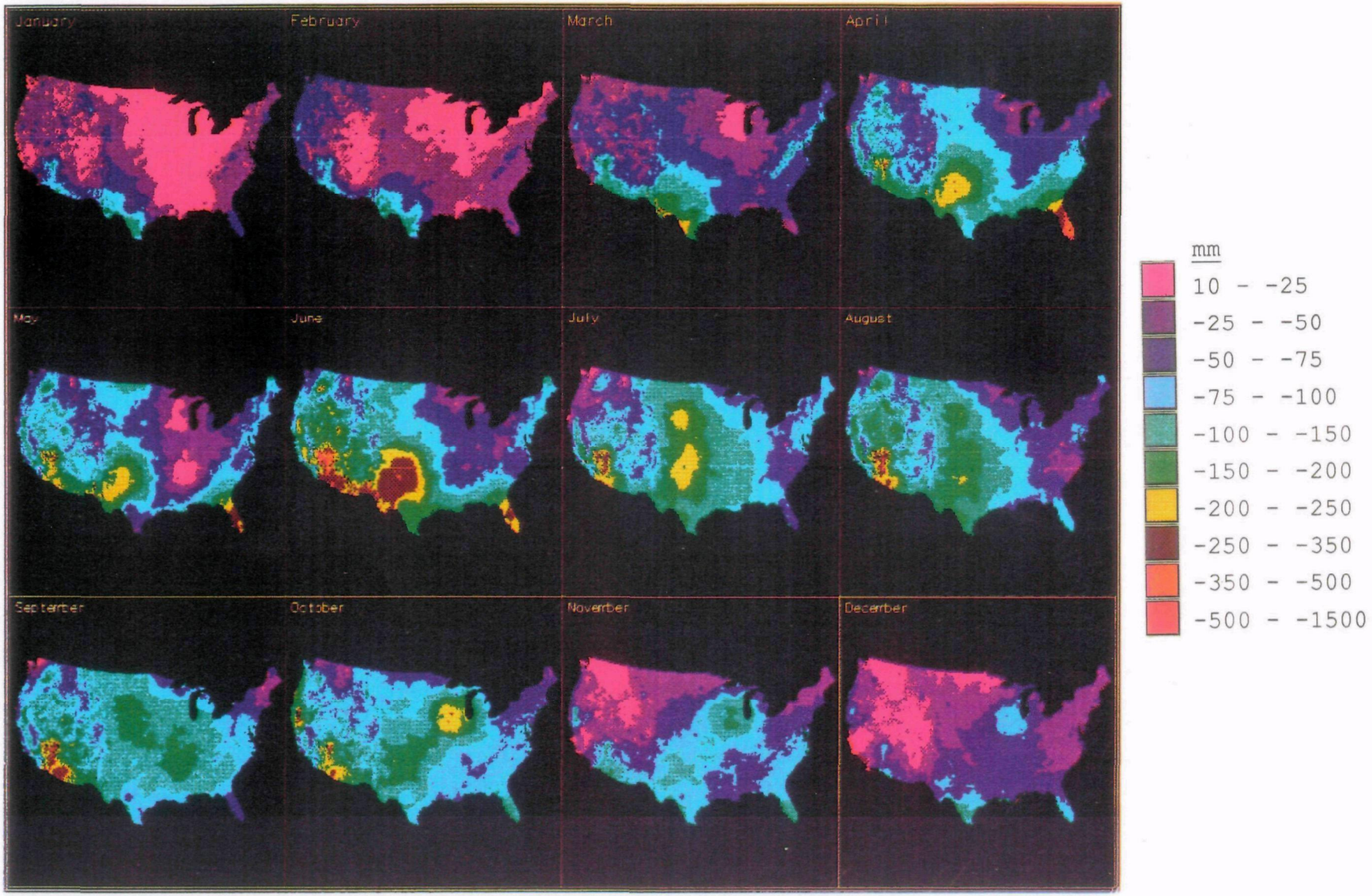

FIGURE 18: Difference Between 2×CO_2 and historical climate predictions for the GISS model.

6. DISCUSSION

The distribution of air and surface temperature, humidity, and wind are strongly affected by topographic structure [*Marks*, 1988; *Dozier, et al.*, 1988]. The detail of topographic structure shown in **Figure 1** illustrates variability of topography across the continental U.S. The $10\,km$ grid resolution for DEM shows significant topographic detail for continental-scale analysis, while keeping the number of grid points (≈140,000) computationally acceptable. The T_a, e_a, and u_{10m} surfaces presented in **Figures 3, 4,** and **5** clearly show that even relatively simple corrections for topographic effects show the topographic influence on the distribution of climatic parameters, and substantially improve our ability to use historic data to estimate these distributions at ecologically meaningful resolutions.

Wind data over the U.S. are limited. The u_{10m} surfaces shown in **Figure 4** are long-term seasonal averages derived from unspecified periods during the last 40 years. Monthly wind surfaces would be more compatible with the T_a and e_a surfaces. Hopefully, such data will be available in the near future.

$E_{T,P}$ calculated from these data surfaces, using the turbulent transfer model show increases into the southwestern U.S. starting in spring, with maximum $E_{T,P}$ occurring during summer, and dominating the western U.S. This is contrary to the result when $E_{T,P}$ is estimated using a temperature-regression approach such as *Thornthwaite* [1948] (**Figure 14**) which doesn't account for either wind or humidity gradients. At large scales, where wind and humidity vary considerably, the temperature-regression approach shows a strong temperature bias, and gives an incorrect result showing $E_{T,P}$ maximized in the southeastern U.S. during July. The relationship between temperature and $E_{T,P}$ is weak, at best, as shown in Eqs. 3, 4, and 6. Clearly, for analysis at large regional to continental scales, where humidity and wind will vary considerably, it is important to use a model of $E_{T,P}$ which is based on the variation of humidity and wind.

Temperature-regression methods were developed primarily for application over agricultural areas, where the assumption of uniform humidity and wind conditions were reasonable. They were not designed for application under changing climatic conditions and should not be used for large regional or continental scale analysis, where these assumptions are unrealistic. In the late 1940's, climatological databases did not exist, nor did the the technology to process and display them. The analysis presented in this paper required 10^9 bytes of data storage, and computer processing capabilities approaching that of a super computer. Even a few years ago, this would have required affiliation with a major computer research facility, such as NCAR, GFDL, or GISS, where most GCM research has been conducted. The combined power and storage of networked, desk-top workstations, has made this type of analysis possible at relatively low cost, without the specialized technical support required for GCM runs.

Figures 7 thru **12** show T_a, e_a, and u_{10m} surfaces for predicted $2\times CO_2$ conditions for the GFDL and GISS GCM models. As is shown in **Figure 6**, T_a and e_a differences between the models are slight, but differences in u_{10m} are large. The GFDL model predicts warmer, drier, and much windier conditions during summer, while the GISS model predicts warmer, wetter, and less windy conditions during the same time of year. These differences have a profound effect on the calculated summer $E_{T,P}$, as shown in **Figures 15** thru **18**. $E_{T,P}$ calculated from the GFDL model conditions is extremely high in summer, while GISS model predicts $E_{T,P}$ that is only slightly higher than the base conditions predicted from the historical data.

Similar results were reported by *Martin, et al.*, [1990] from their analysis using very similar methods to predict actual E_T on a grassland, a wheat field, and a forest, for current climate conditions, and $2\times CO_2$ conditions predicted by the GISS and GFDL GCMs. If the GISS scenario were realized, there would be an impact on vegetation and agriculture in the U.S. If the GFDL scenario were realized, much of the agricultural grain-belt of the mid-western U.S. would be desicated by increased evaporative demand. This could have profound implications on the economy of the United States, as reported by *Smith and Tirpak*, [1989]. Until more realistic feedbacks between terrestrial ecosystems and the climate system are built into the GCMs, it will be impossible to achieve better agreement between the models, or to use GCM predictions to estimate the likely ecological consequences of climate change.

There is considerable uncertainty in the absolute magnitude of these calculations. There is no way to verify the accuracy of the T_a, e_a, or u_{10m} surfaces for either the current or $2\times CO_2$ conditions. The elevation-correction methods and interpolation method discussed above maintain the original data points, however, so only the distribution between points is uncertain. The turbulent transfer model has been tested [*Stewart*, 1982] and verified [*Marks*, 1988] over snow where both the surface temperature and vapor pressure, and the scaling parameters can be measured or approximated. For continental scale applications over heterogeneous surfaces that are not well characterized, uncertainty in the scaling parameters, a_E, k, and z_0, over a large region, could cause uncertainty in the magnitude of $E_{T,P}$, as could approximating the surface temperature from the average monthly air temperature. The basic trends in the spatial distribution of $E_{T,P}$ should not change, however.

In general, the magnitudes of $E_{T,P}$ shown for the base case in **Figure 13** are in agreement with other estimates over regions of similar size cited below. † If similar methods can be used to estimate the distribution of surface temperature, net radiation, precipitation, and soil moisture over the U.S., then it will be possible to compute a water balance surface for the U.S. which can be used verify the evaporation calculations. For purposes of this analysis, I have emphasized discussion of the spatial distribution of $E_{T,P}$ shown in the surfaces, rather than the predicted magnitude.

Potential evapotranspiration $E_{T,P}$ has been used to estimate vegetation stress and soil moisture depletion by many investigators, using the regression of T_a and measured evaporation [*Thornthwaite*, 1948; *Holdridge*, 1967; *Mather and Yoshioka*, 1968; *Woodward*, 1987; and drought [*Palmer*, 1965; *Shugart*, 1984; *Solomon*, 1986]. This approach may work when it is limited to a brief time period, and to a small field or region, where wind and humidity can be assumed constant, but it is not appropriate for application over a large region. It is particularly problematic for climate change analysis, where, as shown in **Figure 6**, variations in wind and humidity may in sharp contrast to variations in air temperature. Based on differences in temperature alone, we would not expect $E_{T,P}$ to be very different for the GISS and GFDL predictions.

---

†: This isn't a valid comparison, however, because the other estimates are based on temperature-regression methods of calculating $E_{T,P}$.

7. CONCLUSIONS

This analysis shows the importance of topographic structure in estimating the distribution of meteorological parameters over large areas. Elevation corrected surfaces of the temporal and spatial distribution of T_a, e_a, and u_{10m}, determined from historical data for the U.S. are generated at a 10 km grid spacing. Using these surfaces as a base condition, changes predicted by the GISS and GFDL GCMs can also be mapped over the U.S. The predicted GFDL and GISS surfaces for T_a and e_a are representative of what may be expected to occur under a $2\times CO_2$ climate.

Wind surfaces are more difficult to estimate from historical data, and GCM predictions of wind appear less stable and reliable than temperature or humidity. Erratic variations in wind from one season to the next cause uncertainty in the predicted $2\times CO_2$ u_{10m} surfaces. It is difficult to determine if this is because of the seasonal aggregation, or because GCM wind predictions are more closely related to the atmospheric dynamics of the models than to surface conditions. A monthly time-series of wind data would be desirable for this type of analysis, as would improved GCM wind predictions.

The calculations of $E_{T,P}$ by the turbulent transfer model are substantially different from previous estimates of $E_{T,P}$ based on temperature-regression approaches. Base case calculations of $E_{T,P}$ show maximum evaporative stress during summer over the western U.S., in strong contrast to the maximum shown over the southeastern U.S. by the temperature-regression methods. This discrepancy illustrates the poor relationship between air temperature and evaporation shown in Eqs. 3, 4, and 6. It also points out that a regression relationship between two physically unrelated parameters is likely to be inconsistent over an area as large as the U.S. It is essential that regional to continental-scale estimates of $E_{T,P}$ be based on estimates of wind speed and humidity gradients.

The $E_{T,P}$ surfaces calculated for predicted $2\times CO_2$ conditions show an increase in evaporative stress in the western and midwestern U.S. The GFDL model predicts conditions that would severely impact the agriculture of the midwestern grain-belt of the U.S. To verify these calculations, and improve our confidence in the magnitudes of the estimated $E_{T,P}$, we must 1) improve our ability to estimate the distribution of climatic parameters over large regions, accounting for topographic effects (this is particularly important in regard to development of a synoptic wind database which is at a monthly time-scale); 2) include surface temperature T_s, derived from satellite data, to make the estimate of $E_{T,P}$ more realistic, and to allow evaluation of sensible H and latent L_vE as well as $E_{T,P}$; 3) incorporate synoptic vegetation patterns into the turbulent transfer model, to account for the distribution of surface roughness, stomatal resistance, and leaf area index (LAI) [*Martin, et al.*, 1990]; 4) test the model and a daily time-step for selected years of particular climatic interest, such as the 1988 drought, or selected flood years.

This analysis of $E_{T,P}$ sensitivity is the first step toward a comprehensive evaluation of the energy and mass balance over a continent at a spatial resolution that is ecologically and hydrologically meaningful. It will lead to a better understanding of the interactions between climatic conditions and surface processes, and feedbacks between regional processes and vegetation and the climate system under current and $2\times CO_2$ conditions.

8. REFERENCES

Baumgartner, A. and E. Reichel, *The World Water Balance*, 179 pp., Elsevier Scientific Publications, Amsterdam, 1975.

Beaty, C. B., Sublimation or melting: observations from the White Mountains, California and Nevada, U.S.A., *Journal of Glaciology, 14*, 275-286, 1975.

Benton, G. S., R. T. Blackburn, and V. O. Snead, The role of the atmosphere in the hydrologic cycle, *EOS Transactions of the American Geophysical Union, 31*, 61-73, 1950.

Botkin, D. B., J. F. Janak, and J. R. Wallis, Some ecological consequences of a computer model of forest growth, *Journal of Ecology, 60*, 849-872, 1972.

Broecker, W. S., Unpleasant surprises in the greenhouse?, *Nature, 329*, 123-126, 1987.

Brutsaert, W., *Evaporation into the Atmosphere*, 299 pp., D. Reidel, Dordrecht, 1982.

Brutsaert, W., Catchment-scale evaporation and the atmospheric boundary layer, *Water Resources Research, 22*, 39S-45S, 1986.

Budyko, M. I., *Climate and Life*, 508 pp., Academic Press, New York, 1974.

Budyko, M. I. and O. A. Drozdov, Characteristics of the moisture circulation in the atmosphere, *Izv. Akad. Nauk SSSR, 4*, 5-14, 1953.

Businger, J. A., J. C. Wyngaard, Y. Izumi, and E. F. Bradley, Flux-profile relationships in the atmospheric surface layer, *Journal of the Atmospheric Sciences, 28*, 181-189, 1971.

Byers, H. R., *General Meteorology*, vol. Fourth Edition, 461 pp., McGraw-Hill, New York, 1974.

Campbell, W. G., D. Marks, J. J. Kineman, and R. T. Lozar, A geographic database for modeling the role of the biosphere in climate change, *submitted to Climatic Change*, (1990).

Center, National Oceanographic and Atmospheric Administration, National Geophysical Data, *Geophysics of North America: Users Guide*, U.S. Department of Commerce, Boulder, Colorado, 1989.

Chamberlain, A. C., Transport of gasses to and from grass and grass-like surfaces, *Proceedings of the Royal Society of London, A290*, 236-265, 1966.

Davis, R. E., J. Dozier, and D. Marks, Micrometeorological measurements and instrumentation in support of remote sensing observations of an alpine snow cover, *Proceedings of the Western Snow Conference, 51*, 161-164, 1984.

Dickinson, R. E., Land surface processes and climate--Surface albedos and energy balance, *Advances in Geophysics, 25*, 305-353, 1983.

Dickinson, R. E. and R. J. Cicerone, Future global warming from atmospheric trace gasses, *Nature, 319*, 109-115, 1986.

Dickinson, R. E. and B. Hanson, Vegetation-albedo feedbacks, in *Climate Processes and Climate Sensitivity*, edited by J. E. Hansen and T. Takahashi, Geophysical Monograph, vol. 5, pp. 180-187,

American Geophysical Union, Washington, D.C., 1984.

Dozier, J., J. M. Melack, D. Marks, K. Elder, R. Kattlemann, and M. Williams, Snow deposition, melt, runoff, and chemistry in a small alpine watershed, Emerald Lake basin, Sequoia National Park, *Final Report, CARB Contract A3-106-32*, 367 pp., Computer Systems Laboratory, University of California, Santa Barbara, CA, 1988.

Eagleman, J. R., *The Visualization of Climate*, Heath, Lexington, Mass, 1976.

Eagleson, P. S., Climate, soil, and vegetation I. Introduction to water balance dynamics, *Water Resources Research, 14*, 705-712, 1978.

Eagleson, P. S., Land Surface Processes in Atmospheric General Circulation Models, in *Proceedings of Greenbelt Study Conference*, p. 560, Cambridge University Press, New York, 1982.

Eagleson, P. S., The emergence of global-scale hydrology, *Water Resources Research, 22*, 6S-14S, 1986.

Eagleson, P. S. and R. I. Segarra, Water-limited equilibrium of savanna vegetation systems, *Water Resources Research, 21*, 1483-1493, 1985.

Elliott, D. L., C. G. Holladay, W. R. Barchet, H. P. Foote, and W. F. Sandusky, *Wind Energy Resource Atlas*, Solar Technical Information Program, 210 pp., U.S. Department of Energy, 1987.

Eubank, R. L., *Spline Smoothing and Nonparametric Regression*, Statistics: Textbooks and Monographs, vol. 90, 455 pp., Marcel-Dekker, New York, 1989.

Fichtl, G. H. and G. E. McVehil, Longitudinal and lateral spectra of turbulence in the atmospheric boundary layer at Kennedy Space Center, *Journal of Applied Meteorology, 9*, 51-63, 1970.

Fleagle, R. G. and J. A. Businger, *An Introduction to Atmospheric Physics*, 2nd ed., 432 pp., Academic Press, New York, 1980.

Frew, J. E., The Image Processing Workbench, Ph.D. Thesis, 382 pp., Department of Geography, University of California, Santa Barbara, CA, 1990.

Gates, W. L., The use of general circulation models in the analysis of the ecosystem impacts of climatic change, in *Report of the Study Conference on Sensitivity of Ecosystems and Society to Climatic Change*, World Climatological Impact Study Program, World Meteorological Organization, Geneva, 1983.

Hansen, J., I. Fung, A. Lacis, D. Rind, S. Lebedeff, R. Ruedy, and G. Russell, Global climate changes as forecast by Goddard Institute for Space Studies three dimensional model, *Journal of Geophysical Research, 93D*, 9341-9364, 1988.

Hansen, J., A. Lacis, D. Rind, G. Russell, P. Stone, I. Fung, R. Ruedy, and J. Lerner, Climate sensitivity, analysis of feedback mechanisms, in *Climate Processes and Climate Sensitivity*, edited by J. E. Hansen and T. Takahashi, Geophysical Monograph, vol. 5, pp. 130-163, American Geophysical Union, Washington, D.C., 1984.

Holdridge, L. R., Determination of world formulations from simple climatic data, *Science, 105*, 367-368, 1947.

Holdridge, L. R., *Life Zone Ecology*, Tropical Science Center, San Jose, Costa Rica, 1967.

Isaaks, E. H. and R. M. Srivastava, *Applied Geostatistics*, 561 pp., Oxford University Press, New York, 1989.

Jenne, R. L., *The NMC Octagonal Grid*, National Center for Atmospheric Research, Boulder, CO, 1970.

Jenne, R. L., *Data From Climate Models; the CO_2 Warming*, National Center for Atmospheric Research, Boulder, CO, 1990.

Jenne, R. L., D. Joseph, C. Mass, E. Recker, M. Albright, and H. Edmon, *National Meteorological Center Grid Point Data Set, Version II*, Department of Atmospheric Sciences, University of Washington, and National Center for Atmospheric Research, Seattle, WA, 1990.

Karl, T. R., C. N. Williams, F. T. Quinlan, and T. A. Boden, *United States Historical Climatology Network (HCN) Serial Temperature and Precipitation Data*, 391 pp., U.S. Department of Energy, Carbon Dioxide Information Anslysis Center, Oak Ridge, TN, 1990.

Keeling, C. D., Industrial production of carbon dioxide from fossil fuels and limestone, *Tellus, 25*, 174-198, 1973.

Keeling, C. D. and R. B. Bacastow, Impact of industrial gasses on climate, in *Energy and Climate*, pp. 72-95, National Academy of Sciences, Washington, D.C., 1977.

Kondo, J., Observations on wind and temperature profiles near the ground, *Science Reprints from Tohoku University, 14*, 91-124, 1962.

Korzoun, V. I., *Atlas of World Water Balance*, USSR National Committee for the International Decade, UNESCO Press, Paris, 1977.

Korzun, V. I., *World water balance and water resources of the earth*, USSR National Committee for the International Decade, 663 pp., UNESCO Press, Paris, 1978.

Kramer, P. J., *Water Relations of Plants*, 489 pp., Academic Press, San Diego, 1983.

Larcher, W., *Physiological Plant Ecology*, 303 pp., Springer-Verlag, New York, 1980.

Legates, D. R. and C. J. Willmott, Mean seasonal and spatial variability in global surface air temperature, *Theoretical and Applied Climatology, 41*, 11-21, 1990.

Lettau, H., K. Lettau, and L. C. B. Molion, Amazonia's hydrologic cycle and the role of atmospheric recycling in assessing deforestation effects, *Monthly Weather Review, 107*, 227-237, 1979.

Lettenmaier, D. P. and S. J. Burges, Climate change: Detection and its impact on hydrologic design, *Water Resources Research, 14*, 679-687, 1978.

Lettenmaier, D. P. and T. Y. Gan, Hydrologic sensitivities of the Sacramento-San Joaquin river basin, California, to global warming, *Water Resources Research, 26*, 69-87, 1990.

Lettenmaier, D. P. and D. P. Sheer, Assessing the effects of global warming on water resources systems: An application to the Sacramento-San Joaquin River Basin, California, *Journal of Water Resources Planning and Management (in press)*, (February, 1991).

Manabe, S. and R. T. Wetherald, The effects of doubling the CO_2 concentration on the climate of a general circulation model, *Journal of Atmospheric Sciences, 32*, 3-15, 1975.

Manabe, S. and R. T. Wetherald, On the distribution of climate change resulting from an increase in CO_2 content of the atmosphere, *Journal of Atmospheric Sciences, 37*, 99-118, 1980.

Marks, D., Climate, energy exchange, and snowmelt in Emerald Lake watershed, Sierra Nevada, Ph.D. Dissertation, 158 pp., Departments of Geography and Mechanical Engineering, University of California, Santa Barbara, CA, 1988.

Marks, D. and J. Dozier, Climate and energy exchange at the snow surface in the alpine region of the Sierra Nevada, *(submitted to Water Resources Research)*, (1990).

Marks, D. and J. Dozier, A clear-sky longwave radiation model for remote alpine areas, *Archiv für Meteorologie, Geophysik und Bioklimatologie, Series B, 27*, 159-187, 1979.

Martin, P., N. J. Rosenberg, and M. S. McKenney, Sensitivity of evapotranspiration in a wheat field, a forest, and a grassland to changes in climate and direct effects of carbon dioxide, *Climatic Change, 14*, 111-117, 1990.

Mather, J. R. and G. A. Yoshioka, The role of climate in the distribution of vegetation, *Annals of the American Association of Geographers, 58*, 29-41, 1968.

Palmer, W. C., *Meteorological Drought*, Research Paper, U.S. Weather Bureau, Washington, D.C., 1965.

Parry, M. L. and T. R. Carter, An assessment of the effects of climatic change on agriculture, *Climatic Change, 15*, 95-116, 1989.

Parry, M. T., T. R. Carter, N. Konijin, and J. Lockwood, The impact of climatic variations on agriculture, in *Introduction to the IIASA/UNEP Case Studies in Semi-Arid Regions*, International Institute for Applied Systems Analysis, Laxenburg, Austria, 1987.

Perrier, A., Land surface processes: vegetation, in *Land Surface Processes in Atmospheric General Circulation Models*, Proceedings of Greenbelt Study Conference, Cambridge University Press, New York, 1982.

Quinlan, F. T., T. R. Karl, and C. N. Williams, *United States Historical Climatology Network (HCN) Serial Temperature and Precipitation Data*, 160 pp., U.S. Department of Energy, Carbon Dioxide Information Anslysis Center, Oak Ridge, TN, 1987.

Ramanathan, V. R., R. J. Cicerone, H. B. Singh, and J. T. Kiehl, Trace gas trends and their potential role in climate change, *Journal of Geophysical Research, 90*, 5547-5566, 1985.

Rind, D., The influence of vegetation on the hydrologic cycle in a global climate model, in *Climate Processes and Climate Sensitivity*, edited by J. E. Hansen and T. Takahashi, Geophysical

Monograph, vol. 5, pp. 73-92, American Geophysical Union, Washington, D.C., 1984.

Rind, D., R. Goldberg, J. Hansen, C. Rosenzweig, and R. Ruedy, Potential evapotranspiration and the likelihood of future drought, *Journal of Geophysical Research, 95*, 9983-10005, 1990.

Rosenzweig, C. and R. Dickinson, *Climate-Vegetation Interactions*, Workshop Proceedings , 156 pp., NASA/Goddard Space Flight Center, 1986.

Salati, E. and P. Vose, The Amazon basin: a system in equilibrium, *Science, 225*, 129-138, 1984.

Schlesinger, M. E., Quantitative analysis of feedbacks in climate model simulations of CO_2-induced warming, in *Physically-Based Modelling and Simulation of Climate and Climatic Change*, edited by M. E. Schlesinger, C: Mathematical and Physical Sciences; NATO ASI Series, vol. 243, pp. 653-737, Kluwer, Boston, 1988.

Shugart, H. H., *A Theory of Forest Dynamics*, 278 pp., Springer-Verlag, New York, 1984.

Shugart, H. H. and D. C. West, Development of an appalachian deciduous forest succession model and its application to assessment of the impact of the chestnut blight, *Journal of Environmental Management, 5*, 161-179, 1977.

Shukla, J. and Y. Mintz, Influence of land-surface evapotranspiration on the Earth's climate, *Science, 215*, 1498-1501, 1982.

Smith, J. B. and D. A. Tirpak, *The Potential Effects of Global Climate Change on the United States*, Report to Congress, vol. PM-221, 412 pp., United States Environmental Protection Agency, Washington, D.C., 1989.

Snyder, J. P. and P. M. Voxland, *An Album of Map Projections*, Professional Paper, 249 pp., U.S. Geological Survey, 1989.

Solomon, A. M., Transient response of forests to CO_2-induced climate change: Simulation modeling experiments in eastern North America, *Oecologia, 68*, 567-579, 1986.

Spangler, W. M. L. and R. L. Jenne, *World Monthly Surface Station Climatology (and Associated Datasets)*, National Center for Atmospheric Research, Boulder, CO, 1989.

Stephenson, N. L., Climatic control of vegetation distribution: the role of the water balance, *submitted to American Naturalist*, (1989).

Stewart, B. J., Sensitivity and significance of turbulent energy exchange over an alpine snow surface, M.A. Thesis, 41 pp., Department of Geography, University of California, Santa Barbara, CA, 1982.

Strain, B. R., Physiological and ecological controls on carbon sequestering in terrestrial ecosystems, *Biogeochemistry, 1*, 219-232, 1985.

Sutton, O. G., *Micrometeorology*, 333 pp., McGraw-Hill, New York, 1953.

Thompson, S. L. and S. H. Schneider, Carbon dioxide and climate: The importance of realistic geography in estimating the transient temperature response, *Science, 217*, 1031-1033, 1982.

Thornthwaite, C. W., An approach toward a rational classification of climate, *Geographic Review*, *38*, 55-89, 1948.

Thornthwaite, C. W. and J. R. Mather, *The Water Balance*, Publications in Climatology, vol. 8, 104 pp., Laboratory of Climatology, 1955.

U.S. Army Corps of Engineers, *GRASS Users and Programmers Manual*, U.S. Army Corps of Engineers, Construction Engineering Research Laboratory, Champagne, IL, 1988.

WeatherDisc Associates, Inc., *World WeatherDisc: Climate Data for the Planet Earth*, WeatherDisc Associates, Inc., Seattle, WA, 1990.

Whittaker, R. H., *Communities and Ecosystems*, MacMillian, New York, 1975.

Woodward, F. I., *Climate and Plant Distribution*, Cambridge, New York, 1987.

Characterizing the Distribution of Precipitation Over the Continental United States Using Historical Data

JAYNE DOLPH
DANNY MARKS

NSI Technology Services, Inc.

U.S. Environmental Protection Agency
Environmental Research Laboratory
200 S.W. 35th Street
Corvallis, OR 97333
(503) 757-4657

Abstract

Characterizing the distribution of precipitation at regional scales is a requirement for the development of regional scale, spatially distributed hydrologic water balance models. This study performs a preliminary assessment of the utility and limitations of historical hydro-meteorological data for providing spatially distributed precipitation estimates at large scales. The historical data are used in a spatial analysis to characterize regional patterns of precipitation and runoff across the continental United States. Precipitation and runoff "surfaces" generated from interpolation of point measurements capture broad regional patterns. A distributed water balance is calculated over the continent using long-term (1948 -1988) and seven-year (1982 -1988) annual average values to check the reliability of precipitation estimates. The resulting "input-output surfaces" illustrate the deficiency (low elevation bias) of historical precipitation measurements in the mountainous western United States where snowmelt is an important component of the annual runoff. The incorporation of high elevation snow measurements into the precipitation record for the seven-year average significantly improves the water budget in these regions and enhances the utility of historical data for providing distributed precipitation estimates at regional and continental scales. The analysis presented in this study is exploratory in nature, and will ultimately have implications for the development of large scale hydrological and ecological modeling and climate change research.

1. Introduction

Spatially distributed hydrological and ecological analyses are required to assess the effects of climate change on water resources and vegetation (Eagleson, 1986; Dooge, 1986; Neilson et al., 1989). The development of spatially distributed models requires spatially distributed precipitation estimates at regional[1] to continental scales. What is not well understood is whether historical data can be used effectively to characterize large scale precipitation patterns and thereby provide the necessary input to spatially distributed models. This study provides a preliminary assessment of the utility of historical data for providing spatially distributed, large scale precipitation estimates, and is the first step in characterizing surface hydrology at scales compatible with climate change research.

The global hydrologic cycle is an important component of the coupled ocean-atmosphere-land surface system. It contributes to atmospheric circulation and exerts a strong influence on weather and climate. Global climate change, predicted to occur due to increasing concentrations of green-house gases in the atmosphere, will cause changes in the earth's hydrologic cycle (Smith and Tirpak, 1989). These changes may significantly alter physical processes of the terrestrial biosphere, because changes in hydrologic regimes directly affect land surface properties such as soil moisture, vegetation health and distribution, and surface albedo (Rasmusson et al., 1990; Hall et al., 1988; Hansen et al., 1984; Rind, 1984; Shugart and West, 1977).

[1] For this study, "regional" refers to areas on the order of roughly 50,000 to 500,000 km^2, or approximately the size of one water resources region as defined by the US Water Resources Council (1978).

A major uncertainty at this time is the effect that climate change will have on regional hydrology and the distribution of biomes (e.g. Dooge, 1990; Neilson et al., 1989). In particular, it is not well understood how the spatial patterns and seasonality of precipitation may change. While much research has been directed toward understanding historical temperature records (eg. Hanson and Lebedeff, 1987; Jones et al., 1986; Wigley et al., 1985), relatively little attention has been given to large-scale precipitation patterns.

Presently, the only tool for predicting the effects of climate change on physical processes at large scales is the General Circulation Model (GCM). GCMs are global scale numerical models of atmospheric circulation that simulate the fundamental physical relationships of the ocean-atmosphere-land surface system (Manabe and Wetherald, 1975; Hansen et al., 1988; Dickinson and Cicerone, 1986). GCMs predict that global precipitation is likely to increase (e.g. Smith and Tirpak, 1989), but it is not clear how regional precipitation patterns will be affected. Furthermore, the geographical distribution of predicted change differs from model to model (Schlesinger and Mitchell, 1987; Rind 1988). These inconsistencies are due, in part, to the unrealistic parameterization of land surface processes in the models which is a function of their coarse resolution (Eagleson, 1986; Rind et al., 1990). The GCM distributes precipitation uniformly over one grid cell, tens to hundreds of thousands of km^2 in size. However, precipitation is a highly variable process, particularly at large spatial scales, and in topographically diverse regions. Given the simplified treatment of precipitation distribution in these models, their predictions of hydrologic sensitivity to climate change are unreliable. A more realistic representation of the global hydrologic cycle in the models would improve the reliability of precipitation estimates. This improvement requires a better understanding of basic hydrologic phenomena at regional scales (e.g. Eagleson, 1986).

An important step towards improving precipitation estimates for large scale modeling and climate change research is the characterization of past and present spatial distributions of precipitation at regional scales using historical data. This will better link surface hydrology to large scale climatic processes by providing spatially distributed precipitation estimates at resolutions which are ecologically and hydrologically meaningful.

2. Objectives

The objectives of this study are:

1) the development of a comprehensive database of historical precipitation and runoff data for analyses at large scales;

2) a preliminary assessment of the utility of historical precipitation data for characterizing the spatial distribution of precipitation at regional and continental scales using water balance techniques;

3) the identification of those regions where the use of historical precipitation data may be most limited;

4) the recommendation of improvements to the historical data, and alternatives to its use for large scale precipitation estimation.

3. Related Research and Databases

Historical hydro-meteorological data are an important source of information on past and present hydrologic conditions (e.g. Karl and Riebsame, 1989). In the United States, extensive networks of precipitation and runoff measurement sites have been established, and historical data are becoming widely available in digital

form. The development of comprehensive national information bases and data bases has substantially increased the amount of observational information available on hydro-climatic dynamics. The goal of these efforts is primarily inventory-oriented, aimed at data collection and the identification and projection of water resource problems. Thus far, a high-quality geographic database, combining the historical hydro-meteorological data into a single usable form for spatial analysis and modeling at the continental scale has not been developed.

Several studies in recent years have investigated the utility of historical data for describing hydrologic parameters at large scales. Rasmusson (1985) and Ropelewski et al. (1986,1987) have analyzed global precipitation patterns associated with anomalous climate events such as the El Nino Southern Oscillation (ENSO) cycle. Trends in precipitation fluctuations over the northern and southern hemisphere have been studied with the objective of assessing the significance of projected climate change from GCMs as compared with the variability evident in precipitation and temperature records (e.g. Diaz, et al., 1989, Bradley, et al., 1987). Additionally, multi-year fluctuations in temperature and precipitation at the continental scale have been investigated in sensitivity studies to assess the utility of historical data for detecting secular climate change (Karl 1987; Karl and Riebsame, 1989).

These studies have emphasized the need for improved estimates of precipitation at regional scales, and a better understanding of the spatial and temporal variability of land surface processes at resolutions which are hydrologically and ecologically meaningful. As Bradley (1987) points out, the "magnitude of observed trends, their geographic distribution, and differences between seasons need to be examined in more detail.". Initially, this will involve determining the utility and limitations of the historical data for adequately characterizing physical processes

at a variety of spatial scales. Past correlations and empirical relationships describing the spatial distribution and variability of precipitation may be inadequate with climate change conditions because changes are predicted to be more severe and rapid than the historical record indicates (e.g. Hansen et al. 1988). By using historical data to characterize precipitation and runoff patterns at regional to continental scales, we can begin to identify those regions and conditions where historical data are most limited, and where better data networks and more focused research efforts are required.

4. Methods

The approach taken in this study was to utilize Geographic Information System (GIS) technology and historical data to generate "surfaces" that represent the spatial distribution of precipitation and runoff across the continental United States. Distributed water balance techniques were developed using these surfaces to make a preliminary assessment of the utility of historical data to account for the spatial variability of precipitation at the continental scale. The output is spatially distributed, long-term annual average precipitation estimates for the United States.

4.1 Data

Synthesizing the immense volume of historical data at the continental scale is a formidable task, due both to the quantity of data available and data quality uncertainties. Analyzing patterns of precipitation and runoff at this scale requires a substantial amount of data aggregation, manipulation, and quality control. The United States was chosen as the study area for this research because the historical data are abundant, readily available in digital form, and are generally of higher quality than many other parts of the world. The analysis techniques developed here may later be used to characterize precipitation patterns in other regions of

the world, where data may be less reliable.

Historical data were aggregated from existing digital databases and synthesized into a single, geographically-referenced database. Such an effort has only become possible recently with the advent of mass storage devices such as CD-ROM for data collection and storage, improvements in computing efficiency, and the growing availability of GIS technology. These advances have provided the mechanisms necessary to synthesize and analyze historical data in a spatial context.

Runoff Data

Monthly time-series runoff data were obtained from a newly-created hydro-meteorological database for the United States (Wallace et al., in review). The database consists of 1014 unregulated or minimally regulated gauging sites with streamflow data that have been corrected for station moves and missing values. The database was compiled from the EarthInfo (EarthInfo, 1990) database of daily runoff values on CD-ROM which is a digital compilation of the USGS daily and peak values files. Runoff measurements from this database are for the period 1948 to 1988. Figure 1. is a map of gauging station locations and illustrates the spatial distribution of measurement sites across the country.

The historical runoff data used in this analysis had to meet several criteria. The first criterion was a representative range of drainage area sizes so that runoff contributed from large drainage basins and tributary flow from smaller basins would be represented. The drainage area sizes from the database range from

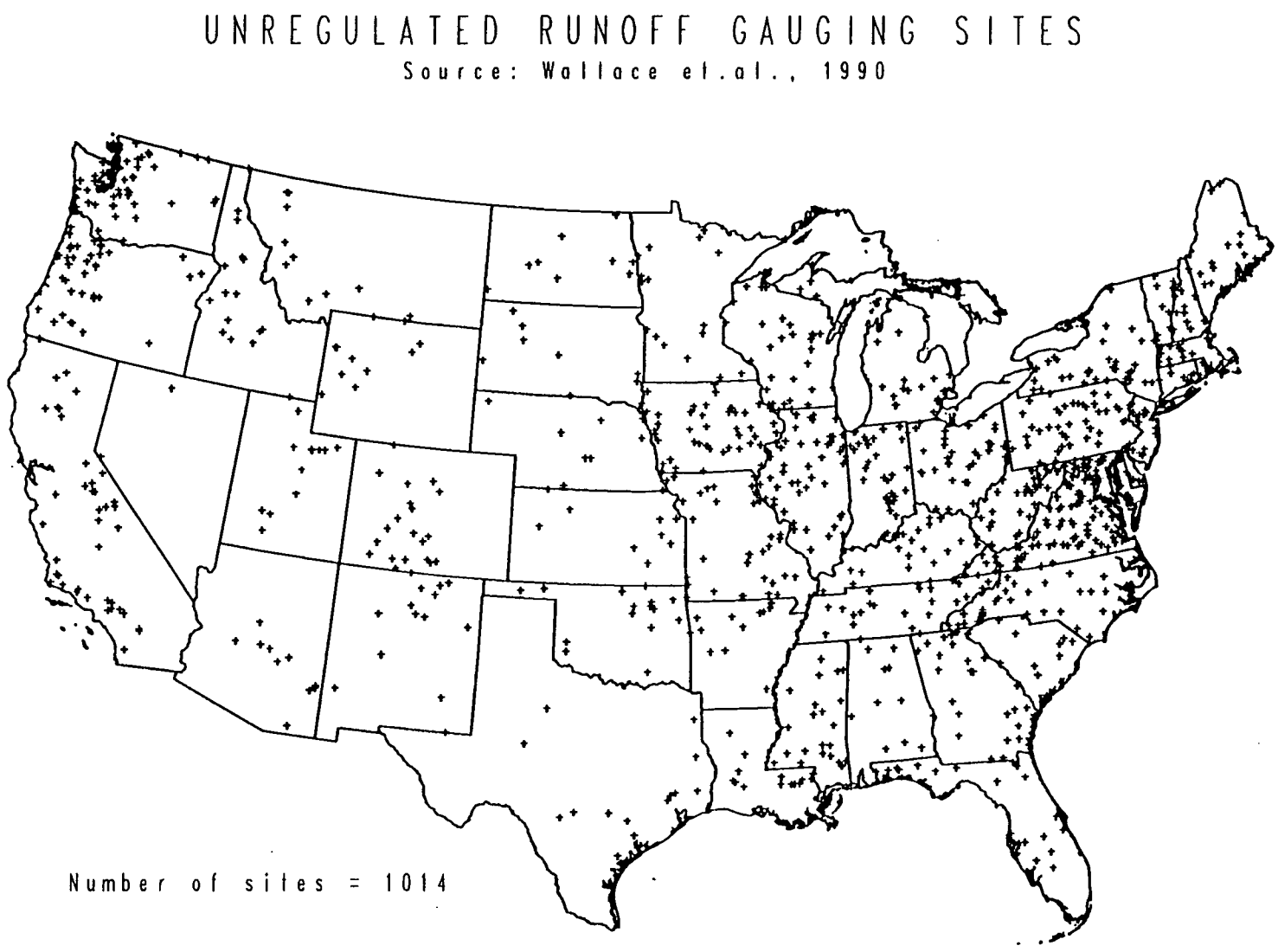

Figure 1. Runoff gauging station location map

4.14 km^2 to 35,224 km^2. Figure 2. is a histogram showing the distribution of drainage area sizes.

The second criterion was that each runoff gauge be operational for a substantial number of years and have a continuous measurement record so that average conditions could be represented. Where discontinuities in runoff records did arise, data filling techniques were used and are described by Wallace, et al. (in review).

Precipitation Data

Precipitation measurements were obtained from the Carbon Dioxide Research Division of the United States Department of Energy and the National Climatic Data Center of NOAA's Historical Climatology Network (HCN) (Quinlan et al., 1987). The HCN data represent a high-quality dataset of monthly precipitation measurements for 1211 stations which are free from anthropogenic and localized effects on precipitation. Each station has a continuous eighty year record and is quality-controlled to account for missing data. The dataset was specifically designed for analyses of climate change at the regional scale (Quinlan et al., 1987).

Figure 3. is a map of station locations showing the spatial distribution of HCN measurement sites across the country. The spatial distribution of HCN stations is adequate across much of the United States, except for the southwest. A greater density of measurement sites in mountainous regions is desirable for characterizing precipitation, because in topographically diverse areas precipitation is highly variable due to orographic influences. Unfortunately most precipitation gauges in the United States are located in low-lying areas. Therefore, mountainous regions are not well represented by the historical data

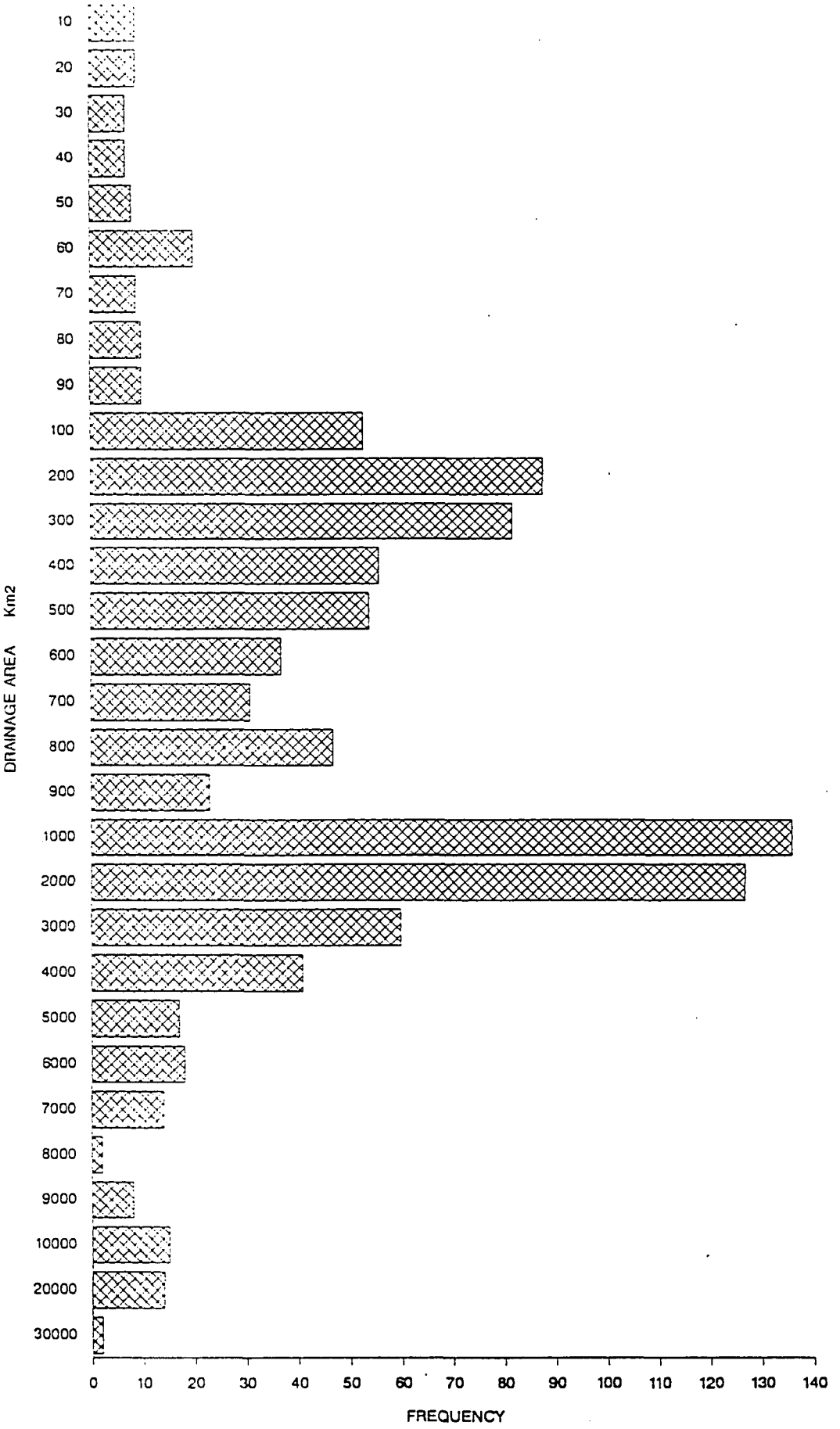

Figure 2. Histogram of runoff gauging station drainage areas

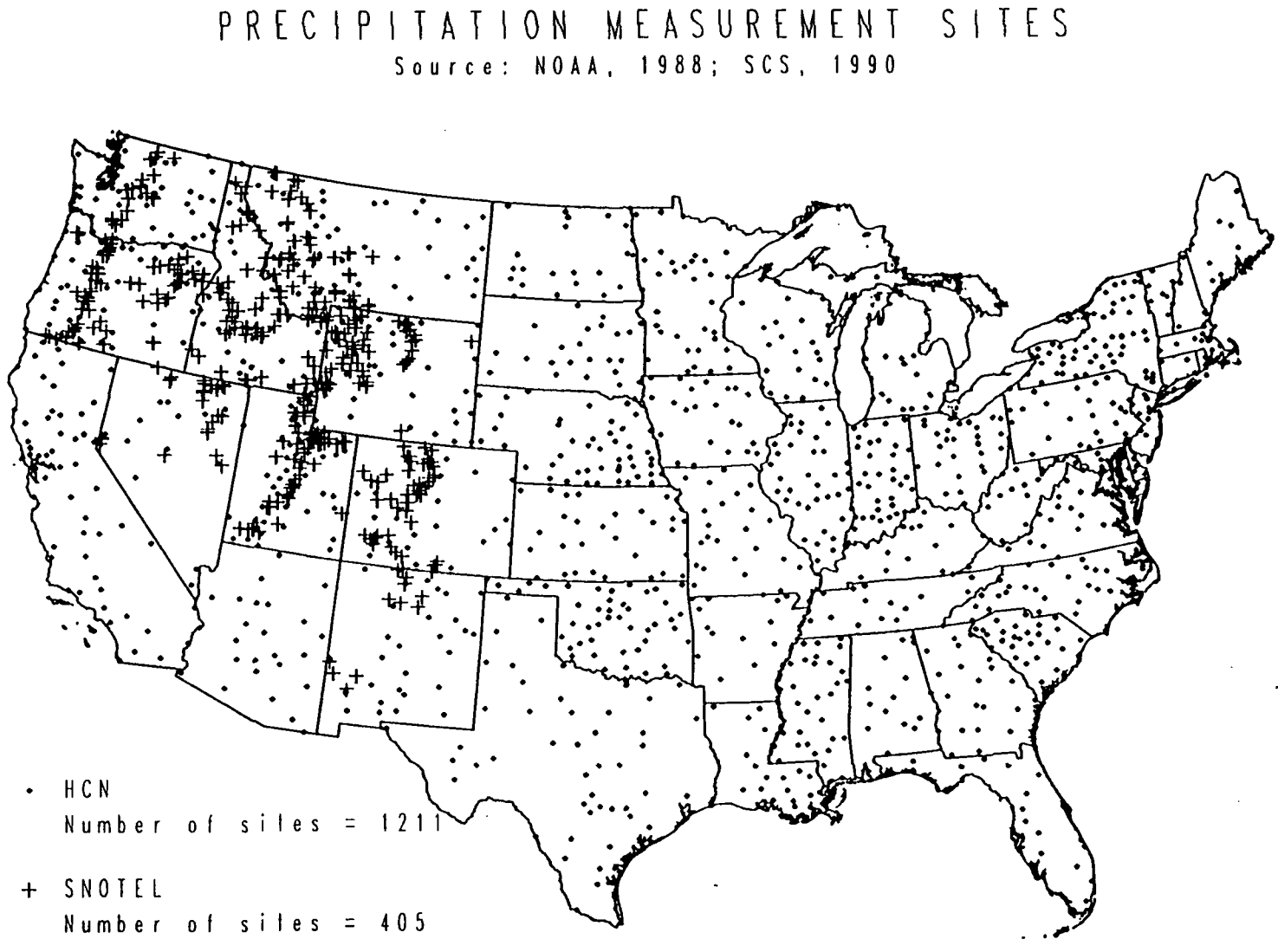

Figure 3. HCN and Snotel station location map

and the density of measurement sites is actually lowest in high elevation areas. HCN data from 1948 - 1987 were used for near-compatibility with the runoff data, as 1988 data was not yet available at the time of this analysis.

Monthly precipitation measurements were also obtained from the Soil Conservation Service's Snotel database (USDA-SCS, 1988) to increase the elevational range of precipitation measurement sites. Snotel measurements are available for twelve states in the western United States and represent snow water equivalent measured at snow course locations. These stations are located in mountainous regions and measure precipitation (rainfall and snowfall) at high elevations on a year-round daily basis. A limitation of these data are their relatively short period of record. Measurements are only available in digital form for about a ten year period, on average. In several states (ie. California), the data are unavailable before 1989 and could not be used for this analysis. Monthly values from 1982 through 1987 for 405 stations were used for this study. Figure 3. shows the locations of the Snotel measurement sites.

Figure 4. illustrates the low elevational range of HCN stations as compared with the Snotel sites. The majority of HCN sites are located below 1,300 meters with several sites located at 2,700 meters. The inclusion of 405 Snotel sites increases the elevational range to 3,500 meters.

4.2 Continental Data Surfaces

Continental surfaces were generated using these data to characterize general spatial patterns of precipitation and runoff across the country and to illustrate precipitation-runoff relationships at the continental scale. Monthly runoff values for the 1014 gauging stations were normalized by converting values of cfs-days to unit runoff for comparability with precipitation data. This resulted in an

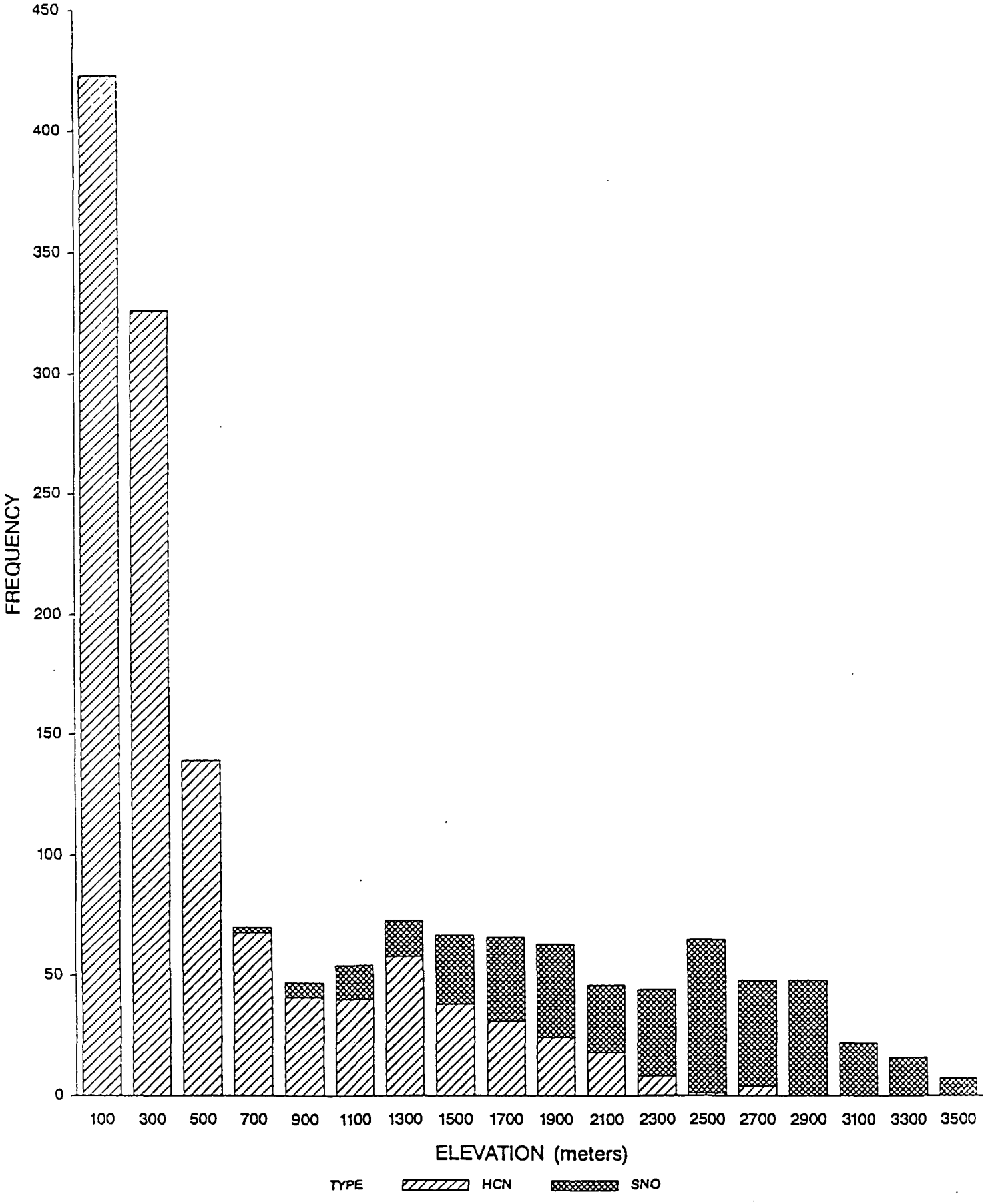

Figure 4. Histogram of HCN and Snotel station elevations

average volume of flow, or depth, at each gauge relative to that gauge's drainage area. Average annual values of runoff were computed for each gauge for a 41-year time period, from 1948 through 1988. Monthly precipitation measurements from the 1211 HCN stations were aggregated to annual precipitation averages for the period 1948 through 1987.

A raster-based GIS (USACE, 1988) was used to distribute the point values of precipitation and runoff to a 5 minute digital elevation grid (approximately 10km X 10km resolution) (NOAA, 1989) for the continental United States. An inverse distance-squared algorithm (Isaaks and Srivastava, 1989) was used to interpolate the point values of precipitation and runoff to annual precipitation and runoff surfaces. The interpolation algorithm fills the grid cell matrix with interpolated values generated from the input data points (eg. precipitation or runoff measurement sites), keeping the original data values. The twelve nearest data points are used to determine the interpolated value of each cell in the surface. The boundary of the continental United States was used as a mask so that only those cells falling within the study area were assigned interpolated values. Numerical approximation techniques such as weighted-averaging interpolation provide a mechanism for representing complex, irregular surfaces by employing restrictions to the spatial influence of measurement errors that may otherwise bias results (Isaaks and Srivastava, 1989). Figure 5. shows the 41-year average annual runoff and precipitation surfaces.

The continental surfaces illustrate the general spatial extent of runoff and precipitation across the United States. The use of long-term average values tends to smooth out the influence of extreme hydrologic events. What is readily apparent from viewing the surfaces is the magnitude of spatial variability of runoff and precipitation at the continental scale, and the steep gradients which

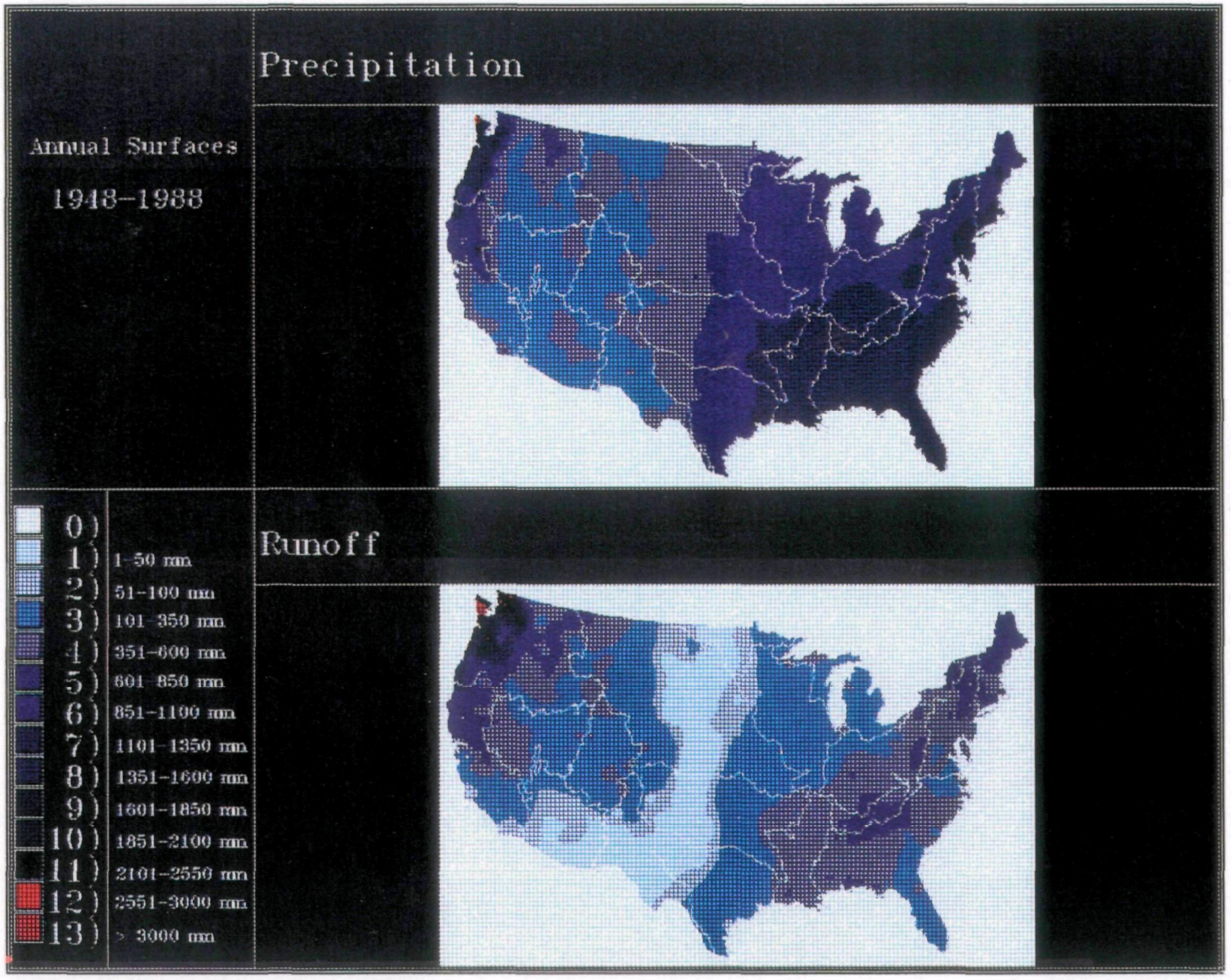

Figure 5. Average annual runoff (1948-1988) and precipitation (HCN) (1948-1987) surfaces

exist between major hydrologic regions.

Figures 4. and 5. suggest that precipitation in the western United States may be under-represented by the historical data, due to the poor spatial distribution of measurement sites in mountainous regions. With limited precipitation measurements at high elevations, the interpolation of precipitation can not capture orographic influences on precipitation variability. Furthermore, the elevational range of measurement sites in the west can not account for the substantial portion of precipitation deposited as snow.

4.3 Distributed Water Balance Calculation

A distributed water balance was calculated over the continent using the long-term average annual runoff and precipitation surfaces to provide a general idea of areas where obvious inconsistencies exist and where better precipitation estimation techniques beyond simple linear interpolation algorithms, better data, or a combination of both are needed.

The water balance equation (Linsley et al., 1982) is:

$$P = Q + ET + \Delta S + R$$

where
P = Precipitation
Q = Runoff
ET = Evapotranspiration
ΔS = Change in storage
R = Data measurement error and model error

The water balance calculation used for this analysis is a variation on this equation. When a long-term average is used, changes in storage can be assumed negligible (Linsley et al., 1982) and therefor are unaccounted for here. Evapotranspiration (ET) represents a significant portion of water movement through the hydrologic cycle and is an important component of the annual water balance. ET has been estimated to be 50% or more of the annual precipitation at continental to global scales (Budyko, 1974; Brutsaert, 1986). Rind et al. (1990) have reported that transpiration alone may account for as much as 70% of precipitation in the United States. The remaining percentage appears as streamflow, as indicated in the water balance equation. The difference, then, between measured precipitation and measured runoff over sufficiently long periods of time is a measure of losses primarily by ET (Chow, 1964). Given these assumptions, the continental water balance equation simplifies to:

$$P = Q + R$$

where R is now a residual term which includes ET, data measurement error, and model measurement error.

The terms (P and Q) of the water balance equation were represented by the average annual precipitation and runoff surfaces. Precipitation (P) should exceed or equal runoff (Q) across the continent if the historical data adequately account for the spatial distribution and total amount of precipitation input. Theoretically, the residual (R) should be positive or zero. For this analysis however, we did not expect that the water budgets would actually 'balance' because: 1) measurement errors are inherent in the historical data; 2) the interpolation of point values to a surface has limitations; and 3) precipitation measurement sites in mountainous regions are poorly distributed, spatially and

topographically. We did expect the water balance to indicate broad regions where measured runoff is substantially greater than measured precipitation, and thus point out those areas where the historical data may poorly characterize the spatial distribution of precipitation.

5. Results

Using the 1948-1988 long-term average precipitation and runoff surfaces, a distributed water balance was calculated over the continent by subtracting the annual runoff surface from the annual precipitation surface. Figure 6. illustrates the resulting annual "input-output surface". The blue areas represent regions where the water balance calculation produced residuals which are positive (measured precipitation exceeds runoff), with light blue representing those regions having residual values falling within 20 cm of balance and dark blue representing regions with larger positive residuals. These regions occur consistently throughout the eastern and midwestern states and to a much lesser extent in the mountainous west. Red areas depict regions of the country where the water balance calculation produced residuals which are negative (measure runoff exceeds measured precipitation), with lighter red representing regions with residuals falling within 20 cm of balance (negative), and dark red representing those regions with large negative residuals. These dark red regions are areas where inconsistencies in the measured data are most severe. This occurs almost exclusively in the mountainous west, most notably in the Pacific Northwest, the Great Basin, and to a lesser extent in parts California. The input-output surface illustrates the inadequacy of historical data to account for the amount and spatial distribution of precipitation in the mountainous western United States.

Snotel data were incorporated into the precipitation record to increase the

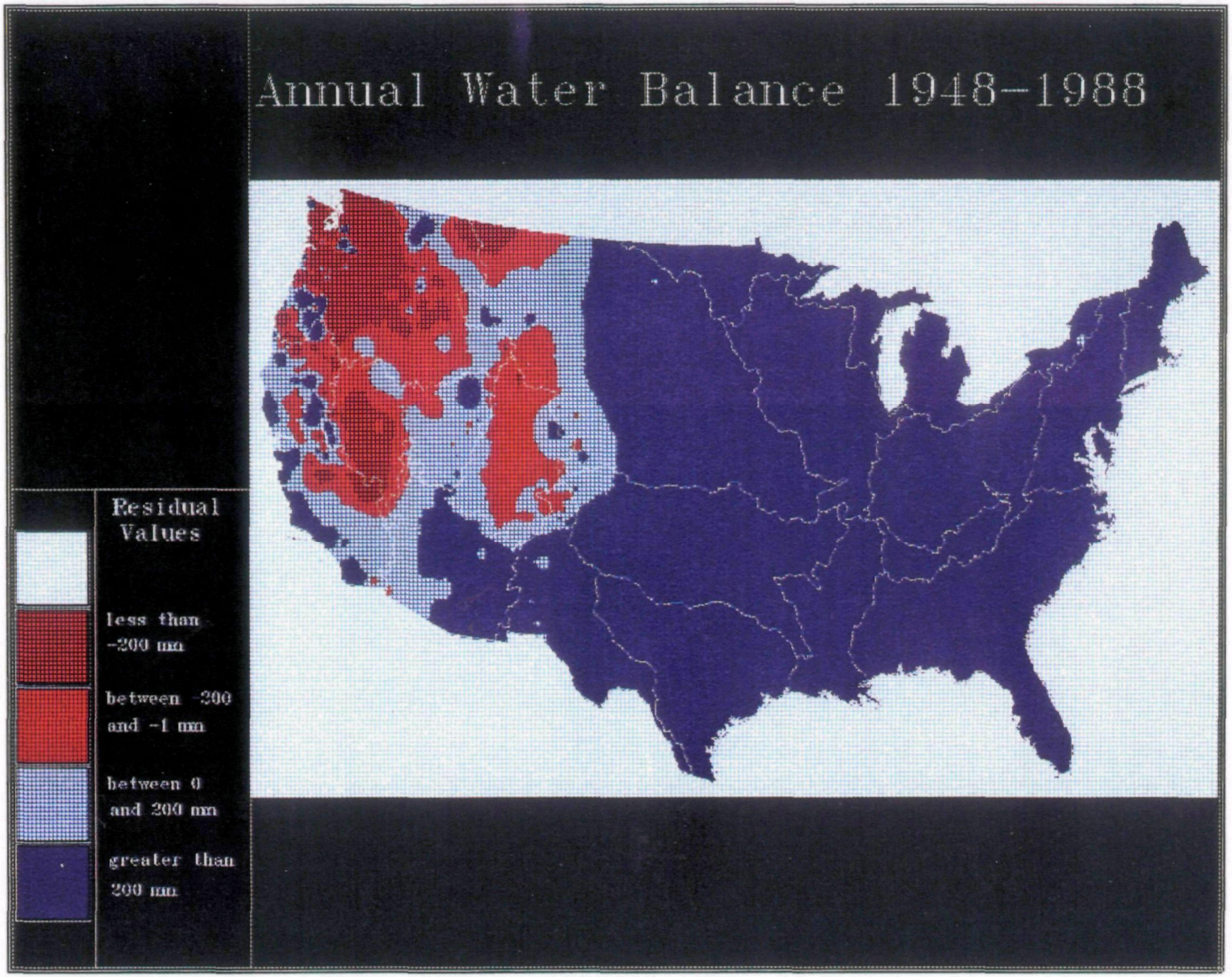

Figure 6. Annual input-output surface 1948-1988

elevational range and spatial density of precipitation observations and to improve the distributed water balance calculations. Average annual precipitation values were calculated from monthly HCN and Snotel site data for the period 1982 to 1988. Monthly runoff values for 1982 to 1988 were aggregated to annual averages. These values were interpolated using the procedure described earlier to create new annual precipitation-snow and runoff surfaces. Additionally, precipitation surfaces were generated using only the HCN data for the period 1982 to 1987 to compare the spatial distribution of precipitation with and without the incorporation of snow data in the precipitation record (Figure 7.).

The spatial patterns of the short-term surfaces were visually compared to the 41-year surfaces and found to be highly similar. While average annual precipitation values are greater during the 1948 to 1988 period, particularly in parts of the west, the general patterns of precipitation and runoff across the country do not vary significantly when short-term average values are used rather than the 41-year average values. However, comparing the short-term precipitation-snow surfaces to the short-term precipitation surfaces calculated using only the HCN data, illustrates a significant increase in measured precipitation input in the mountainous west with the inclusion of the Snotel data, most notably in the Pacific Northwest, Great Basin, and Upper Colorado regions.

The short-term precipitation-snow and runoff surfaces were used to calculate a new distributed water balance across the continent. An annual water balance was also calculated using the short-term precipitation surfaces generated using only the HCN data to compare and quantify the improvement when including snow in the calculations (Figure 8). The input-output surfaces calculated with the incorporation of Snotel data illustrate a substantial improvement in the distributed water balance. As compared with the input-output surfaces calculated using only

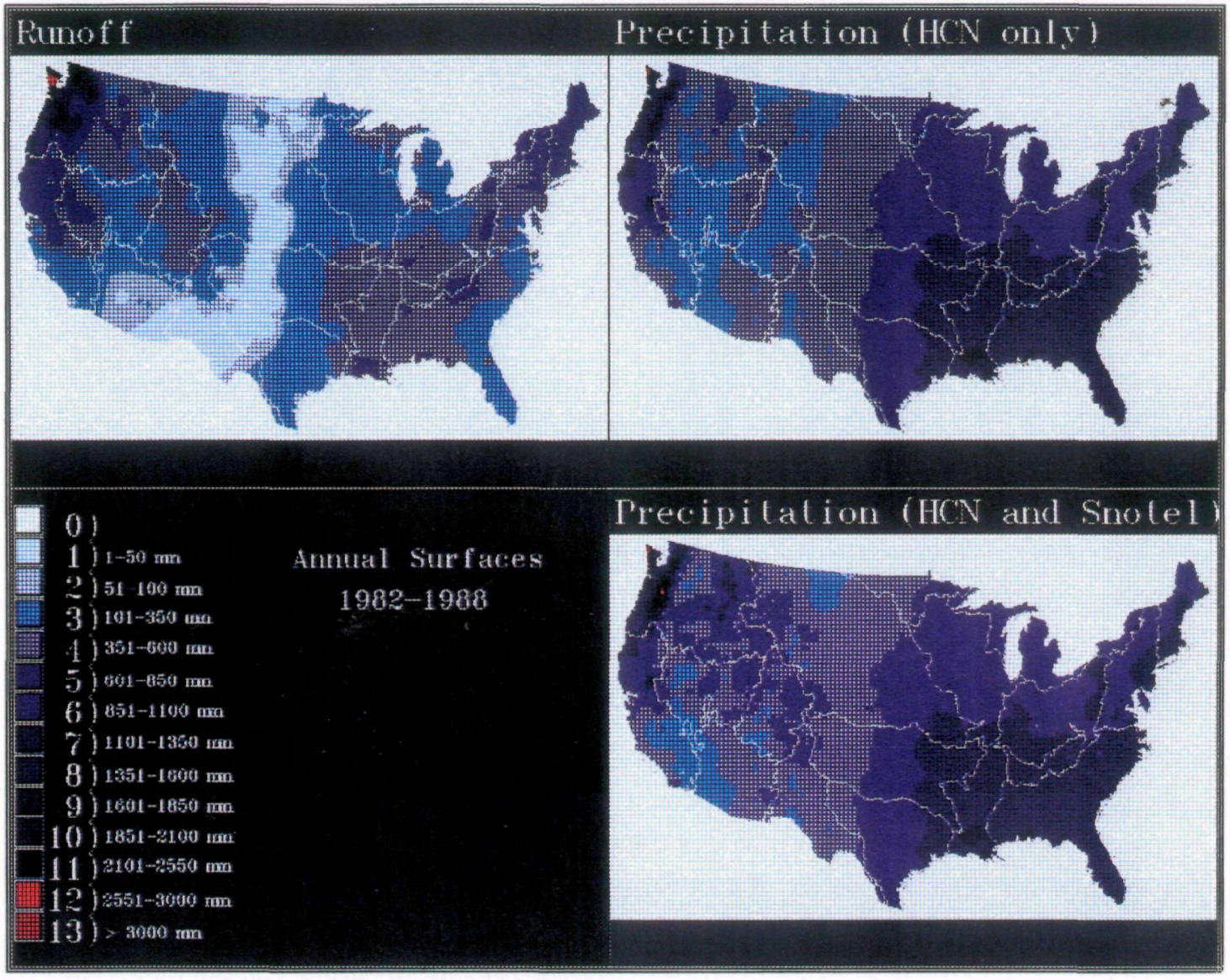

Figure 7. Average annual runoff (1982-1988), precipitation (HCN) (1982-1987), and precipitation-snow (1982-1988) surfaces

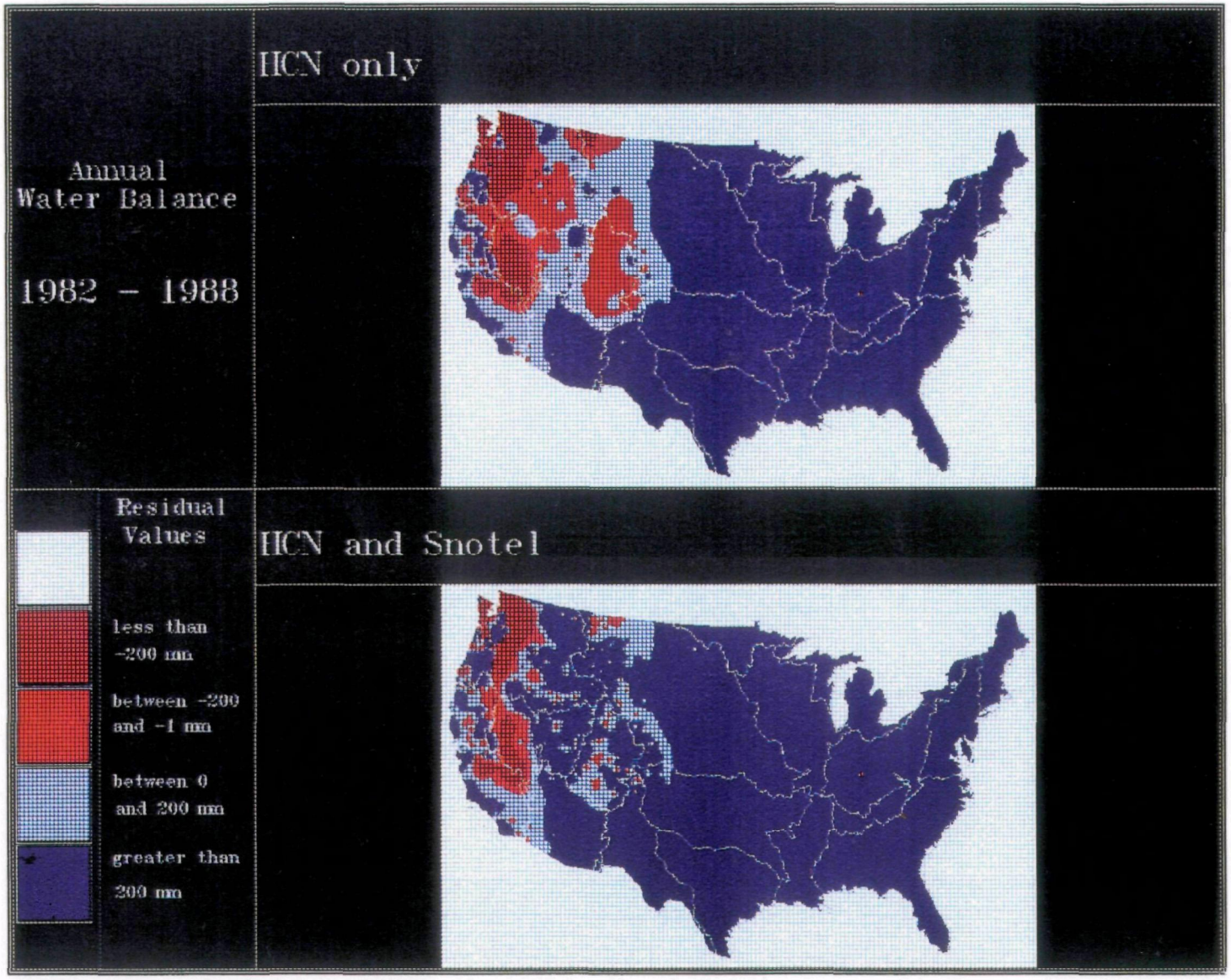

Figure 8. Annual input-output surfaces with and without snow 1982-1988

the HCN data, a greater portion of the mountainous west, particularly large regions of the Pacific Northwest, Great Basin, and Upper Colorado have positive rather than negative residuals. This analysis illustrates that care must be taken in the use of historical precipitation estimates to avoid under-estimation in mountainous regions, and that the inclusion of snow into the precipitation record enhances the utility of the historical data for characterizing the spatial distribution of precipitation by increasing the elevational range and spatial density of measurement sites. It also points out the need to consider orographic effects on the spatial distribution of precipitation in mountainous regions.

Annual average runoff, precipitation, and precipitation-snow values from the short-term surfaces were calculated for four major hydrologic regions in the western United States to quantify the improvement in measured precipitation volume with the inclusion of snow deposition data into the precipitation record. The size of this region is 173.34 km^2 and includes the Columbia Basin, the Great Basin, the Upper Colorado River Basin and the Lower Colorado River Basin. These values (in depths of water) are shown in Figure 9. The average annual runoff value for this region is 50.6 cm. The average annual precipitation value using only HCN data, at 46.5 cm, does not even equal the measured runoff. With the inclusion of Snotel data, this value increases to 68 cm, accounting for the total measured runoff plus a positive residual of 17.4 cm.

6. Limitations

The analysis presented is exploratory in nature, and part of a larger effort aimed at the development of large scale ecological, hydrological, and biogeochemical models for climate change research. It is important to note the limitations associated with the data and the techniques which were used.

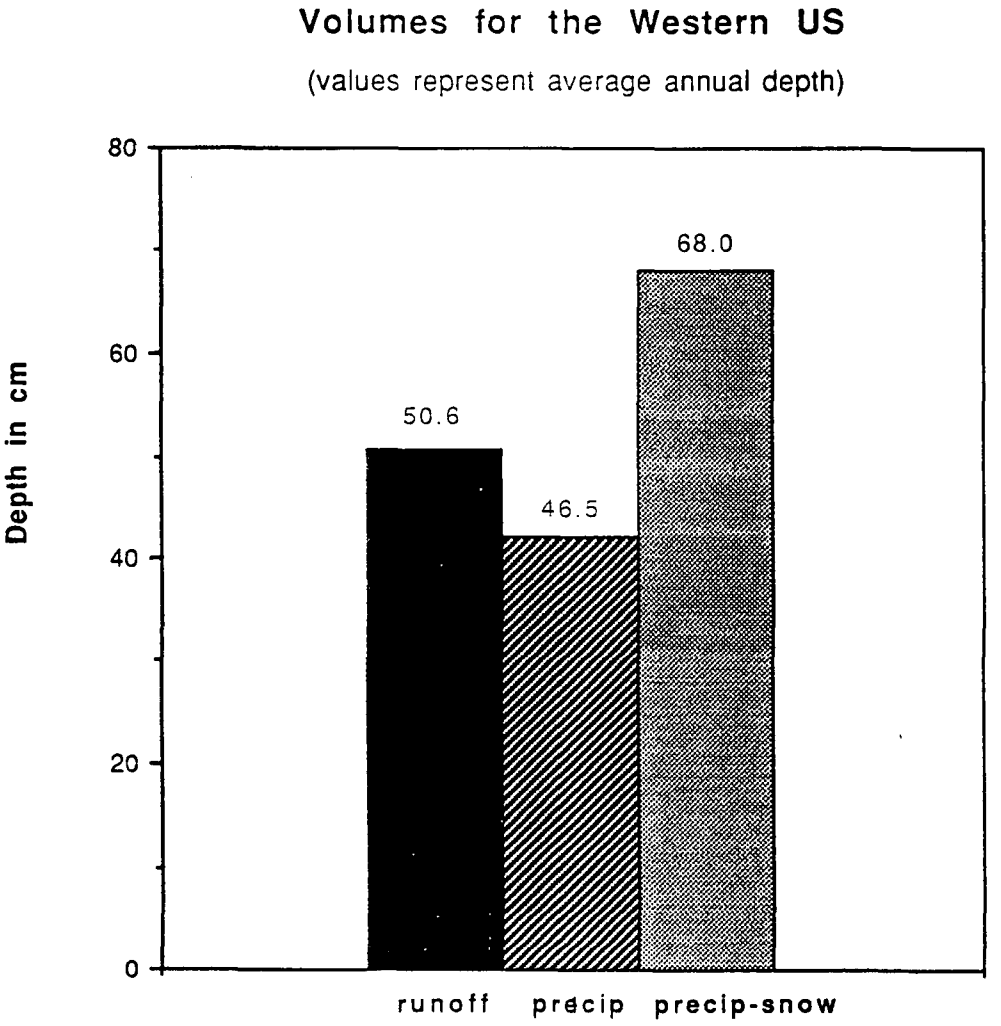

Figure 9. Bar graph showing the improvement in the annual water balance calculation for the western US with the inclusion of snow data

The use of unregulated gauges rather than the entire gauging network limits the spatial density of point measurements, particularly in areas of the western United States. Additionally, the extrapolation of runoff from one drainage to another possibly quite distant drainage, has obvious limitations. However, at the continental scale, detailed basin information is difficult to consider and the use of a time-consistent, quality-controlled data set of unregulated flow measurements was the natural place to begin. In some areas, we will need to incorporate more measurement sites for future work, and undoubtedly include flow records from regulated basins (for example, in the southwest data measurements are sparse and regulated flow comprises a substantial portion of the measured runoff). The use of regulated flow exclusively will become particularly critical for regional scale, seasonal analyses using monthly time series data rather than long-term averages. The point here is that while augmentation of the precipitation-runoff database with additional data is required, we must also develop better techniques for distributing these data both spatially and temporally in topographically diverse regions.

Our use of unregulated gauging stations exclusively for this study, introduced a small drainage area bias. This bias may actually tend to over-estimate runoff, as smaller basins yield greater depth of flow per unit area. Conversely, unregulated gauging stations having large drainage areas are typically "drier". In any event, we do not feel that by using unregulated flow exclusively, our runoff estimates are off by an order of magnitude, or any substantial amount for the purposes of this analysis. The emphasis in this study was not to attempt to simulate runoff distribution or predict runoff at a point, but rather to use the runoff surfaces as a check on our precipitation estimates in a general sense, to identify those regions where severe inconsistencies exist in the measured values of precipitation and runoff.

The procedure used to generate the precipitation and runoff surfaces is a simple, linear interpolation algorithm. As such, it may introduce estimate bias in areas of high topographic relief. However, while other interpolation algorithms may yield precipitation and runoff estimates which are different, we do not feel that they would contradict the conclusions from this analysis - that precipitation is underestimated in regions of the western United States by the historical data, and that the inclusion of snow data into the historical record improves the precipitation estimates in mountainous regions. This analysis is a first-cut effort at spatially distributing precipitation at the continental scale for the identification of regions where more detailed analyses should be directed. Other models and interpolation algorithms which can include elevation and other variables as factors to better simulate the spatial distribution of precipitation-elevation relationships should be considered in future work at a variety of spatial scales.

7. Conclusions

The development of large scale ecological and hydrological models requires spatially distributed estimates of precipitation. While historical hydro-meteorological data may be used to characterize the spatial distribution of precipitation across large regions, geographic scale and topographic variability must be considered. In the United States, historical data characterize precipitation best in regions with minimal topographic variability, namely the eastern and mid-western regions. However, the historical data may be severely limiting in mountainous regions of the west, in part, because the data do not account for precipitation inputs at high elevations.

This study has illustrated that the integration of snow measurements into the precipitation record is essential for improving precipitation estimates. The incorporation of snow data into the precipitation record for four major

hydrologic regions of the western United States improved the precipitation input by roughly 40%. While the addition of snow data significantly improves the spatial distribution and elevational range of measurement sites, these data have a limited geographical extent and period of record. Additionally, the inclusion of these data will not, in itself, resolve the temporal variability of precipitation-runoff relationships. Resolving the seasonal cycle of winter snow deposition followed by spring snowmelt runoff is a more complex issue which is critical for predicting water availability under both current and predicted $2XCO_2$ climate conditions in water-stressed areas of the western United States. Ultimately, techniques must be developed to use these and other sources of data to account for snow depletion and runoff timing in mountainous regions.

This research has established a database for precipitation and runoff analyses at regional and continental scales and has produced spatially distributed precipitation estimates for the United States at a resolution which is ecologically meaningful. Most importantly, it has demonstrated that it is insufficient to simply use historical data to characterize precipitation at large scales, particularly in mountainous regions where dramatic precipitation gradients exist. Spatially distributed precipitation estimates that account for the spatial arrangement of measurement sites, precipitation-elevation relationships, and topographic constraints on precipitation distribution are needed.

REFERENCES

Bradley, R.S., H.F. Diaz, J.K. Eischeid, P.D. Jones, P.M. Kelly and C.M. Goodess, Precipitation fluctuations over northern hemisphere land areas since the mid-19th century, *Science*, 1987.

Brutsaert, W., Catchment-scale evaporation and the atmospheric boundary layer, *Water Resources Research*, 22, 39S-45S, 1986.

Budyko, M.I., *Climate and Life*, pp. 508, Academic Press, New York, 1974.

Chow, Ven Te, *Handbook of Applied Hydrology*, McGraw-Hill, New York, 1964.

Diaz, H.F., R.S. Bradley, and J.K. Eischeid, Precipitation fluctuations over global land areas since the late 1800's, *Journal of Geophysical Research*, vol. 94, 1989.

Dickinson, R.E. and R.J. Cicerone, Future global warming from atmospheric trace gases, *Nature*, 319, 109-115, 1986.

Dooge, James, C.I., Looking for hydrologic laws, in *Trends and Directions in Hydrology*, ed. Stephen J. Burges, pp. 46S-58S, American Geophysical Union, Washington, D.C., 1986.

Dooge, James, C.I., Hydrologic models and climate change, keynote address *Chapman Conference on Hydrologic Aspects of Global Climate Change*, 1990.

Eagleson, P.S., Land Surface Processes in Atmospheric General Circulation Models, in *Proceedings of Greenbelt Study Conference*, p. 560, Cambridge University Press, New York, 1982.

Eagleson, P.S., The emergence of global-scale hydrology, *Water Resources Research*, 22,6S-14S, 1986.

EarthInfo, *Hydrodata User's Manual - Daily and Peak Values*, Denver, CO, 1988.

Hall, F.G., D.E. Strebel, and P.J. Sellers, LInking knowledge among spatial and temporal scales: vegetation, atmosphere, climate, and remote sensing, *Landscape Ecology*, vol. 2, 1988.

Hansen, J., I. Fung, A. Lacis, D. Rind, S. Lebedeff, R. Ruedy, and G. Russell, Global climate changes as forecast by Goddard Institute for Space Studies three dimensional model, *Journal of Geophysical Research*, 93D, 9341-9364, 1988.

Hansen, J., and S.Lebedeff, Global trends of measured surface air temperature, *Journal of Geophysical Research*, 92, 13345-13372, 1987.

Hansen, J., A. Lacis, D. Rind, G. Russell, P. Stone, I. Fung, R. Ruedy, and J. Lerner, Climate sensitivity, analysis of feedback mechanisms, in *Climate Processes and Climate Sensitivity*, edited by J.E. Hansen and T. Takahashi, Geophysical Monograph, vol. 5, pp. 130-163, American Geophysical Union, Washington, D.C., 1984.

Isaaks, E.H. and R.M. Srivastava, *Applied Geostatistics*, pp. 561, Oxford University Press, New York, 1989.

Jones, P.D., T.M.L. Wigley, and P.B. Wright, Global temperature variations between 1861 and 1984, *Nature*, 322, 430-434, 1986.

Karl, T.R., Multi-year fluctuations of temperature and precipitation: the gray area of climate change, *Climatic Change*, vol. 12, 1987.

Karl, T.R. and W.E. Riebsame, The impact of decadal fluctuations in mean precipitation and temperature on runoff: a sensitivity study over the United States, *Climatic Change*, vol. 15, 1989.

Linsley, R.K., M.A. Kohler, and L.H. Paulhus, *Hydrology for Engineers*, McGraw Hill, 1982.

Manabe, S. and R.T. Wetherald, On the distribution of climate change resulting from an increase in CO_2 concentration on the climate of a general circulation model, *Journal of Atmospheric Sciences,* 32, 3-15, 1975.

National Oceanographic and Atmospheric Administration, National Geophysical Data Center, *Geophysics of North America: Users Guide,* U.S. Department of Commerce, Boulder, Colorado, 1989.

Neilson, R.P., G.A. King, R.L. DeVelice, J. Lenihan, D. Marks, J. Dolph, B. Campbell, and G. Glick. Sensitivity of ecological landscapes and regions to global climate change. *U.S. Environmental Protection Agency,* Environmental Research Laboratory, Corvallis, Oregon, 1989.

Quinlan, F.T., T.R. Karl, and C.N. Williams, *United States Historical Climatology Network (HCN) Serial Temperature and Precipitation Data,* U.S. Department of Energy, Carbon Dioxide Information Analysis Center, Oak Ridge, TN, 1987.

Rasmusson, E.M., El Nino and variations in climate, *American Scientist,* 73, 168-177, 1985.

Rasmusson, E.M. and P.A. Arkin, Measuring and understanding global precipitation variability, *in Symposium on Global Change Systems - Special Sessions on Climate Variations and Hydrology,* Anaheim, CA, 1990.

Rind, D., The influence of vegetation on the hydrologic cycle in a global climate model, in *Climate Processes and Climate Sensitivity,* edited by J.E. Hansen and T. Takahashi, Geophysical Monograph, vol. 5, pp. 73-92, American Geophysical Union, Washington, D.C., 1984

Rind, C., The doubled CO_2 climate and the sensitivity of the modeled hydrologic cycle, *Journal of Geophysical Research,* 93, 5385-5412, 1988.

Rind, D., R. Goldberg, J. Hansen, C. Rosenzweig, and R. Ruedy, Potential evapotranspiration and the likelihood of future drought, *Journal of Geophysical Research,* 95, 9983-10005, 1990.

Ropelewski, D.F.and M.S. Halpert, North American precipitation and temperature patterns associated with the El Nino Southern Oscillation Cycle, *Monthly Weather Review,* 1986.

Ropelewski, D.F. and M.S. Halpert, Global and regional scale precipitation patterns associated with the El Nino Souther Oscillation Cycle, *Monthly Weather Review,* 1987.

Schlesinger, M.E. and J.F.B. Mitchell, Climate model simulations of the equilibrium climatic response to increasing carbon dioxide, *Reviews of Geophysics,* 25, 760-798,1987.

Shugart, H.H. and D.C. West, Development of an appalachian deciduous forest succession model and its application to assessment of the impact of the chestnut blight, *Journal of Environmental Management*, 5, 161-179, 1977.

Smith, J.B. and D.A. Tirpak, *The Potential Effects of Global Climate Change on the United States,* Report to Congress, vol. PM-221, United States Environmental Protection Agency, Washington, D.C. 1989.

U.S. Army Corps of Engineers, *GRASS Users and Programmers Manual*, U.S. Army Corps of Engineers, Construction Engineering Research Laboratory, Champagne, IL, 1988.

U.S. Water Resources Council, *The Nation's Water Resources 1975-2000*, Volume3 Analytical Data Summary, Washington, D.C. 1978

U.S.D.A. Soil Conservation Service, *Snow Survey and Water Supply Products Reference*, West National Technical Center, Portland, OR, 1988.

Wallace, J.R., D.P. Lettenmaier, and E.F. Wood, A daily hydroclimatological data set for the continental United States, *Water Resources Research,* (in review), 1990.

Wigley, T.M.L., J.Angell, and P.D. Jones, Analysis of the temperature record, in *Detecting the Climatic Effects of Increasing Carbon Dioxide,* DOE/ER-0235, pp. 198, Dept. of Energy, Washington, D.C., 1985.

A COMPARISON OF GEOSTATISTICAL PROCEDURES FOR SPATIAL ANALYSIS OF PRECIPITATION IN MOUNTAINOUS TERRAIN

Donald L. Phillips
U.S. Environmental Protection Agency

Jayne Dolph
NSI Technology Services, Inc.

Danny Marks
NSI Technology Services, Inc.

U.S. EPA Environmental Research Laboratory
Corvallis, OR 97333

The information in this document has been funded wholly or in part by the U.S. Environmental Protection Agency. It has been subject to the agency's peer and administrative review, and it has been approved for publication as an EPA document. Mention of trade names or commercial products does not constitute endorsement or recommendation for use.

ABSTRACT

Application of simulation models to assessment of global climate change effects often requires spatially distributed estimates of precipitation, both under current and future climate scenarios. Simple interpolation methods fail to consider the effects of topography on precipitation and may be in considerable error in mountainous regions. The performance of three geostatistical methods for making mean annual precipitation estimates on a regular grid of points in mountainous terrain was evaluated. The methods were (1) kriging, (2) kriging elevation-detrended data, and (3) cokriging with elevation as an auxiliary variable. The study area was the Willamette River Basin, a 2.9 million hectare region spanning the area between the Coast Range and the Cascade Range in western Oregon. Compared to kriging, detrended kriging and cokriging both exhibited better precision (coefficients of variation of 16% and 17% vs. 21%; average absolute errors of 19 cm and 20 cm vs. 26 cm) and accuracy (average errors of -1.4 cm and -2.0 cm vs. -5.2 cm) in the estimation of mean annual precipitation. Contour diagrams for kriging and detrended kriging exhibited smooth zonation following general elevation trends, while cokriging showed a patchier pattern more closely corresponding to local topographic features. Detrended kriging and cokriging offer improved spatially distributed precipitation estimates in mountainous terrain on the scale of a few million hectares. Application of these methods for a larger region, the Columbia River drainage in the U.S. (57 million hectares), was unsuccessful due to the lack of a consistent precipitation-elevation relationship at this scale. Precipitation estimation incorporating the effects of topography at larger scales will require either piecewise estimation using the methods described here or development of a physically-based orographic model.

INTRODUCTION

A substantial portion of the assessment of the potential effects of climate change on natural resources and ecosystems has utilized simulation models in conjunction with climate scenarios. For example, the EPA Congressional Report on climate change effects in the United States (Smith and Tirpak, 1989) gave results from models simulating hydrologic processes, crop growth, and forest dynamics. These models used climate scenarios derived from general circulation models (GCMs) of the atmosphere simulating conditions of doubled atmospheric CO2 concentrations. Typically, changes in modeled temperature and precipitation between current and doubled CO2 concentrations have been used to adjust the historical weather record from weather stations in the area of interest. However, U.S. Weather Service stations are located in an irregular, coarse grid. Many areas, particularly in the western United States, have only sparse coverage. In addition, topographic relief has large effects on precipitation. Precipitation generally increases with elevation, and mountain ranges also create "rain shadows" on the leeward side. Weather stations tend to be sited at low elevations and may thus underestimate the regional precipitation (Dolph, in review). Precipitation at higher (or lower) elevations near a weather station may not be accurately reflected by the weather station measurements.

For these reasons, especially in areas of high topographic relief, it will often be insufficient to use data from the nearest weather station as the climate input for hydrology or vegetation models to assess climate change impacts. This is especially true if the models are being applied to a spatial distribution of points to represent different facets of the landscape (Marks, in review). Spatially distributed precipitation data, which take into account the spatial arrangement of weather station data, precipitation-elevation relationships, and topographic relief are needed.

Geostatistical interpolation methods, such as kriging, were originally developed for spatial analysis of ore reserves in mining (Matheron, 1971), but have since been applied to a number of other problems, including spatial interpolation of precipitation (Dingman et al., 1988; Istok et al., 1990a,b;

Tabios and Salas, 1985). Tabios and Salas (1985) found kriging to be superior to other commonly used interpolation techniques such as Thiessen polygons, polynomial trend surfaces, inverse distance, and inverse square distance methods for precipitation estimation in a 52,000 km^2 region in Nebraska and Kansas.

Kriging does not explicitly account for the influence of elevation on precipitation in mountainous areas except as reflected in the precipitation of surrounding weather stations. If, however, the neighboring stations are at different elevations than the point being estimated, then the estimate is likely to be in error. To address this problem, Chua and Bras (1982) and Dingman et al. (1988) performed linear regressions on precipitation vs. elevation, subtracted the regressed elevation effect, and performed kriging on the elevation-adjusted data. Cokriging is another geostatistical method which uses a second correlated auxiliary variable to aid in estimation of the primary variable. Cokriging may be especially advantageous in situations where the auxiliary variable is highly correlated with the primary variable ($r > 0.5$) and is oversampled compared to the primary variable (Vauclin et al., 1983; Yates and Warrick, 1987). Only recently has this been applied to precipitation estimation using elevation as the auxiliary variable (Istok et al., 1990a,b). Both of these methods seem to hold promise for improved spatially distributed estimation of precipitation. The purpose of this paper is to evaluate the effectiveness of geostatistical procedures which utilize topographic information (cokriging and elevation-detrended kriging) and those which do not (kriging), for estimating precipitation across mountainous terrain, in order to provide spatially distributed climate data for models assessing climate change effects.

OVERVIEW OF GEOSTATISTICAL THEORY

The basic goal of geostatistical methods such as kriging and cokriging is to interpolate values for points or areas which have not been sampled, using data from surrounding sampled points. Any interpolation scheme must assign a series of weights to the neighboring points to be used in order to compute an interpolated value of the variable of interest (e.g., precipitation). Simple

interpolation schemes may assign equal weights to each of n nearest neighbors, for example, or they may assign weights inversely proportional to the distance to the estimation point. The first of these methods does not take into account the spatial proximity of the neighboring points in interpolating a value for the estimation point. The second does, but assumes a particular relationship (inverse) between the weight and the distance. Thus, the weights are not necessarily optimal. Kriging and cokriging are interpolation methods which attempt to optimize the weights assigned to the neighboring data points in computing the interpolated value.

Kriging and cokriging consist of three steps: (1) an examination of the covariation of data values depending on their distances apart; (2) fitting theoretical models to these relationships; and (3) using these models to calculate the weights for a particular set of neighboring points and computing the interpolated value. The first step is referred to as constructing a sample semivariogram. All possible pairs of data points are examined, the pairs are grouped by distance classes, and one half the variance of the difference in values (the semivariance) is graphed vs. the distance. Second, a theoretical curve (model semivariogram) is fit to these points either by eye or using least squares regression. Lastly, this model determines the weights to be used for each neighboring point to compute the interpolated values. For kriging, interpolations are made using only the semivariogram for the variable to be interpolated. For cokriging, additional semivariograms for other correlated variables are also used to help make the estimate.

The theoretical semivariogram model is defined by the nugget variance (the variance at zero distance), the sill (the variance to which the semivariogram asymptotically rises), and the range (the distance at which the sill or some predetermined fraction of the sill is reached). See Figure 3 for an example semivariogram.

In their simplest form, kriging and cokriging assume that there is no "trend" or "drift" in the data, that is, no consistent, directional gradient in the variable(s). This is often not the case, but the assumption may be made if the neighborhood of points used in interpolation is smaller than the distance

over which the trend is apparent (Journel and Rossi, 1989). A related concept is isotropy, the condition under which the semivariance is the same for a given distance, regardless of direction. Again, this is often not strictly true, but small differences may be ignored and isotropy is often assumed for procedural simplicity.

METHODS

Study Area

The study area is the Willamette River basin in Oregon. The Willamette River begins in southwestern Oregon and flows north into the Columbia River at Portland, Oregon. The basin is approximately 170 km wide and 270 km long and covers 2.9 million hectares. It is bordered by two major topographic features, the Coast Range to the west and the Cascade Range to the east. The elevation ranges from near 0 m above sea level at the confluence with the Columbia River to 3200 m at the peak of Mt. Jefferson in the Cascade Range (Fig. 1). Annual precipitation ranges from approximately 100 cm to 300 cm. The area has a Meditteranean climate with wet winters and dry summers. Cyclonic storms are carried in on the polar front jet stream which dips southward into the region in the winter and retreats northward in the summer. The high mountains have minor convective activity in the summer.

Precipitation and Elevation Data

Precipitation data were obtained from 37 U.S. Weather Service stations (EarthInfo, 1990) and 15 Soil Conservation Service SNOTEL (snow telemetry) stations in the basin (Soil Conservation Service, 1988) [Fig. 2]. The SNOTEL data were added to increase the elevation range for precipitation data and to give a better regional representation of precipitation patterns (Dolph, in review). The U.S. Weather Service stations ranged in elevation from 46 m to 1095 m. The SNOTEL stations ranged in elevation from 610 m to 1494 m. Precipitation from both sources includes rainfall and snow water equivalents. Because of the recency of the SNOTEL network and our desire for a uniform period of record for the two data sources, we used data from water years 1982-

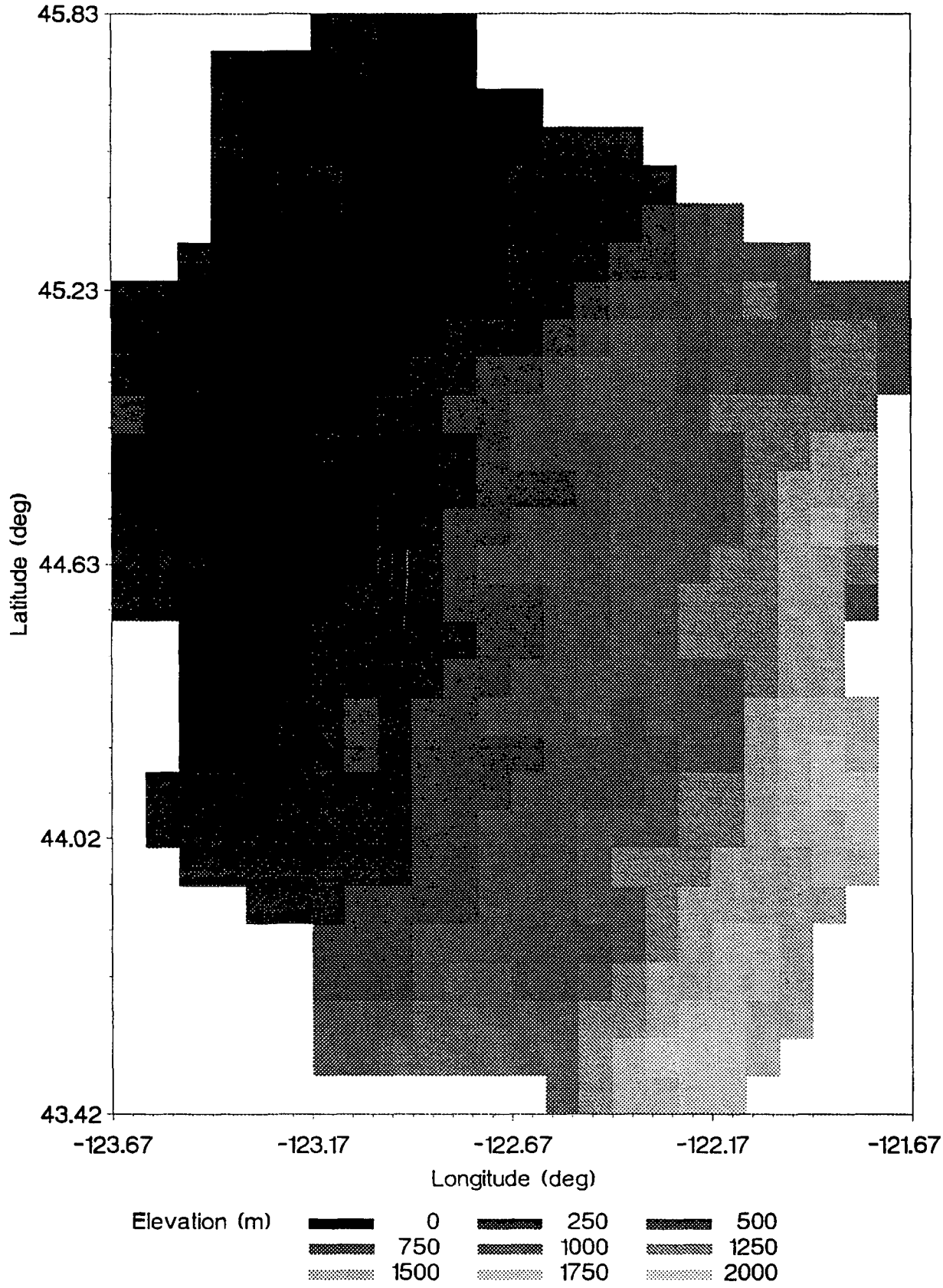

Figure 1. Elevation contour diagram of the study area.

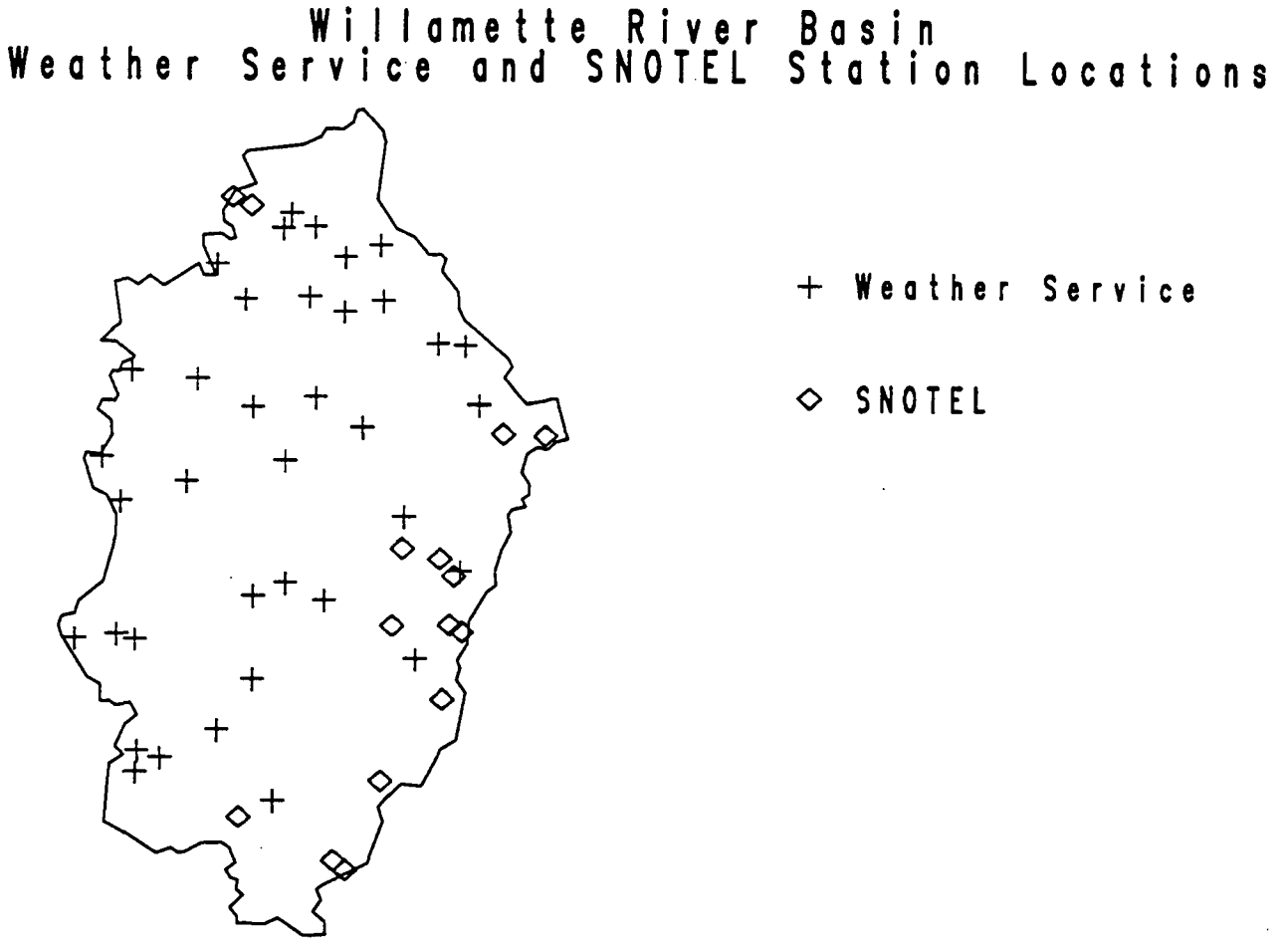

Figure 2. Locations of the 52 U.S. Weather Service and SNOTEL weather stations.

1988 (10/81-9/88). The results reported here will focus on mean annual precipitation, but additional analyses are being done on a seasonal and monthly basis. The 52 stations had a grand mean annual precipitation of 162 cm, with a range of 99 cm to 293 cm. The distribution of mean annual precipitation for the 52 sites was skewed right ($p<.01$ for Kolmogorov-Smirnov normality test). The data were decimal log transformed to approximate a normal distribution ($p>.05$ for Kolmogorov-Smirnov normality test).

The elevation data set included the elevations for the 52 precipitation stations, plus 478 additional points on a 5-minute latitude/longitude grid covering the basin. Elevation values for this grid were derived from a Digital Elevation Model with 5-minute resolution (National Geophysical Data Center, 1989; Campbell and Marks, 1990). The mean elevation for the 530 data points was 629 m with a range of 2 m to 2250 m. The distribution of elevation values was also right skewed ($p<.01$ for Kolmogorov-Smirnov normality test), so the data were decimal log transformed to approximate a normal distribution ($p>.05$ for Kolmogorov-Smirnov normality test).

Semivariograms

For all semivariograms and cross-semivariograms, both isotropic and anisotropic variograms were constructed. To examine possible anisotropy, pairs of perpendicular directional semivariograms with tolerances of ± 45 degrees were calculated for angles of 0 to 90 degrees (relative to Albers projection; 0 degrees is approximately north) in increments of 15 degrees. For ordinary kriging of log annual precipitation (LAP), the sample semivariograms were constructed using the 52 precipitation data points. The same sample LAP semivariogram was used for cokriging. Also for cokriging, log elevation (LEL) sample semivariograms were constructed using the 478 5-minute grid points plus the 52 weather station elevations. The cokriging sample cross-semivariograms used the 52 stations which had both LAP and LEL values. For elevation-detrending of precipitation data, a linear regression was performed with LAP as the dependent variable and LEL as the independent variable ($n=52$). The residuals (RESID) were then used to construct semivariograms for use in detrended kriging. SAS (SAS Institute, 1985) was

used for the linear regression. The GEOPACK geostatistical software package (Yates and Yates, 1990) was used for all semivariogram, cross-semivariogram, kriging, and cokriging procedures. The GEO-EAS geostatistical software package (Englund and Sparks, 1988) and programs written in SAS were also used for cross-validation procedures described below.

Kriging and Cokriging Procedures

The kriging and cokriging systems of equations are as outlined in Vauclin et al. (1983). For detrended kriging, the elevation-detrended residuals (RESID) were used instead of LAP. This detrending procedure is essentially equivalent to one iteration of the universal kriging procedure for kriging in the presence of trends (Isaaks and Srivastava, 1989).

Cross-Validation Procedures

Semivariograms for LAP and elevation-detrended residuals (RESID), and cross-semivariograms for LAP-LEL were initially fit with a least squares procedure. The model form was selected by visual examination of the sample semivariograms and cross-semivariograms. Several different models were tried for each. A jackknife procedure of cross-validation was used. Data points were deleted one at a time, values were kriged or cokriged for the missing points, and the estimated and actual values were compared. The Reduced Mean and Reduced Variance cross-validation statistics were computed (Vauclin et al., 1983; Yates and Warrick, 1987). For a set of n points at locations x_i and values $z(x_i)$, there are corresponding estimates $z^*(x_i)$ with estimation variances $\sigma_k^2(x_i)$. The values $z(x_i)$ have sample variance s^2. The Reduced Mean (RM) is defined by:

$$RM = \frac{1}{n} \sum_{i=1}^{n} \left[z(x_i) - z^*(x_i) \right] / \sigma_k (x_i)$$

and should be close to 0 if the estimates are unbiased. The Reduced Variance (RV) is defined by:

$$RV = \frac{1}{n}\sum_{i=1}^{n} \{ [z(x_i) - z^*(x_i)] / \sigma_k (x_i) \}^2$$

and should be close to 1 if the estimation variances are consistent. Nugget, sill, and range coefficients were iteratively changed to improve the RM and RV performance of the semivariograms and cross-semivariograms. To insure that the cross-semivariogram was positive definite, an indicator of positive definite condition (PDC) was overlaid on the model cross-semivariogram. This indicator is defined by:

$$PDC = \sqrt{\gamma_{pp}(h)\ \gamma_{ee}(h)}$$

where $\gamma_{pp}(h)$ and $\gamma_{ee}(h)$ are the semivariances at distance h for LAP and LEL, respectively. The cross-semivariogram model was checked to be sure that the semivariance $\gamma_{pe}(h)$ was less than PDC for all distances h.

RESULTS AND DISCUSSION

Precipitation Semivariograms

For LAP, the directional semivariograms oriented at 0 and 90 degrees showed the greatest variability in the semivariances. For spherical models with similar sills (0.020 and 0.018), the ranges were not greatly different (67 and 82). Because of the small size of the precipitation data set, the anisotropy ratio near unity (82/67 = 1.2), and for simplicity of modeling, isotropy was assumed. The semivariogram for LAP is shown in Figure 3, along with the fitted model. The rise of the semivariance above the sample variance is evidence of a trend for distances > 90 km. Model fitting was done for the points in the semivariogram which fell below this distance. The nugget, sill, range, reduced mean, and reduced variance values for the selected model are shown in Table 1.

Elevation-detrended Precipitation Residual Semivariograms

Figure 4 shows the regression line for LAP as a function of LEL. The

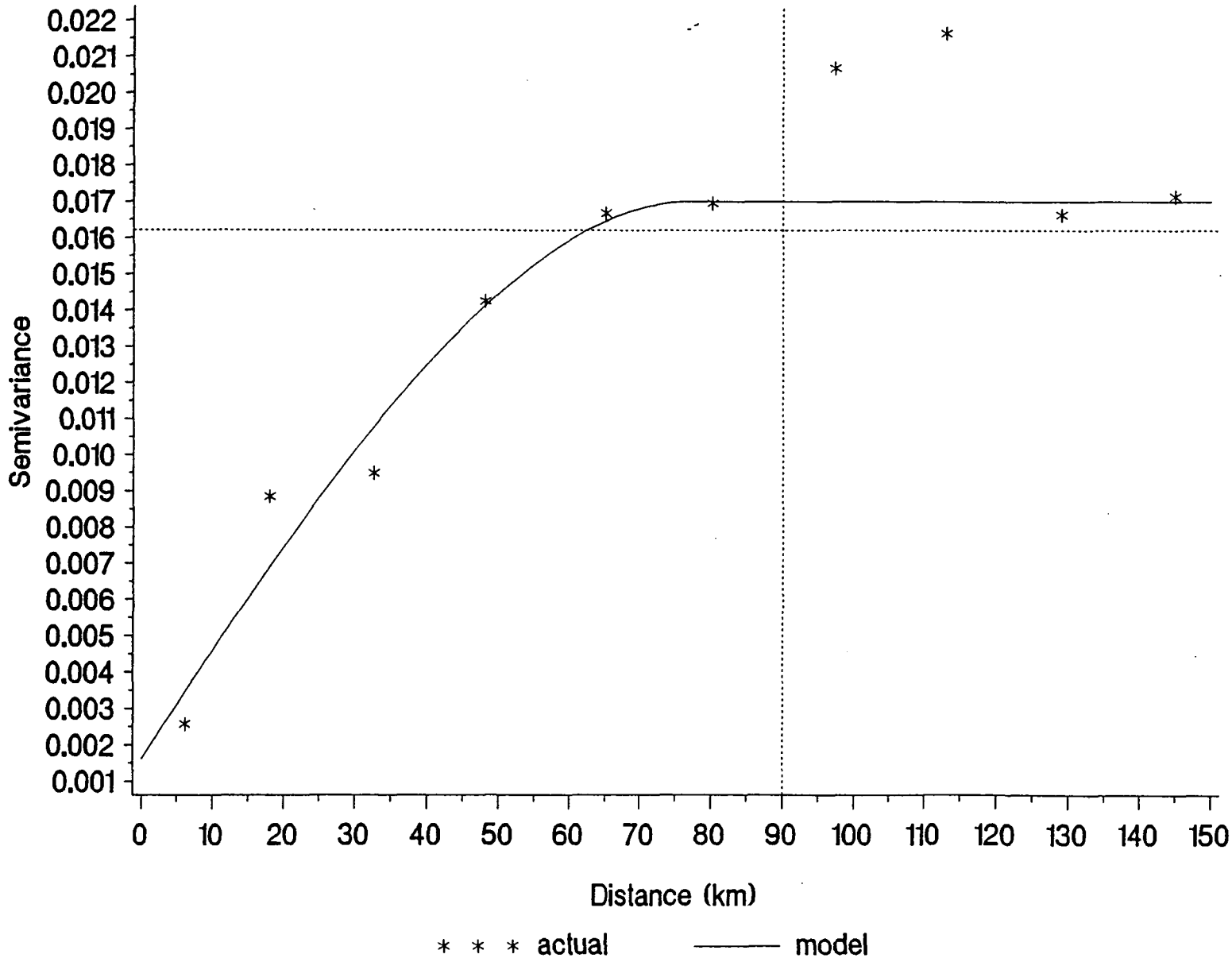

Figure 3. Sample and model semivariograms for LAP (log10 annual precipitation in cm). The model was a spherical model with a nugget of 0.0016, sill minus nugget of 0.0154, and range 77 km. The horizontal dashed line shows the sample variance (n=52).

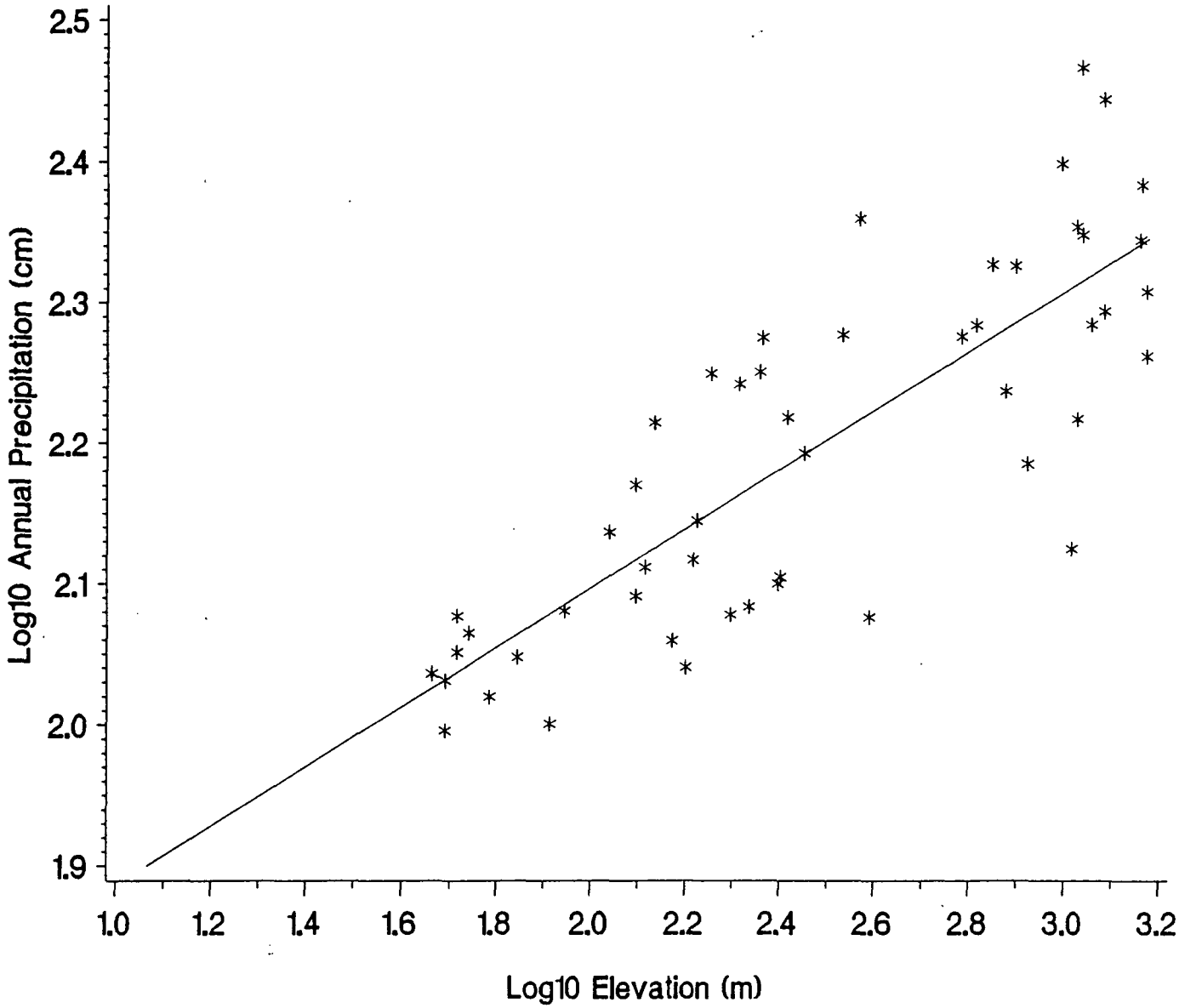

Figure 4. Regression of LAP (log10 annual precipitation in cm) vs. LEL (log10 elevation in m). The regression model is LAP = 1.675 + 0.2108 LEL ($F = 104.8$; $df = 1$; $p < 0.0001$), with a correlation coefficient $r = 0.82$.

TABLE 1. Summary of semivariogram and cross-semivariogram models.

Variable(s)	n	Model	Nugget (C_0)	Sill minus Nugget (C_1)	Range (a)	Reduced Mean	Reduced Variance
LAP	52	Spherical	0.0016	0.0154	77	0.037	0.99
LEL	530	Gaussian	0.029	0.346	86	0.003	0.90
RESID	52	Spherical	0.00167	0.00372	67	0.000	1.00
LAP/LEL	52	Exponential	0	0.0794	71	0.040	0.96

Models:

Spherical:
$$\gamma(h) = \begin{cases} C_0 + C_1\left[1.5\,ha - 0.5\left(\frac{h}{a}\right)^3\right] & \text{if } h \le a \\ C_0 + C_1 & \text{otherwise} \end{cases}$$

Exponential:
$$\gamma(h) = C_0 + C_1\left[1 - \exp\left(-\frac{h}{a}\right)\right]$$

Gaussian:
$$\gamma(h) = 1 - \exp\left(-3\frac{h^2}{a^2}\right)$$

regression equation was:

$$LAP = 1.675 + 0.2108 \times LEL$$

where LAP and LEL are the decimal logs of annual precipitation (cm) and elevation (m), respectively. For the Willamette River basin, the two variables were highly correlated with r = 0.82 (n = 52). Regressions were performed for both log-transformed and untransformed annual precipitation and elevation data. The LAP vs. LEL regression had the highest correlation, the best spacing of data along both axes, used the variables already employed in kriging and cokriging, and thus was chosen for the elevation detrending. The sample semivariogram and model semivariograms for the residuals from this regression (RESID) are shown in Figure 5. The directional semivariograms did not show a great deal of anisotropy so an isotropic model was fit. The rise of the semivariance above the sample variance shows evidence of a trend for distances > 115 km. The model was fit for the 12 points below this distance (see Table 1).

Elevation Semivariograms

Anisotropy was examined by same method as for LAP. The maximum variability of semivariances was evident in directional variograms oriented at 45 and 135 degrees, rather than the 0 and 90 degree orientation for precipitation. Variability among directional semivariances was fairly small for 0 and 90 degrees. Even though anisotropy was evident for distances above 30 km at angles of 45 and 135 degrees, isotropy was assumed for the following reasons:

- This did not coincide with the direction of maximum semivariance variability for LAP, the primary variable.
- With a regular 5 minute grid of elevation values, the number of neighbors (8) used in cokriging would all occur within about 10-20 km of the point being estimated. Anisotropy at these distances was not strongly evident regardless of the angle examined.
- Cokriging estimates of precipitation are to be made at points coinciding with the location of elevation values. Therefore, the

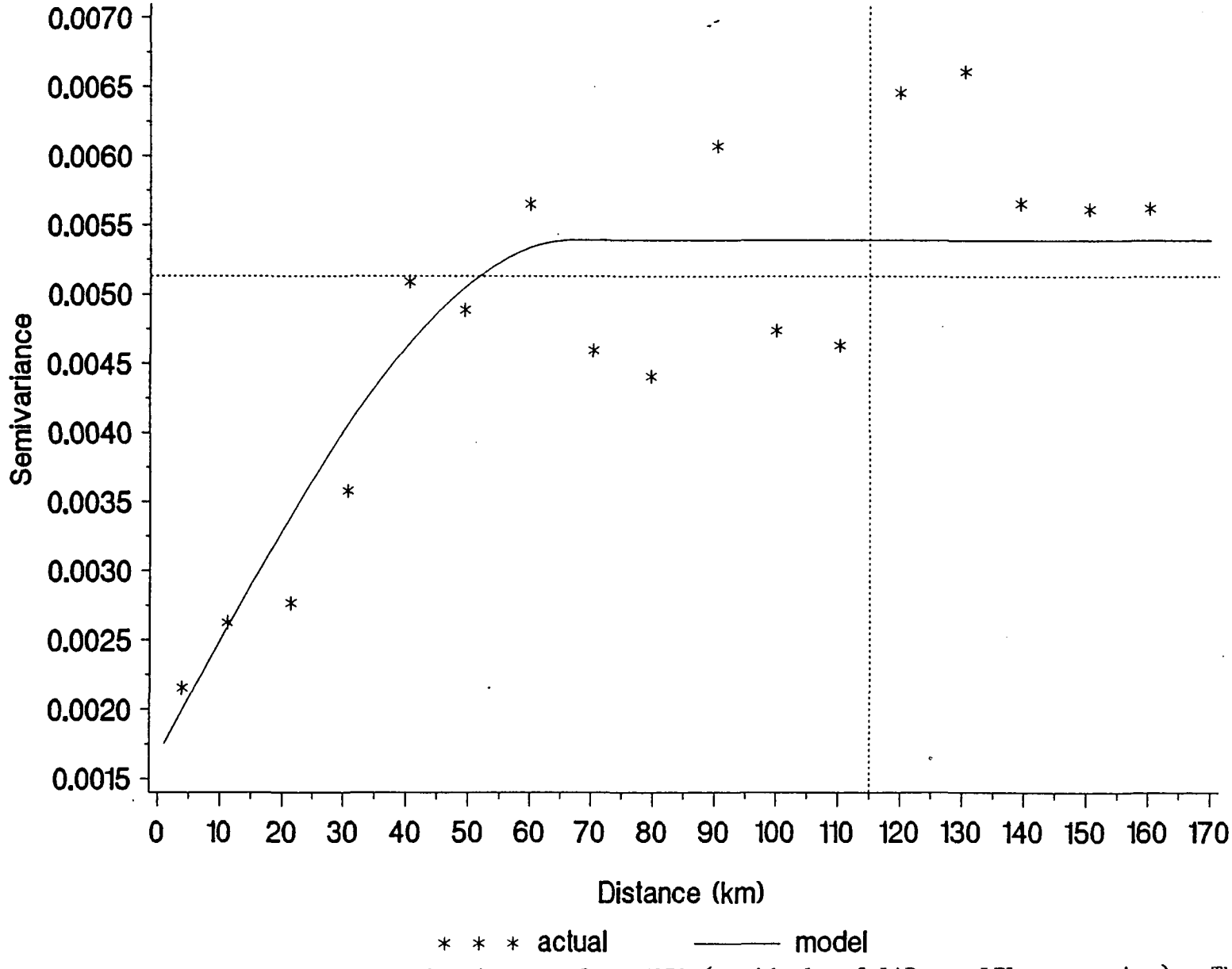

Figure 5. Sample and model semivariograms for RESID (residuals of LAP vs. LEL regression). The model was a spherical model with a nugget of 0.00167, sill minus nugget of 0.00372, and range 67 km. The horizontal dashed line shows the sample variance (n = 52).

influence of surrounding elevation values (within 10-20 km) will be slight, and anisotropy will make little difference.

- o Ease of modeling and cokriging.

The sample and model semivariogram are shown in Figure 6. As was the case with LAP, there was evidence of a trend (rise above sample variance) for distances > 90 km. The model was fit for sample semivariogram points where h $\leq$ 90 km (see Table 1).

Precipitation/Elevation Cross-Semivariograms

The directional cross-semivariograms for LAP/LEL showed patterns very similar to those for the semivariograms for LAP. In the isotropic cross-semivariogram, as with both LAP and LEL semivariograms, there was evidence of a trend (a rise above the sample covariance) for distances > 90 km (Fig. 7). The model was fit for points below this distance (see Table 1).

Precipitation Estimation

Figures 8, 9, and 10 show the precipitation estimates determined by ordinary kriging, elevation detrended kriging, and cokriging, respectively for the 478 5-minute grid points using a search radius of 60 km. The median and range of the precipitation estimates by each method are summarized in Table 2. The associated estimation coefficients of variation (CV) are shown in Figures 11, 12, and 13. The mean CV for precipitation estimates was 21% for kriging, 16% for detrended kriging, and 17% for cokriging. All three methods showed the largest CVs on the edges of the study area. Along the boundary, the size of the neighborhoods incorporating the nearest 8 points were larger, and in some cases less than 8 neighbors occurred within the maximum ellipse radius of 60 km.

The precipitation estimates by ordinary kriging show fairly smooth zonal patterns, with minimum precipitation at low elevations in a band running roughly north-south, and increasing precipitation to the west and east as elevation generally increased up the Coast Range and Cascade mountains. Of

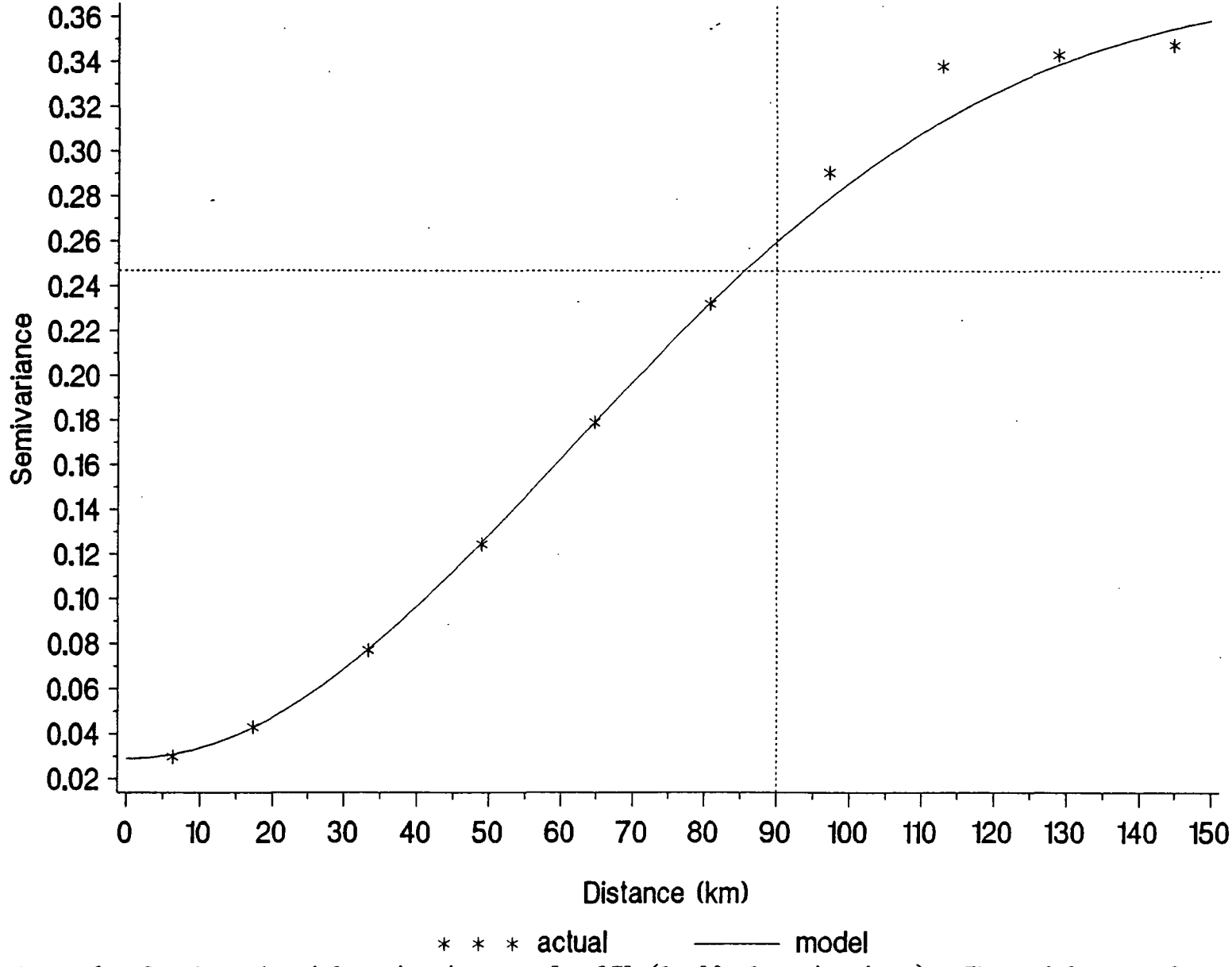

Figure 6. Sample and model semivariograms for LEL (log10 elevation in m). The model was a Gaussian model with a nugget of 0.029, sill minus nugget of 0.346, and range 86 km. The horizontal dashed line shows the sample variance (n = 530).

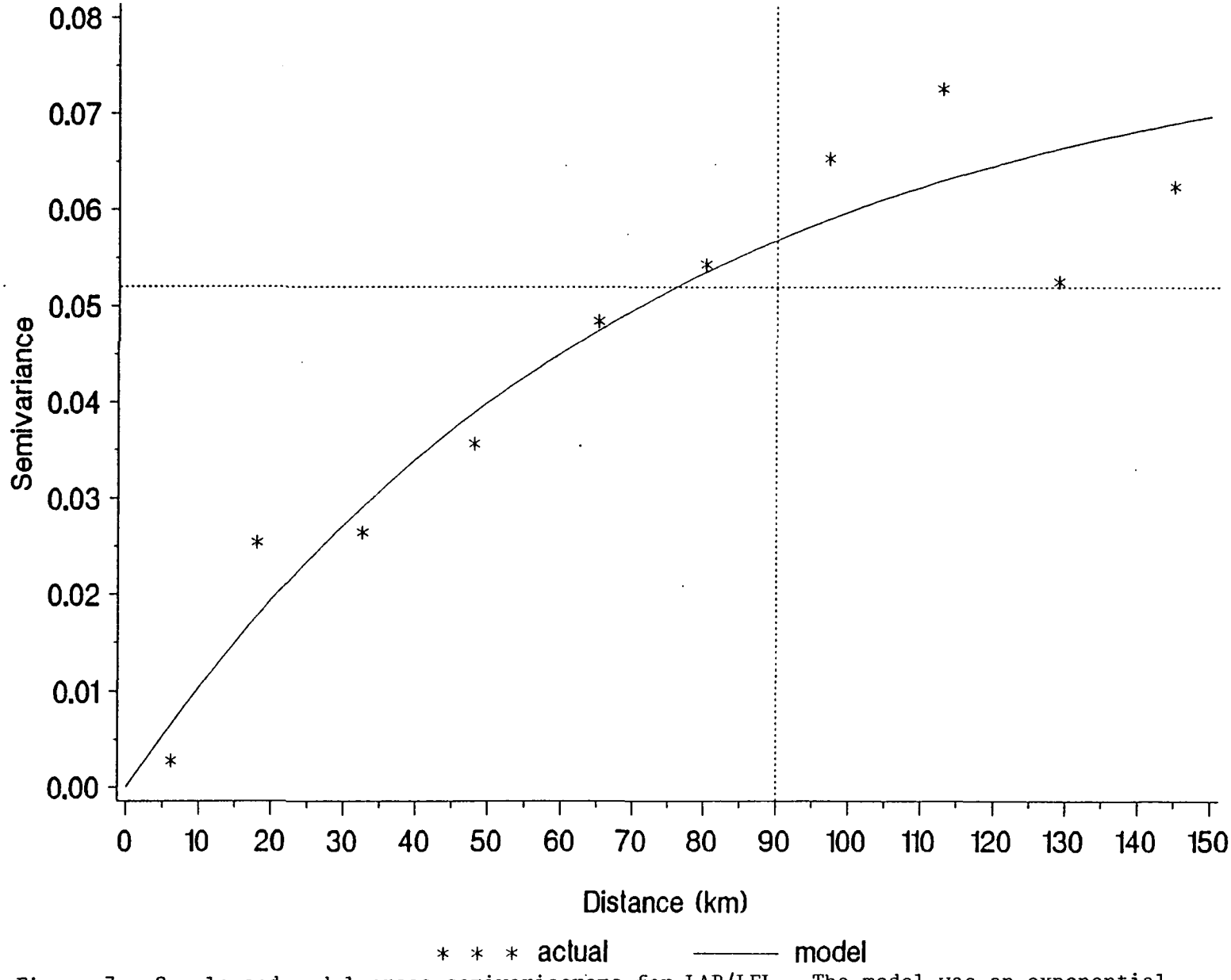

Figure 7. Sample and model cross-semivariograms for LAP/LEL. The model was an exponential model with a nugget of 0, sill minus nugget of 0.0794, and range 71 km. The horizontal dashed line shows the sample covariance (n = 52).

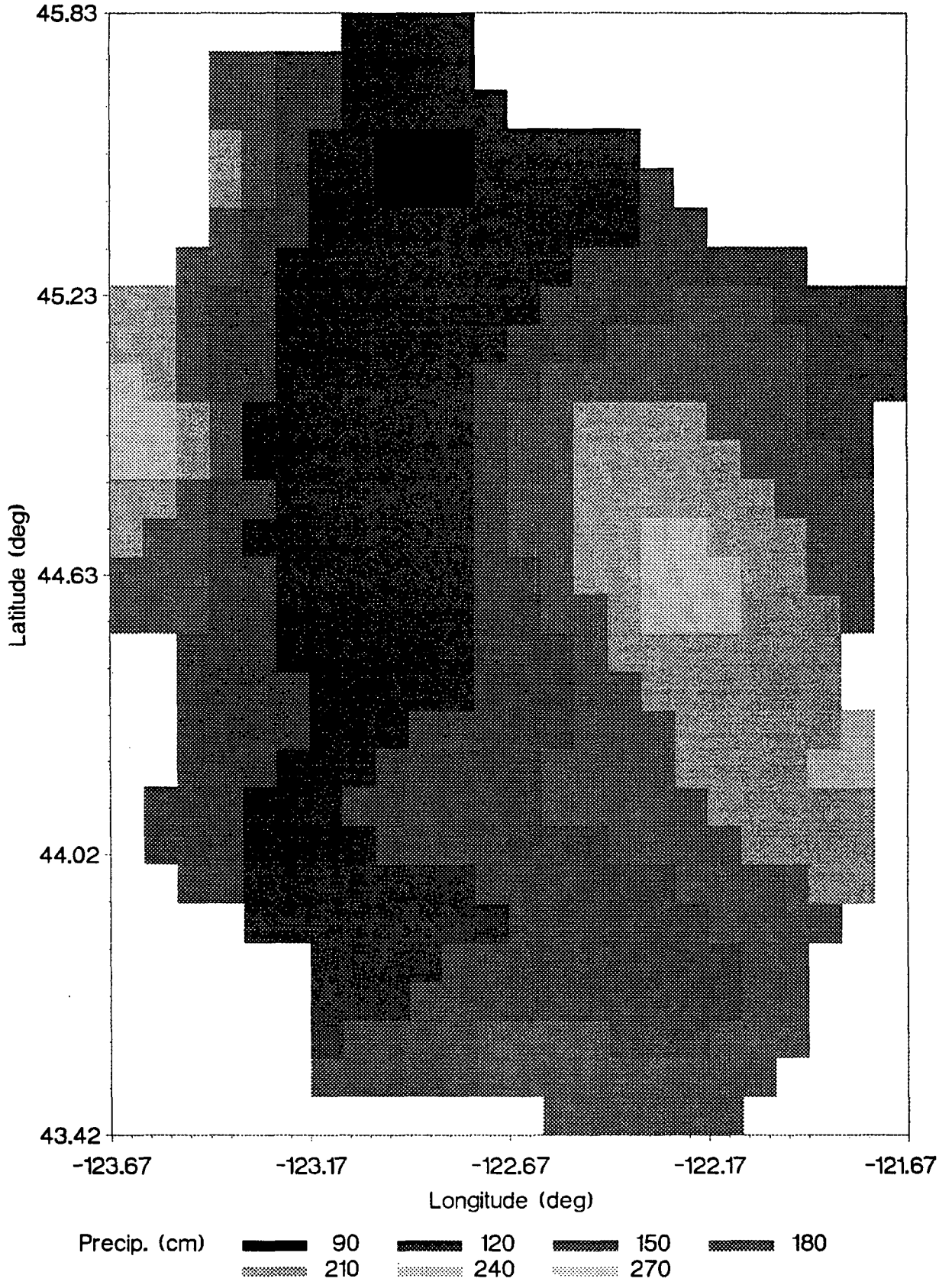

Figure 8. Estimates of annual precipitation (in cm, back-transformed from LAP estimates) from ordinary kriging.

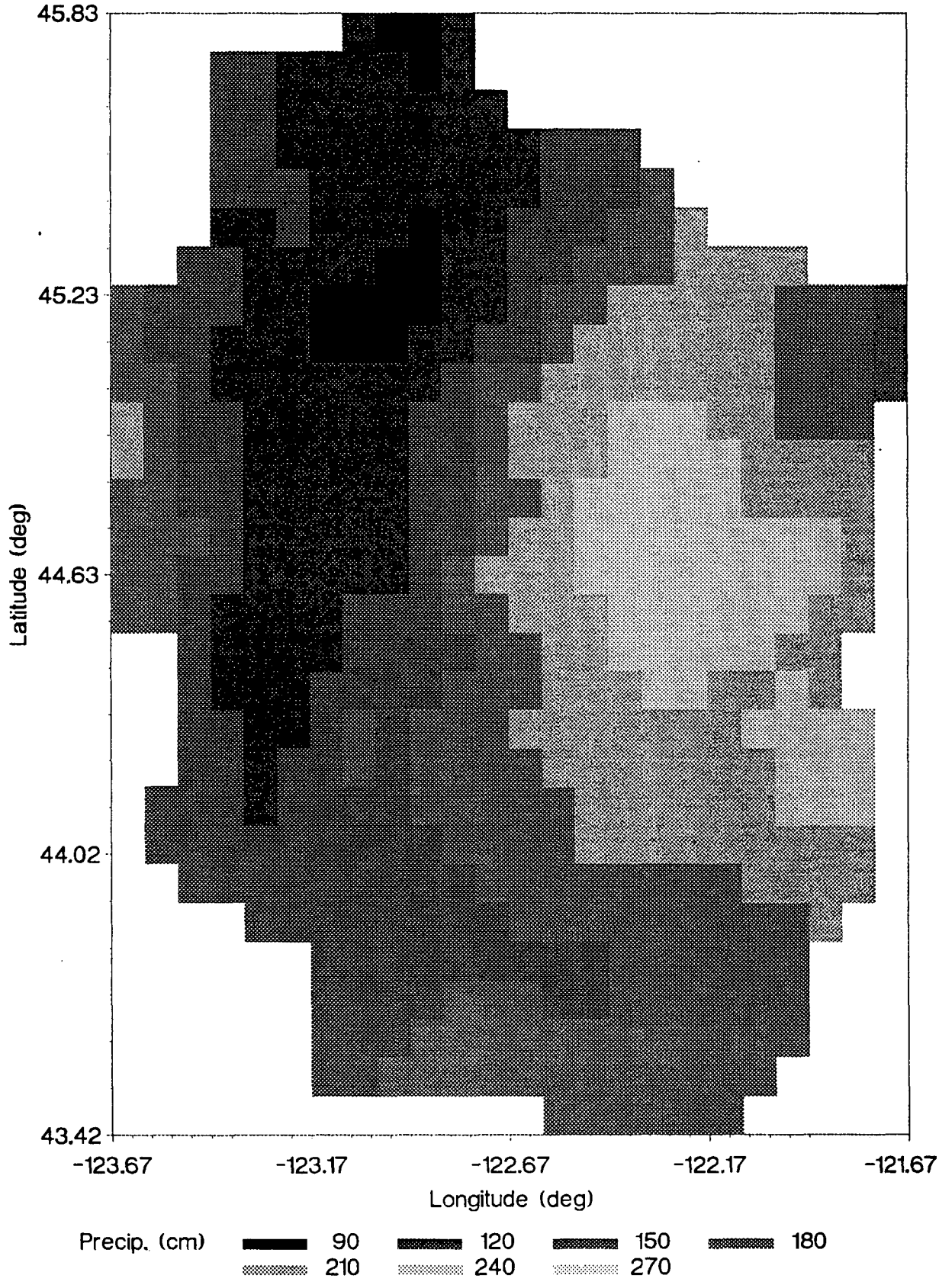

Figure 9. Estimates of annual precipitation (in cm, back-transformed from LAP residual estimates) from detrended kriging.

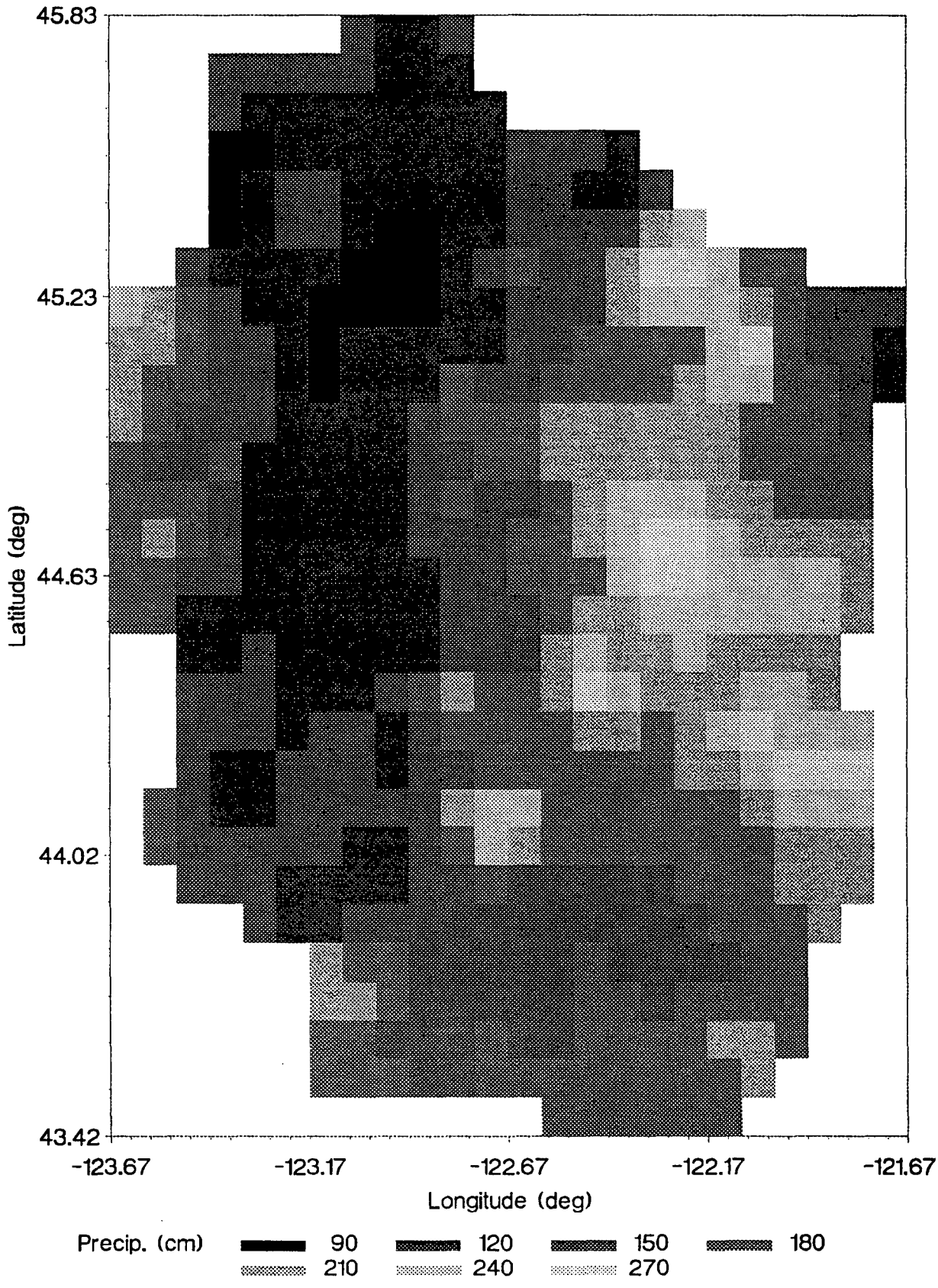

Figure 10. Estimates of annual precipitation (in cm, back-transformed from LAP estimates) from cokriging.

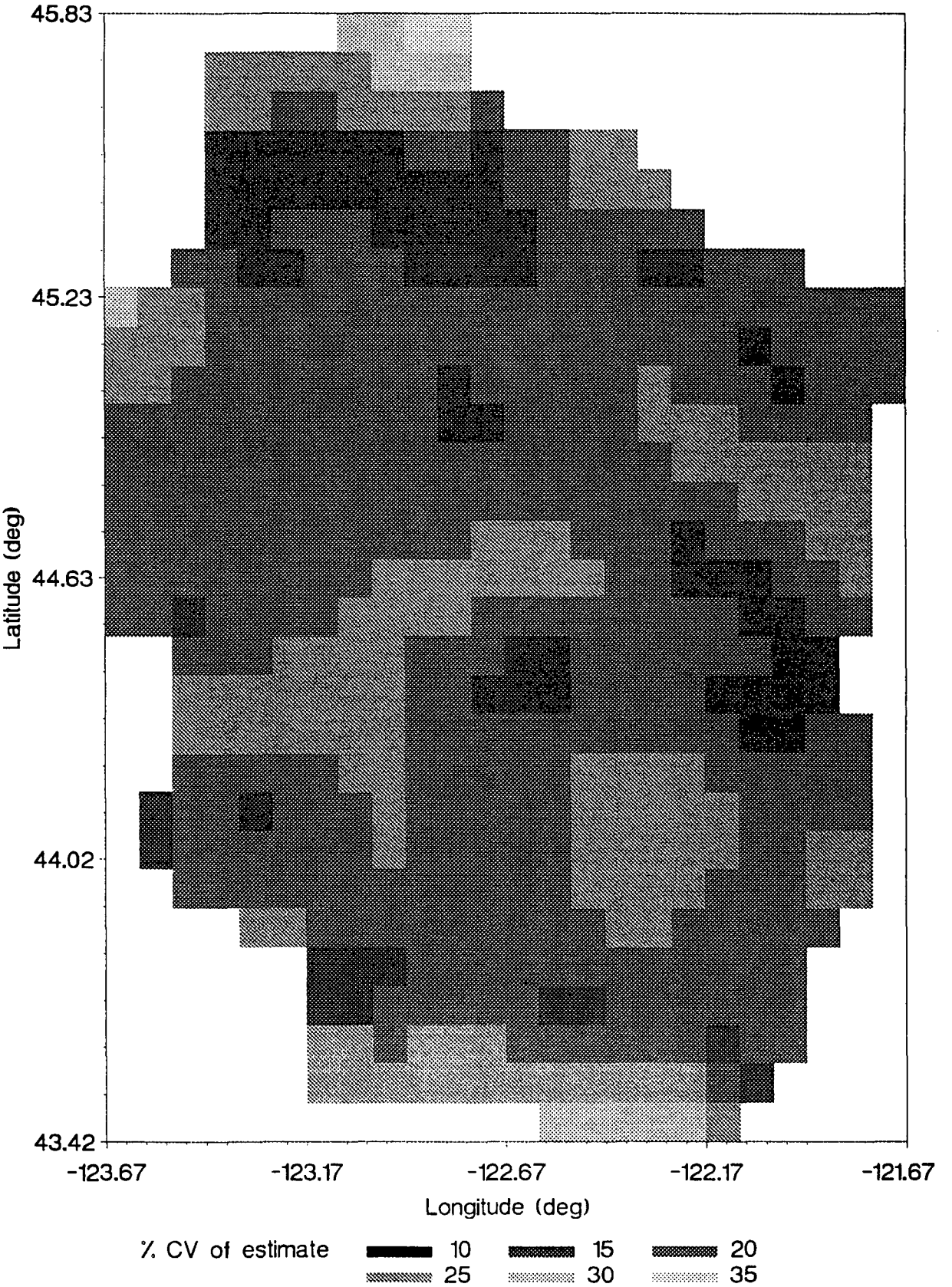

Figure 11. Coefficients of variation (CV, in %) for annual precipitation estimates from ordinary kriging.

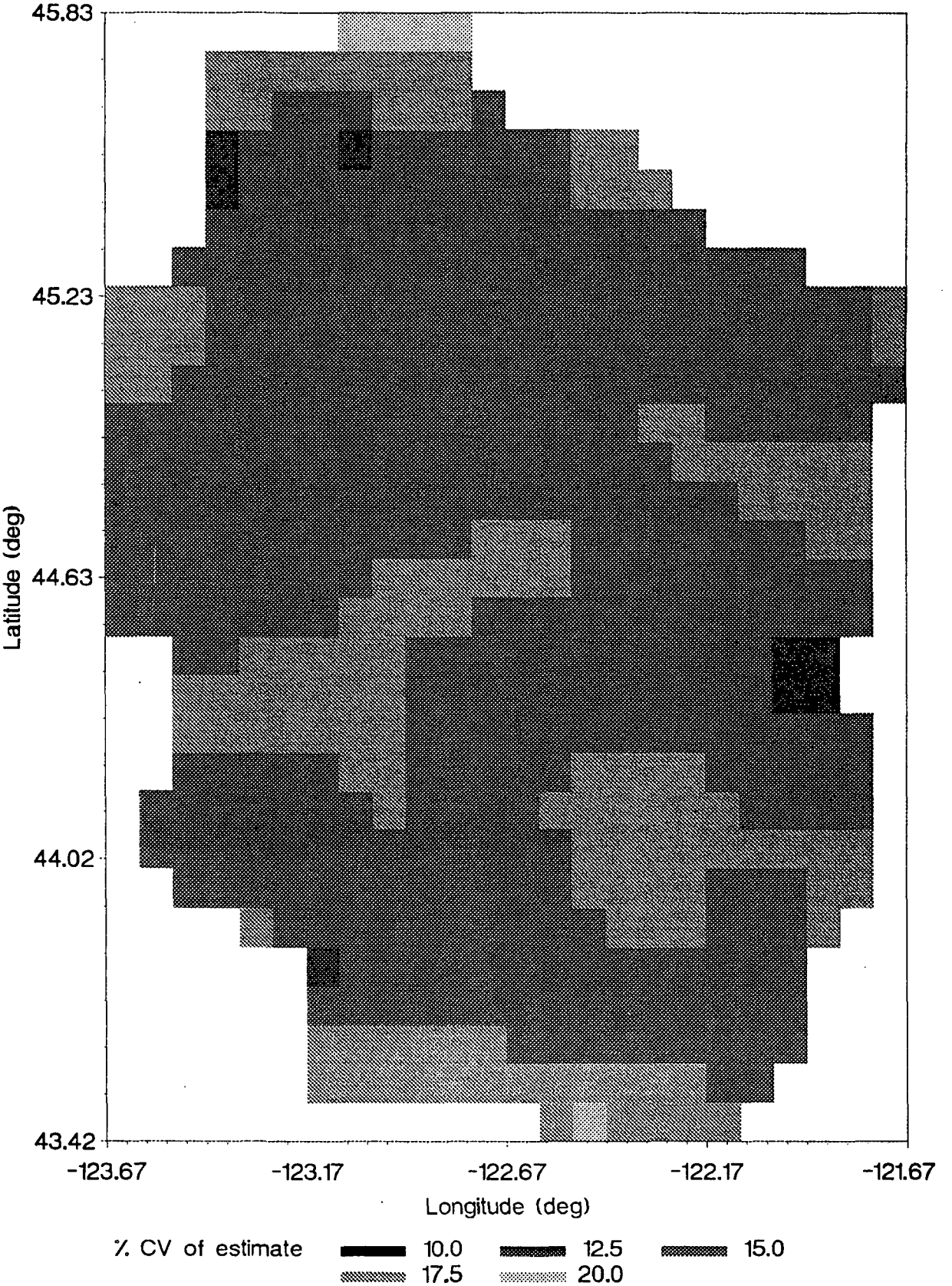

Figure 12. Coefficients of variation (CV, in %) for annual precipitation estimates from detrended kriging.

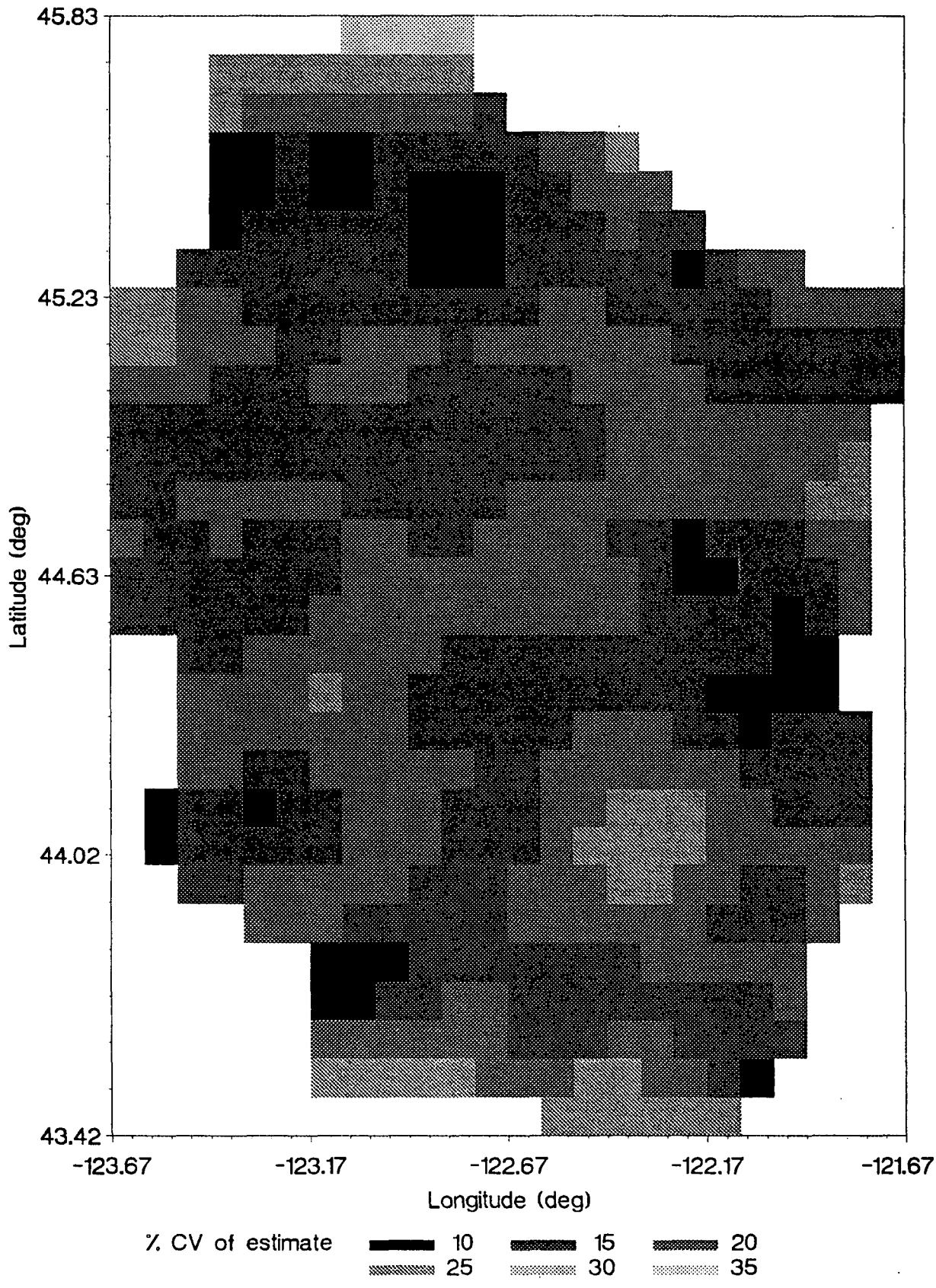

Figure 13. Coefficients of variation (CV, in %) for annual precipitation estimates from cokriging.

TABLE 2. Summary of precipitation estimates by kriging, detrended kriging, and cokriging for 478 points in a 5 minute grid. The estimate statistics are presented in the original (back-transformed) units of cm annual precipitation. The variance ratios are for log10 precipitation values on which the kriging and cokriging were done, and compare the estimation variances of each method with those of ordinary kriging.

Method	Min estimate (cm)	Max estimate (cm)	Median estimate (cm)	Mean % CV for ppt. estimate	mean % variance reduction
Kriging	104	265	151	21	---
Detrended Kriging	97	259	171	16	38
Cokriging	77	319	162	17	28

course, elevation at the kriging estimation points was not taken into account with this method, so these patterns result from the patterns of the weather station data. Interpolation between stations within the search radius of 60 km produced the smoothed contours seen in Fig. 8.

A similar smooth pattern was seen for the detrended kriging method (Fig. 9). The minimum and maximum precipitation estimates were similar to those from ordinary kriging (Table 2), but the contour levels within the basin were shifted westward compared to the kriging contours. Thus, overall the detrended kriging estimates were somewhat higher than the kriging estimates, with a median of 171 cm compared to 151 cm for kriging.

The cokriging estimates exhibited a greater range, with a lower minimum and a higher maximum than either of the other two methods (Table 2). The median estimate (162 cm) was intermediate. The pattern of precipitation contours is much more broken and less smooth (Fig. 10). This same phenomenon was observed by Istok et al. (1990b) and Martinez-Cob (1990) when comparing cokriging (with elevation) estimates with kriging estimates of precipitation and evapotranspiration, respectively. They attributed this to a closer correspondence between the precipitation at a point and local orographic factors which are considered in the cokriging method. While detrended kriging does take elevation into account, it does so by incorporating a regional average effect of elevation into a kriging interpolation of the precipitation data within the search neighborhood. Cokriging, on the other hand, considers not only the local variation of precipitation within the search neighborhood, but the local variation of elevation as well, and thus the estimates are more closely tied to localized orographic features.

Both detrended kriging and cokriging showed considerable average reductions in estimation variance compared to ordinary kriging (Table 2) of 38% and 28%, respectively. Dingman et al. (1988) similarly found reductions in estimation variance for detrended kriging of precipitation, as did Istok (1990b) for cokriging of precipitation, and Martinez-Cob (1990) for cokriging of evapotranspiration. Cross-validation on the 52 weather station points showed average absolute errors of 26 cm for kriging, 19 cm for detrended kriging, and

20 cm for cokriging. Thus, both of the latter two methods seem capable of producing estimates of greater precision than ordinary kriging. Accounting for elevation effects, either by detrending for a regional average effect (detrended kriging) or by incorporation of elevation semivariograms and cross-semivariograms (cokriging), also gave increased accuracy of precipitation estimates. In cross-validation, the average errors for the 52 weather station locations were -5.2 cm for kriging, -1.4 cm for detrended kriging, and -2.0 cm for cokriging.

Issues of Scale

While detrended kriging and cokriging using precipitation-elevation relationships seem to be promising methods for producing spatially distributed precipitation scenarios for global climate change effects research, the scale of the geographic area to which they are applied must be considered. An initial examination was made of the precipitation-elevation relationship in a larger region, the Columbia River drainage area in the United States. This drainage area covers 57 million hectares and includes 8 other major hydrologic subregions besides the Willamette River basin. Because of the dramatic precipitation gradients across this region and the inclusion of major orographic features, the precipitation-elevation relationship was not consistent across the region. The correlation coefficient r for LAP and LEL was 0.00 ($n = 491$). The Willamette River Basin study area covered sizable ranges of both elevation and precipitation, and included several very important orographic features. However, the advantage of using a hydrologically defined area such as this is that the major orographic features occurred on the edge of the region, and all the points in the region fell on the same side of a given orographic feature. Expansion to too large a geographic area includes orographic effects in the interior and weakens the relationship between elevation and precipitation, which is the basis of the improved precipitation estimates by either detrended kriging or cokriging.

There are several alternatives for spatially distributed estimation of precipitation over a large region. The estimates could be done piecewise by using cokriging or detrended kriging on a number of smaller subregions with

consistent precipitation/elevation relationships. Ordinary kriging could be performed over the entire region. However, ordinary kriging was shown to be inferior to the other two methods which explicitly consider elevation when precipitation was strongly correlated with elevation. Also, there would undoubtedly be directional trends and anisotropic effects of considerable magnitude over such a large area. Other geostatistical techniques to be explored include fitting polynomial trend surfaces and using universal kriging, and median polish kriging (Cressie, 1986). Simpler interpolation methods such as inverse distance weighting could be used, but were found to be inferior to geostatistical estimation of precipitation by Tabios and Salas (1985).

Kriging and cokriging are exact interpolation methods, i.e., the surfaces generated always pass through the known data points. Noise in the precipitation data may cause some points to be outliers, especially with fairly short periods of record. Other non-exact interpolation techniques less sensitive to outliers, such as nonparametric trend surface analysis methods, should be explored as well.

A final alternative is the development and use of a physical orographic model incorporating effects of topography, storm tracks, atmospheric thermodynamics, etc. (Peck and Schaake, 1990). However, such a model may be considerably more data-intensive than the statistical methods above.

Future Work

For assessment of impacts on natural resources, global climate change research requires regional scale hydrologic data, including spatially distributed estimates of precipitation (Dooge, 1986; Eagleson, 1986). This paper has demonstrated the utility of several geostatistical methods in providing improved precipitation estimates for hydrologically defined regions. One application for these methods will be estimation of precipitation and temperature for input into forest "gap models" to simulate forest dynamics across a Pacific Northwest landscape under climate change scenarios.

Further analyses will be performed to examine the variation of precipitation patterns in extreme wet and dry years to examine regional patterns of climatic variability as historic analogs to climate change. Seasonal and monthly analyses will be done to increase the temporal resolution of these methods. In addition, methods for spatially distributed estimation of precipitation in larger regions will be examined and tested.

CONCLUSIONS

Detrended kriging and cokriging both provide spatially distributed estimates of precipitation which take into account precipitation-elevation relationships. The inclusion of these relationships leads to precipitation estimates of improved accuracy and precision in mountainous terrain on the scale of a few million hectares. Such estimates are needed for the use of spatially distributed models of hydrology and vegetation to assess the effects of climate change scenarios. Precipitation-elevation relationships weaken at larger scales, necessitating a different approach for providing spatially distributed climate data.

LITERATURE CITED

Campbell, W.G. and D. Marks (1990). A geographic database for modeling the role of the biosphere in climate change. Biospheric Feedbacks to Climate Change: The Sensitivity of Regional Trace Gas Emissions, Evapotranspiration, and Energy Balance to Vegetation Redistribution, Chapter II. EPA report, ERL-Corvallis.

Chua, S. and R.L. Bras (1982). Optimal estimators of mean areal precipitation in regions of orographic influence. Journal of Hydrology 57: 23-48.

Cressie, N. (1986). Kriging non-stationary data. Journal of the American Statistical Association 81: 625-634.

Dingman, S.L., D.M. Seely-Reynolds, and R.C. Reynolds III (1988). Application of kriging to estimating mean annual precipitation in a region of orographic influence. Water Resources Bulletin 24: 329-339.

Dolph, J. (1990). Characterizing the distribution of precipitation and runoff over the continental United States using historical data. Biospheric Feedbacks to Climate Change: The Sensitivity of Regional Trace Gas Emissions, Evapotranspiration, and Energy Balance to Vegetation Redistribution, Chapter IV. EPA report, ERL-Corvallis.

Dooge, J.C.I. (1986). Looking for hydrologic laws. Water Resources Research 22: 465-585.

Eagleson, P.S. (1986). The emergence of global-scale hydrology. Water Resources Research 22: 65-145.

EarthInfo, Inc. (1990). ClimateData User's Manual, TD3200 Summary of the Day - Cooperative Observer Network. EarthInfo, Inc., Denver, Colorado.

Englund, E. and A. Sparks (1988). GEO-EAS (Geostatistical Environmental Assessment Software) User's Guide. U.S. Environmental Protection Agency, Las Vegas, NV.

Isaaks, E.H. and R.M. Srivastava (1989). An introduction to applied geostatistics. Oxford University Press, New York. 561 pp.

Istok, J.D., J.A. Hevesi, and A.L. Flint (1990a). Precipitation estimation in mountainous terrain using multivariate geostatistics: 1. Structural analysis. Unpublished manuscript.

Istok, J.D., J.A. Hevesi, and A.L. Flint (1990b). Precipitation estimation in mountainous terrain using multivariate geostatistics: 2. Isohyetal maps. Unpublished manuscript.

Journel, A.G. and M.E. Rossi (1989). When do we need a trend model in kriging? Mathematical Geology 21: 715-739.

Marks, D. (1990). The sensitivity of potential evapotranspiration to climate change over the continental United States. Biospheric Feedbacks to Climate Change: The Sensitivity of Regional Trace Gas Emissions, Evapotranspiration, and Energy Balance to Vegetation Redistribution, Chapter III. EPA report, ERL-Corvallis.

Martinez-Cob, A. (1990). Multivariate geostatistical analysis of evapotranspiration and elevation for various climatic regimes in Oregon. Ph.D. dissertation, Agricultural Engineering Department, Oregon State University, Corvallis. 228 pp.

Matheron, G. (1971). The theory of regionalized variables and its applications. Cahiers du Centre de Morphologie Mathematique, Ecole des Mines, Fountainebleau, France, 211 pp.

National Geophysical Data Center, National Oceanic and Atmospheric Administration (1989). Geophysics of North America: User's Guide. U.S. Department of Commerce, Boulder, Colorado.

Peck, E.L. and J.C. Schaake (1990). Network design for water supply forecasting in the west. Water Resources Bulletin (in press).

SAS Institute (1985). SAS User's Guide: Statistics, Version 5 Edition. SAS Institute, Inc., Cary, NC.

Smith, J.B. and D.A. Tirpak (1989). The Potential Effects of Global Climate Change on the United States. Report to Congress, U.S. Environmental Protection Agency, Washington, D.C.

Soil Conservation Service, U.S. Department of Agriculture (1988). Snow Survey and Water Supply Products Reference, West National Technical Center, Snow Survey Program, Portland, Oregon.

Tabios, G.Q. and J.D. Salas (1985). A comparative analysis of techniques for spatial interpolation of precipitation. Water Resources Bulletin 21: 365-380.

Yates, S.R. and M.V. Yates (1990). Geostatistics for Waste Management: A User's Manual for the GEOPACK (Version 1.0) Geostatistical Software System. U.S. Environmental Protection Agency, Ada, OK.

EFFECTS OF GLOBAL CLIMATE CHANGE ON GLOBAL VEGETATION

George A. King
NSI Technology Services Corporation
US EPA Environmental Research Agency
200 SW 35th St
Corvallis, OR 97333

Rik Leemans
Global Change Department
National Institute of Public Health and
Environmental Protection, RIVM
P.O. Box 1
3720 BA Bilthoven
the Netherlands

September 1990

ABSTRACT

EFFECTS OF GLOBAL CLIMATE CHANGE ON GLOBAL VEGETATION

The potential redistribution of vegetation types in response to climate change has been estimated in several analyses using climate/vegetation correlation systems such as that of Holdridge combined with GCM climate scenarios. A review of results using five different GCMs revealed a general agreement in terms of the sign of the predicted change in the areal extent of specific vegetation types, i.e., deserts, boreal forest, and tundra biomes decrease, while grasslands and temperate and tropical forests generally increase in area. These changes reflect the increases in precipitation expected in temperate and tropical areas, and the effect of rising temperatures in high latitudes that displace or eliminate tundra and boreal biomes. The proportion of land surface area changing from one vegetation type to another ranged from 16 to 56 % depending on the GCM used.

Introduction

Changes in fluxes of carbon to the atmosphere from the terrestrial biosphere can significantly affect atmospheric CO_2 concentrations (e.g. Tans et al. 1990). Projected changes in global climate (see Appendix A) could result in a significant redistribution of global vegetation, resulting in large changes in carbon pools and fluxes. These changes could provide significant positive or negative feedbacks to climate change. To begin an evaluation of the potential significance of this feedback mechanism, the current best estimates of changes in global vegetation caused by climate change are summarized here. The data presented in this paper forms the basis for calculating changes in terrestrial carbon storage in Turner et al. (1990).

Global Vegetation Models

Several models describing the global distribution of vegetation (or at least classification schemes relating climate to vegetation) are available with which to estimate the redistribution of vegetation in response to climate change. These include models of Holdridge (1947, 1964), Köppen (1900, 1918, 1936), Box (1981), and Lashof (1987). Tuhkanen (1980) and Prentice (1990) have reviewed these models. The original Holdridge (1947, 1964), modified Holdridge (Prentice 1990), Box (1981), and Lashof (1987) approaches have been

used to predict the redistribution of vegetation in response to climate change.

The Holdridge life zone classification uses three climate parameters to define the occurrence of major plant formations: biotemperature, mean annual precipitation, and a potential evapotranspiration (PET) ratio. Biotemperature is a temperature sum over the course of a year, with unit values (e.g., daily values) that are less than 0°C set to 0°C. PET, as Holdridge (1964) defined it, is a linear function of biotemperature, and thus it does not add degrees of freedom to the model. Thus, the Holdridge classification system is really only based on two climate variables, biotemperature and total annual precipitation. The PET ratio is defined as PET/mean annual precipitation. Holdridge created an axis system using these three climate parameters to classify life zones (Figure 1). Mean annual precipitation forms two axes of an equilateral triangle, with the third being the PET ratio. Annual biotemperature forms a separate axis perpendicular to the base of the triangle. The Holdridge classification thus creates hexagons that define specific life zones.

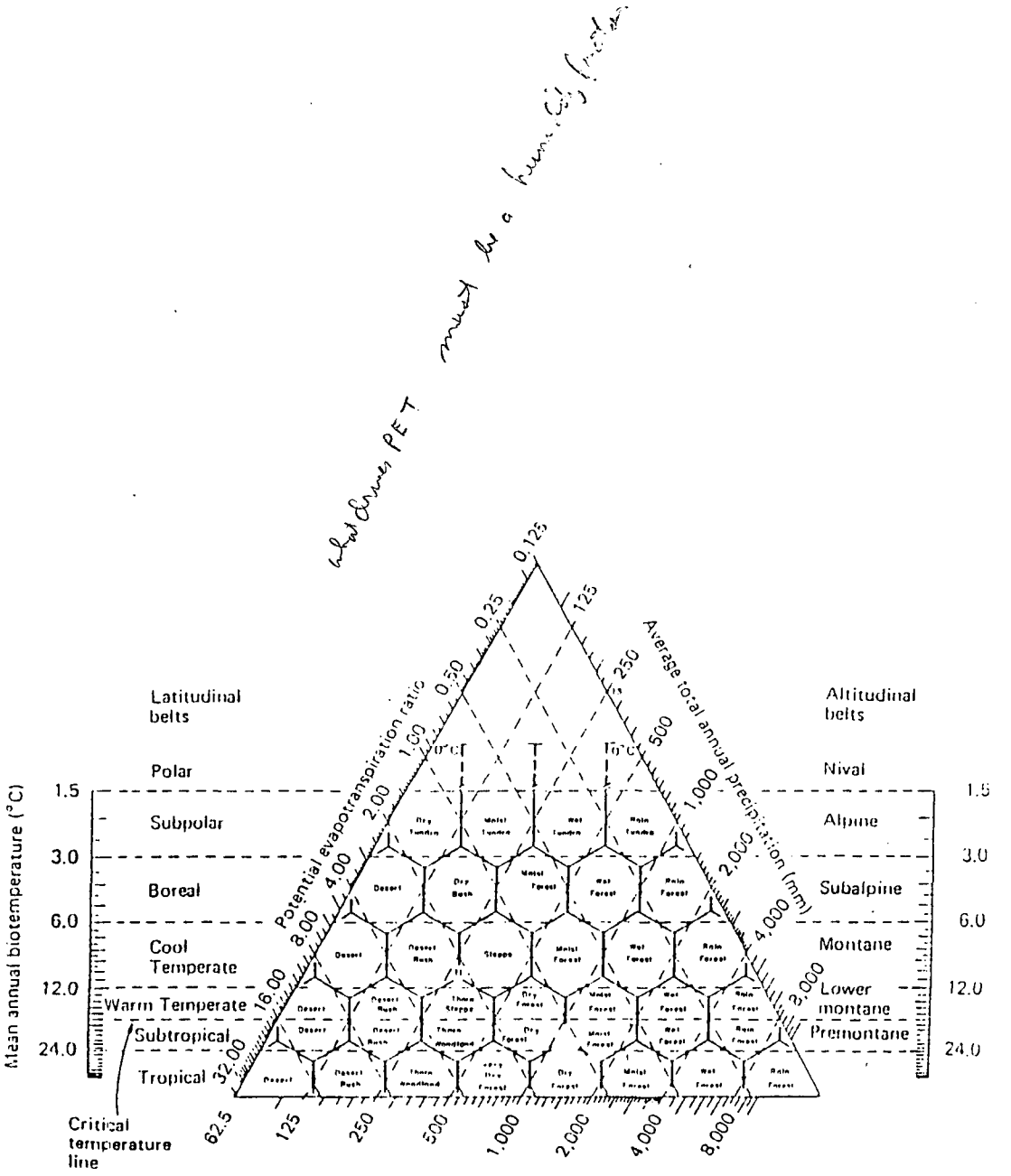

Figure 1. Holdridge life zone classification system (Holdridge 1967).

A significant factor in evaluating simulations of future vegetation patterns is understanding how well the vegetation model simulates current vegetation patterns. The Holdridge life zone classification reproduces broad-scale global vegetation patterns (Leemans 1990), but it is inaccurate for many regions of the world (only vegetation in 40% of $1^{\circ} \times 1^{\circ}$ gridboxes are correctly simulated by the Holdridge system (Prentice 1990)). Prentice (1990) evaluated and refined the Holdridge system to improve its accuracy. In the initial simulation, in which climate space was divided on a finer scale than in the original Holdridge classification, vegetation in 58% of the land gridboxes was correctly simulated. An additional refinement was to aggregate observed vegetation units based on similarity of vegetation and climate. For the final analysis, 18 primary vegetation types and 11 transitional zones were defined. Using this scheme, vegetation in 77% of the gridboxes was correctly predicted.

A more complicated but more biologically realistic global vegetation model was developed by Box (1981). Instead of analyzing climate-biome relationships, Box analyzed the distributions of 77 plant life forms (e.g., summergreen broadleaved trees) throughout the world. For each life form, a set of eight different climate values were correlated with the range limits of the life form. In essence, Box created a set of 77 different climate envelopes within which the life form occurs and outside which the life form is absent. The Box model can predict combinations of growth forms at

any given location, so it is capable of predicting canopy structure.

Box validated his model by simulating life forms present at 74 sites around the world. The actual dominant growth forms were predicted for 92% of the sites, but all dominants and codominants, and no others, were correctly predicted for only 50% of the sites.

Lashoff (1987) developed a statistical model of climate-vegetation relationships using Olson et al.'s (1983) vegetation database. Since this database reflects actual rather than potential vegetation, the Lashoff model is the only currently available approach that incorporates land use.

Limitations of Global Vegetation Models

The four global vegetation models just summarized have significant limitations for predicting future global vegetation patterns. First and foremost, all are steady-state models and non-dynamic. They give no information on how long it would take the vegetation to return to equilibrium with climate. It may take 200-500 years for forest and shrub species to respond to a large climate change (Davis et al. 1986, Webb 1986). Thus, these models cannot be used directly to estimate vegetation patterns that could exist in the next century. Second, the Holdridge and Lashoff approaches, and to a lesser degree the Box approach, are based on empirical

relationships between climate and vegetation. Since future climate regimes in some regions may be different than any present in the world today, vegetation models based on the mechanistic response of species or growth forms to climate must be developed. Third, the models are imperfect predictors of present vegetation, which introduces bias into the simulations of future vegetation patterns. Fourth, none of the models take into account the effect of soils (e.g., nutrient availability, texture) or land use (with the exception of the Lashoff model) on vegetation distribution. Thus, simulating future vegetation using these models assumes that there are appropriate changes in soils to support the predicted vegetation type. In regions where soils have a major effect on vegetating cover, predictions by the vegetation models will likely be incorrect. Fifth, the direct effects of CO_2 on plants are not incorporated into the models.

Equilibrium Simulations of Future Vegetation Patterns

Despite the limitations discussed above, simulations of the potential response of vegetation to future climate change are useful for understanding both the magnitude of possible vegetation change and biospheric feedbacks to climate change. Several global simulations have been recently completed that form the basis for estimating changes in carbon pools and fluxes. Emanuel et al. (1985) made the first global projection of future vegetation

patterns using the Holdridge approach, although only changes in temperature were used to calculate future vegetation patterns. A more recent and complete simulation using the Holdridge approach and five climate scenarios has been completed by Leemans (1990) and Smith et al.(1990). Prentice and Fung (1990) used the refined Holdridge system (Prentice 1990) to project future vegetation patterns and carbon storage. Smith et al. (1990) also used the Box model to project changes in vegetation in the tropical and boreal regions of the world.

Major changes in the distribution of the world's vegetation are projected under all the double-CO_2 climate scenarios and the different vegetation models (Emanuel et al. 1985a,b, Smith et al. 1990, Prentice and Fung 1990). The results of each analysis are briefly summarized here. It should be emphasized that these analyses are for potential natural vegetation, and do not take into account human land-use (e.g., agriculture).

Emanuel et al. (1985a,b) created a future climate scenario using temperature data from Manabe and Stouffer's (1980) simulation of global climate under quadruple-CO_2 concentrations. Temperature changes were divided by two to create a double-CO_2 climate scenario. Under this scenario, tropical forests, grasslands, subtropical deserts, and boreal deserts showed significant expansion, while subtropical forests, boreal forests, warm temperate forests, tundra, and ice contracted significantly (Table

Table 1. Changes in Global Vegetation Distribution in a Double-CO_2 Atmosphere using the Holdridge Classification System as Applied by Emanuel et al. 1985a,b.

Vegetation Type	Current Area ($10^6 \cdot km^2$)	2 x CO_2 Area ($10^6 \cdot km^2$)	Percent Change
Ice	2.22	0.57	-74
Tundra	4.47	3.03	-32
Boreal Deserts	1.31	2.59	98
Boreal Forests	17.26	10.88	-37
Cool Temperate Deserts	4.84	4.04	- 16
Grasslands	22.78	28.52	25
Cool Temperate Forests	11.29	11.63	3
Warm Temperate Deserts	6.75	5.41	20
Warm Temperate Forests	15.81	14.69	- 7
Subtropical Deserts	2.91	3.66	26
Tropical Deserts	10.74	12.63	18
Subtropical Forests	11.96	9.38	-22
Tropical Forests	19.03	24.33	28
Total	131.37	131.36	

1). Smith et al. (1990) used five different climate scenarios generated from output from the four GCMs described in Appendix A. The fifth scenario is a second run of the GFDL model using a more realistic heat flux, and is referred to here as GFDL-QFlux. Under all climate scenarios, the tundra, cold parklands, forest tundra, boreal forest, cool desert, warm temperate forest, and tropical

seasonal forest biomes generally decreased significantly in areal extent (Table 2). The temperate forest, tropical semi-arid, tropical dry forest, and tropical rain forest biomes increased in areal extent. Tropical rain forests doubled in area under the GISS and OSU climate scenarios. The GFDL-Qflux scenario results represent the least change from the present, with only the cold parklands and tropical rain forests changing in size by more than 20%.

Table 2. Changes in Global Potential Vegetation Distribution in a Double-CO_2 Atmosphere using the Holdridge Classification System as applied by Smith et al.(1990).

Biome	Current Area ($10^6 \cdot km^2$)	Percentage Change GFDL	GFDL-QFlx	GISS	OSU	UKMO
Tundra	9.30	-66	- 9	-54	-49	-69
Cold Parklands	2.79	1	-28	-15	- 4	-39
Forest Tundra	8.90	-56	- 1	-34	-33	-62
Boreal Forest	15.03	-36	3	-10	- 6	-32
Cool Desert	4.01	-24	-13	-42	-21	-48
Steppe	7.39	57	-10	- 6	18	- 3
Temperate Forest	9.94	19	17	35	16	31
Hot Desert	20.85	- 1	- 4	-15	- 7	- 4
Chaparral	5.58	33	- 3	- 2	-12	54
Warm Temperate Forest	3.17	-38	7	-40	-23	- 9
Tropical Semi-Arid	9.56	46	-10	75	27	74
Tropical Dry Forest	14.86	32	- 5	30	0	75
Tropical Seasonal Forest	15.13	-34	- 5	-48	-33	-49
Tropical Rain Forest	8.46	82	47	105	137	52
Total	134.97					

Prentice and Fung (1990), using a GISS climate scenario, also reported significant increases in the areal extent of tropical rain forests, as well as savanna, cold deciduous broadleaved forest and woodland, and drought deciduous forest (Table 3). Drought deciduous woodland, arid grassland, desert, evergreen needle-leaved forest, tundra, and temperate evergreen seasonal forest all showed significant decreases in area.

Table 3. Changes in Global Vegetation Distribution in a Double-CO_2 Atmosphere using the Holdridge Classification System as modified by Prentice (1990) and applied by Prentice and Fung (1990)

Vegetation Type	Area ($10^6 \cdot km^2$)	Perc. Change	2 x CO_2 Area
Polar Desert and Ice	3.00	0	3.00
Tundra	7.00	- 63	2.59
Cold-Deciduous Needleleaved Forest and Woodland	16.00	5	16.80
Evergreen Needleleaved Forest and Woodland	6.00	- 66	2.04
Mesic Grassland	2.00	- 17	1.66
Drought-Deciduous Woodland	6.00	- 42	3.48
Arid Grassland and Shrubland	30.00	- 22	23.40
Cold-Deciduous Broadleaved Forest and Woodland	12.00	40	16.80
Temperate Evergreen Seasonal Broadleaved Forest	2.00	- 31	1.38
Mediterranean Forest and Woodland	2.00	4	2.08
Desert	14.00	- 62	5.32
Savanna	5.00	35	6.75
Drought-Deciduous, Drought-Seasonal Broadleaved Forest	9.00	21	10.89
Tropical Rain Forest	19.00	75	33.25
Total Area	133.00		129.44

In contrast to the results using the Holdridge system presented, preliminary estimates using the Box approach suggest that tropical forests will decrease in area rather than increase (Smith personal communication).

To compare the results of Emanuel et al. (1985), Smith et al. (1990), and Prentice and Fung (1990), the vegetation classes they used have been grouped into six broad vegetation types (Table 4, Figure 2). Generally, there is agreement in terms of the sign of the predicted vegetation change. Deserts, boreal forests, and tundra types decreased in areal extent, while grasslands, temperate forests, and tropical forests generally increased in area under double-CO_2 climates. Across the seven different simulations and

six vegetation categories, there are only four differences in the direction of the predicted change. The GFDL-Qflux climate scenario caused the smallest changes in global vegetation. Despite the general agreement in the sign of the changes, there are significant differences in the estimated magnitude of the vegetation changes. For instance, estimates of the future distribution of boreal forest differ by a factor of two.

Table 4. Comparison of Global Vegetation Distribution in a Double-CO_2 Atmosphere using the Holdridge Classification System, as applied by three different teams of investigators.

A. SMITH ET AL. 1990 Predictions

Vegetation Type	Current Area	GFDL	GFDL-QFlx	GISS	OSU	UKMO
		Percentage Change				
Deserts	20.80	- 1	- 4	-15	- 7	- 4
Grasslands/Shrubland	26.60	35	- 9	18	9	30
Temperate Forests	13.10	5	14	17	7	21
Boreal Forests	26.70	-39	- 2	-19	-15	-43
Tropical Forests	38.50	17	6	16	17	21
Tundra	9.30	-66	- 9	-54	-49	-69
TOTAL	135.00					

B. PRENTICE AND FUNG 1990 Predictions

	Current Area	GISS Percentage Change
Deserts	14.00	- 62
Grasslands/Shrubland	38.00	- 25
Temperate Forests	16.00	27
Boreal Forests	22.00	- 14
Tropical Forests	33.00	54
Tundra	10.00	- 44
TOTAL	133.00	

C. EMANUEL ET AL. 1985b Predictions

	Current Area	Percentage Change
Desert	20.40	6
Grasslands	27.62	18
Temperate Forests	27.10	- 3
Boreal Forests	18.57	-27
Tropical Forests	30.99	9
Tundra	6.69	-46
TOTAL	131.37	

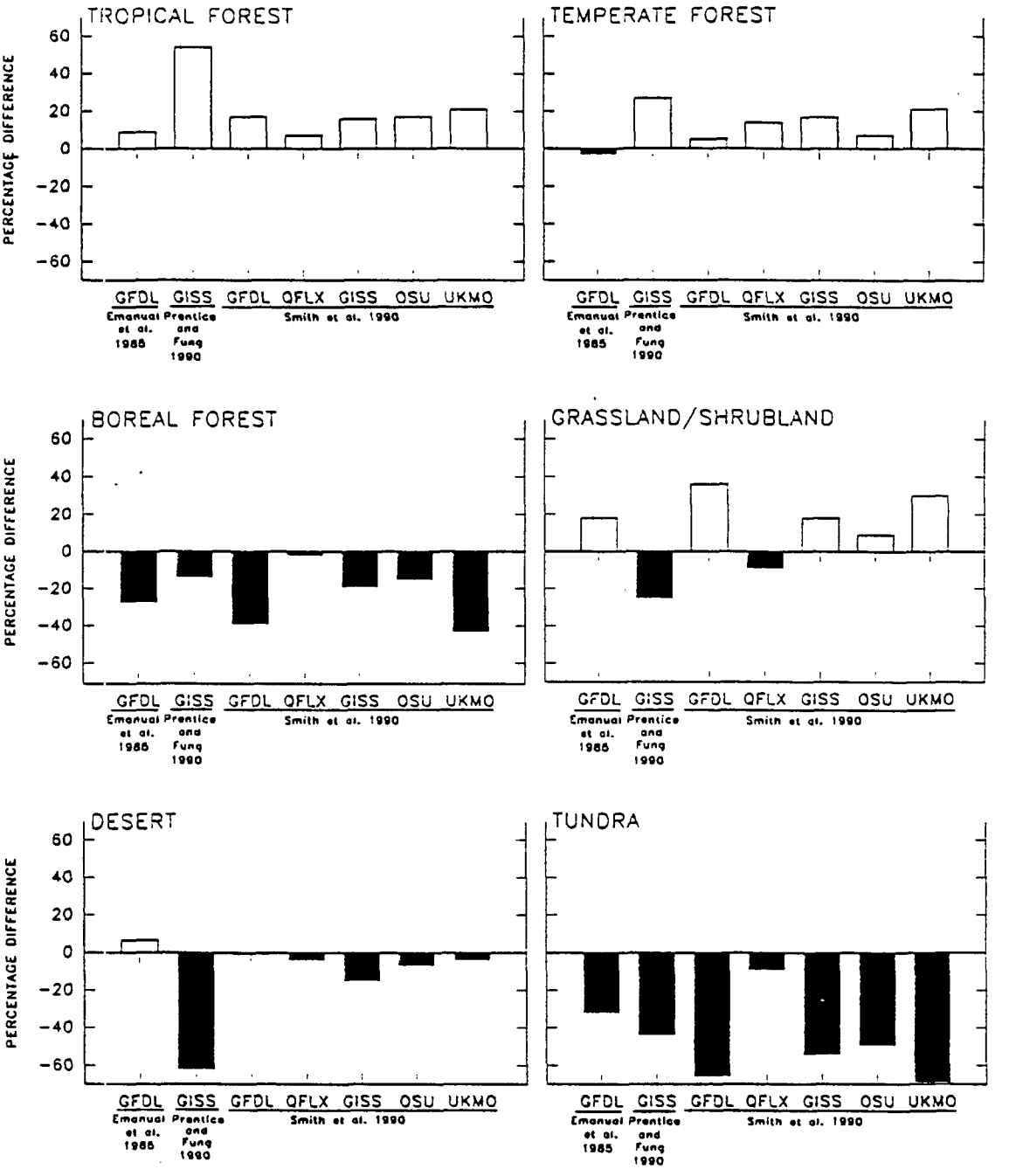

Figure 2. Histograms showing changes in the total area of six major vegetation types after a double-CO2 induced climate change. Emanuel refers to Emanuel et al. 1985; Prentice to Prentice and Fung 1990, and Smith et al. to Smith et al. 1990. Data also summarized in Table 4.

The results presented above in effect are summaries of global vegetation before and after a climate change caused by a doubling of CO_2 concentrations. What is not indicated by these numbers is the amount of land that changed from one vegetation type to another. This could have a significant impact on the global carbon cycle because of the transient release of carbon to the atmosphere from vegetation dieback (see section 3.2 in King et al. 1990). In the Prentice and Fung (1990) scenario, 60% of the vegetated landscape on the globe changed vegetation type. In the Smith et al. (1990) scenarios, 16% (GFDL-QFlux) to 56% (UKMO) of the earth's land surface changed vegetation type (Table 5, Figure 3). Such predicted changes would have significant impacts on biodiversity (discussed next), water resources, forest resources, agriculture, and land management.

Table 5. Areal extent of land on the globe changing vegetation cover under double-CO_2 conditions as estimated using the Holdridge system (Smith et al. 1990).

Climate	Amount of Land Changing Vegetation Cover (10^6 km2)	Perc. of Land Surface Changing
GFDL	65.24	48.34
GFDL-QFlux	21.51	15.94
GISS	60.36	44.72
OSU	53.73	39.81
UKMO	76.21	56.46
Total Land Area	134.97	

Discussion of Vegetation Scenario Results

The fact that the vegetation scenarios are similar (in terms of the sign of the change) using the Holdridge approach is not surprising, given that the GCM scenarios on a global basis predict warmer and wetter conditions than present (see Appendix A). In general, a point in climate space on the Holdridge diagram (Figure 1) can be expected to move down and to the right under double-CO_2 climate conditions. More detailed results from Smith et al. (1990) not presented here in fact show that this is often the case. For instance, areas of current tundra vegetation are estimated to change in the future to forest tundra or boreal forest. Tropical seasonal forest regions that change type tend to change to tropical rain forest.

Estimates of current area of the six vegetation types can differ substantially between investigators. That the Prentice and Fung (1990) areas are different is not surprising, as they used a different vegetation classification system from the original Holdridge system. However, Emanuel et al. (1985b) and Smith et al. (1990) used the same basic vegetation units in their analyses, and they aggregated the units in the same way to obtain the areas for the vegetation types presented in Table 4. For instance, estimates of boreal forest area differ by over 8×10^6 km^2. A possible reason for this is that Emanuel et al. (1985a,b) used monthly temperature values to calculate annual biotemperature, whereas Smith et al.

(1990) used daily values. Consequently, differences in the percent changes listed in Table 4 are in part due to differences in how the current vegetation areas were calculated, and how the individual vegetation units were aggregated to form the vegetation units used in the table.

The other reason the estimated changes in vegetation differ is that there are large differences in the climate scenarios used to drive the vegetation models (see Appendix A).

Conclusions and Research Needs

Global climate change on the order currently projected by GCMs will cause large changes in the distribution of global vegetation. However, because of differences in GCMs, climate scenarios and vegetation models, and the simplifying assumptions on which the vegetation models are constructed, the specifics of future, steady-state, vegetation patterns are highly uncertain. One of the weaknesses of current global vegetation models is that they are based on correlations between climate and vegetation, correlations which may not persist under altered climate conditions. Furthermore, current models do not incorporate soils or the potential effects of CO_2 fertilization on vegetation. Land-use is not treated by many of the models.

In addition, current global vegetation models can not be used to

estimate transient vegetation dynamics. The ability to predict the transient response of global vegetation to climate change is essential for estimating biospheric feedbacks and regional sensitivity to climate change in the next century, and for evaluating the effectiveness of various mitigation strategies (e.g., reforestation).

There is much work to be done in producing a dynamic and realistic global vegetation model. The following areas of research need attention in order to develop such a model:

- Development of a plant life-form classification system that can form the basis of a global vegetation model. Life-forms grouped together should have common autoecological characters, such as physiognomy, seed dispersal and response to macroclimate and soils.

- Determination of the ecological mechanisms through which climate controls the distributions of these life-forms.

- Incorporation of disturbance and migration into global vegetation models.

- Production of global vegetation maps based on remotely sensed data to calibrate and validate vegetation models.

- Generation of digitized databases of soil texture and nutrient availability at a resolution appropriate for global modeling.

- Calculation of the effects of CO_2 enrichment on ecosystem water-use efficiency.

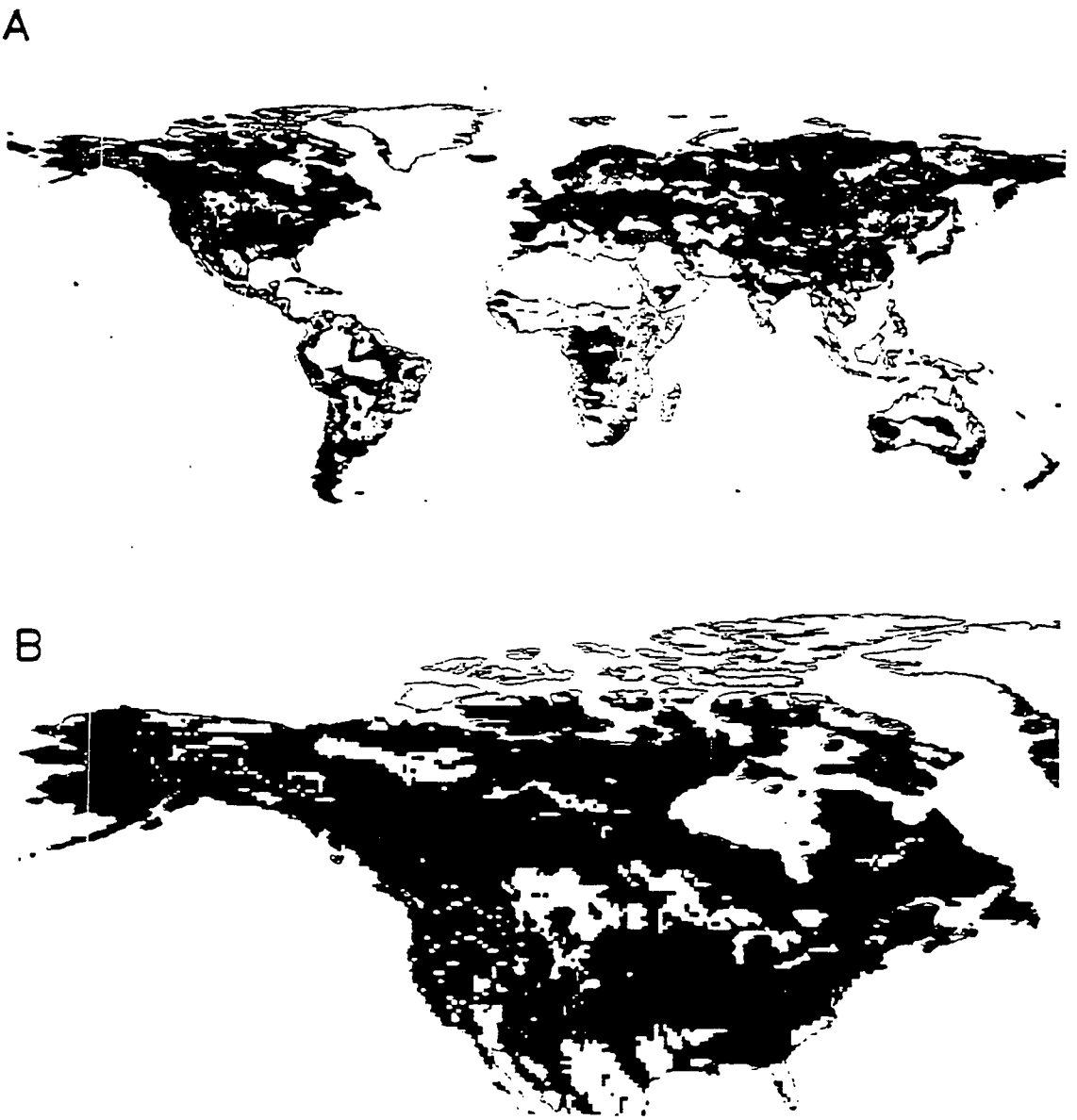

Figure 3. Areas (black) in which predicted future vegetation is different from current vegetation using the UKMO double-CO_2 climate scenario (Smith et al.1990).
a. Global changes in vegetation cover.
b. North American changes in vegetation cover.

LITERATURE CITED

Box, E.O. 1981. Macroclimate and Plant Forms: An Introduction to Predictive Modeling in Phytogeography. Dr. W. Junk Publishers, The Hague.

Davis, M.B. 1986. Climatic instability, time lags, and community disequilibrium. In: J. Diamond and T.J. Case, eds., Community Ecology, Harper and Row, N.Y.

Emanuel, W.R., H.H. Shugart, and M.P. Stevenson. 1985a. Climatic change and the broad-scale distribution of terrestrial ecosystem complexes. Climate Change 7:29-43.

Emanuel, W.R., H.H. Shugart, and M.P. Stevenson. 1985b. Response to comment: Climatic change and the broad-scale distribution of terrestrial ecosystem complexes. Climate Change 7:457-460.

Holdridge, L.R. 1947. Determination of world formations from simple climatic data. Science 105:267-268.

King, G.A., J.K. Winjum, R.K. Dixon, and L.Y. Arnaut, eds. Submitted, 1990. Response and feedbacks of forest systems to global climate change. Report prepared for Environmental Protection Agency, Washington, DC. 204 pp.

Köppen, W. 1936. Das Geographische System der Klimate. In: Handbuch der Klimatologie, by W. Köppen, and R. Geiger, IC, Gebr Borntraeger, Berlin, 46 pp.

Köppen, W. 1900. Versuch einer Klassification der Klimate, vorzugsweise nach ihren Beziehungen zur pflanzenwelt. Geographische Zeitschrift. 6:593-611, 657-679.

Köppen, W. 1918. Klassification der Klimate nach Temperatur, Neidenschlag und Jahreslauf. Petermanns Geogr. Mitt. 64:193-203, 243-248.

Lashof, D. 1987. The role of the biosphere in the global carbon cycle: evaluation through biospheric modeling and atmospheric measurement. Ph.D. Dissertation, Energy and Resources Group, University of California, Berkeley, CA.

Leemans, R. 1990. Possible changes in natural vegetation patterns due to a global warming. Publication Number 108 of the Biospheric Dynamics Project, International Institute for Applied Systems Analysis.

Leemans R. and Prentice, I.C. 1990 (In prep.) Possible changes in natural vegetation patterns using GCM climate scenarios.

Prentice, K.C., and I.Y. Fung. Bioclimatic simulations test the

sensitivity of terrestrial carbon storage to perturbed climates. Nature. In press.

Prentice, K.C. Bioclimatic distribution of vegetation for GCM studies. J. Geo.Res. In press.

Smith, T.M., R. Leemans, W. Cramer, I.C. Prentice, A.M. Solomon, and H.H. Shugart. Submitted. Simulating changes in the distribution of global terrestrial vegetation under CO_2-induced climate change: Comparison among scenarios based on general circulation models. Climate Change.

Tans, P.P., I.Y. Fung, and T. Takahashi. 1990. Observational constraints on the global atmospheric CO_2 budget. Science 247:1431-1438.

Webb, T. 1986. Is vegetation in equilibrium with climate? How to interpret late-quaternary pollen data. Vegetatio 67:75-91.

APPENDIX A: CLIMATE SCENARIOS

In order to determine the possible impacts of global climate change on vegetation, quantitative estimates are needed of the magnitude of trace gas induced climatic change. General Circulation Models (GCMs) of the earth's atmosphere are the only tool available for making quantitative estimates of climate variables on a global scale. GCMs are complex computer models based on fundamental principles of physics and thermodynamics (e.g. Schlesinger 1988). In the past decade, several GCMs have been used to simulate the possible effect on global climate of a doubling of CO_2 concentrations. Results of simulations of four different GCMs (Table A1) are widely available for use by researchers and were used by Smith et al. (1990) in generating their Holdridge vegetation scenarios. Some of the overall conclusions on future climate change and uncertainties in the GCMs are discussed in this appendix, as well as the general methodology for creating the future climate scenarios.

TABLE A1 GENERAL CIRCULATION MODELS USED TO GENERATE DOUBLE CO_2 CLIMATE SCENARIOS

Model Name	Reference
Geophysical Fluid Dynamics Model (GFDL)	Manabe and Wetherald 1987
Goddard Institute for Space Studies (GISS)	Hansen et al. 1988
Oregon State University (OSU)	Schlesinger and Zhao 1989
United Kingdom Meteorological Office (UKMO)	Mitchell et al. 1989

The most recent results suggest that double CO_2 conditions will increase global temperatures from 1.9 to 4.4°C (Schlesinger and Zhao 1989, Washington and Meehl 1989, Mitchell and Warilow 1987, Mitchell et al. 1989, Wetherald and Manabe, In prep.). Global precipitation could increase from 7.8% to 11% (Smith and Tirpak 1989). Regional and seasonal predictions are more variable between models, sometimes differing even in the predicted direction of the change (e.g. whether precipitation increases or decreases in a region). The speed of these changes depends upon the rate of increase of CO_2 concentrations in the atmosphere. Current estimates suggest that CO_2 concentrations will double their pre-industrial level between 2055 and 2080 without any effort at stabilizing emissions (Lashoff and Tirpak 1989). Considering both the magnitude and rate of change, trace gas induced climate change could be greater than any climate change during the last 15,000 years.

Although GCMs are expansive, complicated and computationally intensive computer programs, they are far from perfect in simulating present climate (Grotch 1988, Dickenson 1989, Neilson et al. 1990). For instance, the GFDL model predicts winter temperatures that are 1.8°C cooler than those observed for North America. The GISS model simulates summer temperatures 3.1°C cooler than those observed for this same region. Precipitation estimates are even more problematic. Four major problems exist with how the models simulate climate: 1) poor simulation of cloud processes; 2)

inadequate atmosphere-ocean coupling; 3) overly simplistic biosphere; and 4) poor spatial resolution. Consequently, the accuracy of future climate simulations is considered highly uncertain. Major research efforts are underway to improve GCMs (the Department of Energy's ARM and CHAAMP programs) and to determine how well they simulate past climates as a validation technique (COHMAP 1989).

Despite the limitations of GCM output, especially their poor spatial resolution, they remain the only tool that can provide spatially distributed estimates of future climates based on the principles of atmospheric physics. The challenge for researchers estimating the effects of climate change on some component of the biosphere is to generate reasonable scenarios of future climate for input into their models based on GCM output. The most common technique is to calculate the difference between (or for precipitation, the ratio of) the double CO_2 estimate for a particular gridpoint and the control estimate (current conditions) for that same gridpoint (Parry et al. 1987, Smith and Tirpak 1989, ICF 1989). These differences are then applied to the corresponding historical weather data (often the mean value for the 1951-1980 time period). For instance, if a GCM estimates that July temperatures will be 2°C warmer for a particular gridpoint, then the mean July temperature for a weather station in the grid box is increased by 2° to estimate future July temperatures for that particular location.

LITERATURE CITED

Cooperative Holocene Mapping Project (COHMAP). 1988. Climatic changes of the last 18,000 years: Observations and model simulations. Science 241:1043-1052.

ICF, Inc. 1989. Summary Report: Scenarios Advisory Meeting Report, 31 Aug-1 Sept, Boulder, CO. Report for U.S. Environmental Protection Agency, Office of Policy, Planning and Evaluation, Washington, DC, 14 pp.

Neilson, R.P., G.A. King, R.L. DeVelice, J. Lenihan, D. Marks, J. Dolph, B. Campbell, and G. Glick. 1989. Sensitivity of ecological landscapes and regions to global climate change. U.S. Environmental Protection Agency, Environmental Research Laboratory, Corvallis, OR.

Parry, M., T. Carter, N. Konijin, and J. Lockwood. 1987. The impact of climatic variations on agriculture: Introduction to the IIASA/UNEP Case Studies in Semi-Arid Regions. Laxenburg, Austria.

Schlesinger, M.E. and Z.C. Zhao. 1989. Seasonal climatic change introduced by doubled CO_2 as simulated by the OSU atmospheric GCM/mixed-layer ocean model. J.Climate 2:429-495.

Schlesinger, M.E., ed. 1986. Physically-Based Modelling and Simulation of Climate and Climatic Change (Part 1). Proceedings of the NATO Advanced Study Institute, Erice, Italy.

Smith, J.B., and D. Tirpak, eds. 1989. The Potential Effects of Global Climate Change on the United States. Report to Congress. EPA-230-05-89-050, U.S. Environmental Protection Agency, Washington, DC 413 pp.

Washington, W.M. and G.A. Meehl. 1989. Climate sensitivity due to increased CO_2: experiments with a coupled atmosphere and ocean general circulation model. Climate Dynamics. 4:1-38

Wetherald, R.T., and S. Manabe. 1988. Cloud feedback processes in a general circulation model. J. Atmos. Sci. 45:1397-1415.

TOWARD A RULE-BASED BIOME MODEL

Prepared by:

Ronald P. Neilson
Oregon State University
U.S. EPA Environmental Research Lab
200 S.W. 35th Street
Corvallis, Oregon 97333

George A. King
NSI Technology Services Corporation
U.S. EPA Environmental Research Lab
200 S.W. 35th Street
Corvallis, Oregon 97333

Greg Koerper
Oregon State University
U.S. EPA Environmental Research Lab
200 S.W. 35th Street
Corvallis, Oregon 97333

Toward A Rule-Based Biome Model

Current projections of the response of the biosphere to global climatic change indicate as much as 50% to 90% spatial displacement of extratropical biomes. The mechanism of spatial shift could be dominated by either 1) competitive displacement of northern biomes by southern biomes, or 2) drought-induced dieback of areas susceptible to change. The current suite of global biosphere models cannot distinguish between these two processes, thus determining the need for a mechanistically based biome model. The first steps have been taken toward the development of a rule-based, mechanistic model of regional biomes at a continental scale. The computer model is based on a suite of empirically generated conceptual models of biome distribution. With a few exceptions the conceptual models are based on the regional water balance and the potential supply of water to vegetation from two different soil layers, surface for grasses and deep for woody vegetation. The seasonality of precipitation largely determines the amount and timing of recharge of each of these soil layers and thus, the potential mixture of vegetative life-forms that could be supported under a specific climate. The current configuration of rules accounts for the potential natural vegetation at about 94% of 1211 climate stations over the conterminous U.S. Increased temperatures, due to global warming, would 1) reduce the supply of soil moisture over much of the U.S. by reducing the volume of snow and increasing winter runoff, and 2) increase the potential evapotranspiration (PET). These processes combined would likely produce widespread drought-induced dieback in the nation's biomes. The model is in an early stage of development and will require several enhancements, including explicit simulation of PET, extension to boreal and tropical biomes, a shift from steady-state to transient dynamics, and validation on other continents.

TOWARD A RULE-BASED BIOME MODEL

Ronald P. Neilson[1]

George A. King[2]

Greg Koerper[1]

Introduction

Trace-gas induced global climatic change has been projected to potentially shift the world's major biotic regions by hundreds of kilometers (Smith and Tirpak 1989). Under one scenario as much as 55% of the world's terrestrial vegetation could change to a different type (Smith *et al. in prep.*, King *et al. in prep.*). Such changes could produce complicated feedbacks to the global climate, possibly exacerbating the 'greenhouse effect', and would certainly produce significant ecological and economic upheavals. These projections are based, in part, on the Holdridge life-zone approach that correlates the distribution of major vegetation types to annual precipitation, potential evapotranspiration and biotemperature (Holdridge 1967). Another global biome model (Box 1981), more detailed in climate parameters, is also correlational. The two approaches generally agree on the direction of mid- to high-latitude vegetation changes under $2xCO_2$, but disagree on the sign of the change in the tropics. The tropical forests expand under the Holdridge model, but contract under the Box model (Smith *et al. in prep.*, King *et al. in prep.*). Both approaches assume a steady state, that is, they cannot simulate the transition of biomes from one type to another. The accuracy with which these approaches predict current vegetation ranges from <50% to about 77% (Prentice *in press*, Stephenson 1990). These models also do not simulate biosphere-atmoshere feedbacks. These and other limitations suggest the need for a more mechanistic approach to biome modeling, one that can be incrementally developed to incorporate transient

---

[1]Oregon State University, U.S. EPA Environmental Research Lab, 200 S.W. 35th St., Corvallis, Oregon 97333

[2]NSI Technology Services Corporation, U.S. EPA Environmental Research Lab, 200 S.W. 35th St., Corvallis, Oregon 97333

behavior, ecosystem productivity, trace gas emissions, and disturbance regimes (e.g. wildfire).

A new approach to biome modeling is being developed that is more closely related to physiological plant processes. The intent is to simulate distinct life-forms or physiognomies (Beard 1978), mixtures of which produce different biomes. The model was constructed from the premise that the climate is the principal determinant of global vegetation distribution and that variations in topography, soils, disturbance regimes and biotic interactions modify these distributions (Allen and Starr 1982, Neilson *et al.* 1989, O'Neill *et al.* 1986, Stephenson 1990, Vankat 1979, Woodward 1987). The construction of this preliminary version of the model represents a partial test of this premise. Successful classification of vegetation based exclusively on climatic information will be viewed as supportive of the premise. The present approach is limited to steady-state, potential natural vegetation. Future enhancements should include land-use considerations. Model development has been limited to the conterminous U.S. at this stage, but will be extended to global vegetation in future versions.

Conceptual Development

New developments in biogeography are providing a mechanistic conceptualization of the biosphere (Bryson 1966, Neilson and Wullstein 1983, Neilson 1986, Neilson 1987, Neilson *et al.* 1989, Stephenson 1990, Woodward 1987). The model described here is based on mechanistic, conceptual models described by Neilson *et al.* (1989). These resulted from transect analyses of over 1200 weather stations in the conterminous U.S. (Figs. 1, 2) and over 7,000 USGS gaging stations (Quinlan *et al.* 1987, US West 1988a, US West 1988b). The approach relates the seasonality of temperature, precipitation and runoff patterns to the physiological requirements of plants during different parts of their life-cycles and seasonal cycles. Details of the approach and results are published elsewhere (Neilson *et al.* 1989).

The continental transects of climate and runoff revealed regionalpatterns of climate and runoff seasonality that coincide with the boundaries of the major biomes of the conterminous U.S. (Fig. 1) (Neilson *et al.* 1989). These generalizations form the basis for the model development described here and can be cast as rules for prediction of the occurrence woody

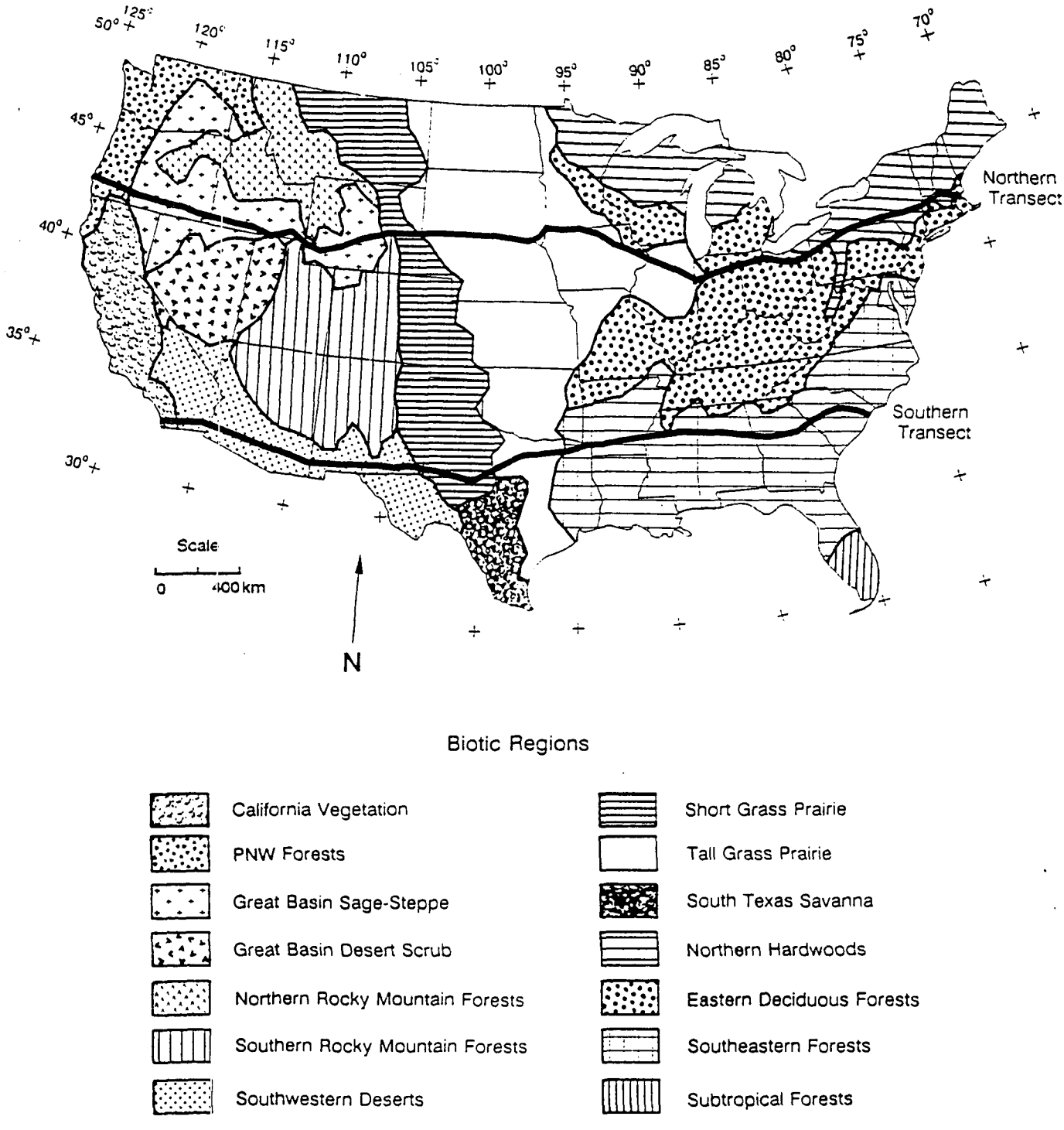

Figure 1. Principle biomes of the conterminous U.S. (simplified from Dice 1943, Küchler 1964). The locations of two transects of the HCN network of weather stations (Fig. 2) are shown (details of these are described elsewhere, Neilson *et al.* 1989).

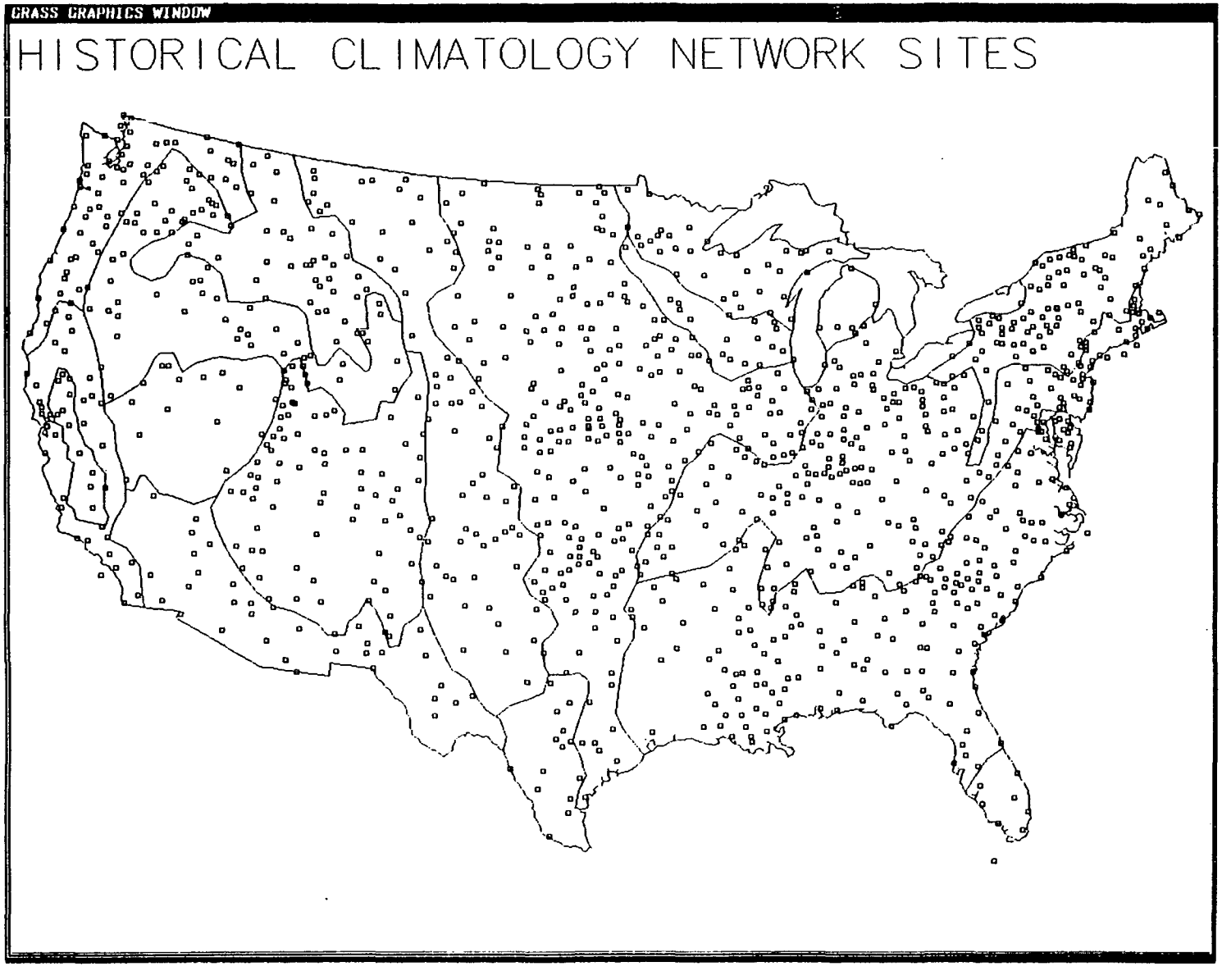

Figure 2. Locations of weather stations in the HCN network (Quinlan et al. 1987). Conceptual models of biomes were developed from a sub-sample of these stations using transect analyses (Neilson *et al.* 1989). The full set of stations was used to calibrate the quantitative model presented here.

vegetation, grasslands and deserts. Woody vegetation in the U.S. appears to receive sufficient winter precipitation to recharge a deep soil reservoir of water. Deep soil water is apparently required to balance the potential evapotranspiration (PET) during the growing season. If the amount of winter precipitation is large, a region will support a closed forest. Intermediate amounts should support a lower stature or open forest (e.g., savanna or pinyon-juniper woodland), while lesser amounts should support a shrubland (Neilson *et al.* 1989). The amount of winter precipitation (i.e., deep soil water) required is, a function of growing season PET and rainfall less runoff. Regional runoff patterns suggest that the deep soil reservoir is virtually depleted each year by transpiration and runoff (Ibid.).

These observations are consistent with current theory and plant physiology (Neilson *et al.* 1989, Stephenson 1990, Woodward 1987). If excess water were available in deep soil layers at the end of a growing season and ecosystems were not energy or nutrient limited, they should increase biomass and leaf area in subsequent seasons, thus increasing the rate of withdrawal of deep soil water. If leaf area over a landscape were so high that the rate of water withdrawal completely depleted deep soil water, then plants would die or leaves and branches would be sloughed (Woodward 1987). Leaf area would be reduced, as would the rate of withdrawal of deep soil water. Thus, in theory, ecosystems should be in dynamic equilibrium (steady state) with the regional water balance by virtue of these intrinsic feedback processes.

While maintenance of woody vegetation appears to require deep soil water, maintenance of grasses appears to require sufficient surface soil moisture during their growth and reproduction, usually the spring to summer months. Mixtures of the two life-forms can occur if there is sufficient moisture in the appropriate soil layers during the growing season and if interference by one life-form does not preclude the existence of the other. Grasslands can occur if the woody canopy is sufficiently open to allow high light penetration to the soil surface and if there is a sufficient supply of surface soil moisture during the active growing season of grasses, generally the spring (Neilson 1987, Neilson *et al.* 1989). This implies a sufficiently low level of deep soil water (i.e., winter precipitation), such that a closed forest would be precluded from the site. If spring rains are accompanied by high mid-summer rains, surface soil will remain moist and a large stature

grassland should be supported, e.g., the Tall Grass Prairie. If both winters and springs are quite dry, maintenance of either woody vegetation or grasses is hindered and a desert may be expected. High mid-summer rains in such a desert area can potentially support a low-stature grassland, as in the Chihuahuan and Sonoran Deserts of the Southwest (Neilson 1986, Neilson 1987).

A few biome boundaries in the U.S. appear to be directly controlled by cold temperature rather than water balance. The most prominent of these in the U.S. are 1) the boundary of the temperate forests with the boreal forest (Burke *et al.* 1976), and 2) possibly the boundary between the Southeast pines and hardwoods with the oak-hickory forest to the north (Neilson *et al.* 1989). The current configuration of our biome model does not address these boundaries.

The model is being developed in stages that will progress from empirical and correlational to simulation of water balance and thermal constraints. The empirical rules described here are generally adequate to define most dominant vegetation types in the conterminous U.S. In our model, threshold values of precipitation amounts during different seasons determine transitions between different life-forms, as described above. This configuration addresses the supply side of the water balance. The demand function, PET, is assumed to be fixed and is not directly factored into the rules. Given the assumption of fixed PET, the current configuration of the rules cannot be used to assess future climate effects. This initial version of the model was constrained by the unavailability of data for the physically based calculation of PET at large spatial scales. PET will be incorporated in later versions.

The rules allow mixtures of life-forms, such as trees and grasses, if the canopy is open. These mixtures can produce complicated biotic interactions and disturbance regimes. For example, the eastern deciduous forest is characterized by both wind and fire disturbances with wind perhaps being the most important (Runkle 1985). However, the adjacent prairie supports a natural, high-frequency fire regime (Abrams *et al.* 1986, Vankat 1979). If the tree canopy is open, such that a well-developed grass layer forms, woody vegetation is at risk from fire. The presence of high grass biomass also places woody vegetation at risk from herbivores and from competition between shrub seedlings and rapidly growing grasses for both light and water. Under these conditions, strictly climatic rules for prediction of

biome physiognomy will not suffice. Secondary influences from disturbance and biotic interactions are important and can remove one or more climatically favored life-forms (Abrams *et al.* 1986, Vankat 1979). Therefore, under certain climatic conditions where specific mixtures are favored, secondary rules are invoked to modulate the biome physiognomy. Variations in soil infiltration rates, water holding capacity and nutrient status will also require secondary rules.

The demand function, PET less growing season rainfall, will determine the amount of supplemental soil water required by different life-forms during different seasons in future versions of the model. Enhanced versions of the model will be operable under future climate. Additional enhancements will include dynamic simulation of regional water balance using an energy balance approach with vegetation and leaf area acting as conduits between the soil and the atmosphere (Federer 1982, Woodward 1987). Model development and calibration are being achieved by using the site-specific monthly data from the 1211 station Historical Climatology Network (Fig. 2, Quinlan *et al.* 1987). Once calibrated, the model will be operated on a distributed climate over a dense grid.

Model Description

The model was constructed as a set of rules based on the conceptual models of Neilson *et al.* (1989). The entire 1200 station HCN network was used to calibrate the rules. Each station was pre-classified to a specific biome based on a map modified from Küchler (1964) and Dice (1943). The stations were then processed through the rule-base and classified accordingly. Accuracy was determined by comparison between pre- and post-classifications. Parameter adjustment and calibration were dependant on visual interpretation of the mapped residuals. Error in classification can arise from either the pre-classification or the rule-based classification. A careful analysis of the residuals is necessary to determine the source of the error.

The most unique feature of the model is the temperature-based definition of seasons. Winter, spring and summer are the principle seasons considered. Temperature thresholds, input as parameters, were used to define the beginning and ending of the seasons (Fig. 3). Therefore, the length of seasons automatically scales with latitude, altitude and continentality. A map of

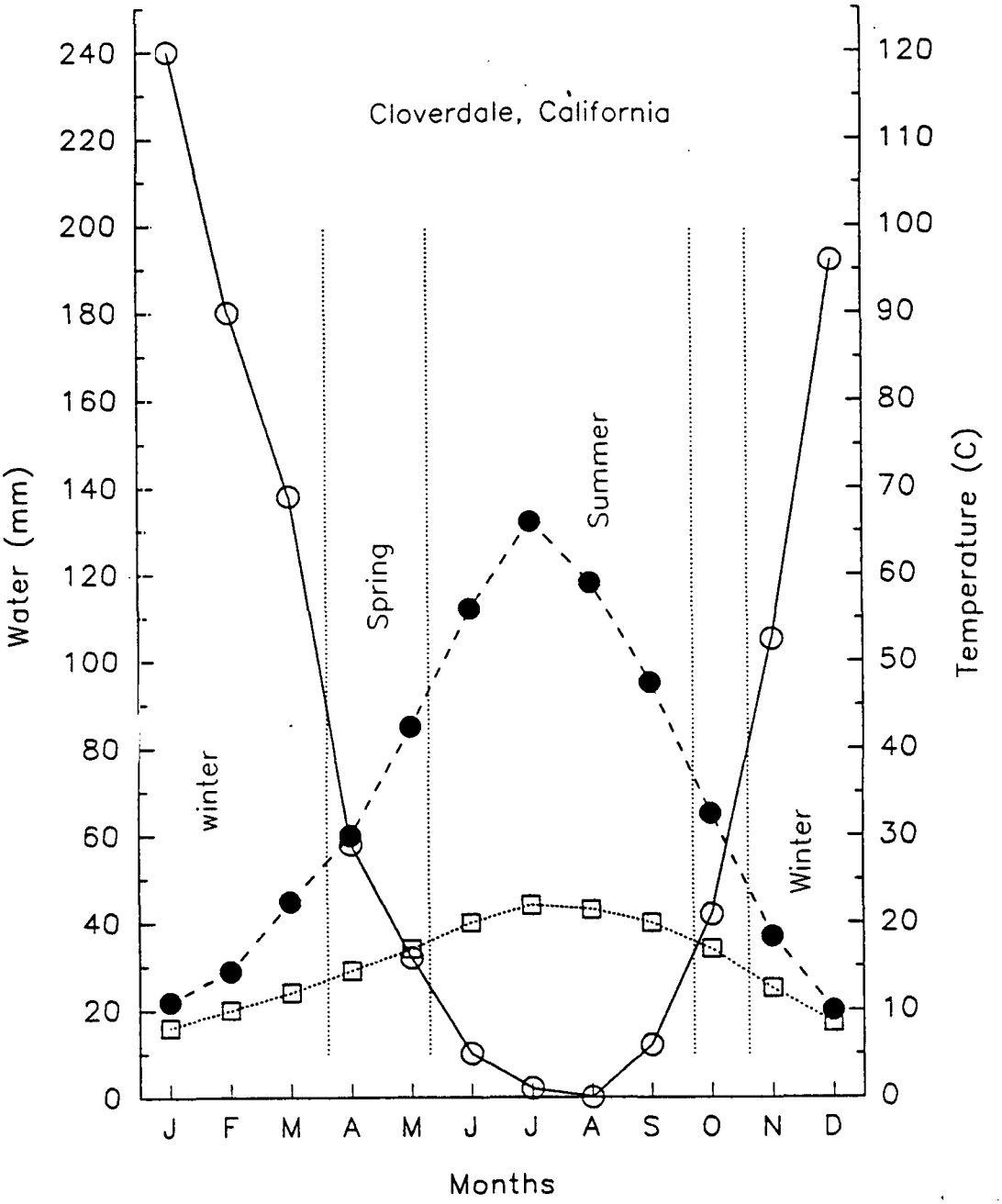

Figure 3. Example of rule-based partitioning of the seasons. Precipitation, open circles; Temperature, open squares; Potential Evapotranspiration, closed circles. Vertical, dotted lines indicate the locations of temperature thresholds used in the model to delineate seasonal transitions. Temperature thresholds are used to define the beginning and ending of seasons for each weather station. Within each season precipitation amounts are accumulated for seasonal totals or examined in terms of precipitation per month. Different rainfall amounts within the different seasons are used by the rule-base to differentiate between different life-forms that would potentially be supported by that climate.

precipitation during any one season would not represent precipitation amounts over the same period of time at all map locations.

The beginning and ending of winter are defined from both hydrologic and biotic perspectives (Fig. 3). In temperate zone summers PET is generally high enough that incident precipitation does not infiltrate to deep soil layers, but either runs off directly or is evapotranspired from vegetation surfaces and surface soil layers (Major 1963, Thornthwaite 1948, Thornthwaite and Mather 1955). In cooler months PET is low enough that incident precipitation can infiltrate to deep soil layers. Accumulated snow will also infiltrate, or run off, upon snowmelt. Thus, we define a temperature threshold above which precipitation cannot reach deep soil layers and below which it can. The infiltration period defines winter in temperate latitudes. The threshold also carries a biotic importance in that it closely relates to the timing of dormancy onset and release in plants.

Spring is viewed from the hydrologic perspective as the period over which the surface soil layer can be depleted (Fig. 3). This period is critical for seedling establishment of woody species and for completion of the life-cycles of grasses and ephemerals. In the temperate zone the surface soil will dry very rapidly in the absence of spring rains, precluding a major grassland development. In northern states under these rules winter can extend to quite late in the year and spring can extend through most of the growing season with little to no summer.

Summer is generally the period of greatest water stress (Fig. 3). Ifthe spring season is sufficiently wet, grasses can complete their life-cycles and senesce before critical mid-summer drought stress (Vankat 1979). However, if summers are also wet, different grass species can continue to grow, producing a mixed or tall-grass environment (Ibid.).

There are two classes of parameters in the model: 1) temperature thresholds that define the beginning and ending of seasons, and 2) precipitation thresholds within seasons that constrain the life-forms dependent upon that season. The model flow chart (Fig. 4) indicates the decision tree applied to each meteorological record of monthly temperature and precipitation. Winter precipitation thresholds are configured as absolute amounts, since the timing of precipitation is not critical. That is, of all the accumulated precipitation during the winter, a fixed fraction is assumed

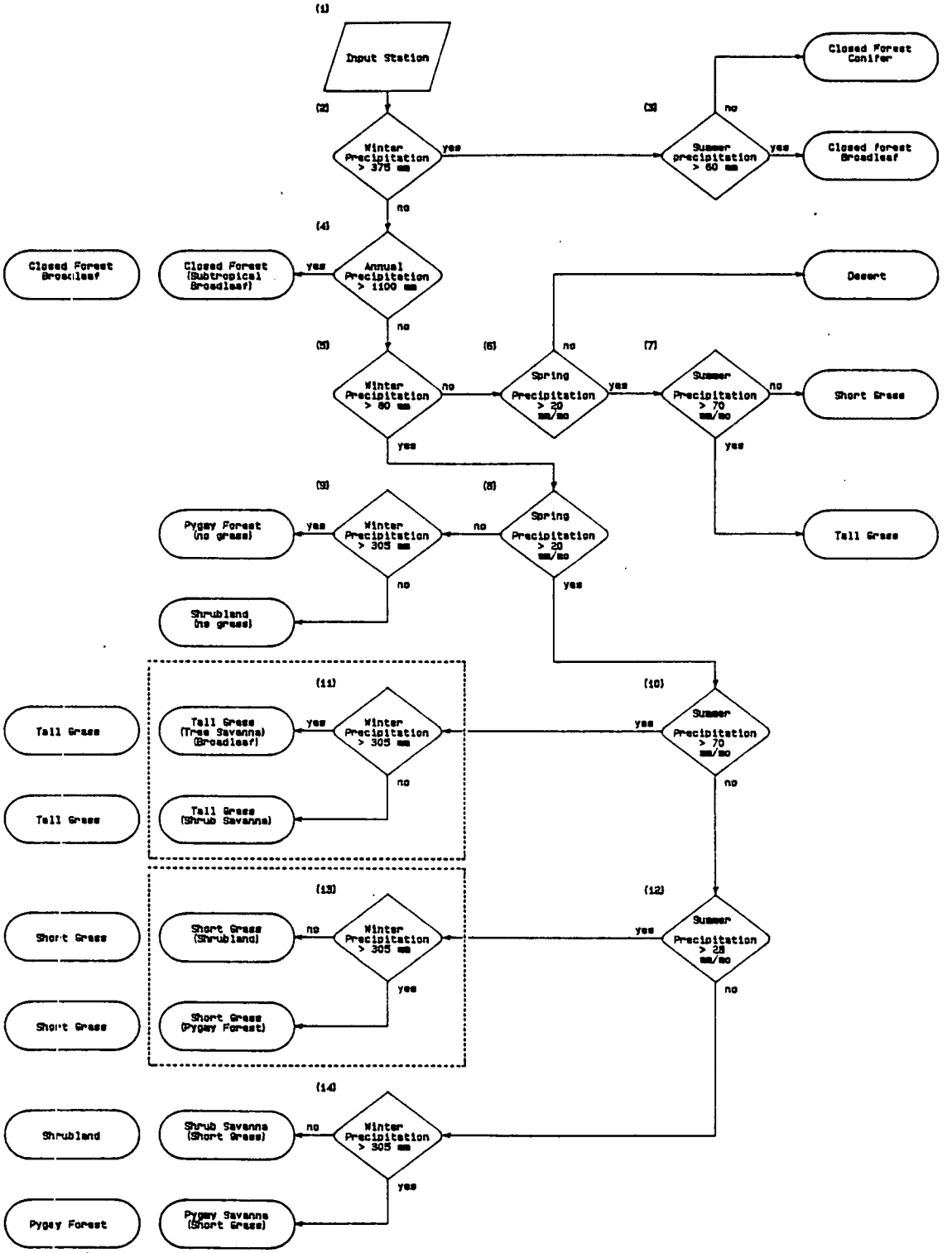

Figure 4. Flow chart of rule-base. Monthly mean temperature and monthly total precipitation are input for each station. Seasons are defined as in Fig. 3 and precipitation amounts are linearly interpolated for each season from the monthly data. The rule-base is a dichotomous key that classifies each station as to the potential natural vegetation based on climate. The enclosed rules (11 and 12, dashed lines) indicate implied, secondary rules (see discussion in text), whereby disturbance regimes and biotic interactions are inferred to constrain one or more life-forms from a dominant expression in the mixture of life-forms.

to infiltrate to deep soil layers at some time during the winter with the remainder being returned to the atmosphere (evaporation, sublimation) or routed to surface waters (runoff). However, during the spring and summer months the supply of water (precipitation) and demand for water (evapotranspiration) are essentially simultaneous when viewed from a monthly time-step. Therefore, precipitation thresholds during spring and summer are defined in units of mm/mo.

The rules (Fig. 4) are equivalent to a dichotomous key with simple yes/no decisions determining the trajectory through the rules and the ultimate declaration of biome type for a station (or cell if applied to a full grid). The flowchart is arranged such that all winter decisions are in the first column of diamond shapes, followed by a column of spring decisions and a column of summer decisions. The decisions enclosed by dashed lines (rules 11, 13) are implied rather than explicitly coded rules in the current configuration. The implied rules arise from assuming the application of secondary biome rules for biotic interaction and disturbance regimes. The bubbles to the left of the flowchart (Fig. 4) are the simplified classifications applied at the termination of the adjacent rule. They indicate the influence of the secondary, implied rules accounting for fire and biotic interactions. For example, a mixture of open-canopy, deciduous trees with tall grass prairie is directly classified as tall grass prairie. Similarly, all Pygmy forests (pinyon-juniper woodland) with or without grass are classified as Pygmy forest. Future versions of the model will retain all such mixtures and distinctions.

The calibrated threshold separating closed forest from non-closed forest is 375 mm of winter precipitation (rule 2, Fig. 4). The amount of summer precipitation per month (rule 3) separates broadleaf from conifer forests. The physiological inference is that broadleaf trees cannot withstand the degree of mid-summer vapor-pressure stress across the leaf surface that conifers can withstand (Marshall and Waring 1984, Neilson *et al.* 1989, Running 1975, Waring and Franklin 1979).

The current configuration of the model becomes inadequate as the stations approach sub-tropical climates. Rule 4 (Fig. 4) is a temporary proxy for a set of rules that will deal with sub-tropical climates. As one approaches the Florida peninsula, winters become ever shorter and eventually

non-existent as defined by the temperature thresholds. Thus, the total amount of precipitation during the winter at these stations is not sufficient to support a forest, a clear artifact of the rules. As the growing season becomes longer, the infiltration period of winter becomes shorter. Under these situations, infiltration can still occur if the amounts of rainfall more than compensate for a high PET. This does occur in forested areas within the subtropical climates of the Southeast U.S. and elsewhere (Neilson *et al.* 1989). However, implementation of such a rule must await a future version of the model that incorporates physically-based PET calculations. A workable place-holder is a threshold for annual precipitation of about 1100 mm, given that winter precipitation is below a closed-forest threshold (rule 4). This correctly classifies closed-forest stations in the far southeastern U.S., yet does not interfere with appropriate winter, rule-based decisions in more northerly latitudes.

After partitioning the high winter precipitation, i.e., closed-forest, stations, rule 5 selects sites with winter precipitation less than 80 mm. These stations are ultimately classified as desert or grassland based on spring precipitation (rule 6, 20 mm/mo) and tall or short grass based on summer precipitation (rule 7, 70 mm/mo).

The remaining stations will be classified as either shrublands, open forest (savanna), or grasslands potentially supporting woody species. Shrubland and open forest are distinguished depending on whether winter rains are above or below 305 mm (rules 9, 11, 13, 14). Each type (shrub or tree) can be broadleaf or microphyllous (small leaf), depending on the level of summer rains (rules 10, 12), reflecting again the inferred vapor pressure gradient across the leaf surface. If summer rains are sufficient to support a broadleaf type (rule 10), the result is either a broadleaf, tall-grass savanna or tall-grass shrub savanna. In either case, secondary rules are invoked to classify these sites as tall grass prairie, with the principle mechanism for grass dominance assumed to be fire.

Given sufficient winter rains to support shrubs or open forest (rule 5), but less than 70 mm/mo of summer rainfall (rule 10), only a xeromorphic leaf structure can be supported. The tree form will be conifer and could be a xeric conifer savanna, such as ponderosa pine or a smaller stature, but more dense pygmy forest of pinyon pine and juniper. In either case the conifer

leaf area is comparatively low. If only the shrub form can be supported (rule 14), the shrubs would be microphyllous. If summer rains are above 28 mm/mo and spring rains are above 20 mm/mo (rule 8), then a well-developed short grass community can be supported. Under these conditions, secondary rules are again invoked to remove the woody component (rule 13) and the communities are classified as short grass. Below 28 mm/mo of summer rains, the grassland is of lower biomass, weakening the secondary rules, resulting in either a shrub or pygmy forest savanna depending on winter rains (rule 14).

Model Calibration

The model parameters were adjusted to provide an optimal fit to the specified biome boundaries. This was accomplished iteratively by visual examination of the residuals and calculations of percent correct classification. Two classes of parameters require calibration: 1) thermal constraints controlling the beginning and ending of seasons, and 2) precipitation thresholds within seasons for different life-forms. These must initially be calibrated in tandem with sensitivity of both classes being examined. However, once the thermal thresholds are set, primary calibration is with the precipitation thresholds. Future versions of the model that incorporate PET will use the PET less precipitation estimates in conjunction with thermal information to control seasonal timing and length.

Most rules exhibit one or more 'balance' points. That is, increasing or decreasing the value of a parameter may continue to increase the correct classification of a particular biome, but there will be a point above (or below) which further adjustment occurs at the expense of correct classification in other biomes. The parameters were adjusted close to these 'balance' points. Some parameters were clearly more sensitive than others, however, we have not attempted a formal sensitivity analysis.

The site-specific accuracy of the calibration was 79% with the highest success being 94% in the eastern U.S. forests and the lowest being 0% for the 11 grassland stations in the central valley of California (Table 1, Fig. 5). The current model does not subdivide the eastern forest into the three different sub-sections. Undoubtedly, when these rules are implemented, errors in classification will occur near the ecotones. A few sites near the border

Table 1. Summary of classifications. *n* is the number of weather stations, C.F. = conifer forest;, Srb. = shrubland; S.D. = southwest deserts; P.J. = pinyon-juniper; S.G. = short grass; T.G. = tall grass; B.F. = broadleaf forest. Entries in the table are percentages. The bold numbers correspond to the groupings of similar biomes. The italics highlight the correct classification category.

	n	C.F.	Srb.	S.D.	P.J.	S.G.	T.G.	B.F.
Conifer Forests	**91**	*82*	**9**		**8**	**1**		
Northwest	58	*91*	2		5	2		
Southwest	33	*67*	21		12			
California Grassland	**11**	**45**	**36**		**18**	*0*		
Shrubland	**78**	**12**	*81*	**1**	**5**	**1**		
Northern Great Basin	63	14	*79*		6			
Southern Great Basin	15		*87*	7		7		
Southwest Deserts	**34**		**12**	*88*				
Mixed Forest	**114**	**15**	**53**	**2**	**11**	**16**	**2**	
Northern Rockies	36	*28*	39		11	22		
Southern Rockies	78	9	59	5	*12*	13	3	
Short Grass Prairie	**81(122)[3]**		**2**	**2**		*84(89)*	**11**	
Central	67(108)		3	1		*93(95)*	3	
South Texas savanna	14			7		*43*	50	
Tall Grass Prairie	**242(201)**					**17(0)**	*70(84)*	**13(16)**
Broadleaf Forests	**560**	**1**		**<1**			**4**	*94*
Northern Hardwood	129	6					8	*86*
Deciduous Forest	234						6	*94*
Southeast Forest	189							*100*
Sub-tropical Forest	8			12				*88*
Total	**1211**	**79(82)**						
Total (drop Rocky Mts.)	**1097**	**85(88)**						
Total (accept Rockies, California, and mixed-grass as correct)	**1211**	**94**						

[3]Numbers in parentheses are the sample sizes (*n*) and percentages if the northern mixed grass prairie of Küchler (1964) is considered to be short grass prairie as determined by the rule-base. The current configuration of rules does not explicitly attempt to distinquish mixed-grass as intermediate between short and tall grass.

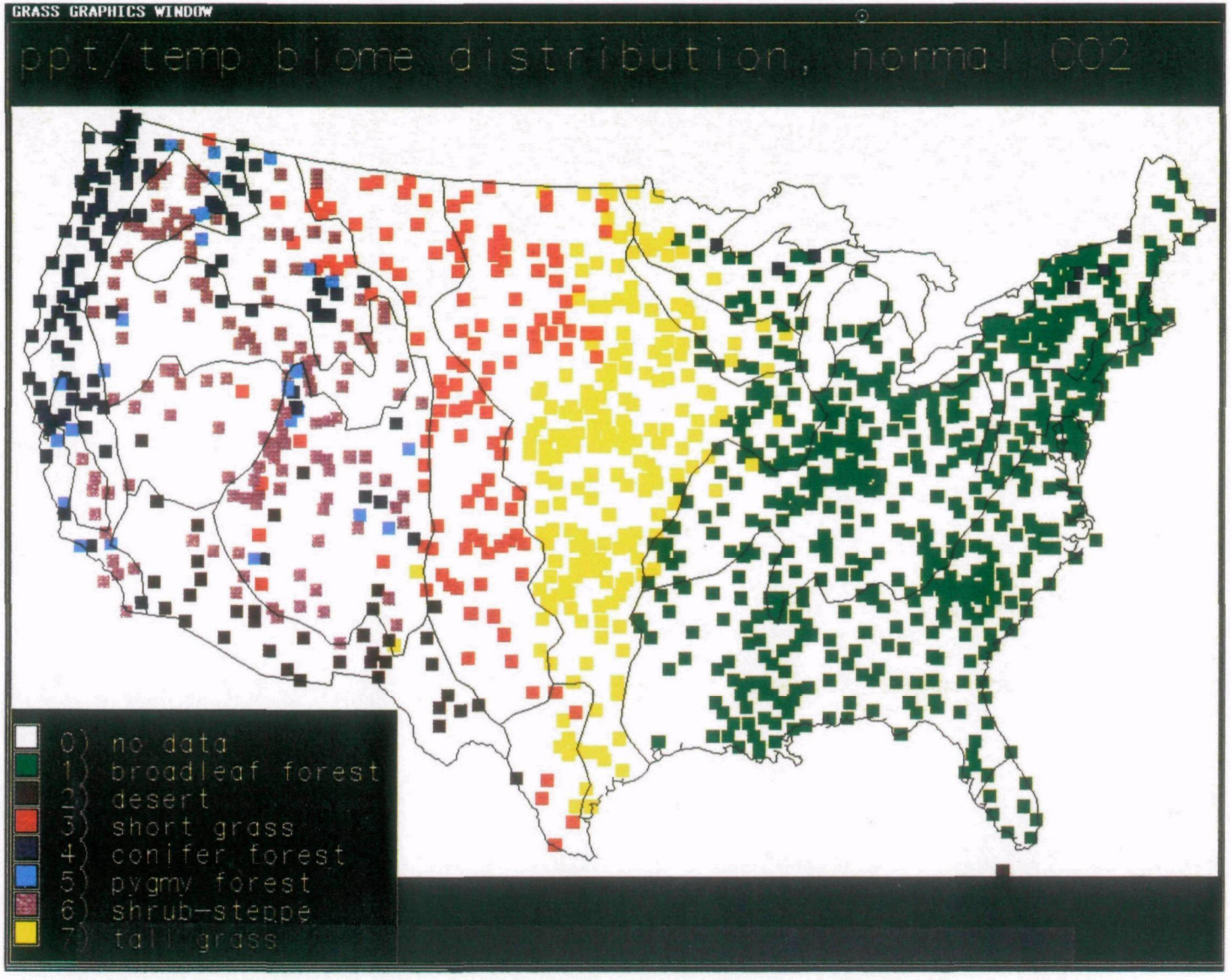

Figure 5. Rule-based classification of the HCN network sites (Fig. 2), overlain on the pre-classification of U.S. biomes (Fig. 1).

between the northern hardwoods and the boreal forest were classified as conifer, a reasonable occurrence. The mixed forests of the Rocky Mountains were only predicted at 17% accuracy (28% northern Rockies, 12% southern Rockies (Table 1). The next lowest success was 70% for the tall grass prairie with the remaining biomes being predicted at better than 80% accuracy.

Closer examination of the residuals (Table 1, Fig. 6) reveals that the model is more accurate than these indications, since pre-classification error is incorporated in the results. The California grasslands were predicted as conifer forest (45%), shrubland (36%) and pinyon-juniper (P-J) woodland (18%). Given the wet winters and very dry summers, these predictions may be quite reasonable. The conifer forest and P-J woodland stations cluster in the north end of the valley and at the boundaries with the neighboring conifer forests. These could be accurate classifications given the potential inaccuracies of the pre-classification biome map. A shrubland classification for the remaining sites may also be acceptable. Recall that the rule-basedclassifications have been simplified to indicate only the dominant life-form, even if a mixture is actually being selected (Fig. 4). The shrubland classification in the current configuration of rules is actually a mixture of shrub and short grass life-forms (rule 14, Fig. 4). Climatically, the mixed shrub-grass classification for the central valley is quite reasonable; however, the relative mix of shrubs and grass is likely inaccurate in that the model does not yet account for the unusually long spring period over which grass biomass would build. Given sufficient grass biomass, the natural and anthropogenic influence of fire could have rendered the valley more of a monotypic grassland (Vankat 1979). Other possibilities for a lack of shrubs in the central valley include 1) the presence of fine surface soils that might hinder percolation of deep soil water, and 2) the lack of sufficient summer rains that are usually necessary for the establishment of shrubs (Neilson 1986).

Both the northern and southern Rocky Mountain regions were poorly predicted (Table 1, Fig. 6). The over-simplistic pre-classification into one category each, conifers in the north and pinyon-juniper in the south, does not capture the vertical zonation of vegetation in these regions. Most of the weather stations in this highly dissected terrain occur in valley bottoms that are often dominated by shrubland or grassland (Küchler 1964, Vankat 1979).

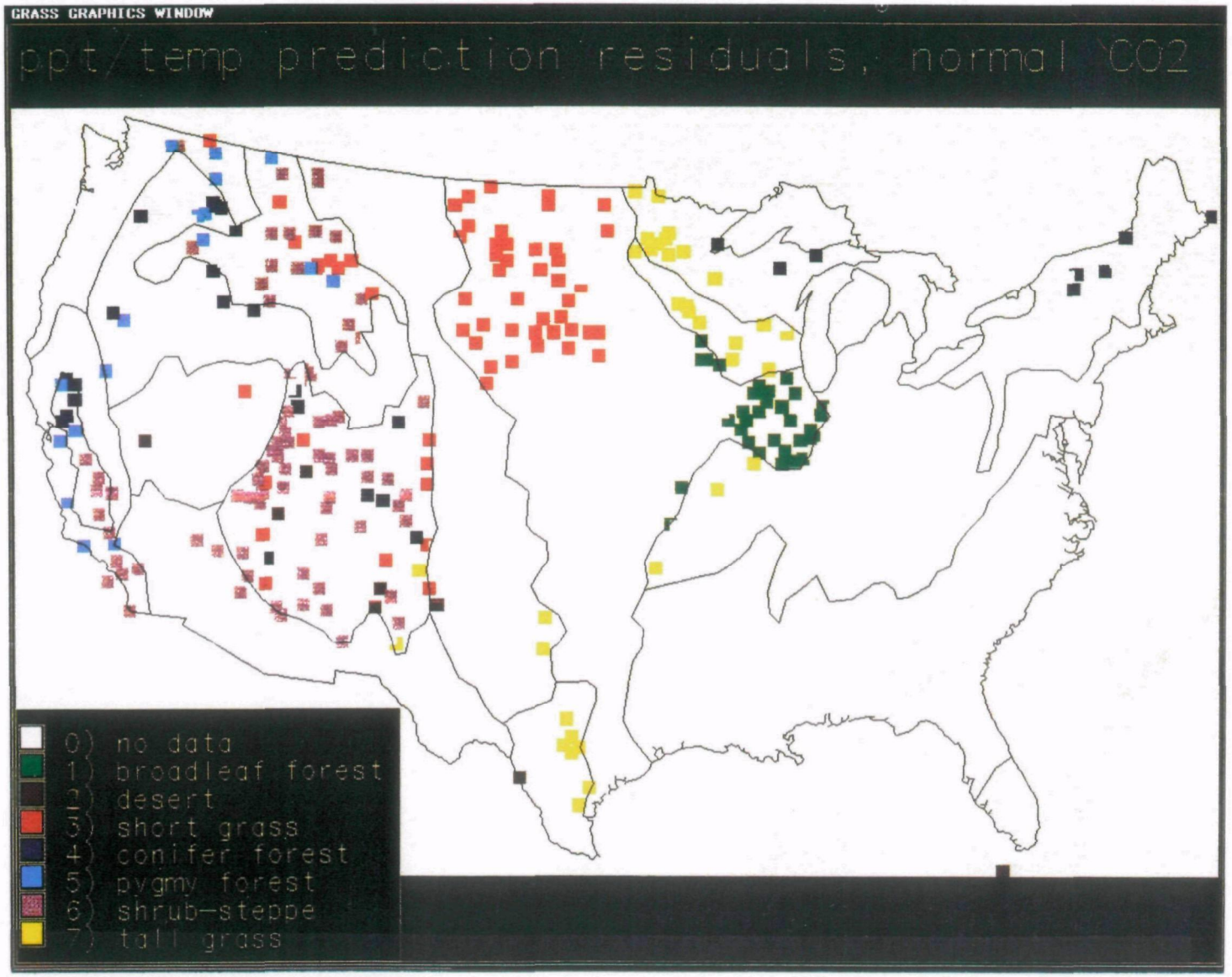

Figure 6. Residuals from the rule-based classification (Fig. 5). Only those sites in Fig. 5 that were not correctly classified according to the pre-classification (Fig. 1) are displayed.

The classifications for the northern Rocky Mountains include conifer (28%), pinyon-juniper (11%), shrubland (39%), and short grass (22%). The southern Rocky Mountains are warmer, more xeric in the winter and wetter in the summer with conifer (9%), pinyon-juniper (12%), shrubland (59%), desert (5%), short grass (13%), and tall grass (3%). We examined most of these stations individually and concluded that these classifications are generally accurate. If the Rocky Mountain, rule-based classifications are accepted as correct, the model performance shifts from 79% to 90% overall. If the Rocky Mountains are removed from the classification the performance is 85% (Table 1).

A third set of residual mis-classifications stems from 17% of the tall grass prairie stations being classified as short grass prairie (Fig. 6, Table 1). These stations occur in a region in the north plains designated by Küchler (1964) as mixed grass, a life-form for which we have not written arule. Thus, our pre-classification as either short or tall grass is arbitrary. If these stations are accepted as a correct classification, the performance of the model in the tall grass shifts from 70% to 84% and the overall rating increases from 79% to 82% (Table 1). If the mixed-grass is accepted, but both the Rockies and the Central Valley are excluded, the accuracy of the model is 88%. If both the Rocky Mountains and the mixed grass classifications are accepted, the overall accuracy shifts to 93%. If the Central Valley classifications are also accepted, the overall accuracy is 94% (Table 1).

The remaining cluster of residuals occurs where much of the prairie peninsula is classified as broadleaf forest rather than grassland. Classification of the prairie peninsula has been a particular challenge to biogeographers and climatologists (Borchert 1950, Corcoran 1982, Küchler 1972, Manogaran 1983, Transeau 1935). There is considerable debate as to whether the prairie peninsula is climatically determined, or whether man historically induced the prairie through fire (Vankat 1979). Fires clearly play a major role in reducing the dominance of woody vegetation. However, a climatic classification of the prairie peninsula, based on a moisture index of Thornthwaite, indicates that the region is climatically unique, (Manogaran 1983). The current configuration of the rule-base lacks the PET calculations that will be necessary to reflect this unique climatology. The next version of the model will incorporate the PET calculations. The prairie peninsula

also occurs at the convergence of two air mass gradients (Bryson 1966). As a consequence, regional rainfall gradients are relatively shallow (Neilson *et al.* 1989) and should exhibit considerable year-to-year variability. We tested the sensitivity of the prairie-forest border to small changes in the winter rainfall threshold. The prairie peninsula was most sensitive to these changes while the border locations to the north and south were more stable. It is possible that year-to-year variability of weather patterns produces extreme years that preclude the long-term maintenance of forest in the prairie peninsula. We expect that the model rendition of the prairie peninsula will improve with future enhancements.

Future Model Developments

The primary limitation of the current configuration of the model is that it simulates only the supply side of the water balance. The next enhancement will be to include the demand side as driven by PET. The precipitation thresholds will be re-evaluated as a function of seasonal PET and seasonal rainfall supply. Within the water balance thresholds for each life-form water balance will be treated as a continuum and calculated using energy balance equations, allowing a prediction of leaf area as well as life-form (Woodward 1987). Regional scale information on soil water holding capacity and texture will be required to fine-tune the regional water balance estimates. The continued use of thresholds in the model recognizes the use of thresholds in defining physiognomic distinctions. It may be possible in the future to loosen this constraint and treat life-form physiognomies as a continuum. Grass physiognomy extends toward large and woody, as in bamboo; and, woody plants extend toward small ephemerals, as in many semi-arid species.

With the incorporation of PET the model will be sufficiently complete for a preliminary estimate of $2xCO_2$ impacts on biome distribution over the conterminous U.S. Qualitative estimates have been made based on the conceptual pre-cursor to this model (Neilson *et al.* 1989). Biome boundaries are expected to shift several degrees of latitude and hundreds of meters of elevation.

Temperature constraints will also be added to the model to differentiate the mixed forests of the southeast U.S. from the eastern deciduous forest (Fig. 1) and the temperate forest from the boreal forest. The model will also

be extended to both boreal and tropical regions. These extensions will require very different kinds of rules than those developed for temperate zone biomes. For example, the current, thermally defined summer shortens with increasing latitude and disappears at about the latitude of the boreal forest. Likewise, the thermally defined winter does not occur in the subtropics, i.e., the vicinity of Florida. Transect analyses, as applied in the U.S. (Neilson *et al.* 1989), will be extended to other parts of the world to assist in the formulation of additional rules.

The calibration of the model with regard to secondary rules, those invoking fire and biotic interactions, will require continuing investigation. Since the natural environment expresses the influence of these processes, it is particularly difficult to assign thresholds that adequately constrain biomes in the absence of secondary rules. For example, the winter precipitation threshold below which shrubs cannot be supported is currently set at 80 mm (rule 5, Fig. 4). This produces shrubland in the Great Basin and desert in the Southwest. It also produces shrubland throughout the Great Plains. The simultaneous presence of grassland in the plains invokes the secondary rules to shift the biome classification to grassland. If the winter threshold (rule 5) is set to 200 mm, fewer plains sites are attributed a shrub component, but the Great Basin becomes a desert. The Great Basin is characterized by a series of parallel mountain ranges separated by narrow valleys, wherein the shrublands occur. The mountains collect winter precipitation which can run off and infiltrate to deep soil layers in adjacent alluvial fans (Schlesinger and Jones 1984) providing greater deep soil water for support of shrubland than incident precipitation alone. Thus, we are left with a choice for secondary rules: 1) invoke fire in the plains to remove shrubs, or 2) invoke 'run on' in the Great Basin to augment deep soil water and support shrubs. Currently, the first option is used. However, there is little information as to the comparative degree to which these processes control shrubland distribution.

The model could be described as a demographic rather than an ecosystem model, since it simulates life-form (Beard 1978), but does not address nutrient dynamics (O'Neill *et al.* 1986). Alternative approaches to simulation of productivity and nutrient dynamics will be explored (e.g., Jarvis and Leverenz 1983). Once the model incorporates an energy balance approach to

determining the life-form thresholds, water flux through the ecosystems will be directly calculated. This information, coupled with water-use-efficiency and energy-use-efficiency parameters (Landsberg and McMurtrie 1985, Linder 1985, Montieth 1977, Tucker *et al.* 1986) should allow estimates of potential primary productivity. Potential productivity could be modulated by nutrient-use-efficiency and soil nitrogen estimates (Prescott *et al.* 1989, Vitousek 1984). Decomposition rates could be parameterized as functions of temperature and moisture (Meentemeyer 1978).

Increased levels of CO_2 are known to increase productivity and water-use-efficiency in many plants (Strain and Cure 1985). The potential importance of these effects at landscape and biome scales is under debate. If these effects are significant at a regional scale, then the impacts of climatic change could be considerably ameliorated, assuming that the gradually increasing influence of direct effects of CO_2 is not preceded by adverse climatic effects of increasing trace gases, such as widespread drought. Also, even if direct effects prove important over a wide array of plants, it is not clear how much influence plant scale water balance, modulated by the stomata, has over landscape scale water balance. The latter appears to be largely driven by radiation and modulated by root density and depth and by leaf area (Federer 1982, Jarvis and McNaughton 1986). Clearly, stomatal processes will control rates of drying; however, the accurate simulation of drying curves may not be important at time steps of one month (Cowan 1965).

A particularly important enhancement to the model will be to move from steady state to transient dynamics. The potential spatial redistribution of biomes could be mediated by major diebacks or declines in some areas and advances in others (Neilson *et al.* 1989, Solomon 1986, Overpeck *et al.* 1990). Simulation of these dynamics will require both demographic and ecosystem processes. The dispersal of important tree types is expected to lag considerably behind the rapidity of climatic change and the potential movement of boundaries (Davis 1986, Smith and Tirpak 1989). It will be important to incorporate functional categories of seed dispersal in the life-history characterizations (Beard 1978). As extra-tropical forests shift toward the poles, large areas of their current distributions could undergo severe, drought induced decline and dieback (Neilson *et al.* 1989, Overpeck *et al.* 1990). These would be susceptible to fire. The release of CO_2 into the

atmosphere from these fires and subsequent decay of the remaining dead biomass could produce a positive feedback to the 'greenhouse effect' (Neilson *et al. in prep.*). The regrowth of burned landscapes and the potential expansion of the tropics could ameliorate this CO_2 pulse to some extent (Ibid.). We have begun modeling these processes and will incorporate these dynamics into future versions of the model described here.

The simulation of transient dynamics could also be necessary for accurate delineation of some biome boundaries. Sensitivity analyses on the winter precipitation parameter separating closed from open forest (375 mm), indicates that the eastern extent of the prairie peninsula is quite sensitive to this parameter. Year to year variability of rainfall could be shifting this climatic transition quite considerably (Coupland 1958, Küchler 1972). Even though the average climate of the prairie peninsula may be suitable for forest establishment and growth, the extremes due to natural climatic variability could preclude their long-term viability in the region.

As model development continues, calibration and validation will be increasingly important. Although the focus has been on enhancements to the model, it is apparent that the calibration is very dependant on the accuracy of the pre-classification. In the Rocky Mountains, for example, correct model calibration will require a much higher spatial resolution of biome type than needed for less mountainous terrain. Literature and existing maps will be useful in this endeavor. However, satellite technology has the potential to provide this classification at a comparatively high resolution (Tucker *et al.* 1985). Remote classification of vegetation should be a high priority for all the world's vegetation.

Three approaches to model validation will be explored: 1) implementation on another continent, 2) simulation of paleoclimates (Webb *et al.* 1990), and 3) rescaling the model to a smaller, but heterogeneous extent. There will be an attempt to validate the model through extension to other continents, and also attempts to reconstruct past vegetation and to rescale the model. Since it is physically driven and is purported to be mechanistically based, it should apply at any scale of resolution. Thus, application to a heterogeneous watershed, such as the Colorado drainage would be a very interesting test of the model.

Conclusions

The initial stage of development of a rule-based, mechanistic model of vegetative life-form distribution has been described. Different life-form mixtures deduced from the rules produce different biomes with demonstrated prediction potential of up to 94% accuracy. The current configuration of rules is based entirely on the seasonal patterns of regional water balance and the relation of these patterns to different plant life-forms. The apparent success of the model makes two important points. First, regional water balance does appear to be a critical climatic mechanism determining plant distributions. Second, the success of the model, even when the demand side of regional water balance (PET) was not directly considered, implies that on regional scales water balance is currently in equilibrium with the vegetation. It follows that the atmospheric demand for water (PET) is in balance with the supply of water through transpiration. The regional rate of transpiration, according to theory (Woodward 1987), should be related to the amount of leaf area (biomass) over that region. The amount of leaf area over a region should be a direct result of ecosystem feedback processes that select for a specific leaf area as a function of water supply and atmospheric demand. The implication is that ecosystems are perched on a precarious balance with respect to regional water balance and that a rapid change in either supply or demand for water could produce a catastrophic response from regional vegetation.

Being mechanistic in concept, future model enhancements to incorporate ecosystem and spatial demographic processes with temporal dynamics should be relatively straightforward, albeit challenging to implement. The value of these efforts, particularly when coupled with global atmosphere models and land-use characteristics, should be realized in a much improved predictive potential of future global change and biosphere-atmosphere feedbacks.

References

Abrams, M.D., A.K. Knapp, and L.C. Hulbert. 1986. A ten-year record of aboveground biomass in a Kansas tallgrass prairie: effect of fire and topographic position. Amer. J. Bot. 73(10):1509-1510.

Beard, J.S. 1978. The physiognomic approach. pp. 35-64. In: Robert H. Whittaker, ed. Classification of Plant Communities. The Hague, Netherlands.

Borchert, J.R. 1950. The climate of the central North American grassland. Annals of the Association of American Geographers 15(1):1-38.

Box, E.O. 1981. Macroclimate and Plant Forms: An Introduction to Predictive Modeling in Phytogeography. Dr. W. Junk Publishers, The Hague.

Bryson, R.A. 1966. Air Masses, streamlines, and the boreal forest. Geographical Bulletin 8(3):228-269.

Burke, M. J., L. V. Gusta, H. A. Quamme, C. J. Weiser, and P. H. Li. 1976. Freezing injury in plants. Annual Review of Plant Physiology 27: 507-528.

Corcoran, W.T. 1982. Moisture stress, mid-tropospheric pressure patterns, and the forest/grassland transition in the south central states. Physical Geography 3(2):148-159.

Coupland, R.T. 1958. The effects of fluctuations in weather upon the grasslands of the Great Plains. The Botanical Review 23(5):273-317.

Cowan, I.R. 1965. Transport of water in the soil-plant-atmosphere system. J. Applied Ecology 2:221-239.

Davis, M.B. 1986. Lags in the response of forest vegetation to climatic change. pp. 70-76. In: C. Rosenzweig and R. Dickson, eds., Climate-Vegetation Interactions. OIES-UCAR, Boulder, CO.

Dice, L.R. 1943. The biotic provinces of North America. University of Michigan Press, Ann Arbor. 1-79.

Federer, C.A. 1982. Transpirational supply and demand: plant, soil, and atmospheric effects evaluated by simulation. Water Resources Research 18(2):355-362.

Jarvis, P.G., and J.W. Leverenz. 1983. Introduction: Temperate Forest. In Productivity of temperate, deciduous, and evergreen forests. IN: Encyclopedia of Plant Physiology. editors. Springer-Verlag, Berlin. 243-280.

Jarvis, P.G., and K.G. McNaughton. 1986. Stomatal control of transpiration: scaling up from leaf to region. Advances in Ecological Research 15:1-

49.

Küchler, A.W. 1964. The potential natural vegetation of the conterminous United States. American Geographical Society Special Publication no. 36.

Küchler, A.W. 1972. The oscillations of the mixed prairie in Kansas. Erdkunde, Archiv für wissenschaftliche Geographie. 26:120-129.

Landsberg, J.J., and R. McMurtrie. 1985. Models based on physiology as tools for research and forest management. pp. 214-228. In: J.J. Landsberg and W. Parsons (eds.), Research for Forest Management. Proceedings of a conference organized by the Division of Forest Research, CSIRO, 21-25 May 1984, Canberra, Australia.

Linder, S. 1985. Potential and actual production in Australian forest stands. p. 11-34. In: J.J. Landsberg and W. Parsons (eds.), Research for Forest Management. CSIRO, Australia.

Major, J. 1963. A climatic index to vascular plant activity. Ecology 44:485-498.

Manogaran, C. 1983. The prairie peninsula: a climatic perspective. Physical Geography 4(2):153-166.

Marshall, J.D., and R.H. Waring. 1984. Conifers and broadleaf species: stomatal sensitivity differs in western Oregon. Can. J. For. Res. 14:905-908.

Meentemeyer, V. 1978. Macroclimate and lignin control of litter decomposition rates. Ecology 59(3):465-472.

Monteith, J.L. 1977. Climate and the efficiency of crop production in Britain. Phil. Trans. R. Soc. Lond. B. 281:277-294.

Neilson, R.P. 1986. High-Resolution Climatic Analysis and Southwest Biogeography. Science 232:27-34.

Neilson, R.P. 1987. Biotic regionalization and climatic controls in western North America. Vegetatio 70:135-147.

Neilson, R.P., G.A. King, R.L. DeVelice, J. Lenihan, D. Marks, J. Dolph, B. Campbell, and G. Glick. 1989. Sensitivity of ecological landscapes and regions to global climate change. U.S. Environmental Protection Agency, Environmental Research Laboratory, Corvallis, OR.

Neilson, R.P., and L.H. Wullstein. 1983. Biogeography of two southwest American oaks in relation to atmospheric dynamics. Journal of Biogeography 10:275-297.

O'Neill, R.V., D.L. DeAngelis, J.B. Waide, and T.F.H. Allen. 1986. A Hierarchical concept of ecosystems. In: Monographs in population

biology. R.M. May, editor. Princeton University Press, Princeton, N.J.

Overpeck, J.T., D. Rind, and R. Goldberg. 1990. Climate-induced changes in forest disturbance and vegetation. Nature 343:51-51.

Prentice, K.C. *in press*. Bioclimatic distribution of vegetation for GCM studies. J. Geo.Res.

Prescott, C.E., J.P. Corbin, and D. Parkinson. 1989. Biomass, productivity, and nutrient-use efficiency of aboveground vegetation in four Rocky Mountain coniferous forests. Can. J. Res. 19:309-317.

Running, S.W. 1975. Environmental control of leaf water and conductance in conifers. Can. J. Res. For. Res. 6:104-112.

Quinlan, F. T. , T. R. Karl, and C. N. Williams, Jr. 1987. United States Historical Climatology Network (HCN) serial temperature and precipitation data. NDP-019, Carbon Dioxide Information Analysis Center, Oak Ridge National Laboratory, Oak Ridge, Tennessee.

Runkle, J.R. 1985 Disturbance Regimes in Temperate Forests. In: S.T.A. Pickett and P.S. White, eds., The Ecology of Natural Disturbance and Patch Dynamics. pp 17-33.

Schlesinger, W.H., and C.S. Jones. 1984. The comparative importance of overland runoff and mean annual rainfall to shrub communities of the Mojave Desert. Bot. Gaz. 145(1):116-124.

Smith, J.B., and D. Tirpak, eds. 1989. The Potential Effects of Global Climate Change on the United States. Report to Congress. EPA-230-05-89-050, U.S. Environmental Protection Agency, Washington, DC 413 pp.

Solomon, D. M. 1986. Transient response of forests to CO_2-induced climate change: simulation modeling experiments in eastern North America. Oecologia 68:567-579.

Stephenson, N. L. 1990. Climatic Control of Vegetation Distribution: The Role of the Water Balance. American Naturalist 135:649-670.

Strain, B.R. and J.D. Cure. 1985. Direct effects of increasing carbon dioxide on vegetation. DOE/ER-0238, U.S. Department of Energy, Carbon Dioxide Research Division, Washington, DC.

Thornthwaite, C.W. 1948. An approach toward a rational classification of climate. Geographical Review 38:55-94.

Thornthwaite, C.W., and J.R. Mather. 1955. The Water Balance. Publications in Climatology, Volume VIII, Number 1. Drexel Institute of Technology. Centerton, New Jersey.

Transeau, E.N. 1935. The prairie peninsula. Ecology 16(3):423-439.

Tucker, C.J., I.Y. Fung, C.D. Keeling, and R.H. Gammon. 1986. Relationship between atmospheric CO_2 variations and a satellite-derived vegetation index. Nature 319:195-199.

Tucker, C.J., J.R.G. Townshend, T.E. Goff. 1985. African land-cover classification using satellite data. Science 227:369-375.

US WEST. 1988a. Climatedata User's Manual: TD3200 Summary of the Day -- Cooperative Observer Network. US WEST Optical Publishing. Denver, CO.

US WEST. 1988b. Hydrodata User's Manual: USGS Daily and Peak Values, Version 2.0. US WEST Optical Publishing. Denver, CO.

Vankat, J.L. 1979. The Natural Vegetation of North America. John Wiley and Sons, New York.

Vitousek, P.M. 1984. Litterfall, nutrient cycling, and nutrient limitation in tropical forests. Ecology 65(1):285-298.

Waring, R.H., and J.F. Franklin. 1979. Evergreen coniferous forests of the Pacific Northwest. Science 204:1380-1386.

Webb, T.III, P.J. Bartlein, and J.E. Kutzbach. 1990. Climatic Change in Eastern North America During the Past 18,000 Years: Comparisons of Pollen Data with Model Results. In: North America and Adjacent Oceans During the Last Deglaciation. Geology of North America. W.F. Ruddiman, and H.E. Wright, eds. Geological Society of America, Boulder, Colorado, *in press*.

Woodward, F.I. 1987. Climate and Plant Distribution, Cambridge University Press, London, England. 174 pp.

EFFECTS OF CLIMATE CHANGE ON CARBON STORAGE IN TERRESTRIAL ECOSYSTEMS: EQUILIBRIUM ANALYSES AT THE GLOBAL LEVEL

David P. Turner
NSI Technology Services Corporation
US EPA Environmental Research Laboratory
200 SW 35th Street
Corvallis, OR 97333

and

Rik Leemans
Global Change Department
National Institute of Public Health & Environmental Protection
Netherlands

Abstract

Storage of carbon in the terrestrial biosphere is dependent on the distribution of vegetation types. This analysis evaluates potential changes in above- and belowground carbon pools associated with redistribution of vegetation types as driven by climate change. The approach makes use of the Holdridge life zone classification system to distribute vegetatation types under the current climate, and doubled-CO_2 climate scenarios from four General Circulation Models (GCMs). An estimate of the global terrestrial carbon pool for a given climate scenario was made by assigning a representative value for above- and belowground carbon to each vegetation type and using the areal extent of the vegetation types to sum stored carbon. All GCMs predicted a net flux of carbon from the atmosphere to the biosphere under a doubled-CO_2 climate when considering just the aboveground biomass. This flux reflected increases in the areal extent of carbon-rich vegetation types such as tropical humid forests. Two of the GCMs predicted a net loss of belowground carbon because of large decreases in the areal extent of tundra ecosystems with a high level of belowground storage. In terms of ppm CO_2, these fluxes represent a range from adding 13 ppm to the atmosphere to removing 84 ppm. These values suggest the potential for a moderate negative feedback to global warming over the long term via this mechanism.

Introduction

Since at least the time of the 18th century geographer Alexander von Humbolt, it has been recognized that vegetation type or physiognomy is correlated with climate. The constraints on plant form imposed by climate mean that climate also strongly regulates the maximum aboveground carbon in terrestrial ecosystems. Correlations of belowground carbon with climate have also been observed (Post et al. 1983). A change in the areal extent of different biomes as a result of global climate change will thus be likely to result in fluxes of carbon to or from the biosphere, with corresponding changes in the atmospheric CO_2 concentration. These changes are of interest in terms of positive or negative feedbacks from the terrestrial biosphere to climate change.

The specific objective of this section is to investigate the potential for a net flux of carbon between the terrestrial biosphere and the atmosphere due to climate change. This is an equilibrium analysis (i.e. the assumption is made that climate and vegetation are always in equilibrium) and a bookkeeping approach is used in which: 1) vegetation types are distributed across the land surface based on the current climate and double-CO_2 climate scenarios using an existing vegetation-climate correlation system (Holdridge 1947); 2) the vegetation types are assigned representative above- and belowground carbon pools; 3) terrestrial carbon storage is summed by climate scenario; and 4) the differences between current storage and future storage are determined.

Methods

The Vegetation/Climate Correlation

A number of systems have quantified the vegetation-climate correlation. Holdridge's is perhaps the earliest and most widely cited (Holdridge 1947, Emanuel et al. 1985). In the Holdridge system, potential vegetation distribution is a function of annual precipitation and temperature. Vegetation is divided into 30 types, and the whole system can be displayed in a triangular grid as in Figure 1. Applying global data sets from weather stations for the climate variables and a modified version of the Holdridge scheme, the system was correct for 77% of current observed vegetation in a recent study (Prentice 1990). Similar vegetation/climate correlation systems (e.g., Box 1981) use additional climate variables such as seasonality of temperature and precipitation. Research is under way at ERL-C to develop a rule-based system that takes into account geographic patterns in the seasonality of precipitation and runoff. In the analysis presented here, the Holdridge scheme is used. However, the original 30 vegetation classes have been aggregated into 14 biome-level classes (Table 1) more appropriate to the level of resolution achievable in assigning carbon pools to specific vegetation types.

Vegetation Distribution under Current and Double-CO_2 Climates

The basic approach to predicting how biomes or vegetation types may be redistributed due to global climate change is to combine a spatially distributed climate scenario and a climate-vegetation correlation system (King 1990). Several investigators have used the Holdridge classification system to predict the future distribution of vegetation types in this manner (Emanuel et al. 1985a; Prentice and Fung, *in press*).

General Circulation Models (GCMs) are used to produce the climate scenarios. Current GCMs are configured with grid cells several hundred km on a side but predictions of climate at a higher spatial resolution can be made by application of the difference between 1 x CO_2 and doubled-CO_2 GCM runs to the hisotrical climate (Smith and Tirpak 1989).

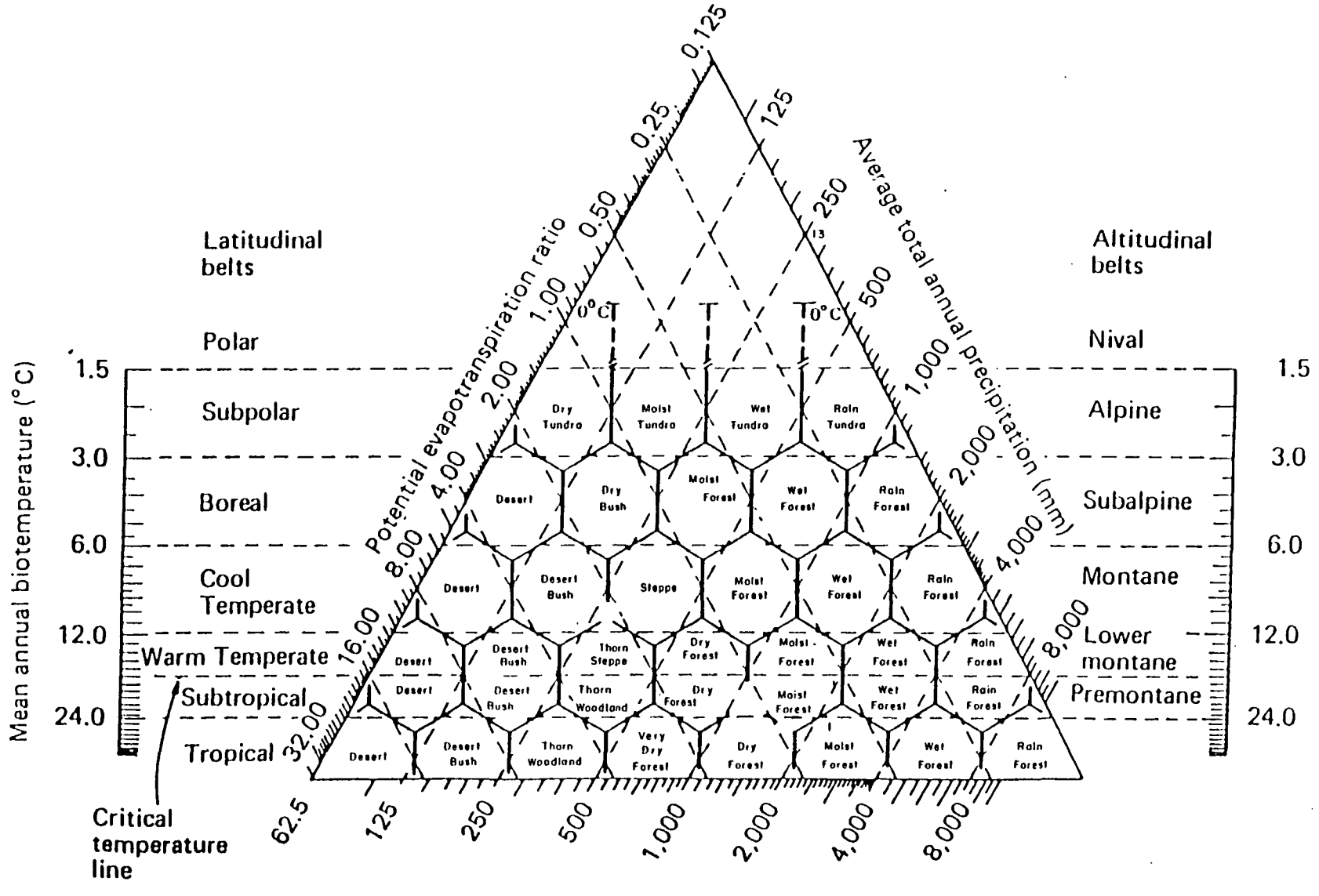

Figure 1. Holdridge life zone classification system. (Holdridge 1967)

As the spatial resolution of the GCMs and their success in recreating the current climate improves, more direct coupling of GCMs to the vegetation will become possible.

In this study, doubled CO_2 runs from the GCMs of four institutions were used: UKMO (United Kingdom Meteorological Organization, OSU (Oregon State University), GISS (Goddard Institute for Space Science, and GFDL (Geophysical Data Center). Current climate was based on long-term weather station data from 13,000 global sites interpolated to 0.5° of latitude and longitude. The assignment of a vegetation type to each grid cell and the determination of the total areal extent of each vegetation type was done by Leemans (1990) using a geographic information systems approach.

Carbon Pools

Aboveground carbon ranges from 25 kg/m^2 in dense forests to less than 0.5 kg/m^2 in the arctic (Olson et al. 1983). The summary of Olson et al. (1983) is used in this study as a basis for assigning aboveground carbon pool values to the aggregated Holdridge vegetation types (Table 2). The assignment of belowground carbon pools to the Holdridge vegetation types (Table 2) was taken from the study of Post et al. (1982) in which data from 2696 global sites were used to construct isolines for belowground carbon storage within the Holdridge climate diagram (Figure 2). Based on the current climate, this analysis estimated totals for aboveground carbon (852 Gt) and belowground carbon (1456) which are consistent with other studies (Schlesinger 1977, Woodwell et al. 1978, Oades 1988).

Certainly there is large spatial heterogeneity in these pools within each vegetation type but evaluation of that heterogeneity will require detailed survey information that is not currently available. Mean values were using in this analysis as a first approximation to accounting for the spatial heterogeneity.

The absolute value of the representative carbon pools is also in question. Recent analysis of boreal forest ecosystems (Botkin and Simpson 1990) suggest that previous estimates of aboveground carbon in these and other ecosystems have been uniformly high. Additional

Table 1. Aggregation Scheme for Combining Holdridge Life Zones into Biomes.

Biome		Holdridge Zone
1	Tundra	Ice Polar Desert Subpolar Dry Tundra Subpolar Moist Tundra Subpolar Wet Tundra Subpolar Rain Tundra
2	Cold Parklands	Boreal Desert
3	Forest Tundra	Boreal Dry Scrub
4	Boreal Forest	Boreal Moist Forest Boreal Wet Forest Boreal Rain Forest
5	Cool Desert	Cool Temperate Desert Cool Temperate Desert Scrub
6	Steppe	Cool Temperate Steppe
7	Temperate Forest	Cool Temperate Moist Forest Cool Temperate Wet Forest Cool Temperate Rain Forest
8	Hot Desert	Warm Temperate Desert Warm Temperate Desert Scrub Subtropical Desert Subtropical Desert Scrub Tropical Desert Tropical Desert Scrub
9	Chapparal	Warm Temperate Thorn Steppe
10	Warm Temperate Forest	Warm Temperate Dry Forest Warm Temperate Moist Forest Warm Temperate Wet Forest Warm Temperate Rain Forest
11	Tropical Semi-Arid	Subtropical Thorn Woodland Tropical Thorn Woodland Tropical Very Dry Forest
12	Tropical Dry Forest	Subtropical Dry Forest Tropical Dry Forest
13	Tropical Seasonal Forest	Subtropical Moist Forest Tropical Moist Forest
14	Tropical Rain Forest	Subtropical Wet Forest Subtropical Rain Forest Tropical Wet Forest Tropical Rain Forest

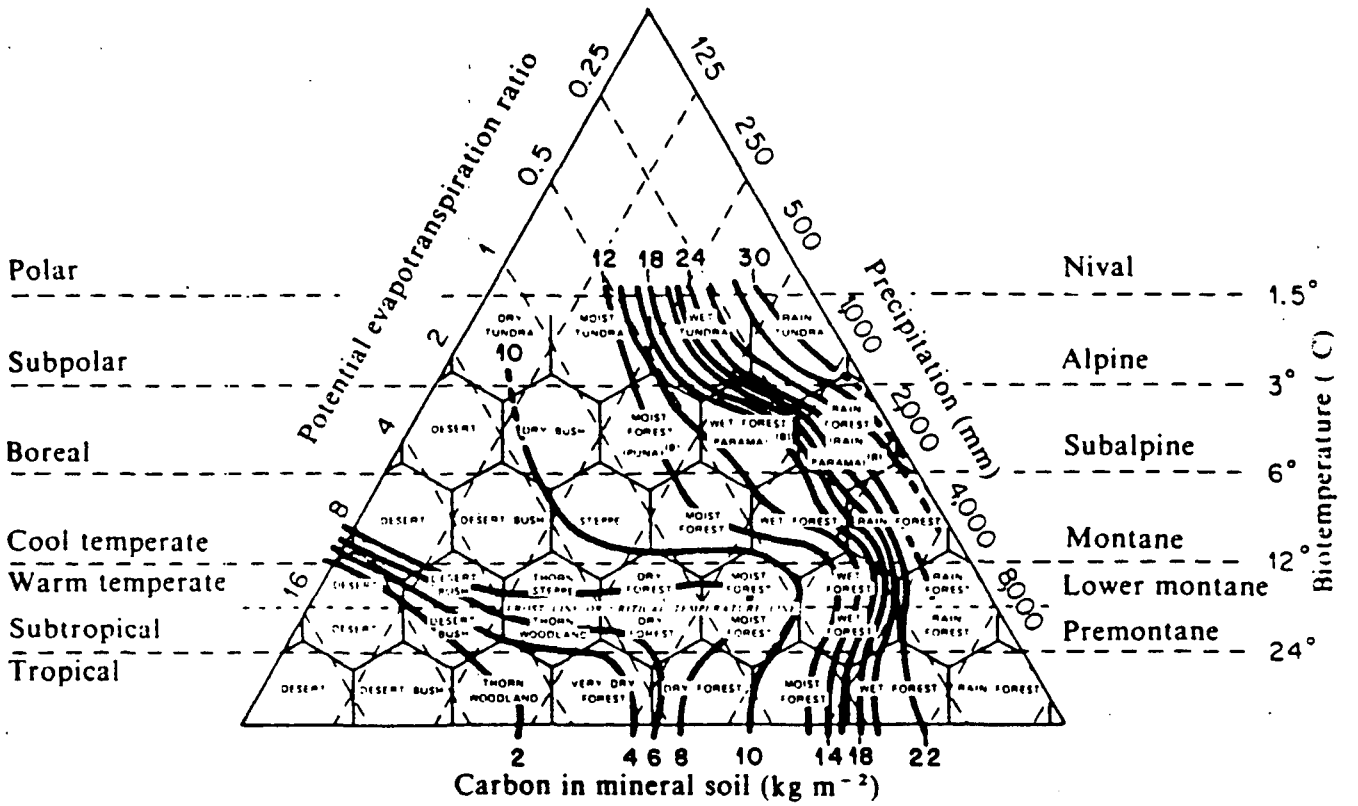

Figure 2. Relationship of belowground carbon pools to holdridge life zones. (Post et al. 1982)

studies, probably coordinated with remote sensing, are needed to evaluate this question. In the present analysis, the carbon pools (Kg/m2) associated with each vegtation type are held constant, and a difference between current and future storage is calculated. Thus, the approach is not particularly sensitive to a consistent overestimate of above- or belowground carbon across all vegetation types.

Table 2. Above- and Belowground Pools for World Biomes

	Biome	Aboveground Carbon Density (kg/m^2)	Belowground Carbon Density (kg/m^2)
1	Tundra	0.5	22.0
2	Cold Parklands	0.8	10.0
3	Forest Tundra	6.0	11.0
4	Boreal Forest	11.0	15.0
5	Cool Desert	0.6	9.0
6	Steppe	1.5	13.0
7	Temperate Forest	11.0	18.0
8	Hot Desert	0.4	1.0
9	Chaparral	4.0	8.0
10	Warm Temperate Forest	10.0	10.0
11	Tropical Semi-Arid	5.0	4.0
12	Tropical Dry Forest	7.0	7.0
13	Tropical Seasonal Forest	10.0	11.0
14	Tropical Rain Forest	15.0	19.0

Aboveground data after Olson et al. 1983

Belowground data after Post et al. 1982

Results and Discussions

Differences in the areal extent of the biomes, as predicted by four GCMs, are listed in Table 3. Results for the four GCMs show some basic similarities. At middle to high latitudes, tundra and boreal forests contract, and temperate forest (mostly coniferous) expands. In the tropics, both the semi-arid woodland and the tropical rain forest have large increases in areal extent, mostly at the expense of tropical seasonal forests.

Analysis of changes in carbon storage reveals that all climate scenarios predict an uptake of carbon from the atmosphere for the aboveground component of the biosphere (Figure 3), ranging from 37 to 116 Gt. There are great discrepancies between the model runs for the change in belowground carbon storage. The UKMO model predicts a flux to the atmosphere of 126 Gt, while the OSU model predicts a belowground accumulation of 37 Gt. The large fluxes to the atmosphere appear to be associated with loss of carbon from reduction in the area of tundra and boreal forest, both having relatively high levels of belowground carbon.

The net change of above- and belowground carbon ranged from a 169 Gt uptake predicted by the OSU model to a 68 Gt release predicted by the UKMO model. A key question appears to be how great the gains will be in tropical rain forest. Because both above- and belowground components have high carbon storage in these forests, the changes from tropical dry forest to tropical wet forest tend to drive the global trends. In terms of climate, the question is whether precipitation will substantially increase in tropical and subtropical latitudes.

A number of other investigators have made estimates of potential changes in carbon storage based on the climate-vegetation correlation systems and other GCM doubled-CO_2 climate scenarios. For aboveground carbon, Sedjo and Solomon (1988) predicted a net flux of 13.9 Gt to the atmosphere. Much of that change in aboveground carbon was accounted for by loss of boreal forest and increases in savanna. Lashof (1987, 1989), evaluating potential above- and belowground changes, reported a range from a 64 Gt uptake from the atmosphere to a 26 Gt release, again depending on the GCM used. A

Table 3. Changes in Area Extent of Different Vegetation Types as Predicted by 4 GCMs.

Smith & Leemans Aggregated Holdridge Life Zones	Current $\times 10^6 km^2$	GFDL	GISS	OSU	UKMO
1 Tundra	9.30	-6.11	-5.05	-4.56	-6.43
2 Cold Parklands	2.79	0.03	-0.41	-0.01	-1.09
3 Forest Tundra	8.90	-5.02	-3.03	-2.90	-5.50
4 Boreal Forest	15.03	-5.45	-1.54	-0.89	-4.85
5 Cool Desert	4.01	-0.97	-1.67	-0.82	-1.93
6 Steppe	7.39	4.20	-0.46	1.30	-0.21
7 Temperate Forest	9.94	1.92	3.49	1.63	3.04
8 Hot Desert	20.85	-0.20	-3.22	-1.42	-0.92
9 Chaparral	5.58	1.83	-0.13	-0.69	2.99
10 Warm Temperate Forest	3.17	-1.22	-1.25	-0.72	-0.29
11 Tropical Semi-Arid	9.56	4.43	7.18	2.58	7.07
12 Tropical Dry Forest	14.86	4.71	4.49	0.00	11.19
13 Tropical Seasonal Forest	15.13	-5.11	-7.24	-4.98	-7.48
14 Tropical Rain Forest	8.46	6.95	8.85	11.57	4.40
TOTAL	134.97				

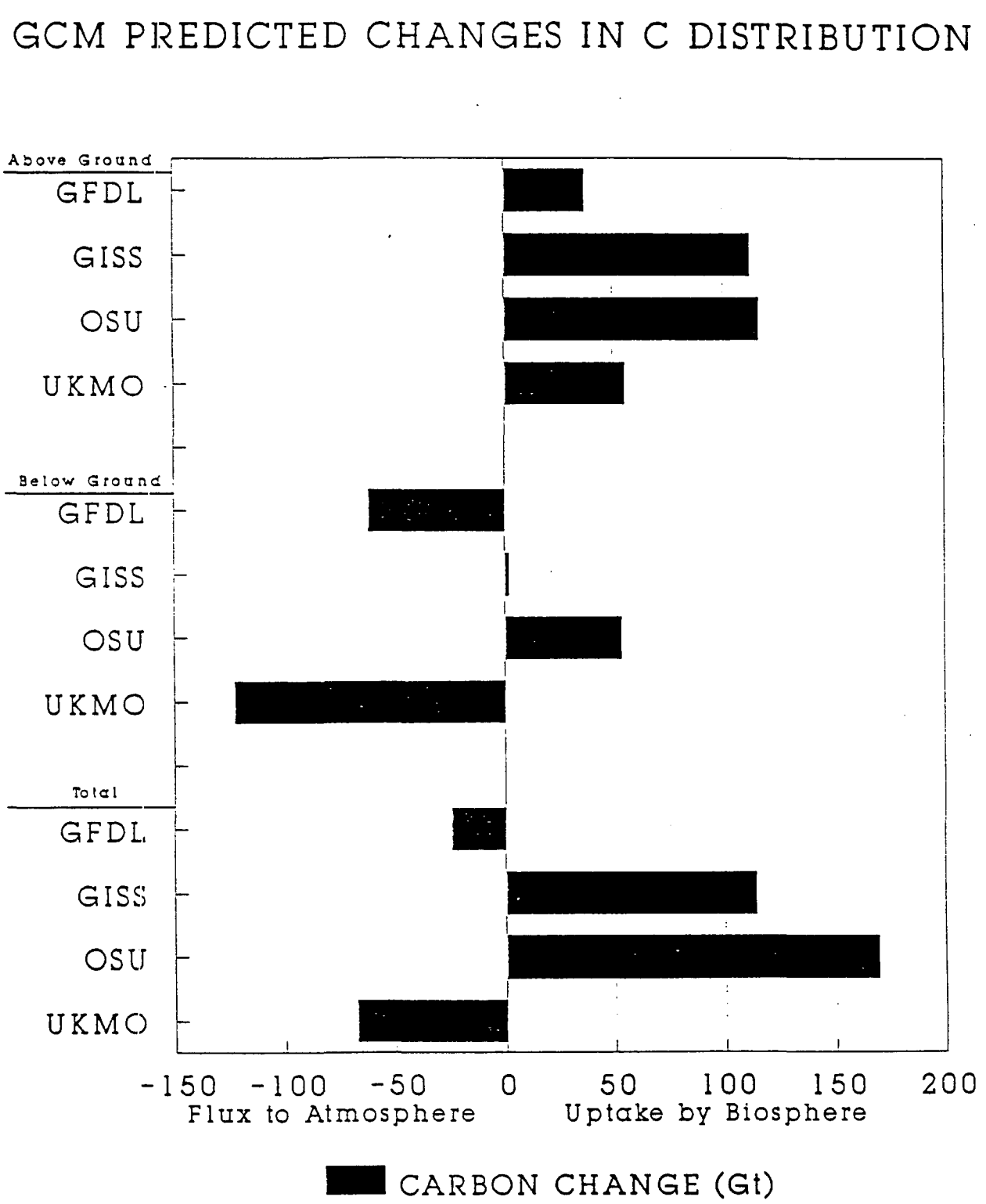

Figure 3. Potential changes in terrestrial carbon storage based on redistribution of vegetation types. Values are differences between stored carbon under the current climate and under doubled-CO_2 climates as predicted by four different general circulation models (GFDL, GISS, OSU, UKMO).

modified Holdridge classification system (Prentice 1990), which better represented the current vegetation, suggested a much greater potential flux of carbon (270 Gt) to the surface (Prentice and Fung, *in press*). As in our analyses, the uptake was related primarily to expansion of the tropical rain forest biome which has relatively high levels of above- and belowground carbon.

To begin evaluating the magnitude of feedbacks associated with these carbon fluxes, it is necessary to know: 1) how much of the carbon would be retained in the atmosphere (in the case of a positive feedback); 2) the radiative forcing of that retained component; and 3) the sensitivity of the climate system to that forcing. Likewise, for a negative feedback, the magnitude can most readily be evaluated via the impact on atmospheric CO_2 concentration.

The proportion of carbon released to the atmosphere due to fossil fuel combustion and deforestation that has accumulated in the atmosphere has been approximated at 40% (International Panel for Climate Change, 1990). The remainder has been taken up by the ocean, in part due to photosynthetic uptake of CO_2 by plankton, and by the terrestrial biosphere via a net imbalance between CO_2 assimilation during photosynthesis and CO_2 loss via plant, animal and microbial respiration. The atmospheric retention factor is difficult to determine because of uncertainties about many terms in the global carbon cycle (Keeling et al. 1989). Assuming a retention factor of 40%, the 68 Gt release of carbon in the case of the maximum positive feedback discussed earlier would result in 27 Gt increase in the atmospheric pool. Given a net change in the atmospheric carbon pool, a conversion to a change in atmospheric CO_2 concentration can be made using an approximation of 2 Gt carbon to 1 ppm CO_2. Thus the increase would be about 13 ppm CO_2. In the case of a negative feedback, Gt can be converted directly into ppm CO_2 extracted from the atmosphere by dividing by two.

The estimation of a climate forcing associated with a change in atmospheric CO_2, independent of feedbacks in the climate system, is relatively straightforward (Hansen et al. 1988) and the GCMs are in general agreement (Cess et al. 1989). Following the approach of Hansen, the climate forcing of 13 ppm added to a reference CO_2 concentration of about

450 ppm for a doubled CO_2 climate (the rest of the warming being provided by other trace gases), is about + 0.05°C. The effect of subtracting 84 ppm (169Gt/2) would be about - 0.28°C. These compare to the doubled CO_2 climate forcing without feedbacks of + 1.25°C. The GCMs are in much less agreement in accounting for various feedbacks in the climate system given an initial forcing (Hansen et al. 1984). The total climate forcing for the given potential changes in CO_2 is thus much less certain. However, they would probably scale to the magnitude of the orginal forcing, so a negative feedback of perhaps 20% of the original forcing could be expected due to changing carbon pools.

Modifiers and Uncertainties

The most troublesome assumption using the equilibrium approach described here is that the climate/vegetation correlation will remain constant. Physiological responses of plants to CO_2 suggests that water use efficiency increases with ambient CO_2 concentration. If this effect is large, aboveground carbon associated with a particular water regime might be expected to increase and thus the magnitude of the predicted feedbacks associated with carbon pool changes would be different.

A second concern is that the analysis described above assumes that climate and vegetation are now, and will remain, in equilibrium. In fact, the predicted rates of climate change (>0.1°C per decade) are an order of magnitude faster than what natural systems experienced during the glacial-interglacial cycles of the Pleistocene period. Analyses of tree seed dispersal distances and pollen records indicate that the rate of climate change may exceed rates of vegetation redistribution (Davis 1981). The predicted discrepancy between these rates may have significant implications for changes in aboveground carbon pools. Large transient carbon fluxes could occur if there is a rapid burnoff of carbon as the vegetation drifts out of equilibrium with the climate and vegetation recovery is slow because of limited migration rates for appropriate species and slow regrowth.

There will also be lags in the equilibrium between belowground carbon pools and climate. Where carbon gains are expected, as with the transition from tropical seasonal to tropical

rain forest, there is little data on how rapidly the predicted accumulation would occur. Factors such as soil mineralology and texture may have strong local influences (Oades 1988). Land use considerations will likewise influence carbon storage because of the tendency for cultivation to decrease stored carbon.

Where equilibrium analyses suggest a reduction in belowground carbon, an important consideration will be the fractionation of the soil organic matter. Microbial respiration increases with temperature, assuming optimal moisture, but belowground carbon is not all readily oxidizable. A large proportion of grassland soil carbon pools has been classified as recalcitrant to decomposition, with a turnover time of up to 1000 years (Parton et al. 1988). Forest soils are also characterized by a large recalcitrant fraction, and lags in the reduction of soil organic matter due to warming may be on the order of hundreds of years. Continued research on the mechanisms and modeling of soil organic matter turnover is needed.

These analyses also ignore the human factor which will exert a tremendous influence on rates of vegetation change. Currently anthropogenic factors use or co-opt approximately 40% of the earth's potential net primary production and over large areas the productive capacity of the land is being reduced (Vitousek et al. 1986). Land used for human purposes will probably not be readily transformed to the high-carbon-storage vegetation types predicted in this analysis. However, humanity may be able to promote changes that would favor carbon sequestration. Management options are available for reducing carbon fluxes to the atmosphere and maximizing carbon sinks associated with the terrestrial biosphere. Their implementation will require an understanding of current climate-vegetation-soil relationships and of locations where the climate will favor specific vegetation types in decades to come.

Conclusions

These equilibrium analyses suggest that the changes in terrestrial carbon pools induced by climate warming will be a negative feedback to that warming. That is, as global warming increases, carbon storage will increase and the rate of increase in atmospheric CO_2 concentration will be moderated. The greater the increase in precipitation for the low latitudes, thus creating tropical wet forest, the stronger that feedback will be. These analyses do not consider 1) potential short term fluxes of carbon due to changing disturbance regimes, 2) the relative slow response of belowground carbon pools to climate change, and 3) potential enhancements or reductions of carbon storage due to management practices.

Acknowledgements

Distribution of the Holdridge vegetation types under current and doubled-CO_2 climates were generously provided by Rik Leemans and Tom Smith from the International Institute for Applied Systems Analysis.

References

Botkin, D.B. and L.G. Simpson. 1990. Biomass of the North American boreal forest: A step toward accurate global measures.
Biogeochemistry. 9:161-174.

Box, E.O. 1981. Macroclimate and Plant Forms: An Introduction to Predictive Modeling in Phytogeography. Dr. W. Junk Publishers, The Hague.

Cess, R.D., G.L. Potter, J.P. Blanchet, G.J. Boer, S.J. Ghan, J.T. Kiehl, H. Le Treut, Z.-X Li, X.-Z Liang, J.F.B. Mitchell, J.-J Morcrette, D.A. Randall, M.R. Riches, E. Roeckner, U. Schlese, A. Slingo, K.E. Taylor, W.M. Washington, R.T. Wetherald, and I. Yagai. 1989. Interpretation of cloud-climate feedback as produced by 14 atmospheric general circulation models. Science. 245:513-516

Davis, M.B. 1981. Quaternary history and the stability of forest communities. In: D.C. West, H.H. Shugart & D.B. Botkin, eds., Forest Succession: Concepts and Application. Springer-Verlag, New York. 517 pp.

Emanuel, W.R., H.H. Shugart, and M.P. Stevenson. 1985. Climatic change and the broad-scale distribution of terrestrial ecosystem complexes. Climatic Change 7:29-43

Hansen, J., A. Lacis, D. Rind, G. Russel, P. Stone, I. Fung, and J. Lerner. 1984. Climate sensitivity: Analysis of feedback mechanism. In: Climate Processes and Climate Sensitivity, Geophys. Monogr. Ser., AGU, Washington, DC. 29:130-163.

Hansen, J., I. Fung, A. Lacis, D. Rind, S. Lebedeff, R. Ruedy, G. Russell, and P. Stone. 1988. Global climate changes as forecast by Goddard Institute for Space Studies Three-Dimensional Model. J. Geophys. Res. 93:9341-9364.

Holdridge, L.R. 1947. Determination of world formulations from simple climatic data. Science 105:367-368.

Intergovernmental Panel on Climate Change. 1990. Scientific Assessment of Climate Change. Report for WGI Plenary Meeting.

Keeling, C.D., R.B. Bacastow, A.F. Carter, S.C. Piper, T.P. Whorf, M. Heimann, W.G. Mook, and H. Roeloffzen. 1989. A three-dimensional model of atmospheric CO_2 transport based on observed winds: analysis of observational data. Geophysical Monograph 55:165-236.

King, G.A. 1990. Effects of global climate change on global vegetation. This document.

Lashof, D.A. 1989. The dynamic greenhouse: feedback processes that may influence future concentrations of atmospheric trace gases and climatic change. Climatic Change 14:213-242.

Lashof, D.A. 1987. The role of the biosphere in the global carbon cycle: evaluation through biospheric modeling and atmospheric measurement. PH.D. Dissertation, Energy and Resources Group, Univ. of Ca, Berkeley.

Oades, J.M. 1988. The retention of organic matter in soils. Biogeochemistry 5:35-70.

Olson, J.S., J.A. Watts, and L.J. Allison. 1983. Carbon in live vegetation of major world ecosystems. ORNL-5862. Oak Ridge National Laboratory, Oak Ridge, Tn. 180 pp.

Parton, W.J., J.W.B. Stewart, and C.V. Cole. 1988. Dynamics of C,N, P and S in grassland soils: a model. Biogeo. 5:109-131.

Post, W.M., W.R. Emanuel, P.J. Zinke & A.G. Stangenberger. 1982. Soil carbon pools and world life zones. Nature. 298:156-159.

Prentice, K.C. 1990. Bioclimatic distribution of Vegetation for General Circulation Model Studies. J.Geophy. Res. 95:11811-11830.

Prentice, K.C., and I.Y. Fung. Bioclimatic simulations test the sensitivity of terrestrial carbon storage to perturbed climates. Nature. In press.

Schlesinger, M.E. and Z.C. Zhao. 1989. Seasonal climatic change introduced by doubled-CO_2 as simulated by the OSU atmospheric GCM/mixed-layer ocean model. J. Climate 2:429-495.

Schlesinger, W.H. 1977. Carbon balance in terrestrial detritus. Ann. Rev. Ecol. Syst. 8:51-81.

Vitousek, P.M., P.R. Ehrlich, A.H. Ehrlich, and P.A. Matson. 1986. Human appropriation of the products of photosynthesis. BioScience 36:368.

CLIMATE CHANGE
AND
ISOPRENE EMISSIONS FROM VEGETATION

D.P. Turner[1], J.V. Baglio[1], D. Pross[3], A.G. Wones[1],
B.D. McVeety[2], R. Vong[3], D.L. Phillips[4]

[1]NSI Technology Services, Corvallis, Oregon
[2]Pacific Northwest Laboratories, Richland, Washington
[3]Oregon State University, Corvallis, Oregon
[4]U.S. Environmental Protection Agency, Corvallis, Oregon

ABSTRACT

A global model was developed for estimating spatial and temporal patterns in the emission of isoprene from vegetation under the current climate and doubled CO_2 climate scenarios. Current emissions were estimated on the basis of vegetation type, foliar biomass (derived from the satellite-generated Global Vegetation Index), and global databases for air temperature and photoperiod. The model had a monthly time step and the spatial resolution was 0.5 degrees latitude and longitude. Doubled CO_2 climate emissions were estimated based on predicted changes in the areal extent of different vegetation types, each having a specific rate of annual isoprene emissions. The global total for current emissions was 560 Tg, which agrees reasonably well with estimates generated by other means. The isoprene emissions under a doubled CO_2 climate were about 25 % higher than current emissions due mainly to the expansion of tropical humid forests which had the highest vegetation-specific emission rates. An increase in isoprene emissions is expected to increase atmospheric concentrations of ozone and methane which are important greenhouse gases; however, detailed treatment of this question awaits incorporation of these emission surfaces into 3-D atmospheric chemistry models.

INTRODUCTION

Measurements of chemical emissions from plants began over two decades ago (Rasmussen and Went, 1965) and since then it has become evident that plants emit a great variety of volatile compounds. The most commonly studied chemical species of plant origin are the nonmethane hydrocarbons (NMHCs). In terms of the flux of NMHCs, isoprene (C_5H_8) and the monoterpenes such as alpha-pinene ($C_{10}H_{16}$) are the most important. However, hundreds of other biogenic nonmethane hydrocarbons (NMHCs) have been identified and different plant species vary greatly in the type and quantities of hydrocarbons emitted (Winer, 1989). Although plants may expend up to a few percent of their fixed carbon on NMHC emissions (Zimmerman et al. 1988, Monson and Fall 1989), there is limited understanding of their physiological and ecological significance (Harborne, 1988).

The goal of evaluating of NMHC emissions in the context of global climate change lies in relating their emissions to the current and future tropospheric concentrations of radiatively important trace gases (RITG) such as methane (CH_4), ozone (O_3), and chloroflorocarbons (CFCs). These compounds are also know as greenhouse gases. A schematic depiction of some of the important tropospheric chemical reactions involving these gases is given in Figure 1.

Over the next 50 years, the effect on Earth's radiation balance of increasing concentrations of radiatively important biogenic and anthropogenic trace gases is expected to equal that of increasing CO_2 (Ramanathan et al. 1985). Methane and many other important trace species are removed from the atmosphere primarily by the hydroxyl radical, which is also consumed in the oxidation of NMHCs. Because NMHCs consume the hydroxyl, NMHC emission rates will influence the atmospheric lifetime, and hence the concentration, of other RITG species. NMHCs are also important in relation to photochemical production of ozone in the troposphere (Logan 1985).

This report describes an approach to estimating global patterns of plant emissions under the current climate and under climate scenarios associated with a doubling of atmospheric CO_2. We have initially focused on isoprene emissions to facilitate the development of

spatially distributed estimation methods. In the future, we anticipate the refinement of this technique followed by the application of this approach to additional biogenic species. Isoprene was chosen as the test case because it has a relatively short atmospheric lifetime, and therefore, knowledge of its spatial and temporal emission patterns is important to evaluating its role in regional and global atmospheric chemistry. There are also several other global emission estimates that have been derived using methods different than described here, and thus can be used for intercomparison and validation (Zimmerman et al. 1978, Crutzen and Gidel 1983, Logan et al. 1985, Rasmussen and Khalil 1988).

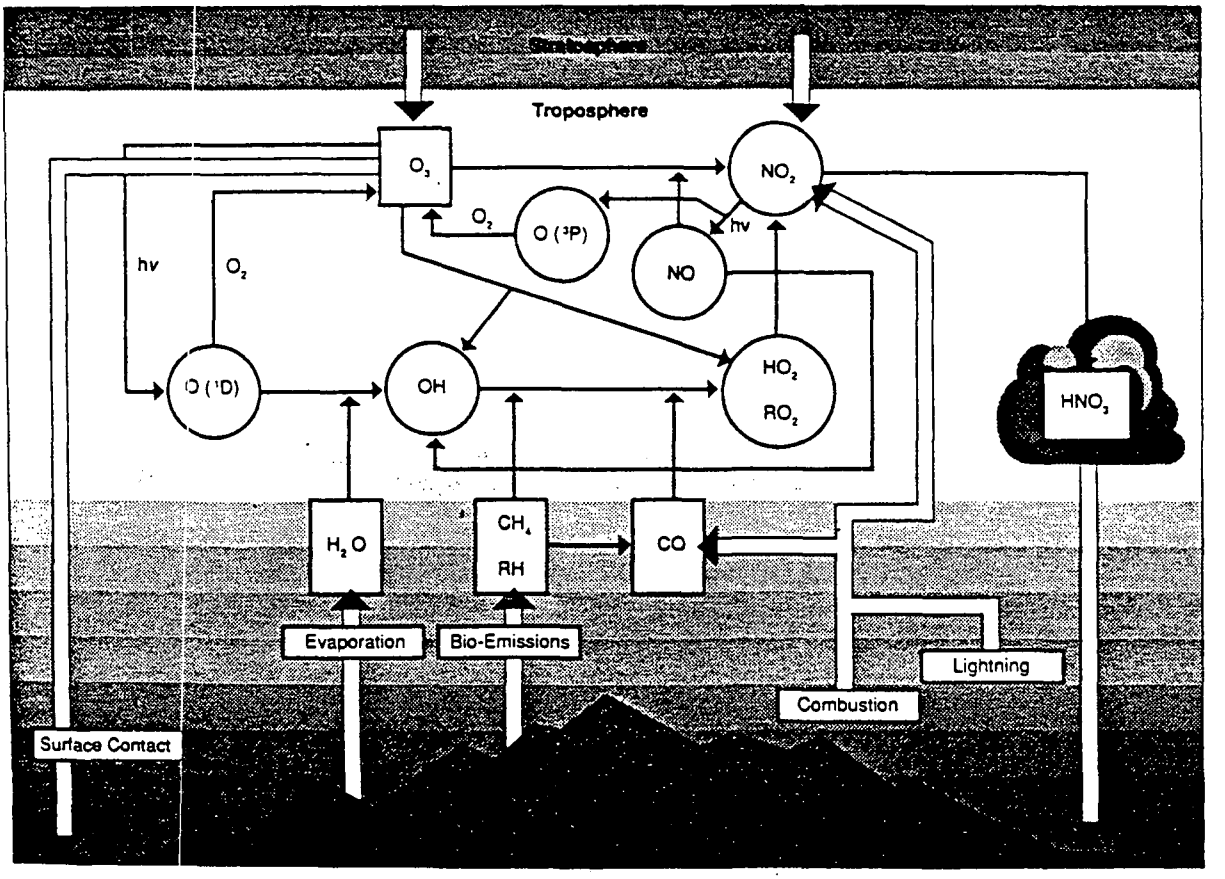

Figure 1. Principal chemical reactions relevant to tropospheric chemistry (from NASA, 1988). RH indicates hydrocarbons.

The approach in this study to estimating current emissions was to apply satellite based remote sensing for characterization of global spatial and temporal patterns in foliar biomass, and a global temperature database for driving temperature/emissions relationships. The projected emissions for a doubled CO_2 climate are based on an equilibrium approach. Here, the average annual emission rate is determined for each vegetation type under current conditions, and the predicted change in the areal extent of the vegetation types due to climate change is used to estimate future emissions. This approach makes the obviously unreal assumption that vegetation and climate always stay in equilibrium. However, it is a start towards determining the sign and magnitude of possible feedbacks to climate change mediated by biogenic NMHC emissions.

The primary objectives of this work were thus to 1) provide a basis for estimating terrestrial biogenic emissions under current climate conditions and forecasting emissions under future climate scenarios, 2) develop a spatial-temporal terrestrial biogenic emissions model that could be incorporated into the three dimensional global atmospheric chemistry model, and 3) establish an ecosystem model framework based on remote sensing that will be able to take advantage of the increasingly refined satellite remote sensing capability being developed by NASA under the EOS (Earth Observation System) program.

The background material which follows summarizes the relationship of NMHC emissions to the concentrations of radiatively and photochemically important trace gas species in the troposphere, and provides information on plant and environmental factors influencing emission rates.

Atmospheric Chemistry

NMHCs are representative of the general pattern of biogenic release of reduced chemical species which are oxidized in the atmosphere and returned to the surface via precipitation scavenging, biological uptake or surface deposition. NMHCs have relatively short atmospheric lifetimes (hours to days) due to rapid oxidation by hydroxyl radicals (OH)

and ozone (Warneck 1988). They may be only partially oxidized, and scavenged as organic acids, or further oxidized to CO and eventually CO_2. It is currently believed that a significant proportion of the global CO budget is related to biogenic NMHC emissions (Logan et al. 1981). Total biogenic NMHC emissions are approximately an order of magnitude larger than anthropogenic NMHC (volatile organic compound) emissions associated with fossil fuel combustion (Hanst et al. 1980).

Relationship to Tropospheric Ozone

The oxidation of NMHCs, and products such as CO, can result in the formation of tropospheric ozone when atmospheric NO_x concentration is greater than about 20 - 200 ppbv. It is unlikely that the oxidation of most biogenic NMHCs currently involves ozone production because of the low NO_x levels (Crutzen 1988). However, NO_x levels are rising over large geographical areas. On a global basis, anthropogenic sources of NO_x via fossil fuel burning are already greater than biogenic NO_x emissions (Logan 1983). Fossil fuel NO_x emissions have decreased in the U.S. in the last decade but may be expected to increase globally due to rapid fossil-fuel-based industrialization in less developed countries (Kavenaugh 1987). In the northern hemisphere, tropospheric ozone is increasing at a rate of about 1 % per year and there is some evidence that anthropogenic NO emissions are the cause of the increase (Crutzen and Gidel 1983, Dignon and Hameed 1985, Liu et al. 1987). NO_x levels in rural Pennsylvania, in combination with both biogenic and anthropogenic NMHCs, are high enough to promote ozone buildup to over 100 ppbv in the summer (Trainer et al. 1987), i.e., more than twice the probable background level.

Where NO_x is not high enough to promote ozone formation during hydrocarbon oxidation, ozone can be consumed by interactions with NMHCs. Several authors have suggested that the terrestrial land masses located in the tropics play a significant role in the global ozone budget (e.g., Thompson et al. 1989), acting mainly as a sink. The ozone sink strength is a function of both plant uptake and interactions with NMHCs. The exception to

this would be during periods of extensive biomass burning (Delany et al. 1985) when the combination of NO_x and hydrocarbons, produced during combustion, produces ozone.

Hydroxyl Radical

A second major impact of biogenic NMHC emissions on tropospheric chemistry concerns the hydroxyl radical (see Figures 1 and 2). The NMHCs are an important sink for OH radicals in the planetary boundary layer (Jacob and Wofsy 1988) but also to a great extent, via oxidation of carbon monoxide (an intermediate in the NMHC oxidation pathway), in the free troposphere. The hydroxyl radical is one of the most reactive species in the troposphere, having an atmospheric lifetime on the order of seconds. Its concentration largely controls the atmospheric lifetime and degree of escape into the stratosphere of important species such as methane, a greenhouse gas, and NO_x, a catalyst for ozone formation. The variety of atmospheric chemical reactions that involve the hydroxyl radical are shown in Figure 2.

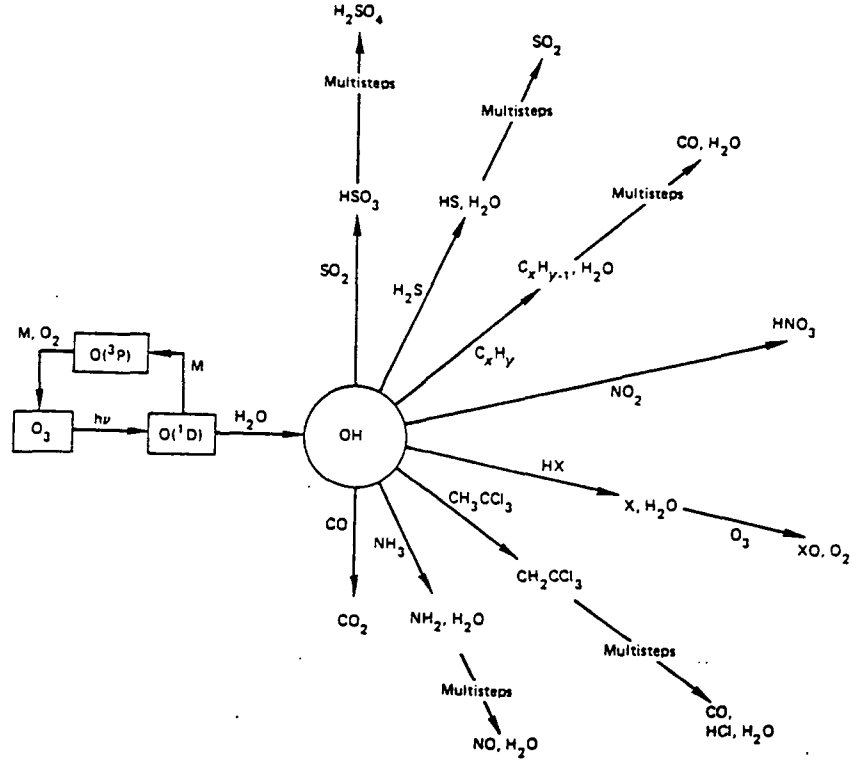

Figure 2. A depiction of the central role OH plays in the oxidation of tropospheric trace gases (from NRC, 1984).

To the degree that current and future NMHC emissions reduce OH, they will contribute to global warming because of an increased atmospheric lifetime for methane and HCFCs, the less inert substitutes for stratospheric ozone depleting CFCs. Models of atmospheric chemistry suggest a global decrease in OH (Thompson and Cicerone 1986) due to increasing methane and carbon monoxide emissions over the last century. Concentrations of CO and CH4 are increasing at rates of 1-2% per year (Khalil and Rasmussen 1990) and as much as half of the methane increase may be due to OH decrease (Thompson and Cicerone 1986). Some modeling efforts indicate instability in the OH concentration under the influence of increasing NMHC, CO or CH_4 emissions (Thompson and Cicerone 1986, Thompson et al. 1990, Guthrie 1990), however, there may be unidentified or poorly modeled feedbacks which would come into play as the chemical climate changes.

Peroxyacetyl Nitrate

Another important chemical reaction involving NMHCs is the formation of peroxyacetyl nitrate (PAN), an intermediate in NO_x oxidation. Gaseous hydrocarbon emissions favor production of PAN (Singh 1987). In addition to being toxic to plants and humans, PAN effectively prevents NO from acting as an agent in further ozone production. Later thermal breakdown of PAN releases NO, and this mechanism provides a reservoir of NO_x and a means for long range transport of NO_x to areas of relatively clean air. Such transport will increase tropospheric ozone formation in rural areas.

Aerosols

NMHCs originating in forest habitats may also participate in formation of aerosols, particularly in areas of high NMHC emission such as over wet tropical forests (Talbot et al. 1988). The blue haze seen over the Great Smoky Mountains before heavy industrialization was probably from this source. Aerosols participate in the climate system as cloud condensation nuclei and absorbers of solar radiation, thus influencing the

precipitation regime and the distribution of heat in the atmosphere. Many aspects of these phenomena are as yet poorly understood.

Isoprene Emissions Rates

A great variety of plant species have been examined for biogenic emissions using field and laboratory enclosures (Zimmerman 1979, Evans et al. 1982, Winer et al. 1989). Techniques differ considerably between investigators, but some comparisons among species are possible by standardizing emissions to a common temperature using experimentally determined algorithms (e.g., Tingey et al., 1979). There is a tendency for either isoprene or monoterpenes to dominate emissions in a given species. For species with mainly isoprene emissions, the rates tend to fall below 40 ug C gdw^{-1} hr^{-1}, where gdw is the grams dry weight of plant tissue. In the study of Evans et al. (1982), for example, emission of isoprene ranged from 0.01 to 38 ug C gdw^{-1} hr^{-1} for a group of 16 tree species of various physiognomic types. These surveys unfortunately have been limited primarily to plant species of the U.S.

In isoprene emitting plants, temperature and light strongly regulate the rate of emissions (Tingey et al. 1979). Emissions typically increase exponentially with temperature (Monson and Fall 1989) and are directly coupled to the light regime, and hence most likely to photosynthesis (Monson and Fall 1989). Unlike the monoterpenes which accumulate in glands and are emiited a rates independent of light intensity, isoprene biosyntheses and thus emissions are quite low in the absence of light.

METHODS

Current Global Isoprene Emissions

The current global isoprene flux was estimated at a spatial resolution of 0.5 latitude by 0.5 longitude and a monthly time step. The general approach was as follows: 1) assign a monthly active foliar biomass (Kg/m^2) to each grid cell based on vegetation type and the satellite derived Global Vegetation Index , 2) reduce that biomass by a vegetation type-specific proportion (%) of non-isoprene emitting biomass, 3) calculate an emission rate based on mean monthly temperature ($ug\ g^{-1}\ hr^{-1}\ m^{-2}$) and 4) multiply by daylight hours in the month (hrs). Total annual global isoprene emissions (in Tg) was computed by multiplying the flux per unit area times the cellular area for each grid cell and summing over the entire terrestrial surface (59,049 grid cells) and over the year.

Annual Emissions = (foliar biomass per grid cell) * (% plant species emitting isoprene per grid cell) * (temperature driven emission rate per grid cell) * (hours of daylight per grid cell).

The assignment of vegetation type to each grid cell was based on the global vegetation database of Olson et al. (1983). Because of limited knowledge about the ranges of foliar biomass and the proportion of isoprene emitters, the 52 vegetation classifications in this database were aggregated into 19 vegetation types as illustrated in Figure 3. The areal extent, maximum foliar biomass and proportion of foliar biomass emitting isoprene for these vegetation types are given in Table 1.

The spatial and temporal patterns in active foliar biomass density (FBD) were estimated using the Global Vegetation Index (GVI). The GVI satellite imagery was obtained from The U.S. Army Corps of Engineers Construction Engineering Research Laboratory for the year 1988 at a weekly time step. It originated from the National Oceanic and Atmospheric Association (NOAA) satellite series which carries the Advanced Very High Resolution Radiometer (AVHRR) and generates daily global coverage. The GVI is

essentially the NDVI (Normalized Difference Vegetation Index), a "greenness" index, brought up to a 16 Km spatial resolution and a one week time step by use of a maximum value compositing procedure (Holben and Fraser 1986, Holben 1986). Weekly GVI data were composited using the maximum value proceedure to produce monthly maximums. An example of the GVI surface for the month of July, 1988 is displayed in Figure 4.

NDVI and GVI imagery have considerable value for monitoring the seasonal and annual variability of vegetation at the global scale, (Goward et al. 1985, Townshend and Justice 1986, Tucker et al. 1986, Goward 1989), as illustrated in Figure 5. NDVI and GVI have been correlated with vegetation properties that include leaf area index, primary production, and annual evapotranspiration (Asrar et al. 1984, Sellers 1985, and Tucker and Sellers, 1986, Box et al. 1989). Nevertheless there are definite limitations in its use, including its sensitivity to factors such as topography, atmospheric turbidity and illumination angle (Townshend and Justice 1986). These problems will be addressed to some degree by the satellite sensors currently being developed for the EOS Platforms. For the present analysis, NDVI (GVI) was used to estimate the amount of active foliar biomass. The intent was to use available satellite imagery to gain an indication of foliar biomass which was potentially emitting isoprene.

To create an active foliar biomass density (FBD) surface based on GVI, an equation relating the two was developed for each vegetation type. Empirical studies have found GVI to be generally related to the natural logarithm of variables such as leaf area index (Box et al. 1989, Running 1988, Running et al. 1989). This relationship has been expressed in the following form:

$$\text{GVI (or NDVI)} = b * \ln(X/a)$$

where

X = Leaf area index, annual evapotranspiration, or net primary production

a, b = empirically determined constants.

Table 1. Areal extent (Olson et al. 1983), maximum foliar biomass (Box 1981; Cannell 1982), and proportion of biomass emitting isoprene (Rasmussen and Khalil 1988) for the vegetation types.

	Vegetation Type	Area (10^6 Km^2)	Maximum Foliar Biomass Density (Kg/m^2)	Proportion Emitting Isoprene (%)
1	Ice	1.24	0	0
2	Desert	18.36	0.09	25
3	Tundra	11.68	0.10	20
4	South Temperate Broad-Leaved Forest	0.71	0.40	50
5	Grassland	21.31	0.50	10
6	Farms and Towns	12.21	0.50	10
7	Non-Paddy Irrigated Dryland	1.57	0.50	10
8	Forest/Field/Woods	9.19	0.50	30
9	North Temperate Broad-Leaved Forest	0.78	0.35	50
10	Cool Conifer & Hardwood	3.54	0.64	40
11	Tropical Montane	1.17	0.75	30
12	Wetlands, Shore & Hinter-Lands	3.15	0.80	25
13	Woodlands	19.87	0.80	30
14	Warm Conifer	0.40	0.89	40
15	Paddyland	1.94	1.00	10
16	Taiga	11.50	1.00	60
17	Tropical Seasonal Humid Forest	6.12	1.05	50
18	Tropical/Subtropical Humid Forest	4.22	1.05	50
19	Cool Conifer	3.09	1.46	60
	TOTAL:	132.05		

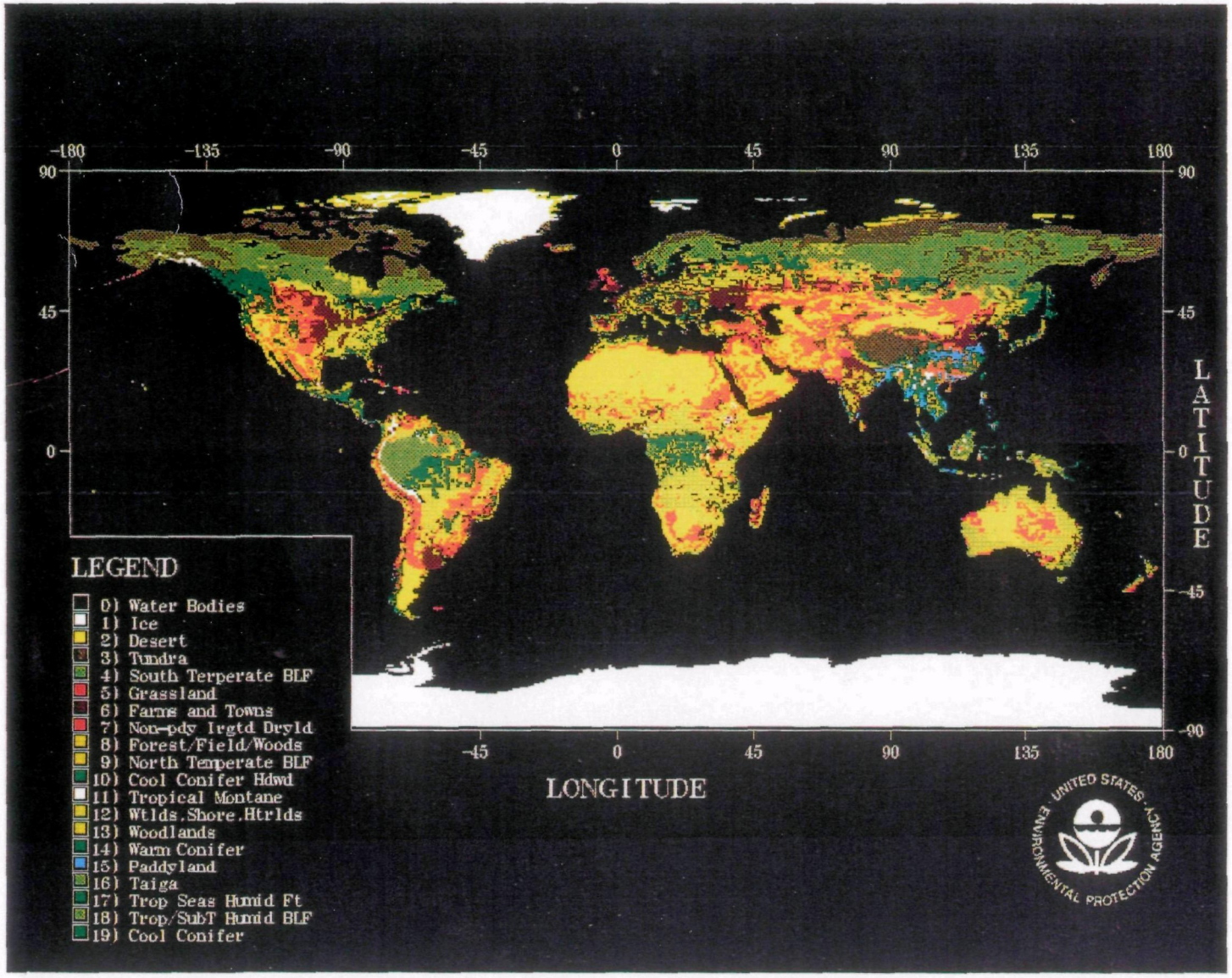

Figure 3. Global Vegetation Distribution (after Olson et al. 1983).

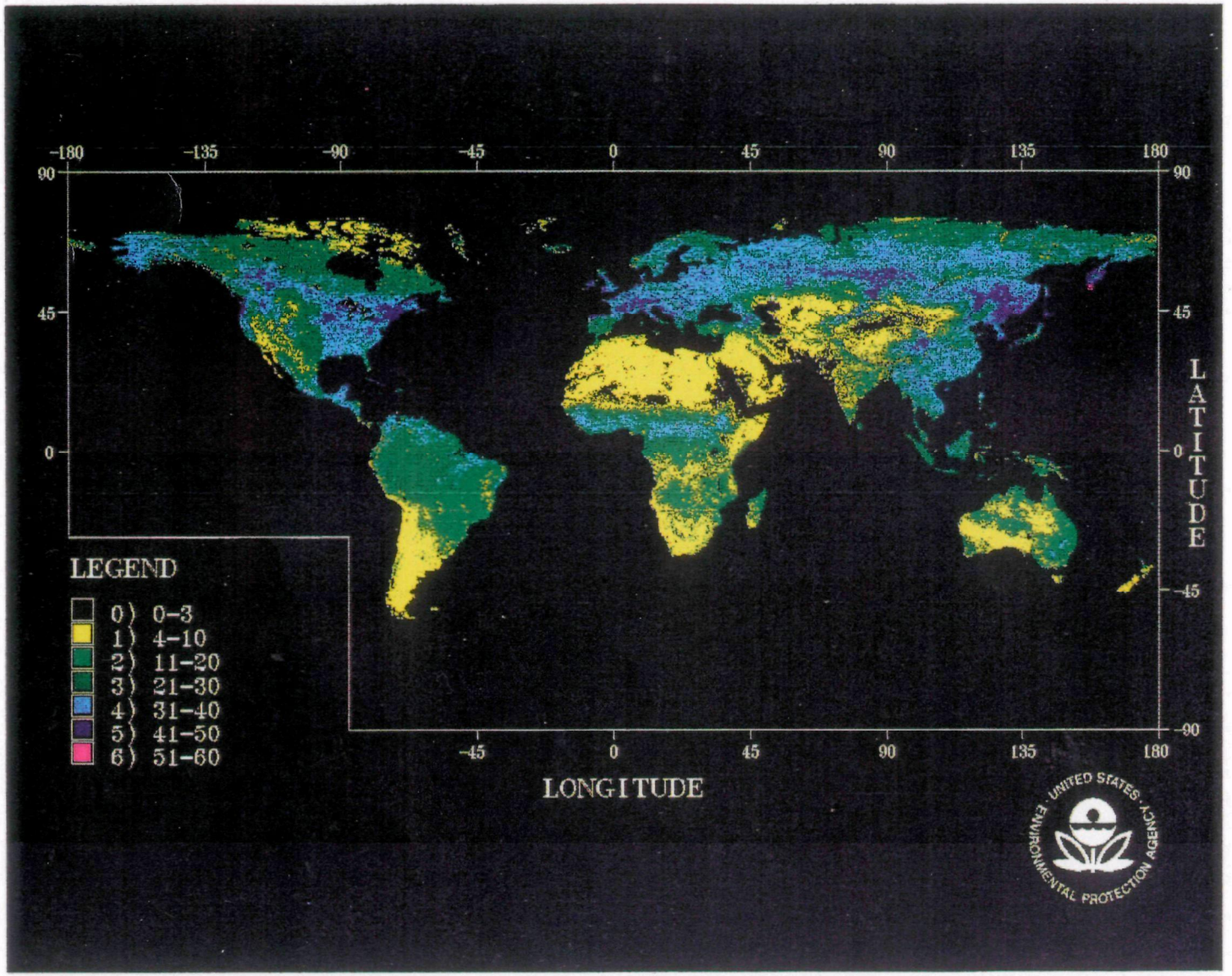

Figure 4. Maximum-value composite of Global Vegetation Index (GVI) data for July, 1988.

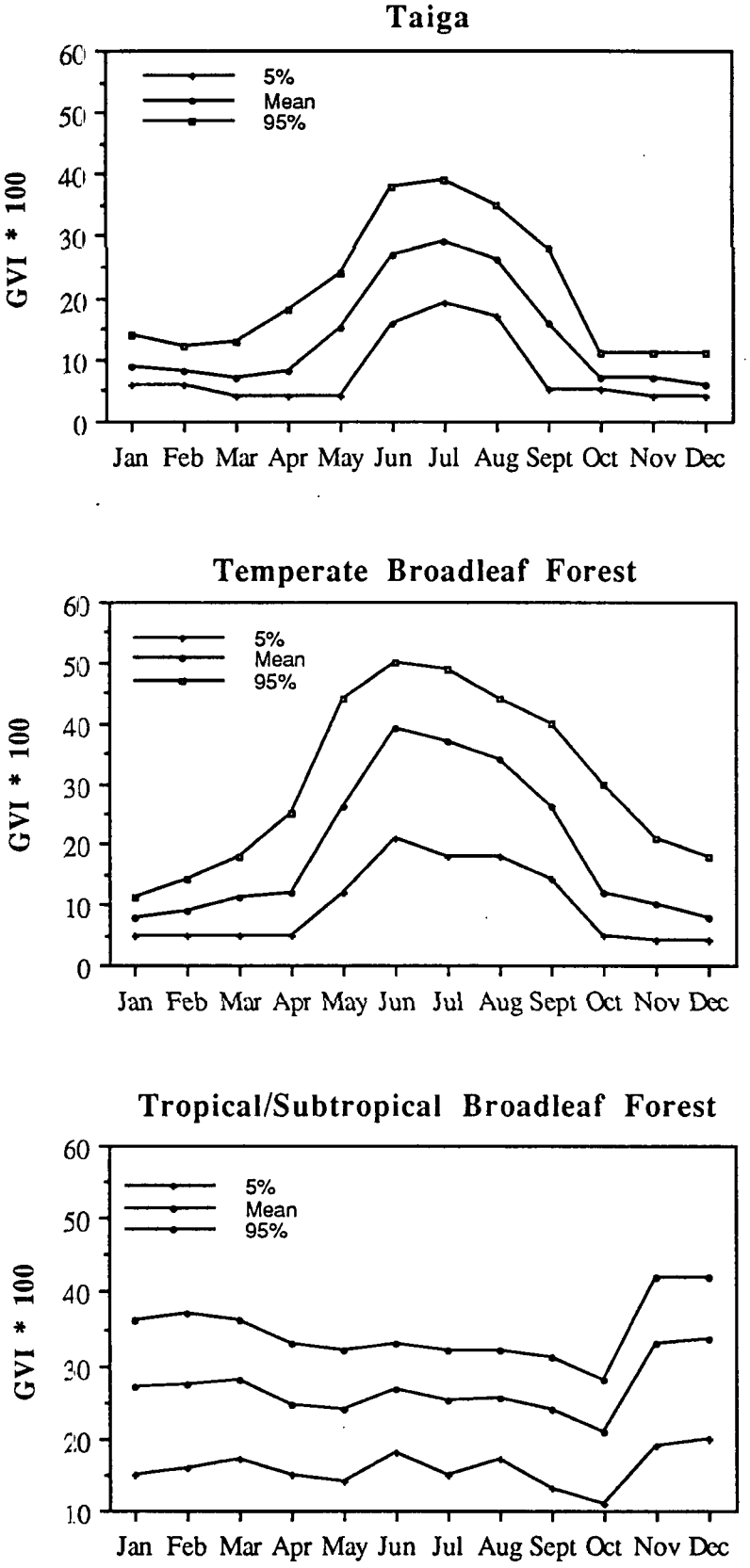

Figure 5. Annual time series of Global Vegetation Index for three vegetation types. All the GVI values of 0 (unreliable data) were deleted. The values are otherwise area weighted. These graphs display the mean, 5th, and 95th percentile values by month for the year 1988. They represent only the northern hemisphere portion of these biomes.

To estimate FBD from GVI, we inverted this relationship and scaled the observed range of GVI to literature values for the range of FBD within each vegetation type. The resulting model for the relationship of GVI to FBD mimics results of the earlier empirical studies in that foliar biomass change is most sensitive to GVI at the higher GVI values. The equation relating GVI and FBD was of the form:

$$FBD = a * e^{(GVI / b)}$$

where

FBD = foliar biomass density

$b = G_{max} - G_{min} / \ln(F_{max} / F_{min})$

$a = F_{max} \exp(-G_{max} / b)$

G_{max} = 95 percentile of GVI values per vegetation type

G_{min} = 5 percentile of GVI values per vegetation type

F_{max} = FBD maximum per vegetation type

F_{min} = FBD minimum per vegetation type

FBD maximums were taken from Box (1981), Cannell (1982), and Whittaker (1975). Literature values also indicated a range of foliar biomass of about an order of magnitude within a vegetation type, so F_{min} was set an order of magnitude lower than F_{max}. G_{max} and G_{min} for each vegetation type by month were determined from annual time series of mean monthly GVI values (as shown in Figure 5). For GVI that are greater than the value of the 95 percentile, FBD is set to a constant value in order to eliminate anomalous occurrences of exceedingly high GVI that would convert to exaggerated FBD. This upper FBD limit was specific for each vegetation type. Figure 6 presents an example of the FBD model used for cool conifer forests.

The global FBD surface for the month of July is displayed in Figure 7. Using the FBD for July in the northern hemisphere and January in the southern hemisphere, total active foliar biomass using this approach was 60 Pg. This estimate compares well to a published estimate of 75 Pg (Box 1981).

The percentage of isoprene emitting plants from particular vegetation types was adapted from Rasmussen and Khalil (1988). Their values were based on surveys of species-specific isoprene emission rates. A number of such surveys have been published (Zimmerman 1979, Evans et al. 1982, Cronn et al. 1982, Winer 1989).

Several equations have been developed that relate the rates of vegetation isoprene emission to air temperature (Tingey et al. 1979, Lamb et al. 1985). These are based on laboratory chamber studies where temperature is regulated, or field enclosure studies where temperature is monitored. Comparisons of field emission rates based on enclosure and non-enclosure techniques reveal reasonable agreement (Lamb et al. 1986). Lamb et al. (1987) compiled existing data across a broad range of plant types and temperatures and found the best fit correlation to be the following exponential relationship:

$$\log (\text{Rate}) = -0.109 + 0.0416 * T$$

where

Rate = isoprene emission rate (ug/g/hr)
T = ambient temperature in C

Foliar Biomass versus GVI

Cool Conifer

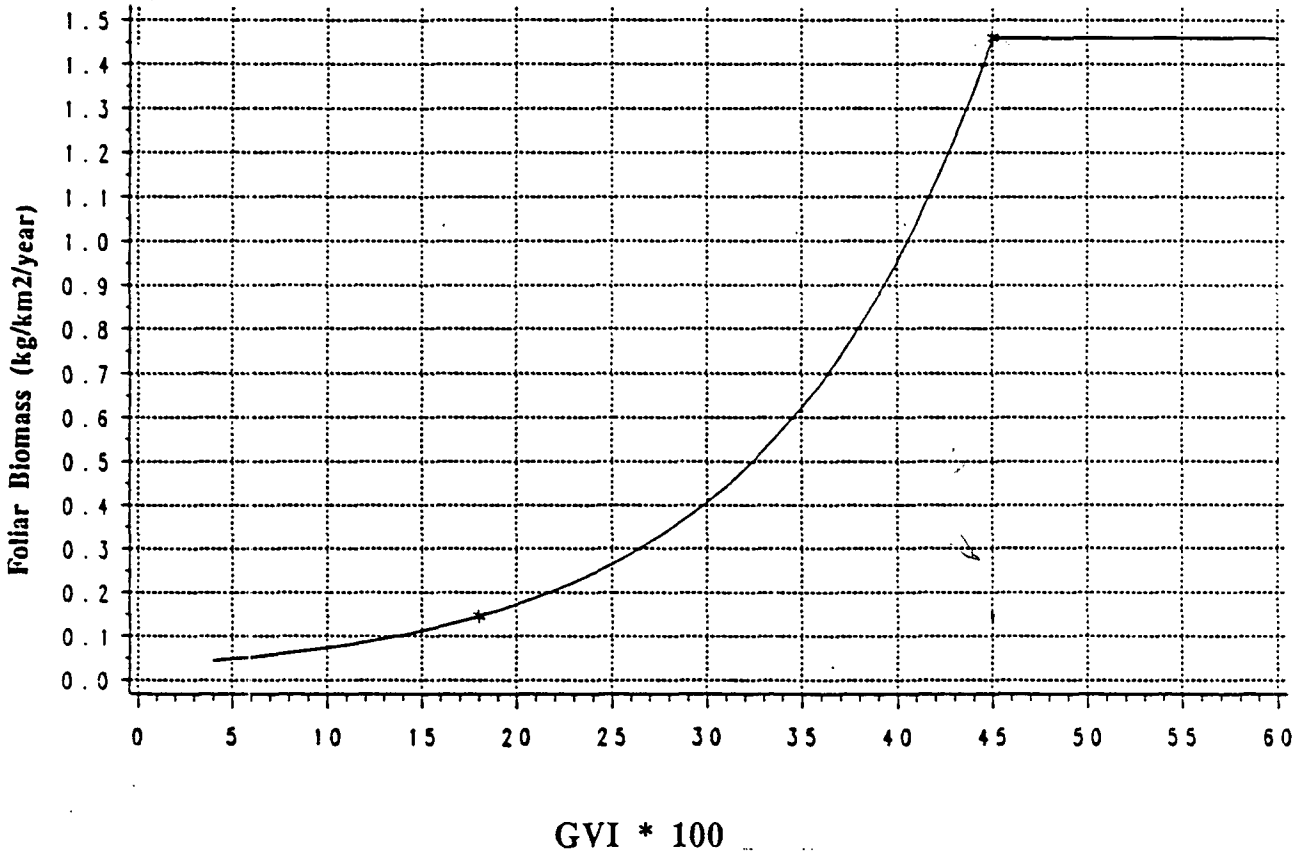

Figure 6. A graphical example of the model used to estimate foliar biomass density based on observed Global Vegetation Index values. The above case is for the cool conifer vegetation type. The 5th and 95th percentiles of GVI values are indicated by stars.

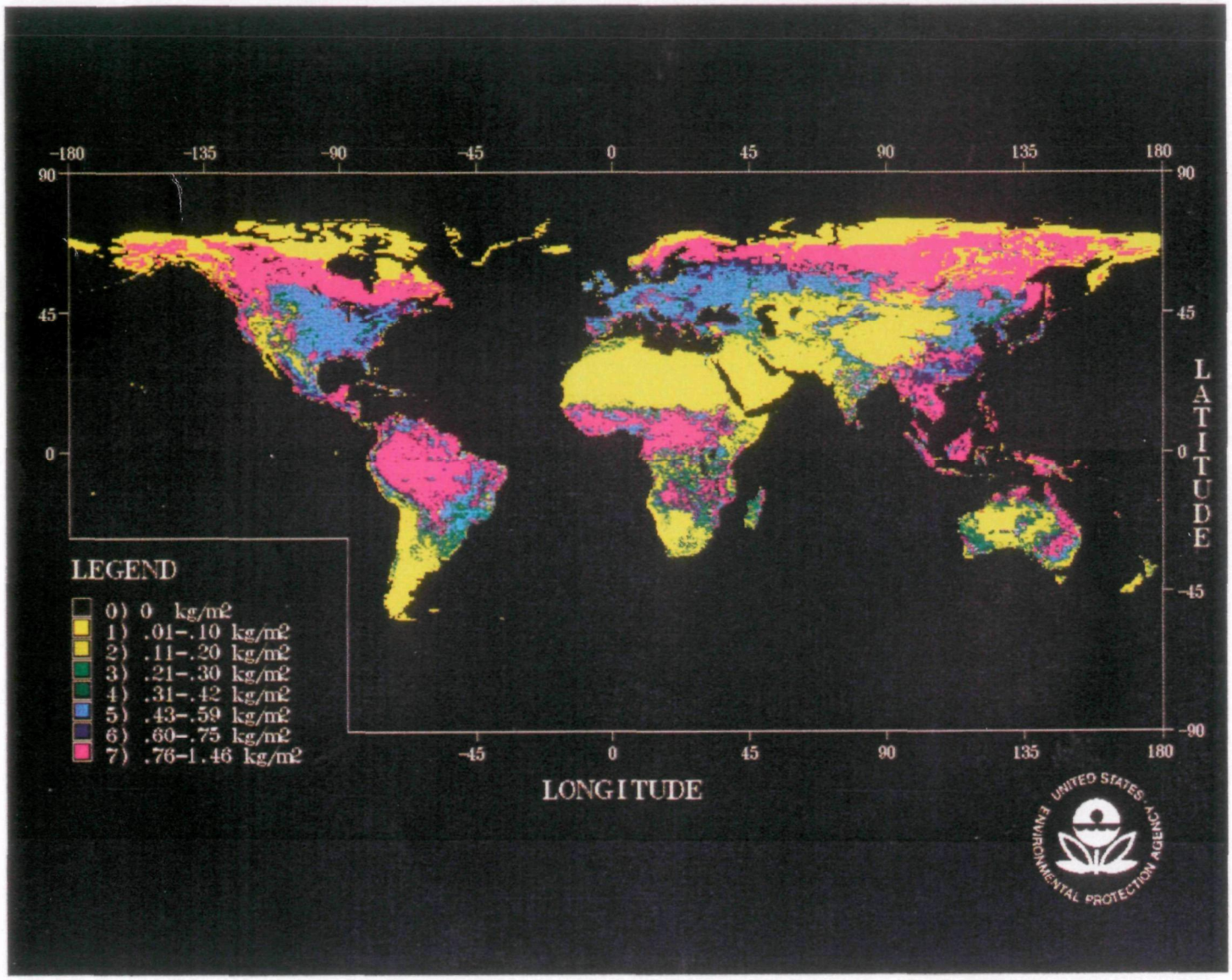

Figure 7. Global distribution of estimated active foliar biomass for July, 1988.

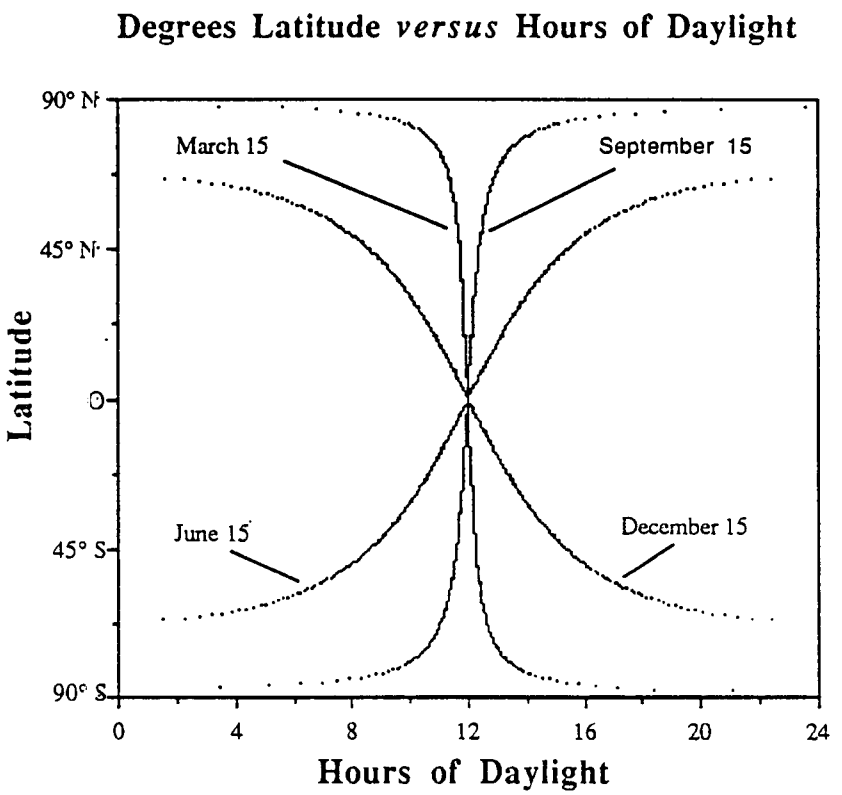

Figure 8. Hours of daylight at 0.5° latitude increments. Light curves shown for the 15th day of four months.

For the present study we have used this relationship across all vegetation types and at a monthly time step. A global air temperature data base developed by Legates and Willmott (1990) was used for mean monthly temperatures. The data base is comprised of mean monthly air temperatures for each 0.5 by 0.5 cell covering the globe. Legates and Willmott (1990) interpolated the land surface air temperatures into each cell based on data collected from 17,986 terrestrial air temperature stations. The photoperiod during each monthly time step (Figure 8) was computed using spherical-geometric equations and parameters as presented in Sellers (1985).

Isoprene Emissions Under A Doubled CO_2 Climate

An equilibrium approach, described previously (Turner 1990, King 1990), was used to estimate future isoprene emissions. Area weighted mean emissions values were assigned to current vegetation types and potential changes in the areal extent of those types were determined based on General Circulation Models (GCMs) and current vegetation-climate correlations. The Holdridge climate-vegetation correlation system and its application to prediction of vegetation redistribution is discussed in King (1990). Vegetation-specific emission factors for the Holdridge types were determined by overlaying the current distribution of the aggregated Holdridge vegetation types (Table 2, Figure 9) on the current annual emissions surface. All areas within each aggregated Holdridge vegetation type were used to calculate an area weighted mean emission. These means were then multiplied by the areal extent of the associated vegetation type under doubled CO_2 climate scenarios (Table 3, Figure 10) as determined by Leemans (1990). The four GCMs were those of Oregon State University, Goddard Institute for Space Studies, Geophysical Fluid Dynamics Laboratory and United Kingdom Meteorological Office.

Table 2 Aggregation Scheme for Combining Holdridge Life Zones into Biomes.

Biome		Holdridge Zone
1	Tundra	Ice Polar Desert Subpolar Dry Tundra Subpolar Moist Tundra Subpolar Wet Tundra Subpolar Rain Tundra
2	Cold Parklands	Boreal Desert
3	Forest Tundra	Boreal Dry Scrub
4	Boreal Forest	Boreal Moist Forest Boreal Wet Forest Boreal Rain Forest
5	Cool Desert	Cool Temperate Desert Cool Temperate Desert Scrub
6	Steppe	Cool Temperate Steppe
7	Temperate Forest	Cool Temperate Moist Forest Cool Temperate Wet Forest Cool Temperate Rain Forest
8	Hot Desert	Warm Temperate Desert Warm Temperate Desert Scrub Subtropical Desert Subtropical Desert Scrub Tropical Desert Tropical Desert Scrub
9	Chapparal	Warm Temperate Thorn Steppe
10	Warm Temperate Forest	Warm Temperate Dry Forest Warm Temperate Moist Forest Warm Temperate Wet Forest Warm Temperate Rain Forest
11	Tropical Semi-Arid	Subtropical Thorn Woodland Tropical Thorn Woodland Tropical Very Dry Forest
12	Tropical Dry Forest	Subtropical Dry Forest Tropical Dry Forest
13	Tropical Seasonal Forest	Subtropical Moist Forest Tropical Moist Forest
14	Tropical Rain Forest	Subtropical Wet Forest Subtropical Rain Forest Tropical Wet Forest Tropical Rain Forest

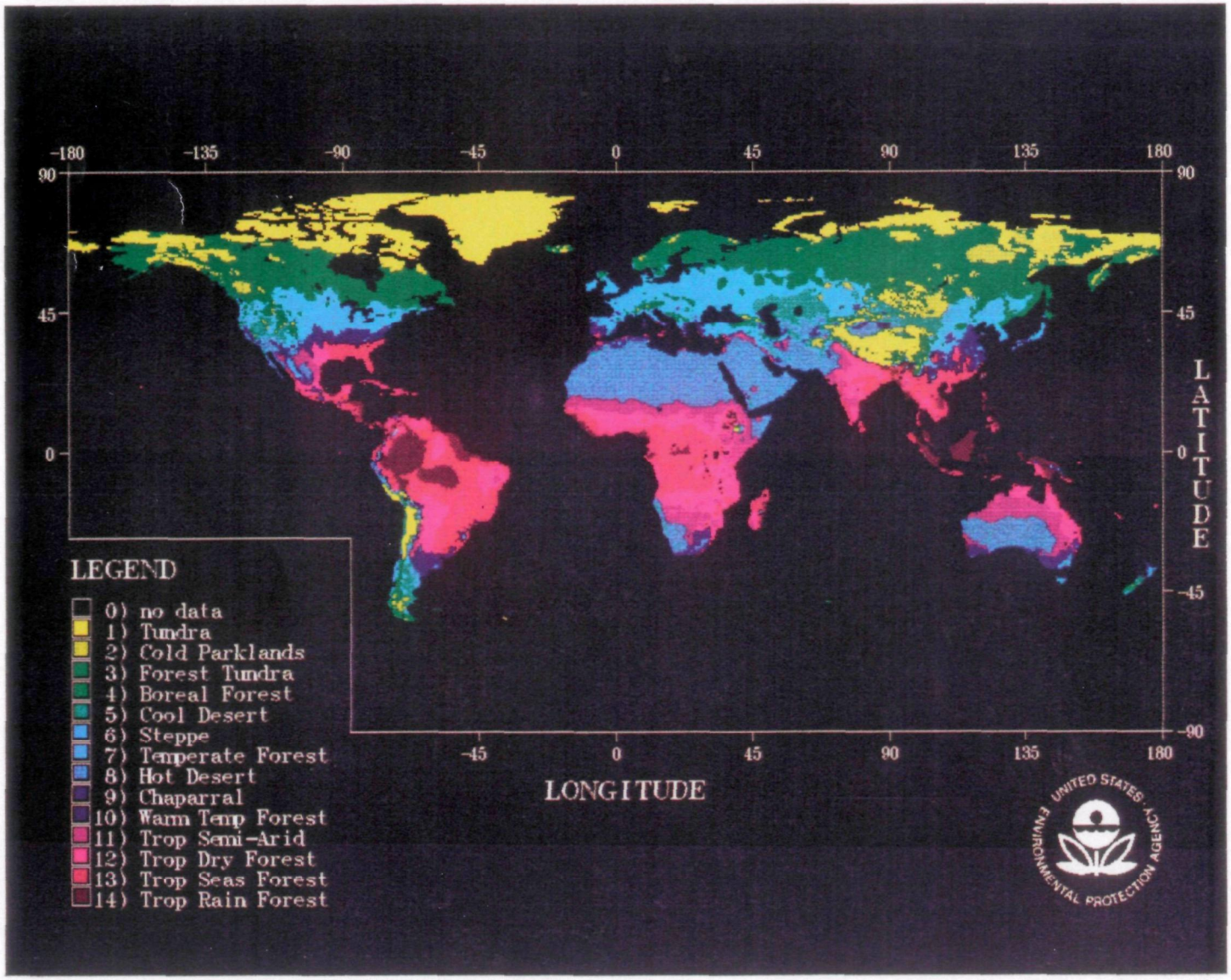

Figure 9. Global distribution of modified Holdridge vegetation types for current climatic conditions (adapted from Leemans, 1990).

Table 3. Annual Isoprene Flux by Different Vegetation Types. Values Are Area-Weighted Means Rounded to the Nearest 100 Kg/Km²/yr.

	Vegetation Type	Isoprene Flux Mean (Kg/Km²/yr)	Isoprene Flux Standard Deviation (Kg/Km²/yr)	Total Emissions (Tg/Yr)
1	Ice	0	0	0
2	Desert	500	300	10.07
3	Tundra	100	100	0.97
4	South Temperate Broad-Leaved Forest	2,000	1,100	1.40
5	Grassland	900	700	19.64
6	Farms and Towns	1,000	600	12.32
7	Non-Paddy Irrigated Dryland	900	600	1.47
8	Forest/Field/Woods	4,300	3,200	39.67
9	North Temperate Broad-Leaved Forest	2,200	900	1.74
10	Cool Conifer & Hardwood	4,200	2,900	14.88
11	Tropical Montane	7,700	3,400	9.06
12	Wetlands, Shore & Hinter-Lands	5,300	4,800	16.84
13	Woodlands	7,700	3,300	153.87
14	Warm Conifer	7,800	4,200	3.13
15	Paddyland	3,600	1,600	7.04
16	Taiga	3,100	800	35.45
17	Tropical Seasonal Humid Forest	19,400	5,200	118.77
18	Tropical/Subtropical Humid Forest	21,500	5,500	90.87
19	Cool Conifer	7,000	2,500	21.53

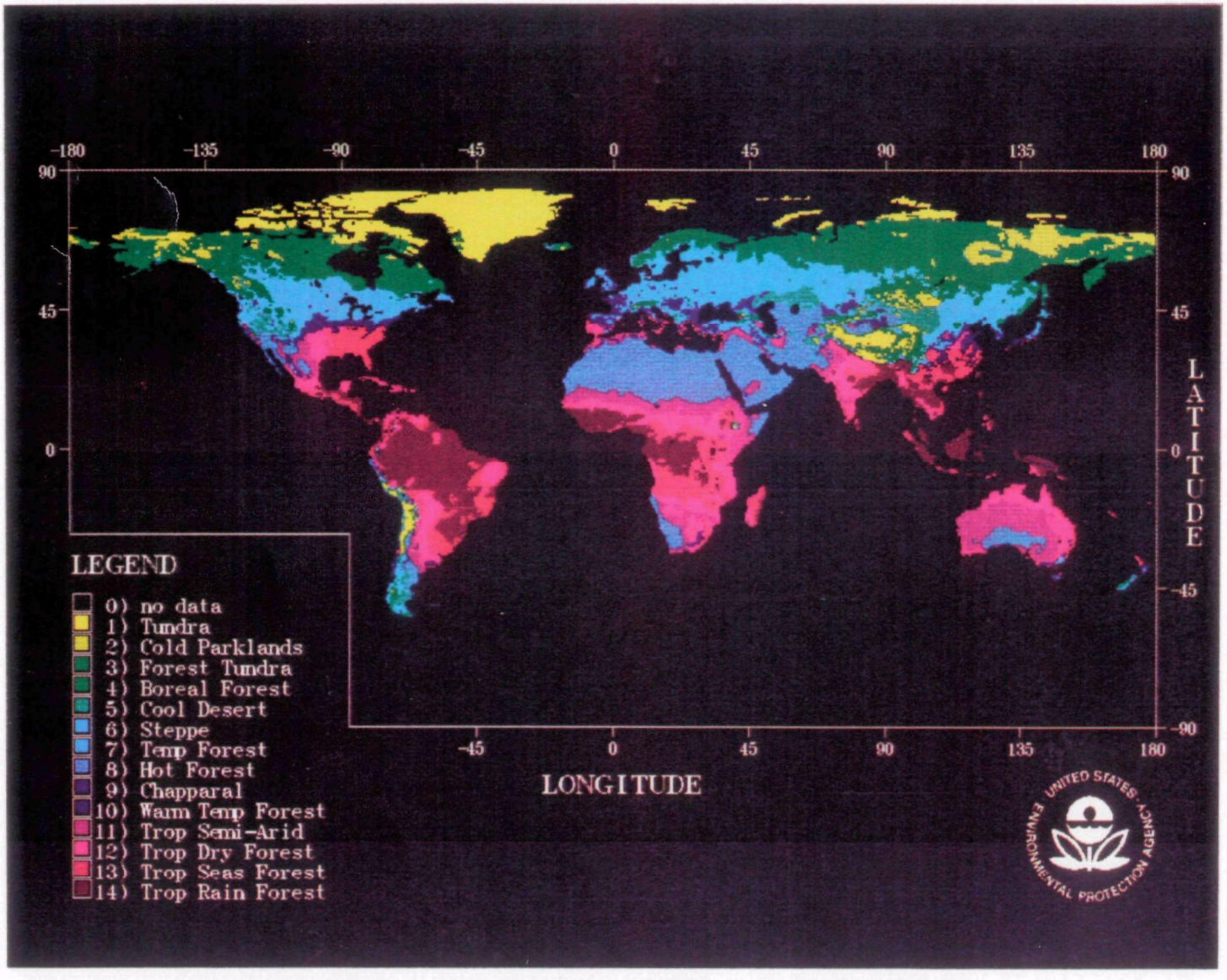

Figure 10. Global distribution of modified Holdridge vegetation types for 2× CO_2 climatic conditions produced by the Oregon State University GCM (adapted from Leemans, 1990).

RESULTS

Annual isoprene emissions by vegetation type are listed in Table 4. On a per unit land area basis, emissions are highest from the equatorial humid forests and lowest in the arctic tundra. There is a general trend towards increasing emissions with increasing foliar biomass and mean annual temperature. The standard deviation is a larger proportion of the mean for the lower biomass vegetation types, probably reflecting the aggregation of somewhat dissimilar types. The estimated global isoprene emissions for the month of July 1988 is given in Figure 11. Using the methods described above, the global annual isoprene emissions for 1988 was estimated at 560 Tg (Figure 12).

The overlay of spatially distributed Holdridge biomes on the annual total emissions surface (Figure 12) yielded average isoprene fluxes for each biome (column one of Table 4). The mean fluxes for different biomes are roughly consistent with patterns of biomass and temperature, with a range from 300-16,000 kg $km^{-2}y^{-1}$. These means reflect current patterns of land use and foliar biomass.

The change in areal extent of the different Holdridge vegetation types (Table 5) indicates a general trend towards reductions in the area of boreal forests and tropical seasonal forests, and increases in tropical rain forests and temperate forests (Leemans 1990; King et al. 1990, Leemans and Prentice 1990). The global isoprene emission totals (Table 4) for the vegetation distributions as predicted by the different GCMs were quite similar, ranging from 670-710 Tg. Because of the relatively high annual emissions from tropical forests, the increase in their area tends to account for most of the predicted increase in emissions.

Table 4. Annual Isoprene Emission (Tg) from Holdridge Life Zones for Current and Doubled CO_2 GCM Scenarios.

Smith & Leemans Aggregated Holdridge Life Zones	Average* (Kg/Km²/yr)	Current	GFDL	GISS	OSU	UKMO
1 Tundra	297	2.77	0.95	1.27	1.42	0.86
2 Cold Parklands	1373	3.83	3.89	3.27	3.69	2.35
3 Forest Tundra	1446	12.87	5.61	8.49	8.68	4.90
4 Boreal Forest	2807	42.20	26.90	37.88	39.70	28.58
5 Cool Desert	546	2.19	1.66	1.29	1.74	1.14
6 Steppe	100	7.41	11.63	6.96	8.72	7.20
7 Temperate Forest	2245	22.32	26.63	30.15	25.96	29.14
8 Hot Desert	984	20.52	20.33	17.35	19.12	19.63
9 Chaparral	1898	10.60	14.07	10.33	9.29	16.27
10 Warm Temperate Forest	4128	13.09	8.09	7.88	10.11	11.89
11 Tropical Semi-Arid	4197	40.13	58.72	70.26	50.95	69.80
12 Tropical Dry Forest	7519	111.75	147.17	145.51	111.75	195.90
13 Tropical Seasonal Forest	9859	149.08	98.73	77.74	100.01	75.38
14 Tropical Rain Forest	15823	133.87	243.85	273.91	316.95	203.50
TOTAL		572	668	692	708	666

*Average isoprene flux for individual life zones.

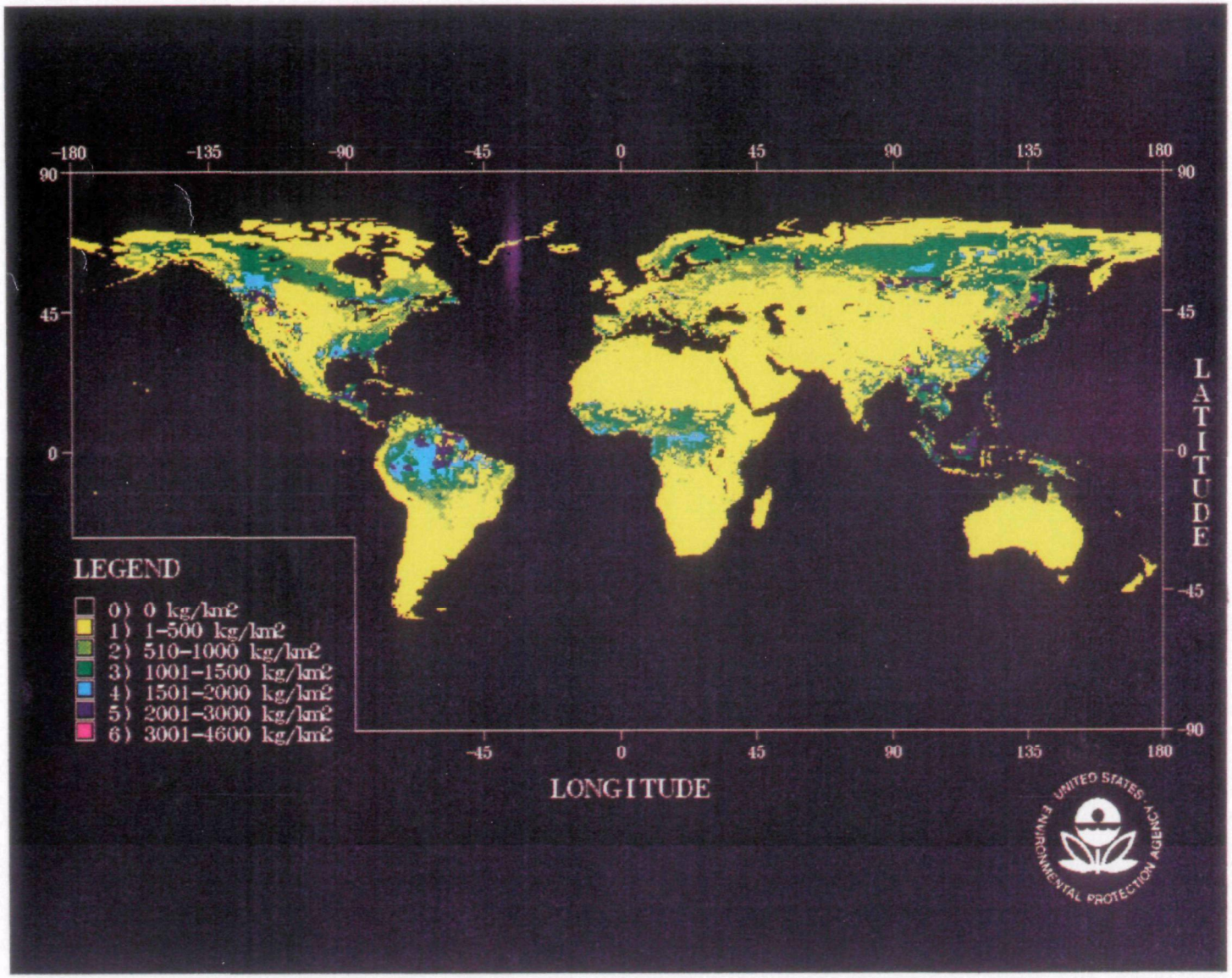

Figure 11. Global distribution of isoprene emissions for July, 1988.

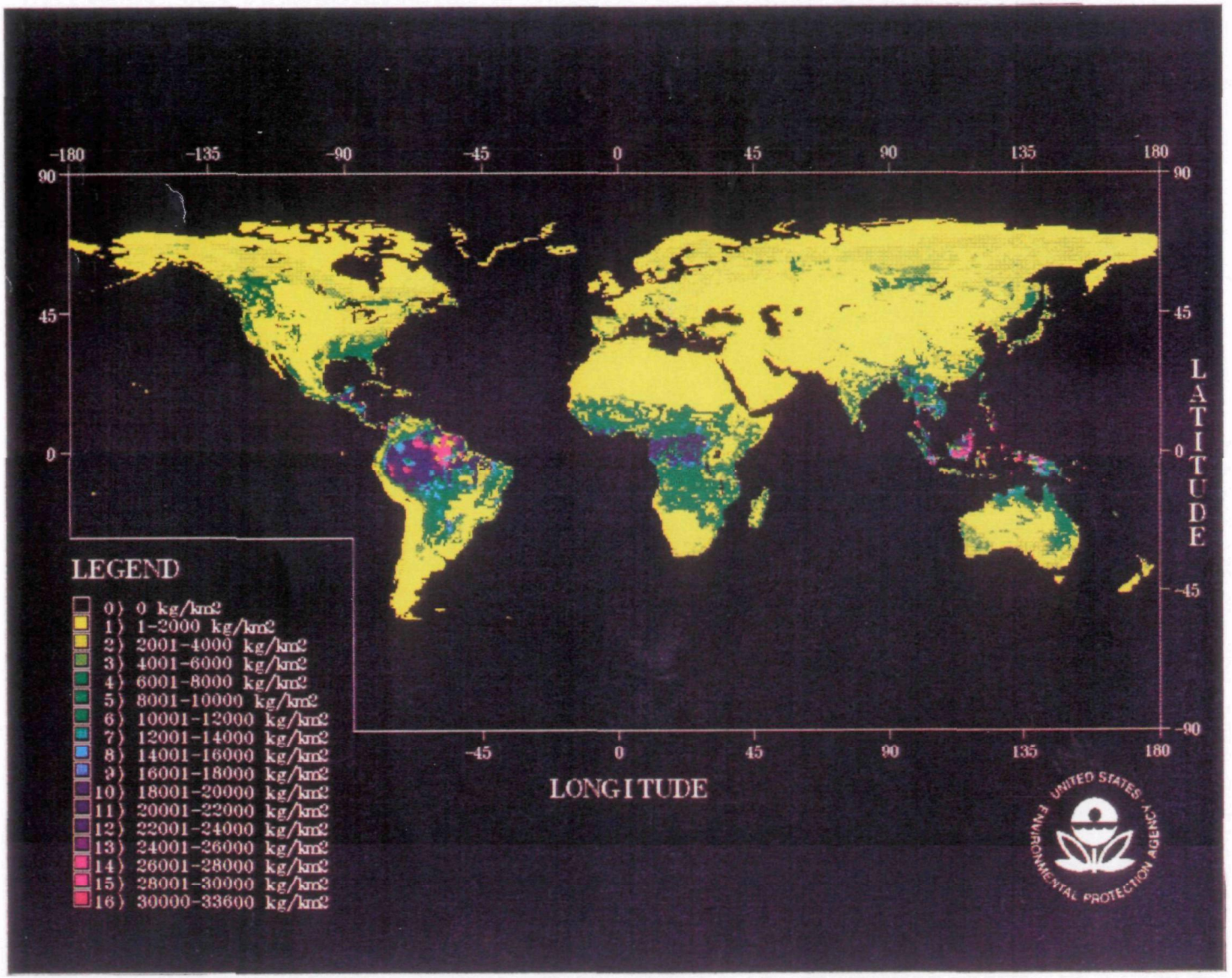

Figure 12. Global distribution of total annual isoprene emissions for 1988. Total emission summed over the globe equalled 560 Tg.

Table 5 Changes in Areal Extent of Different Vegetation Types as Predicted by 4 GCMs.

Biome		Area (10^6 Km^2)	Difference in Biome Area (10^6 Km^2) GFDL	GISS	OSU	UKMO
1	Tundra	9.30	-6.11	-5.05	-4.56	-6.43
2	Cold Parklands	2.79	0.03	-0.41	-0.10	-1.09
3	Forest Tundra	8.90	-5.02	-3.03	-2.90	-5.50
4	Boreal Forest	15.03	-5.45	-1.54	-0.89	-4.85
5	Cool Desert	4.01	-0.97	-1.67	-0.82	-1.93
6	Steppe	7.39	4.20	-0.46	1.30	-0.21
7	Temperate Forest	9.94	1.92	3.49	1.63	3.04
8	Hot Desert	20.85	-0.20	-3.22	-1.42	-0.92
9	Chaparral	5.58	1.83	-0.13	-0.69	2.99
10	Warm Temperate Forest	3.17	-1.22	-1.25	-0.72	-0.29
11	Tropical Semi-Arid	9.56	4.43	7.18	2.58	7.07
12	Tropical Dry Forest	14.86	4.71	4.49	-0.00	11.19
13	Tropical Seasonal Forest	15.13	-5.11	-7.24	-4.98	-7.48
14	Tropical Rain Forest	8.46	6.95	8.85	11.57	4.40
	Total:	134.97 x 10^6 Km^2				

DISCUSSION —

Uncertainty Analysis

The largest uncertainties in this analysis lie in the estimation of active foliar biomass, the use of a mean monthly temperature rather than a diurnal temperature cycle, the application of the same temperature/emissions relationship to all emitting vegetation, and the estimation of the vegetation-specific proportion of foliar biomass which emits isoprene.

The approach in this paper insures that foliar biomass is not overestimated in comparison with literature values. However, it is just a first step in getting away from assigning a constant foliar biomass to a given vegetation type. Continued research linking remote sensing to vegetation characteristics is needed. Specific uncertainties include the shape of the curve relating GVI to FBD, which may not be the same for all vegetation types and the same at all times of the year. In addition, active foliar biomass would tend to be overestimated using the approach described here in that the scheme by which GVI is assigned to each pixel selects for the greenest (highest NDVI) 1 Km^2 pixel within a 16 x 16 Km square. Thus spatial heterogeneity at scales less than 16 x 16 Km is not accounted for. Higher resolution NDVI data sets are available and an important sensitivity analysis to be conducted in the near future will be to compare results for limited areas using a 1 Km^2 spatial resolution and the results using GVI.

The use of mean monthly temperatures instead of hourly temperatures to drive emission rates is likely to produce fluxes which are artificially low. Since the relationship of emissions to temperature is exponential, a model using an hourly time step and a diurnal temperature cycle, which had the mid-day high temperatures, would result in higher predicted emissions. We have recently obtained a global database with daily temperature ranges and that will allow us to more fully evaluate the impact of this factor on regional and global emissions estimates.

Because cloudiness is not accounted for, the light regime used in this model will tend to produce an overestimate of emissions. This factor is balanced to some extent by not attempting to correct for low GVIs due to cloudiness. Estimates of cloud cover for specific sites, and globally, are available and may be used to evaluate the sensitivity of the emissions estimates to this factor.

There is no obvious direction which the use of the same relationship between temperature and emissions for all vegetation types would tend to drive emission estimates. Studies are in progress to extend the range of observations to a greater number of species. If there are clear patterns with respect to vegetation types we will develop separate curves for each vegetation type. The uncertainty relative to the proportion of biomass emitting isoprene in each vegetation type is bounded by the range from 10 - 60 %. In general, the limited number of field and laboratory measurements on which the vegetation factors in this model are based, highlights the need for extensive and intensive measurement programs.

There are of course large uncertainties in current estimates of the magnitude of climate change to be expected under doubled-CO_2 conditions. These uncertainties relate to oceanic factors and to feedbacks involving water vapor, clouds, sea ice, and the biosphere. There are likewise large uncertainties in using vegetation-climate correlations approaches to predicting the distribution of vegetation types (King 1990). In both cases research is progressing on a broad front to reduce uncertainties. In the meantime, sufficient progress has been made to begin making the type of analysis described in this paper.

Comparisons to Other Estimates

The estimate for global annual isoprene emission using the present model was 560 Tg, expressed as carbon. This estimate compares with earlier estimates of 350 Tg (Zimmerman et al. 1978) and 450 Tg (Rasmussen and Khalil 1988). Zimmerman et al. (1978) based their estimate on a fixed ratio between isoprene production and net primary productivity (0.7%) and a global net primary productivity of 118 Gt yr^{-1}. Rasmussen and Khalil (1988) broke out the land surface by vegetation type, then used literature values for

foliar leaf surface area, reduced that by their estimate of the proportion of non-isoprene emitters, estimated annual hours of daylight during the growing season, and predicted emissions by applying a universal emission factor (648 g km^{-2} of leaf area hr^{-1}). At a continental scale, our estimates are also generally greater than those of earlier investigators for the U.S. (Zimmerman 1979b, Lamb et al. 1987) but lower than an estimate made by Ayers and Gillett (1988) for tropical Australia (16 Tg vs 25 Tg).

Others have estimated hydrocarbon emissions by using atmospheric chemistry models to calculate how large a CO source would be needed to balance the global CO budget. Crutzen and Gidel (1983) estimated a CO source on the order of 1400 Tg (as carbon) which was thought to originate largely from vegetation NMHCs. Similarly derived estimates ranged from 560 - 1250 Tg in the study of Logan et al. (1981). Assuming that the CO yield of isoprene oxidation is two CO molecules per isoprene molecule (Logan et al. 1981) and about half of the global NMHC-CO is from isoprene oxidation (Zimmerman et al. 1978), then the associated isoprene source expressed in terms of carbon mass would be 700 - 1750 Tg. Hanst et al. (1980) and Zimmerman et al. (1978) have suggested higher CO yields for isoprene oxidation. If the yield is actually more on the order of four CO per isoprene, then the derived source would range from 350 - 875 Tg. The 560 Tg estimate from our model falls between an apparent lower bound based on extrapolating from enclosure studies and an upper bound based on balancing the global CO budget.

Only a few estimates of isoprene emissions have been made on local scales using atmospheric concentrations rather than extrapolation from enclosure studies. Zimmerman et al. (1988) estimated the isoprene flux from a "tropical forest" based on changes in concentration in the boundary layer under a capping inversion over a diurnal time frame. His estimate was 25 mg m^{-2} d^{-1} during July. The equivalent estimate using an emissions model coupled to a photochemical model was 38 mg m^{-2} d^{-1} (Jacob and Wofsy 1987). Our July estimates for tropical forests ranged from means of 45 to 54 mg m^{-2} d^{-1}. As more measurements of ambient concentrations are made there will be increased opportunity for calibration and validation of this emissions model.

Perhaps as important as getting another estimate of total annual emissions, the present model provides the spatial and temporal patterns in global isoprene emissions at a reasonably high spatial resolution. The value of this information is in revealing areas where more intensive study is needed and providing the basis for hypotheses that can be tested via field measurements. These emission surfaces can also be used in globally distributed atmospheric chemistry models to begin evaluating the role of biogenic hydrocarbon emissions in local and global tropospheric chemistry.

Doubled-CO_2 Climate Emissions

The 150 Tg increase in annual isoprene emissions that is predicted for the doubled-CO_2 climate scenarios represents an increase in annual emissions of about 25%. To a great degree that increase is concentrated at tropical latitudes. It seems likely that total nonmethane hydrocarbons (TNMHC) will also increase because of the similar relationship of emissions to vegetation type. If they increased at a rate similar to isoprene alone, TNMHC emissions could rise by 400 or more Tg, using the mid range values of Logan et al. (1985) for current emissions. Back calculating to CO produced, as in the analyses above, the total increased CO source due to NMHC could be over 200 Tg.

The potential impact on the climate system of increased NMHC emissions is difficult to assess. The added CO might not be large relative to the global CO budget, but it will probably be accompanied by increased CO from other sources and contribute to a downward trend in on OH concentration (Crutzen 1988) and increased atmospheric lifetime of some greenhouse gases. Possible compensatory factors include increases in concentrations of water vapor and ozone which would favor OH production. However, there is great uncertainty about the interrelationships between these various factors (Thompson et al. 1989, Thompson et al. 1990, Lelieveld and Crutzen 1990).

As noted previously, photochemical production of ozone is largely controlled by the availability of NO_x. Results of the GTE-ABLE (Global Tropospheric Experiment-Atmospheric Boundary Layer Experiment) studies in the Amazon Basin suggested that the

strength of the isoprene flux has little local influence on ozone production because of high background levels of CO and isoprene (Jacob and Wofsy, 1987). Limited NO_x apparently restricts the rate of ozone formation such that local ozone levels rise to only about 20 ppm during the day. Thus, a greater areal extent of tropical forest would probably not produce substantial increases in ozone formation unless the ambient NO_x levels were to increase.

Not considered here in detail, but of potential importance to the total tropospheric ozone burden and climate, is the transport of NMHC to the free troposphere (that area above the PBL and relatively isolated from the surface, i.e. low deposition rates) by convection, especially in the tropics (Garstang et al. 1988). This convection may be accompanied by lightning, which forms NO_x, leading to potentially significant ozone production in the upper atmosphere above the tropics. Thus the normally low NO_x and short lifetime for isoprene that are expected over the Amazon basin would not apply to the NMHC transported upward via convection. The GTE-ABLE results, discussed above, apply to the dry season when this upward transport is at a minimum. A second GTE-ABLE experiment was to examine wet season fluxes and transport. If coupling between the Amazon biosphere (NMHC flux) and the global troposphere is established, it is likely that the importance of NMHC to tropospheric ozone production, and hence climate feedbacks, will increase. Any additional ozone formation in the free troposphere is very effective in causing an increase in surface temperature (Wuebbles et al. 1989).

Overall, these analyses suggest a positive feedback to climate warming is likely via impacts on biogenic emissions of NMHC. Progress in evaluating the potential change in the oxidation state of the troposphere and the concentrations of greenhouse gases will come in part from improved 3-D atmospheric chemistry models. Specific problem areas include the spatial and temporal pattern in source strengths for reduced species, the kinetics and products of NMHC oxidation, the heterogeneous chemistry of cloud droplets, and patterns in vertical and horizontal transport. Increased coupling of general circulation models, atmospheric chemistry models and ecosystem emissions models will promote rapid advances on these fronts in the coming years.

Transient Increases in NMHC Emissions

The equilibrium approach to estimating isoprene emissions under a doubled-CO2 climate has several obvious limitations (see Turner 1990) including the fact that there may be a significant transient effect. Trees often live hundreds of years, yet climate change will occur on a much shorter time scale. As temperatures rise, climate will gradually drift out of equilibrium with the vegetation. Given the exponential increases in NMHC emissions with increases in temperature, there may be many situations where NMHC emissions rise substantially before the vegetation changes.

An evaluation of this prospect requires process based models which can be run using particular climate scenarios. The Global Change Research Program at ERL-C is currently developing such a model. The Forest BGC model (Running and Couglan 1988), which accounts for hydrology, nutrient cycling and photosynthesis, is being modified to include NMHC emissions. Laboratory and field measurements are now underway to develop response surfaces relative to light and temperature for particular tree species. Ultimately the model will be used for site-specific simulations and will be spatially distributed using remote sensing to initialize variables such as vegetation type and foliar biomass. The prospects of coupling a GCM to an ecosystem model that predicts NMHC emissions are good.

Conclusions

Isoprene emissions have significant effects on atmospheric chemistry and ultimately on climate via their influence on the concentrations of greenhouse gases such as methane and ozone. The global model presented here for isoprene emissions under the current climate indicates that highest emissions occur at low latitudes, particularly in wet tropical forests. Equilibrium analyses of potential vegetation change suggest that emissions under a doubled-CO2 climate may rise by about 25%, based largely on predicted increases in the areal extent of wet tropical forests. Higher levels of isoprene emission are expected to increase concentrations of methane and ozone but 3-D atmospheric chemistry models are needed to

evaluate these effects. Future studies incorporating transient responses and impacts of land use practices are needed to refine these equilibrium analyses.

Acknowledgements

Special thanks to Tom Smith and Rik Leemans for sharing their doubled-CO_2 climate data used here for the vegetation redistribution analysis.

References

ACE. 1988. GRASS Users and Programmers Manual. U.S. Army Corps of Engineers Construction Engineering Research Laboratory, Champaign, Illinois.

Asrar, G., M. Fuchs, E.T. Kanemasu, and J.L. Hatfield. 1984. Estimating absorbed photosynthesis radiation and leaf area index from spectral reflectance in wheat. Agron. J. 76:300.

Ayers, G.P. and R.W. Gillett. 1988. Isoprene Emissions from vegetation and hydrocarbon emissions from brushfires in tropical australia. J. Atmos. Chem. 7:177-190.

Box, E.O., B.N. Holben & V. Kalb. 1989. Accuracy of the AVHRR vegetation index as a predictor of biomass, primary productivity and net CO_2 flux. Vegetation. 80:71-89.

Box, E.O. 1981. Foliar biomass: Data base of the international biological program and other sources. In: J.J. Bufalini and R.R. Arnts, Eds., Atmospheric Biogenic Hydrocarbons, Vol. 1. Ann Arbor Science Publishers, Inc., Ann Arbor, MI.

Cannell, M.G.R., ed. 1982. World Forest Biomass and Primary Production Data. Academic Press, New York, NY.

Cronn, D.R., and Nutmagul, W. 1981. Analysis of atmospheric hydrocarbons during winter MONEX. Tellus 34:159-165.

Crutzen, P.J. 1988. Variability in atmospheric-chemical systems. In: T.Rosswall, R.G. Woodmansee and P.G. Risser, eds. Scales and Global Change. John Wiley & Sons Ltd., New York, NY.

Crutzen, P. J., and L. T. Gidel. 1983. A two-dimensional photochemical model of the atmosphere 2: The tropospheric budgets of the anthropogenic chlorocarbons CO, CH_4,

CH3Cl and the effect of various NO_x sources on tropospheric ozone. J. Geophys. Res. 88:6641-6661.

Delany, A.C., P.J. Crutzen, P. Haagenson, S. Walters, and A.F. Wartburg. 1985. Photochemically produced ozone in the emission from large-scale tropical vegetation fires. J. Geophys. Res. 90:1425-2429.

Dignon, J., and S. Hameed. 1985. A model investigation of the impact of increases in anthropogenic NO_x emissions between 1967 and 1980 on tropospheric ozone. J. Atmos. Chem. 3:491-506.

Evans, R.C., D.T. Tingey, M.L. Gumpertz, and W.F. Burns. 1982. Estimates of isoprene and monoterpene emission rates in plants. Bot. Gaz. 143:304.

Garstang, M., J. Scala, S. Greco, R. Harriss, S. Beck, E. Browell, G. Sachse, G. Gregory, G. Hill, J. Simpson, W.-K. Tao, and A. Torres. 1988. Trace gas exchanges and convective transport over Amazonian rain forest. J. Geophys. Res. 93:1528-1550.

Goward, S.N. 1989. Satellite Bioclimatology. J. Climate 2:710-720.

Goward, S.N., C.J. Tucker, and D.G. Dye. 1985. North American vegetation patterns observed with the NOAA-7 advanced very high resolution radiometer. Vegetation 64:3-14.

Guthrie, P.D. In Press. The CH_4-CO-OH Conundrum: A simple analytic approach. Biogeochemical Cycles.

Hanst, P.L., J.W. Spence and E.O. Edney. 1980. Carbon monoxide production in photooxidation of organic molecules in the air. Atmos. Environ. 14:1077-1088.

Harborne, J.B. 1988. Introduction to Ecological Chemistry. Academic Press, New York.

Holben, B.N. 1986. Characteristics of maximum-value composite images from temporal AVHRR data. Int. J. Remote Sensing 7:1417.

Holben, B.N., and R.S. Fraser. 1984. Red and near-infrared response to off-nadir viewing. Int.J. Remote Sensing 5:145.

Isaksen, I.S.A., ed. 1988. Tropospheric Ozone, Regional and Global Scale Interactions. D.Reidel Publishing Co., Dordrecht, FRG.

Jacob, D.J., and S.C. Wofsy. 1988. Photochemistry of biogenic emissions over the Amazon forest. J. Geophys. Res. 93:1477-1486.

Kavanaugh, M. 1987. Estimates of future CO, N_2O and NO_x emissions from energy combustion. Atmos. Environ. 21:3463-3468.

Khalil, M.A.L., and R.A. Rasmussen. 1990. The global cycle of carbon monoxide: Trends and mass balance. Chemosphere 20:227-242.

Kidwell, K.B. 1984. NOAA polar orbital data user's guide. NOAA National Climate Data Center, Washington, DC.

Kidwell, K.B. 1990. Global Vegetation Index User's guide. NOAA National Climate Data Center, Washington, DC.

King, G.A. 1990. Effects of global climate change on global vegetation. Contained within this document.

Lamb, B., A. Guenther, A. Gay, and H. Westberg. 1987. A national inventory of biogenic hydrocarbon emission. Atmos. Environ. 21:1695-1705.

Lamb, B., H. Westberg, G. Allwine, and T. Quarles. 1985. Biogenic hydrocarbon emissions from deciduous and coniferous trees in the U.S. J. Geophys. Res. 90:2380.

Lamb, B., H. Westberg, and G. Allwine. 1986. Isoprene emission fluxes determined by an atmospheric tracer technique. Atmos. Environ. 20:1-8.

Legates, D.R., and C.J. Willmott. 1990. Mean seasonal and spatial variability in global surface air temperature. Theor. Appli. Climatol. 41:11-21.

Leemans, R. 1990. Possible changes in natural vegetation patterns due to global warming. IIASA WP-90-08, International Institute for Applied Systems Analysis.

Leemans, R. and I.C. Prentice. 1990. Possible changes in natural vegetation patterns using GCM climate scenarios. In preparation.

Lelieveld, J. and P.J. Crutzen. 1990. Influences of cloud photochemical processes on tropospheric ozone. Nature 343:227-233.

Lieth, H., and R.H. Whittaker. 1975. Primary productivity of the biosphere. Springer-Verlag. New York.

Liu, S. C., M. Trainer, F. C. Fehsenfeld, D. D. Parrish, E. J. Williams, D. W. Fahey, G. Hubler, and P. C. Murphy. 1987. Ozone production in the rural troposphere and the implications for regional global ozone distributions. J. Geophysical Research 92:4191-4207.

Logan, J. A. 1983. Nitrogen oxides in the troposphere: global and regional budgets. J. Geophys. Res. 88:10,785-10,807.

Logan, J.A. 1985. Tropospheric ozone: Seasonal behavior, trends and anthropogenic influences. J. Geophys. Res. 90:10463:10482.

Logan, J.A., M.J. Prather, S.C. Wofsy, and M.B. McElroy. 1981. Tropospheric ozone: A global perspective. J. Geophys. Res. 86:7210-7254.

Monson, R. K., and R. Fall. 1989. Isoprene emission from Aspen leaves: Influence of environment and relation to photosynthesis and photorespiration. Plant Physiol. 90:267-274.

NASA. 1988. Earth System Science: A Closer Look. Report of the Earth System Sciences Committee. NASA. 208pp.

NRC. 1984. Global Tropospheric Chemistry: A Plan for Action. National Academy Press, Washington, DC. 194pp.

Olson, J.S., J.A. Watts, and L.J. Allison. 1983. Carbon in live vegetation of major world ecosystems. ORNL-5862. Oak Ridge National Laboratory, Oak Ridge, TN. 180 pp.

Ramanathan V., R.J. Cicerone, H.B. Singh, and J.T. Kiehl. 1985. Trace gas trends and their potential role in climate change. J. Geophys. Res. 90:5547-5566.

Rasmussen, R.A., and M.A.K. Khalil. 1988. Isoprene over the Amazon basin. J. Geophys. Res. 93:1417-1421.

Rasmussen, R.A., and F.W. Went. 1965. Volatile organic material of plant origin in the atmosphere. Proc. Nat. Acad. Sci. 53:215-220.

Running, S.W., and R.R. Nemani. 1988. Relating seasonal patterns of the AVHRR vegetation index to simulated photosynthesis and transpiration of forests in different climates. Remote Sens. Environ. 24:347-367.

Running, S.W., R.R. Nemani, D.L. Peterson, L.E. Band, D.F. Potts, L.L. Pierce, and M.A. Spanner. 1989. Mapping regional forest evapotranspiration and photosynthesis by coupling satellite data with ecosystem simulation. Ecology 70:1090-1101.

Running, S.W., and J.C. Coughlan. 1988. A general model of forest ecosystem processes for regional applications. I.Hydrological balance, canopy gas exchange and primary production processes. Ecol. Mod. 42:125-154.

Sellers, P.J. 1985. Canopy reflectance, photosynthesis and transpiration. Int. J. remote Sensing 6:1335.

Sellers, W.D, 1965. Physical Climatology. University of Chicago Press, Chicago, 272 pp.

Singh, H. B. 1987. Reactive nitrogen in the troposphere. Environ. Sci. Technol. 21:320-327.

Talbot, R.W., M.O. Andreae, T.W. Andreae, and R.C. Harriss. 1988. Regional aerosol chemistry of the Amazon Basin during the dry season. J. Geophys. Res. 93:1499-1508.

Tarpley, J.P., S.R. Schneider, and R.L. Money. 1984. Global vegetation indices from NOAA-7 meteorological satellite. J. Climate appli. Meteorol. 23:491.

Thompson, A.M., and R.J. Cicerone. 1986. Possible perturbations to atmospheric CO, CH_4 and OH. J. Geophys. Res. 91:10853-10864.

Thompson, A.M., R.W. Stewart, M.A. Owens, and J.A. Herwehe. 1989. Sensitivity of tropospheric oxidants to global chemical and climate change. Atmos. Environ. 23:519-532.

Thompson, A.M., M.A. Huntley, and R.W. Stewart. 1990. Perturbations to tropospheric oxidants, 1985-2035. 1. Calculations of ozone and OH in chemically coherent regions. J. Geophys. Res. 95:9829-9844.

Tingey, D.T., M. Manning, L.C. Grothaus, and W.F. Burns. 1979. The influence of light and temperature on isoprene emission rates from live oak. Physiol. Plant. 47:112-118.

Townshend, J.R.G., and C.O. Justice. 1986. Analysis of the dynamics of African vegetation using the normalized difference vegetation index. Int. J. remote Sensing 7:1435.

Trainer, M., E. J. Williams, D. D. Parrish, M. P. Buhr, E. J. Allwine, H. H. Westberg, F. C. Fehsenfeld, and S. C. Liu. 1987. Models and observations of the impact of natural hydrocarbons on rural ozone. Nature 329:705-707.

Tucker, C.J., C.O. Justice, and S.D. Prince. 1986. Monitoring the grasslands of the Sahel 1984-1985. Int.J. Remote Sensing 7:1571.

Tucker, C.J., and P.J. Sellers. 1986. Satellite remote sensing of primary production. Int. J. Remote Sensing 7:1395.

Turner, D.P. 1990. Effects of climate change on carbon storage in terrestrial ecosystems: equilibrium analysis at the global level. (Contained within this Document)

Wardley, N.W. 1984. Vegetation index variability as a function of viewing geometry. Int.J. Remote Sensing. 5:861-870.

Whittaker, R.H. 1975. Communities and Ecosystems, 2nd Edition. MacMillan Publishing Co., New York, NY. 385 pp.

Winer, A.M. 1989. Hydrocarbon Emissions from Vegetation Found in California's Central Valley. Final Report, A732-155, for California Air Resources Board, Sacramento, CA.

Wuebbles, D.J., K.E. Grant, P.S. Connell, and J.E. Penner. 1989. The role of atmospheric chemistry in climate change. J. Air Poll. Control Agency. 39:22-28.

Zimmerman, P., Chatfield, R.B., Fishman, J., Crutzen, P.J. and Hanst, P.L. 1978. Estimates on the production of CO and H2 from the oxidation of hydrocarbon emissions from vegetation. Geophy. Res. Lett. 5:679-682.

Zimmerman, P.R. 1979a. Tampa Bay Area Photochemical Oxidant Study: determination of emission rates of hydrocarbons from indigenous species of vegetation in the Tampa/St. Petersburg, Fl. area. Final Appendix C, February 2, 1979. EPA 904/9-77-028.

Zimmerman, P.R., R.B. Chatfield, J. Fishman, P.J. Crutzen, and P.L. Hanst. 1978. Estimates on the production of CO and H_2 from the oxidation of hydrocarbon emissions from vegetation. Geophys. Res. Lett., 5:679.

Zimmerman, P.R., J.P. Greenberg, and C.E. Westberg. 1988. Measurements of atmospheric hydrocarbons and biogenic emission fluxes in the Amazon boundary layer. J. Geophys. Res. 93:1407-1416.